Characterisation of Interacting Partner(s) for *EYS*, a Major Gene Implicated in Autosomal Recessive Retinitis Pigmentosa

A Thesis Submitted to the University College London
for the Degree of Doctor of Philosophy

Przemysław Mateusz Kruczek
MSc

Department of Molecular Genetics
Institute of Ophthalmology
University College London
2015

Declaration

I, Przemysław Mateusz Kruczek, confirm that the work presented in this thesis is my own. Where information has been derived from other sources, I confirm that this has been indicated in the thesis.

Signed

Przemysław Mateusz Kruczek

Date:

Abstract

Mutations in *EYS* are a common cause of autosomal recessive retinitis pigmentosa (arRP). *EYS* is one of the largest genes expressed in the retina and the role of the protein it encodes is presently unclear. It has been shown, however, that EYS localises to the outer segments of porcine photoreceptors and that the *Drosophila* orthologue of EYS is essential in the biogenesis of the ommatidium, where it interacts with prominin, a highly conserved protein implicated in retinopathies. The aim of this project was to examine the role of EYS in the retina by investigating its subcellular localisation and by identifying its interacting partners.

Characterisation of the genetic structure of *EYS* has revealed that it has at least four isoforms expressed in the retina and testis. Immunocytochemistry studies have shown that EYS isoforms predominantly localise to the cytoplasm of cultured cells whereas immunohistochemistry studies in the primate retina have revealed that it localises to the photoreceptor ciliary axoneme. Yeast 2-hybrid screening has resulted in identification of one potential interacting partner of EYS, AIPL1, which is a molecular chaperone required for the proteostasis of the retina. Further analysis by co-immunoprecipitation and immunofluorescence has confirmed that AIPL1 interacts with the N-terminal fragment of EYS isoforms 1 and 4 as well as EYS isoforms 2 and 3. Furthermore, co-immunoprecpietation assays and immunofluorescence studies have suggested that the human orthologues of EYS and Prominin-1 do not interact. The mutation screening of *PROM1* has resulted in identification of seven heterozygous novel variants in six unrelated arRP patients; however, pathogenicity of the changes could not be established.

Altogether, the results of the study have demonstrated that EYS may be a novel protein associated with the photoreceptor ciliary axoneme, where it could play a role in maintenance of the photoreceptor outer segments. Furthermore, the analysis of the interacome of EYS has demonstrated that it may require the activity of AIPL1 for correct folding and trafficking, and that the functional link of EYS and Prominin-1 described in *Drosophila* is unlikely to be conserved in humans. The knowledge gained from the study presented herein has brought us closer to unravelling the molecular mechanisms underlying arRP and adds to the overall understanding of the physiology of the retina in health and disease.

List of Publications

Przemysław M Kruczek, Giovanna Alfano, Barbara Czub, Amna Z Shah, Andrew C Zelhof and Shomi S Bhattacharya (2014). 'Understanding the role of EYS by identification and characterisation of its retinal interacting partners'.
Poster presented at the American Society of Human Genetics Meeting 2014, San Diego, California (USA)

Przemysław M Kruczek, Giovanna Alfano, Amna Z Shah and Shomi S Bhattacharya (2014). 'Mutation screening of *PROM1* gene implicated in hereditary retinal degenerations'.
Poster presented at the UCL Neuroscience Symposium 2014, London, UK

Acknowledgments

I would like to express my sincere gratitude to my supervisor Professor Shomi Bhattacharya for the continuous support and guidance of my PhD study. I would also like to thank my subsidiary supervisor Doctor Jacqueline van der Spuy for her invaluable advice and for generously providing reagents essential for this project.

Besides my supervisors, I would like to thank my fellow lab mates: Amna, Giovanna, Barbara, Quincy, Beverley, Naushin, Vanita and Christina for their help and friendship. The past few years have been a difficult but a wonderful time and I could not have made it without your everyday support.

A special thank you goes to Amna who has generously supported me from day one of the project and has been an eminent tutor and an amazing friend. I am also especially grateful to Giovanna who has joined the project at its most difficult stage and contributed her knowledge and expertise to the progress of the work; this thesis would not have been completed to the standard it is now without your help.

I also wish to acknowledge Fight for Sight and Rosetrees foundations for providing the financial support for the study.

Last but not least, I would like to thank my beloved Tomasz for his tremendous support throughout writing this thesis and presence in the happiest and the most miserable times. I would also like to thank my family, especially my grandmother Zofia, my mother Małgorzata and my brothers Konrad and Miłosz, who have always believed in me, even when I could not believe in myself.

Table of Contents

Table of Figures

Table of Tables

Abbreviations

A, AbA	Aureobasidin A
˚C	degree Celsius
A	Ampers
A	adenine
aa	Amino acid(s)
Ab(s)	Antibody (-ies)
ad	autosomal dominant
AD	Activation domain
adRP	Autosomal dominant retinitis pigmentosa
APS	Amonium persulfate
arRP	Autosomal recessive retinitis pigmentosa
ATP	Adenosine triphosphate
att	attachment site (on Gateway cloning vectors)
b/bp	Base/base pair
BBS	Bardet-Biedl Syndrome
BCA	Bicinchoninic acid
DBD	DNA binding domain
BSA	Bovine Serum Albumin
C	Cytosine
CC	Connecting cilium
cDNA	Complementary deoxyribonucleic acid
cGMP	Cyclic guanosine monophosphate
cGMP	Cyclic guanosine monophosphate
CNS	Central Nervous System
Co-IP	Co-immunoprecipitation
CTS	Ciliary Targeting Sequence
Cys	Cysteine
kDa	kilodaltons
DAPI	4', 6-diamidino-2-phenylindole
dbcAMP	N6,2'-O-dibutyryladenosine 3'5'-cyclic monophosphate

ddH_20	Double-distilled water
ddNTP	Dideoxynucleotide
DDO	Double Dropout
dH2O	Distilled water
DMEM	Dulbecco's modified Eagle's medium
DMSO	Dimethyl sulfoxide
DNA	Deoxyribonucleic acid
dNTP	Deoxynucleotide
EDTA	Ethylenediaminetetraacetic acid
FCS	Foetal Calf Serum
FL	Full-length
G	Guanine
g	Gram
Gal	Galactose
GCL	Ganglion cell layer
gDNA	Genomic DNA
GDP	Guanosine diphosphate
GTP	Guanosine triphosphate
h	hours
HeLa	Human adenocarcinoma cell line
His	Histidine
HRP	Horseradish peroxidase
INL	Inner nuclear layer
IP	Immunoprecipitation
IPL	Inner plexiform layer
IPM	Inter-photoreceptor matrix
IRBP	Interphotoreceptor retinoid-binding protein
IS	Inner segment
LB	Lysogeny broth
LD-PCR	Long-distance PCR
Leu	Leucin
LRAT	Lecithin:retinol acyl transferase
Lys	Lysine

Lys/His	Lysine-Histidine-rich motif
M	Mol
Mata	Mating type a
Matα	Mating type alpha
min	Minute
ml	Mililitre
mM	Milimol
mRNA	Messenger ribonucleic acid
NaCl	Sodium chloride
NDS	Normal Donkey Serum
ng	Nanogram
nt	Nucleotide
OD	Optical density
ONL	Outer nuclear layer
OPL	Outer plexiform layer
OS	Outer segment
PAGE	Polyacrylamide gel electrophoresis
PBS	Phosphate-buffered saline
PCR	Polymerase chain reaction
PFA	Paraformaldehyde
PMSF	Phenylmethylsulfonyl fluoride
PNA	Peanut agglutinin
PPI	Protein-Protein Interaction
PSMC1	Regulatory subunit 4 of the 26 S protease
PVDF	Polyvinylidene fluoride
QDO	Quadruple drop-out
RHO	Rhodopsin
RK	Rhodopsin kinase
RNA	Ribonucleic acid
RP	Retinitis pigmentosa
RPE	Retinal pigment epithelium
rpm	Revolutions per minute
RT	Room temperature

RT-PCR	Reverse transcription polymerase chain reaction
SD	Synthetic drop-out
SDM	Site-directed mutagenesis
SDO	Single drop-out
SDS	Sodium dodecyl sulphate
SDS-PAGE	Polyacrylamide gel electrophoresis
Sec	Second
T	Thymine
TAE	Tris base, acetic acid and EDTA buffer
TBS	Tris-buffered saline
TDO	Triple drop-out
TEMED	Tetramethylethylenediamine
Tm	Melting temperature
TOPORS	Topoisomerase I binding RS domain protein
TRIS	Tris(hydroxymethyl)aminomethane
Trp	Tryptophan
U	unit(s)
UAS	Upstream activation sequence
Ub	ubiquitin
UPS	ubiquitin-proteasome system
USH	Usher Syndrome
UTR	Untranslated region
UV	Ultra violet
UVP	UV transilluminator
V	Volt
WB	Western Blot
X	X-α-Gal aka 5-bromo-4-chloro-3-indolyl α-D-galactopyranoside
xlRP	X-linked retinitis pigmentosa
X-α-Gal	5-bromo-4-chloro-3-indolyl α-D-galactopyranoside
X-β-Gal	5-bromo-4-chloro-3-indolyl-β-D-galactoside
Y2H	Yeast 2-hybrid
YPD	Yeast extract peptone dextrose medium
YPDA	Yeast peptone dextrose adenine medium

µl	Microlitre
µm	Micrometre
NFL	Nerve fiber layer
ILM	Inner limiting membrane
OLM	Outer limiting membrane
PR	Photoreceptors

Chapter 1: Introduction

1.1 The Eye

The eye is an organ specialised in mediating vision, one of the most fundamental human senses. It detects and converts light energy into electrical impulses that are transmitted to and processed in the visual cortex of the brain.

The eyeball is set in a protective cavity called the orbit and it is protected by the eyelids that secure the anterior surface of the eyeball and contain glands producing lubricating tear film. Muscles are attached to the outer coat of the eye and control movement and coordination of the eyeballs. A network of blood vessels supplies nutrients and a system of nerves provides innervation to the eye and surrounding tissues. The eyeball is made up of three distinct layers: 1) the external layer, formed by the sclera and cornea; 2) the intermediate layer is the uvea, which is divided into an anterior part comprising of iris and ciliary body, and a posterior part formed by the choroid; and 3) the internal, sensory layer, known as the retina (Figure 1.1) (Remington, 2005). The interior of the eye is divided into three chambers: 1) anterior chamber that lies between the cornea and the iris; 2) posterior chamber, located between the iris and the lens; and 3) vitreous chamber, which extends from lens to the retina. The first two chambers are continuous with each other and are filled with the aqueous humour whereas the vitreous chamber is replete with the viscous vitreous humour (Kolb *et al.*, 1995).

The sclera is the opaque white of the eye whereas the cornea is transparent and it allows light to enter the eye. A black-looking aperture on the anterior of the eyeball is the pupil, through which light enters the eye. The intermediate layer of the eye comprises of the iris, ciliary body and choroid. The most anterior is the iris, which acts as a diaphragm regulating the amount of light entering through the pupil and is controlled by two iris muscles. The crystalline lens is a transparent body located behind the iris, in the posterior chamber. It is attached to the ciliary body by means of ligaments called zonule fibres. The ciliary body is continuous with the iris and it produces the components of the aqueous and vitreous humour and contains the muscle that controls the shape of the lens. As a consequence of

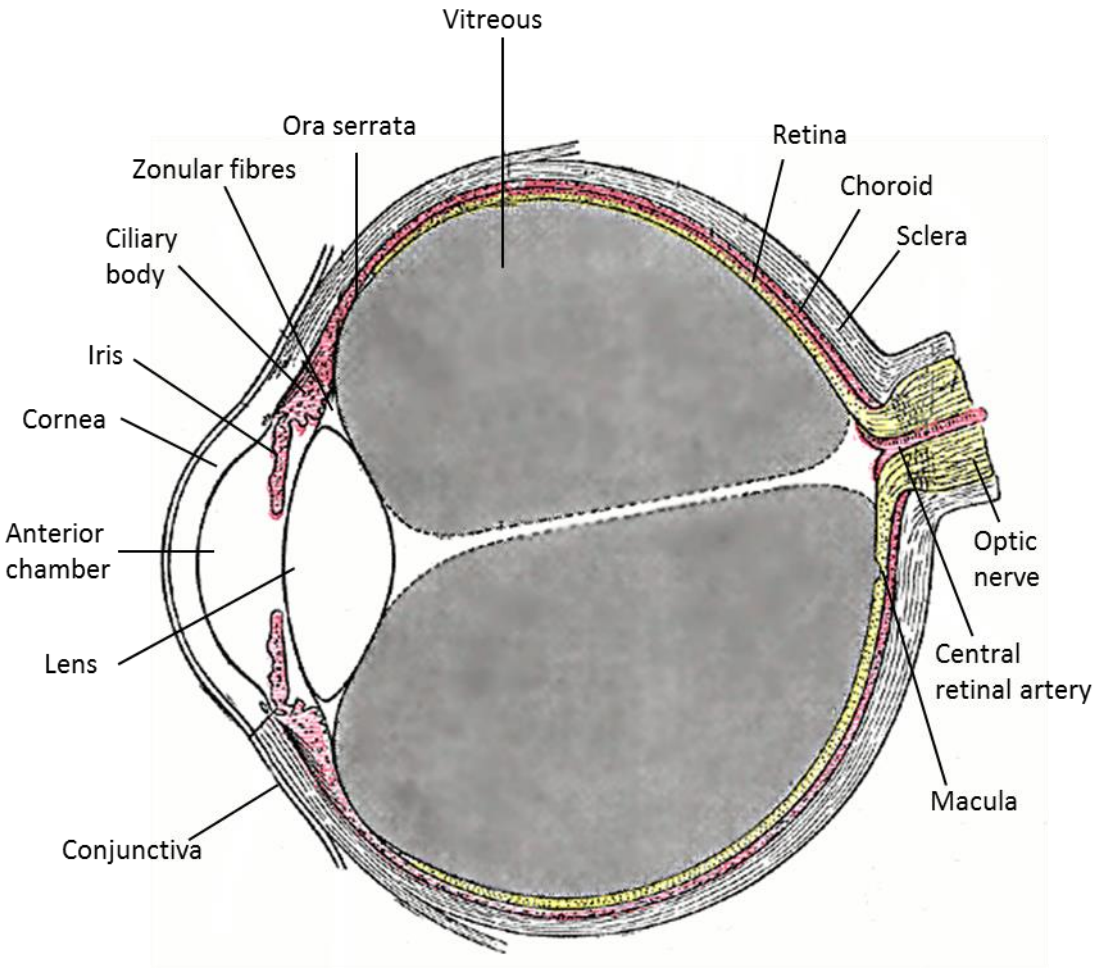

Figure 1.1 A schematic view of a horizontal section through the eyeball (Image adapted from http://www.ganfyd.org/index.php?title=File:Eye.png; public domain).

ciliary muscle action, zonule fibres are subject to contraction and relaxation that affect the shape of the lens. This process is called accommodation and allows a sharp image to be focussed on the retina (Kolb *et al.*, 1995).

The posterior part of the uvea is the choroid that consists of a network of blood vessels. It surrounds the retina and transports nutrients to the outer retinal layers. The retinal neural tissue is located most internally; by a complex biochemical process, it changes light energy into a signal that is processed in the retina and exits the eye via the optic nerve which then forwards the signal to the brain (Remington, 2005). The structure that is of interest in this study is the retina.

1.2 The Retina

The retina is the innermost coat of the eye located between the choroid and the vitreous. It has been intensively studied for many years and it is believed to be the best understood sensory tissue. The retina, which is composed of the neural retina and the retinal pigment epithelium (RPE), develops from the neural ectoderm and it is the outermost layer of the central nervous system. It has a characteristic synaptic organisation and it is a useful and relatively easily accessible model for studying the biology of the central nervous system (Kandel *et al.*, 1991).

1.2.1 Organisation of the Human Retina

The vertebrate retina contains one class of non-neural cells, which are retinal pigment epithelium cells (RPE), and five classes of neurons, which include photoreceptor cells, bipolar cells, amacrine cells, horizontal cells and ganglion cells. The retina has a laminar structure and there can be ten layers identified histologically (Figure 1.2):

- The outermost layer of the retina is the retinal pigment epithelial layer (RPE), to which the neural retina adheres.
- The photoreceptor layer (PR) comprises of the outer and inner segments of the photoreceptor cells.
- The outer limiting membrane (OLM) is formed of intercellular junctions between photoreceptor cells and between photoreceptor cells and Müller

cells at the level of the photoreceptor inner segments; it is not a true membrane but a feature distinguished on the light micrograph.

- The outer nuclear layer (ONL) comprises of photoreceptor cell bodies containing the nuclei.
- The outer plexiform layer (OPL) is formed by the synapses between photoreceptor cells and, bipolar cells, and horizontal cells.
- The inner nuclear layer (INL) contains the cell bodies of the retinal interneurons: bipolar, horizontal and amacrine cells.
- The inner plexiform layer (IPL) is formed by the synapses between bipolar, amacrine and ganglion cells.
- The ganglion cell layer (GCL) comprises of ganglion cell bodies.
- The nerve fibre layer (NFL) if formed of axons of ganglions cells which form the optic nerve exiting the eye.
- The inner limiting membrane (ILM) forms the innermost boundary of the retina and is composed of extensively expanded terminations of the Müller cells. It is a diffusion barrier between the neural retina and the vitreous humour (Kaufman & Alm, 2003).

In the vertebrate retina, the photons of light are captured in the photoreceptor cells, where they are converted into an electric impulse that is subsequently forwarded to the brain through a series of neurons. The retinal neurons form complex networks that permit extensive processing of the visual stimuli, which makes it possible to derive different kinds of information from the responses generated by photoreceptors (Kaufman & Alm, 2003).

RPE is formed of cells that are regularly arranged in single-layered cuboidal epithelium that contains melanin, a black pigment responsible for absorbing any light not captured by photoreceptors. This mechanism prevents from the light being reflected back into the retina, which could cause distortion of the visual image. What is more, RPE cells play an important role in assisting photoreceptors in re-synthesis of the visual pigment and phagocytosis of outer segment tips. For this reason photoreceptors contact the epithelial tissue directly. It makes the light travel through all other layers of the retina and, therefore, these cells are unmyelinated and transparent (Kolb *et al.*, 1995).

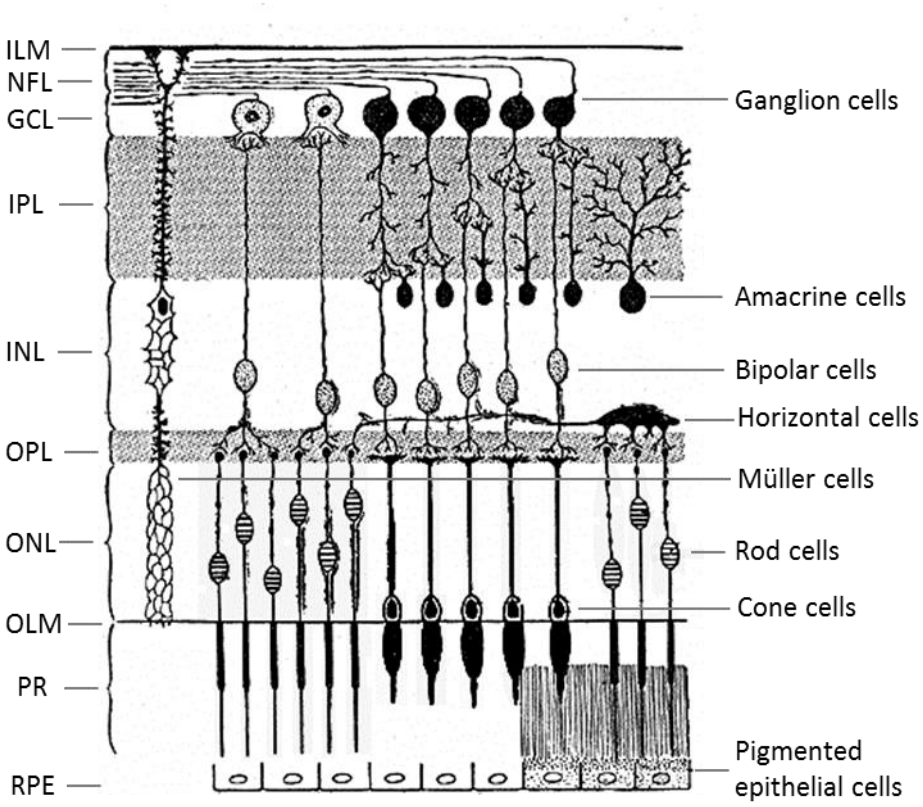

Figure 1.2 A schematic structure of the vertebrate retina. RPE - retinal pigment epithelium layer, PR - photoreceptor cell layer, OLM - outer limiting membrane, ONL - outer nuclear layer, OPL – outer plexiform layer, INL – inner nuclear layer, IPL – inner plexiform layer, GCL – ganglion cell layer, NFL – nerve fibre layer, ILM - inner limiting membrane (Image adapted from http://www.ganfyd.org/index.php?title=Retina; public domain).

1.2.2 Photoreceptor Cells

There are two types of photoreceptor cells in the human retina, rods and cones. Rod photoreceptors perform best at dusk or at night in the dim light conditions and therefore, they mediate night vision (scotopic vision). Most stimuli in the dim light are too weak to excite cone cells. The cone photoreceptors function more effciently in bright light and mediate colour vision (photopic vision). Cones provide higher acuity and better resolution of rapid changes in the visual image (Kandel *et al.*, 1991). Due to the differences in the tasks assigned to each type of photoreceptor cells, rods contain more photosensitive pigment and can be excited by as little as a single photon of light whereas hundreds of photons are required to induce a similar response in cones (Kaufman & Alm, 2003).

Although rods outnumber cones by approximately 20 to 1, the cone system has better spatial resolution. Firstly, cones are densely packed in the central area of macula, fovea, where the visual image is least distorted. Secondly, the rod system is convergent which means that many rods can be connected to the same bipolar cell whereas every cone is synapsed to one or a few bioplar cells. Such arrangment enables visual information to be pooled and reinforces signals received from rods. This in turn increases the ability of the brain to detect dim light and makes the cone system much more efficient in providing spatial resolution (Kandel *et al.*, 1991). Differences between rod and cone systems are summarised in Table 1.1. The general structure of rods and cones is relatively similar. They are composed of several parts, starting nearest the RPE: (1) the outer segment, containing the visual pigment molecules for the conversion of ligh into a neural signal; (2) a connecting stalk, the connecting cilium; (3) the inner segment, containing the metabolic apparatus; (4) the outer fibrer; (5) the cell body and (6) the inner fiber which ends with a synaptic terminal (Figure 1.3).

Rod photoreceptors are slim and rod-shaped. Their outer segments are made up of membranous discs stacked up on each other. The cell membrane is separate from the discs except for a small region at the base where invaginations of the cell membrane are formed and later developed into discs. Discs are gradually displaced outward towards the RPE by the formation of new discs. As they reach the tip of the outer segment they are shed off and phagocytosed by the RPE cells. Disc membranes in rods are shed regularly with the majority of the

process occuring in the morning. The rod inner and outer segments have approximately the same width.

Rods	Cones
• More photopigment • High amplification, single photon detection • Low temporal resolution: slow response, long integration time • More sensitive to scattered light • High sensitivity, specialized for night vision • A single cell has around 2 µm in diameter and is around 100 µm long	• Lower sensitivity, specialized for day vision • Less photopigment • Low amplification • High temporal resolution: fast response, short integration time • Most sensitive to direct axial rays • A single cell has around 4 µm in diameter and is around 50 µm long
Rod system	**Cone system**
• Low acuity: highly convergent retinal pathways, not present in the central fovea • Achromatic: one type of the visual pigment	• High acuity: less convergent retinal pathways, concentrated in fovea • Chromatic: three types of cones, each with different pigment sensitive to a different part of the visible spectrum

Table 1.1 An overview of differences between rod and cone visual systems.

The inner segment makes contact with the cell body by the long and narrow outer fiber. The inner fiber extends from the cell body and terminates with a rounded, pear-shaped structure called a spherule.

Cones are shorter than rods and have a conical shape. Similarly to the rod, the outer segment of the cone houses disc membranes; however, these in cones are continuous with the cell membrane. In many cones discs located at the base of the outer segment are wider than those at the tip giving the characteristic conical shape. Cone disc membranes are also subject to periodical renewal and are most efficiently shed off and phagocytosed by RPE at the end of the day. The shape of the inner segment also contributes to the overall morphology of the cone. It is wider and contains more mitchondria than the rod. The outer fiber is broad and short and may even be abscent in the cone. The inner fiber terminates in a broad, flattened structure called the pedicle (Remington, 2005).

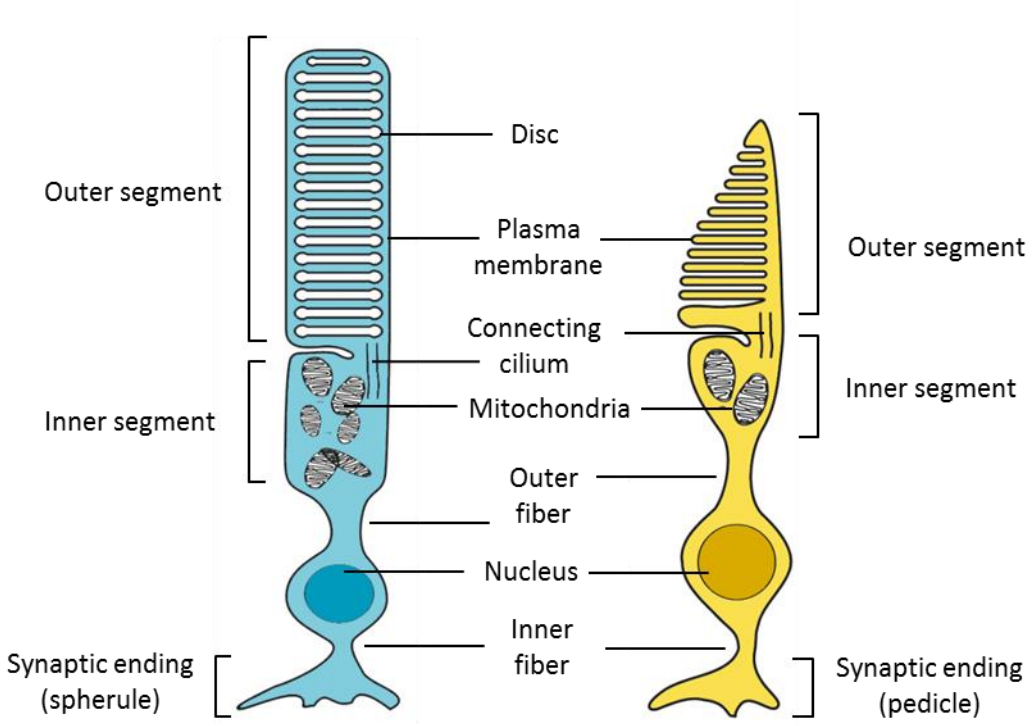

Figure 1.3 A schematic view of rod and cone structure (Image adapted from Shichida & Matsuyama, 2009; open access journal).

1.2.3 Physiology of the Retina

1.2.3.1 Phototransduction Cascade

The process of converting light energy into an electric impulse is called the phototransduction cascade. It takes place in the photoreceptor outer segment, which contains the machinery to conduct this biochemical process.

The cascade begins with absorption of a photon of light by visual pigments embedded on disc membranes. In humans, each type of photoreceptor cells (rods and three types of cones) produce visual pigments with different spectral sensitivity (Nathans, 1999). All of these pigments are G-protein coupled receptors that consist of the protein moiety, opsin, and the chromophore, 11-*cis*-retinal, which is a derivative of vitamin A covalently linked to opsin by a protonated Schiff base. The human cone opsins share less than 50 % of homology with rhodopsin; however, they exhibit similar structure with seven-transmembrane helices. The other phototransduction proteins including transducin, phosphodiesterase and cGMP channel, also have different isoforms in rods and cones. In spite of these differences, the biochemical events of the visual pigment in rods and cones appear to be very similar (Yau & Hardie, 2009). Overview of events the phototransduction cascade is presented in Figure 1.4. The phototransduction cascade can be divided into the following stages:

<u>Activation of the Cascade</u>

In rods, absorption of the photon causes isomeric alteration of 11-*cis*-retinal which is changed to all-*trans*-retinal. Within milliseconds the rhodopsin molecule is transformed to its catalytically active state metarhodopsin II (Rh*). Rh* begins to activate molecules of transducin (Gt) by catalysing GDP/GTP exchange on the Gt α-subunit. The active Gtα dissociates from its partnering subunits βγ and binds to the subunit γ of the cGMP phosphodiesterase (PDEγ). This binding removes the inhibition of PDEγ on the catalytic PDEαβ subunits, allowing the latter to hydrolyse cGMP. Moreover, once GTP has been attached to Gtα, Rh* dissociates from the complex and activates other transducin molecules (Yau & Hardie, 2009).

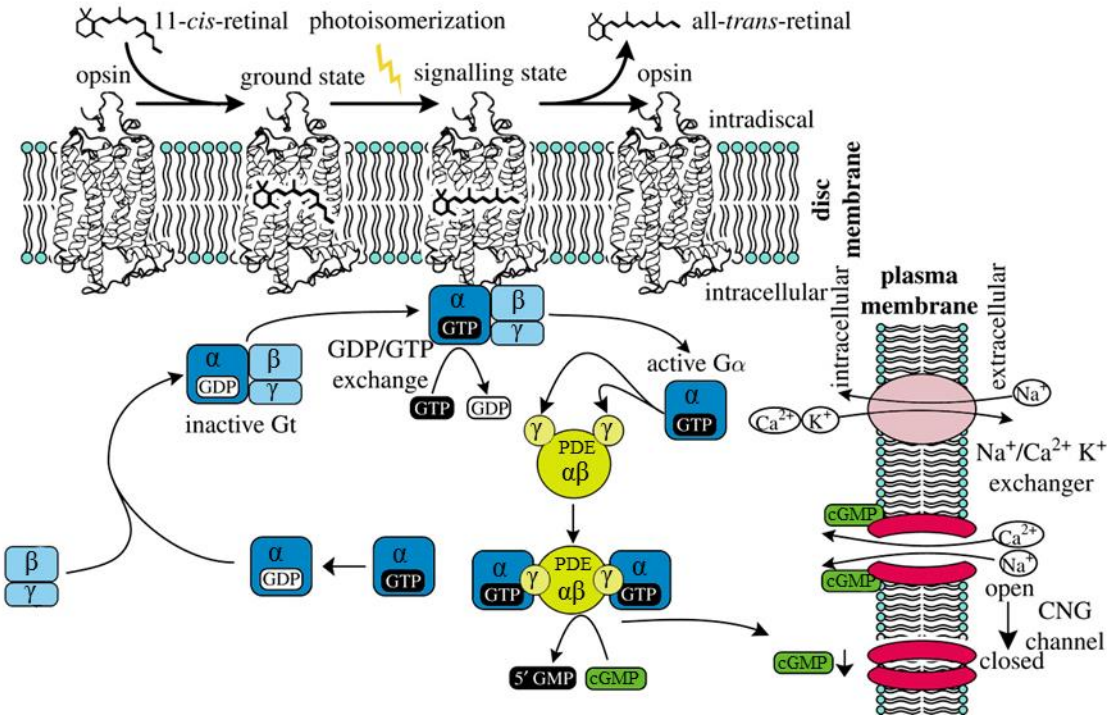

Figure 1.4 Overview of the events of the phototransduction pathway, from the initiation of the photon of light all the way through to the depolarization of the photoreceptor membrane (Image adapted from Shichida & Matsuyama, 2009; open access journal).

The resulting fall in the cGMP concentration causes the cGMP gated channels (CNG channels) in the cell membrane to close, leading to membrane hyperpolarization that reduces the rate of glutamate release onto the second-order retinal neurons.

Deactivation of the Cascade

For complete deactivation of the cascade, each active component of the cascade needs to be shut down. The active state of rhodopsin (metarhodopsin II, Rh*) decays over a minute into an inactive state (metarhodopsin III). However, before that happens, Rh* is phosphorylated by a rhodopsin kinase (also known as G protein-coupled-receptor-kinase 1, or GRK1), which is followed by a rapid binding of arrestin (Arr), which recognises phosphorylated Rh*. Phosphorylated rhodopsin may have some catalytic function; however, in a complex with arrestin it loses all activity. Eventually, rhodopsin in the free-opsin state after metarhodopsin III decay/hydrolysis or in the regenerated rhodopsin state loses its bound arrestin and goes through dephosphorylation.

Transducin deactivates itself by intrinsic GTPase activity, which converts the active Gtα*-GTP to inactive Gtα*-GDP. GTPase activity is facilitated by a GTPase-activating-protein (GAP) complex. In rods, this complex consists of a protein called regulator of G protein signalling 9 (RGS9), a RGS9-anchoring protein (R9AP), an orphan G protein β subunit (Gβ5) and PDEγ, which is the substrate of Gtα*. The requirement for PDEγ ensures that Gtα*-GTP has found and activated its substrate before deactivation. Once GTP has been hydrolysed, the resulting Gtα-GDP dissociates from PDEγ and re-associates with Gtβγ, allowing PDEγ to resume its inhibition of PDEαβ.

Complete recovery from the photoresponse also requires restoration of cytoplasmic cGMP levels. This process is mediated by guanylate cyclase (GC), which is an enzyme transforming GTP to cGMP. GC is activated by guanylate cyclase activating proteins (GCAPs), which sense the intracellular fall in Ca^{2+} concentration. It has been shown that some dark PDE activity exists in order to balance activity of GC (Yau & Hardie, 2009).

1.2.3.2 Calcium Feedback

In photoreceptors the most rapidly acting form of light adaptation is mediated by the level of Ca^{2+} cations. The light induced fall in intracellular Ca^{2+} helps to maintain intracellular levels of cGMP (Burns & Pugh, 2010). In light conditions, closure of the cGMP-gated channels reduces or even stops the Ca^{2+} influx, but the Ca^{2+} efflux continues and therefore the concentration of Ca^{2+} rapidly falls. This decrease has three effects. The first one manifests in the increase of GC activity. The reason is that GC requires two activating proteins, GCAP1 and GCAP2, which are Ca^{2+} binding proteins and they are in an inactive state while Ca^{2+} is bound. In light conditions, the Ca^{2+} decrease disinhibits the GCAPs, thus elevating the GC activity to chase after the light-stimulated PDE activity, producing a negative feedback loop. Second, rhodopsin kinase (GRK1) is negatively modulated by Ca^{2+} binding protein called recoverin or S-modulin, so that Rh* phosphorylation and arrestin binding are moderately slow in dim light but accelerate when Ca^{2+} progressively decreases in brighter light. It therefore reduces the active lifetime of Rh* and the amplification (Yau & Hardie, 2009). The third Ca^{2+} dependent mechanism is the regulation of the sensitivity of the cGMP-gated channels by calmodulin-like proteins. When Ca^{2+} falls during the light response, calmodulin dissociates from the channels increasing the channel's sensitivity to cGMP (Ridge *et al.*, 2003).

1.2.3.3 Visual Cycle

The ability of photoreceptors to function during many hours of continuous illumination requires the inactivated visual pigment to be continuously regenerated. The process of recycling the visual pigment is called the chromophore or visual cycle and involves metabolic processes in the photoreceptors and retinal pigment epithelium (Figure 1.5). After inactivation of rhodopsin, the Schiff base is hydrolysed and free all-*trans*-retinal is released. All-*trans*-retinal is shuttled from the disc membrane to the cytoplasm by a member of an adenosine triphosphate (ATP) binding cassette family, ABCR.

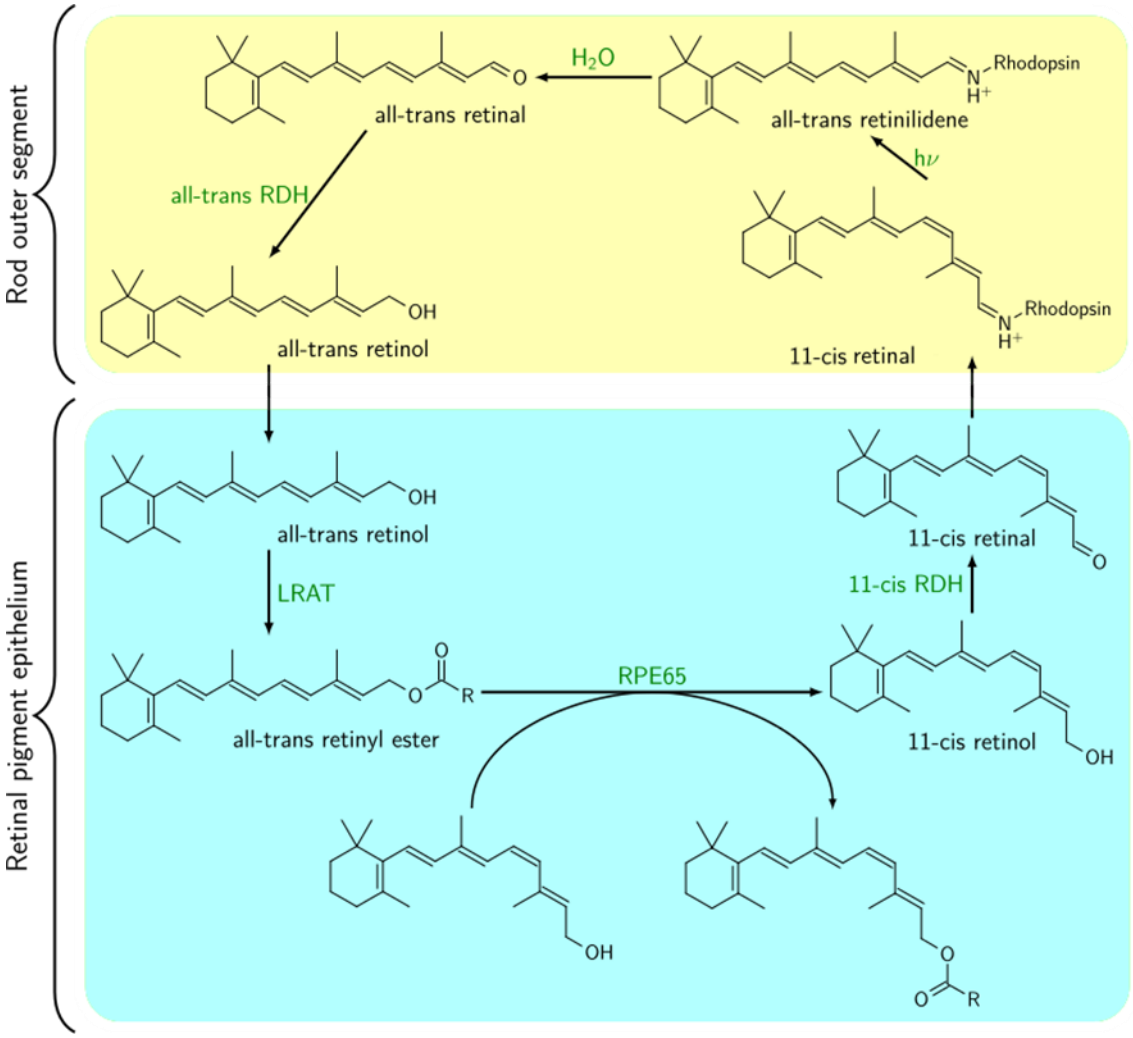

Figure 1.5 A schematic representation of the pigment cycle in human photoreceptors. hν, photon; RDH, retinol dehydrogenase; RPE65 - Retinoid isomerohydrolase; LRAT, lecithin:retinol acyl transferase ("Visual cycle" by Krishnavedala - Own work, Wikimedia Commons - www.commons.wikimedia.org).

Here, all-*trans*-retinal is reduced to all-*trans*-retinol (vitamin A) by all-*trans*-retinal dehydrogenase (RDH). All-*trans*-retinol can subsequently diffuse to the subretinal space where it is bound by the interphotoreceptor retinoid-binding protein (IRBP), a protein that is secreted by photoreceptors and facilitates movements of ligands to the apical membrane of RPE cells. When entering RPE cells, all-*trans*-retinol is bound by the cytosolic retinoid-binding protein type I (CRBP-I) and by that, it is delivered to lecithin:retinol acyltransferase (LRAT) for its esterification into an all-*trans*-retinyl. This ester is then immediately converted by a retinoid isomerohydrolase (RPE65) into 11-*cis*-retinol, after which 11-*cis*-retinol is bound by the cellular retinalaldehyde-binding protein (CRALBP) that enables the 11-*cis*-retinol dehydrogenase (11-*cis*-RDH) to process the final oxidation of 11-*cis*-retinol into 11-*cis*-retinal. Transport of 11-*cis*-retinal back to photoreceptors is stimulated by IRBP, where it can recombine with opsins and continue in the phototransduction (Kaufman & Alm, 2003).

1.3 Retinitis Pigmentosa

Retinitis pigmentosa (RP; OMIM 268000) is a heterogeneous group of retinal dystrophies characterised by progressive degeneration of photoreceptor cells. The worldwide prevalence of the disease is variably reported in about one case for each 3000 to 5000 individuals and there have been about 2 million individuals diagnosed with RP, making it the most common inherited photoreceptor degeneration (Chizzolini *et al.*, 2011).

Clinical hallmarks of RP include night blindness (nyctalopia), pigmentary deposits resembling bone-spicules (initially in the periphery of the retina), attenuation of the retinal vessels, waxy pallor of the optic disk and patchy losses of peripheral vision evolving to tunnel vision. Night blindness is the first symptom; however, it is very often ignored until the time affected individuals begin to live more actively after dusk (Hamel, 2006). The disease tends to manifest in the third decade of life, with the quality of vision progressively deteriorating and leading to complete blindness, usually, by the age of 60 (Hartong *et al.*, 2006).

On the cellular level, RP symptoms correlate with photoreceptors undergoing apoptosis. In most cases, rod photoreceptor system is affected primarily and cone cells degenerate at a later stage of the disease as a secondary effect. Death of photoreceptor cells is reflected in reduced thickness of the outer nuclear layer (ONL), lesions and deposits of pigment in the fundus (Hamel, 2006).

To date, mutations in 84 genes have been identified to be causative of RP (https://sph.uth.edu/Retnet/sum-dis.htm#A-genes; accessed on 25/06/2015) (Table 1.2). This genetically heterogeneous disorder is inherited in all known modes of inheritance, including autosomal dominant (~24 %), autosomal recessive (~41 %) and X-linked (~22 %). The remaining cases could result from non-genetic factors, non-Mendelian inheritance or complex inheritance (Wright *et al.*, 2010). The majority of RP cases are inherited as a monogenic trait but the disease is heterogeneous both clinically and genetically. Most of the genes implicated in RP account for a small portion of cases with the exception of rhodopsin (*RHO*), which leads to about 20 % of dominant RP cases, *USH2A* gene, which might cause up to 20 % of recessive RP, and the *RPGR* gene, which causes approximately 70 % of X-linked RP (Hartong *et al.*, 2006).

Inheritance	Gene
Autosomal dominant (26 genes)	*BEST1, CA4, CRX, FSCN2, GUCA1B, HK1, IMPDH1, KLHL7, NR2E3, NRL, OR2W3, PRPF3, PRPF4, PRPF6, PRPF8, PRPF31, PRPH2, RDH12, RHO, ROM1, RP1, RP9, RPE65, SEMA4A, SNRNP200, TOPORS*
Autosomal recessive (55 genes)	*ABCA4, ARL6, ARL2BP, BBS1, BBS2, BEST1, C2 orf71, C8orf37, CERKL, CLRN1, CNGA1, CNGB1, CRB1, CYP4V2, DHDDS, DHX38, EMC1, EYS, F AM161A, GPR125, HGSNAT, IDH3B, IFT140, IFT 172, IMPG2, KIAA1549, KIZ, LRAT, MAK, MER TK, MVK, NEK2, NEUROD1, NR2E3, NRL, PDE6 A, PDE6B, PDE6G, PRCD, PROM1, RBP3, RGR, RHO, RLBP1, RP1, RP1L1, RPE65, SAG, SLC7A14 , SPATA7, TTC8, TULP1, USH2A, ZNF408, ZNF5 13*
X-linked (3 genes)	*OFD1, RP2, RPGR*

Table 1.2 All genes identified to be implicated in retinitis pigmentosa (RetNet database, https://sph.uth.edu/Retnet/sum-dis.htm#A-genes; accessed on 25/06/2015).

With regards to autosomal recessive RP (arRP), recent reports have suggested a global involvement of the *EYS* gene with the prevalence ranging from 5-23.5 % in different populations (e.g. Spanish, Israeli, French, Japanese), making it one of the major genes for arRP (Abd El-Aziz *et al.*, 2010; Arai *et al.*, 2015; Audo *et al.*, 2010; Bandah-Rozenfeld *et al.*, 2010; Hosono *et al.*, 2012; Iwanami *et al.*, 2012).

Furthermore, a digenic form of inheritance has been reported for RP and the disease was caused by a heterozygous mutation in *ROM1* in combination with a heterozygous mutations in *RDS* (Kajiwara *et al.*, 1994).

Retinitis pigmentosa is in most cases an isolated disease; however, between 20 to 30 % of patients have associated non-ocular symptoms. There have been more than 30 RP syndromes reported with the most prevalent being Usher syndrome and Bardet-Biedl syndrome (Hartong *et al.*, 2006).

Usher syndrome is inherited in a recessive manner and it is the most frequent syndromic form of RP associated with neurosensory deafness. The hearing loss may be profound (type I; *USH1*), moderate to mild in severity and non-progressive (type II; *USH2*) or normal hearing can be present in youth and the gradual hearing loss can occur later in life (type III; *USH3*) (Millán *et al.*, 2011). To

date, 13 genes have been implicated in Usher syndrome (RetNet, https://sph.uth.edu/Retnet/home.htm).

Bardet-Biedl syndrome (BBS) is a rare ciliopathy inherited in an autosomal recessive manner. It is characterised by retinal dystrophy, obesity, post-axial polydactyly, renal dysfunction, learning difficulties and hypogonadism. Renal disease is usually causative of mortality of BBS patients. Weight is very often within standards at birth; however, children with BBS syndrome begin to significantly put on weight in the first year of life. Symptoms of RP usually develop in the first decade of life and most of the BBS patients are legally blind by the second or third decade of life (Forsythe & Beales, 2013). Twenty two genes are currently known to be associated with BBS (RetNet, https://sph.uth.edu/Retnet/home.htm).

1.4 Eys Shut Homolog (EYS)

The *EYS* gene was independently identified at the *RP25* locus by two groups of researchers, who had previously mapped the locus in families with arRP (Abd El-Aziz *et al.*, 2008; Collin *et al.*, 2008). Abd El-Aziz et al. reported six different mutations in five unrelated Spanish families, including four deletions and two nonsense substitutions. All of these changes were predicted to result in a premature stop codon leading to nonsense-mediated decay (NMD) of the resulting mRNA (Abd El-Aziz *et al.*, 2008). Concurrently, Collin and co-workers, using homozygosity mapping, reported a nonsense mutation in three arRP siblings of an unrelated family and a frame-shift mutation in an isolated RP patient. Both changes were predicted to result in a premature termination codon and protein truncation (Collin *et al.*, 2008).

Since its discovery, *EYS* has emerged as a major arRP gene with the estimated prevalence of 11 % in British and Chinese populations (Abd El-Aziz *et al.*, 2007), 12 % in French (Audo *et al.*, 2010), 5 % in Dutch and Canadian (Littink *et al.*, 2010), 7 % in Israeli (Bandah-Rozenfeld *et al.*, 2010), 15.9 % in Spanish (Barragan *et al.*, 2010), and 18-23.5 % in Japanese populations (Arai *et al.*, 2015; Iwanami *et al.*, 2012). There have been at least 150 mutations identified in *EYS* and this number is continuously growing following the publication of new high-throughput sequencing studies of arRP families.

The majority of individuals carrying homozygous mutations in *EYS* present with a typical and rather severe form of arRP. Clinically, they present with night blindness, bone spicule pigmentation and attenuated retinal vessels. On average, it has been estimated that the visual field in patients with homozygous mutations in *EYS* begins to progressively deteriorate at around 30 years of age (Bonilha *et al.*, 2015). Histopathological analysis of retinal tissue derived from patients carrying mutations in *EYS*, revealed advanced retinal degenerative changes with near-total absence of rods at the periphery of the retina and fairly well preserved perifovea (Bonilha *et al.*, 2015). Interestingly, there has been a report of a Japanese individual diagnosed with cone-rod dystrophy caused by a compound heterozygous mutation in *EYS*, suggesting that the protein product of *EYS* may be important for the homeostasis of both rods and cones (Katagiri *et al.*, 2014).

EYS was described as the largest gene known to be expressed in the retina, spanning over 2 Mb of genomic DNA. Abd El-Aziz et al. reported EYS to be composed of 43 exons, of which exons 4-43 encode a protein consisting of 3144 amino acids (Abd El-Aziz *et al.*, 2008). The study conducted by Collin and co-workers revealed a similar gene structure with an additional exon between exon 41 and 42, making the predicted protein slightly larger with a size of 3165 amino acids. The facultative 42nd exon comprises 63 bp and lies just prior to the sequence encoding the fourth LamG domain (Collin *et al.*, 2008).

The predicted human EYS protein consists of a signal peptide followed by 21 epidermal growth factor (EGF)-like domains, putative coiled-coil domain and five Laminin G-like domains that are interspersed by further EGF-like repeats (Figure 1.6). Furthermore, it has been suggested that the signal peptide and its cleavage site consensus sequence located in the N-terminal region of EYS may confer a secretory character to the protein or result in an intracellular or cytoplasmic localisation of the mature protein (Abd El-Aziz *et al.*, 2008; Barragan *et al.*, 2010; Collin *et al.*, 2008).

Both groups reported *EYS* as the human orthologue of the *Drosophila* 'eyes shut' (*eys*) gene, also known as spacemaker or spam, which has been shown to act together with prominin in the development of the *Drosophila* open rhabdom visual system (Husain *et al.*, 2006; Zelhof *et al.*, 2006) (see section 1.6).

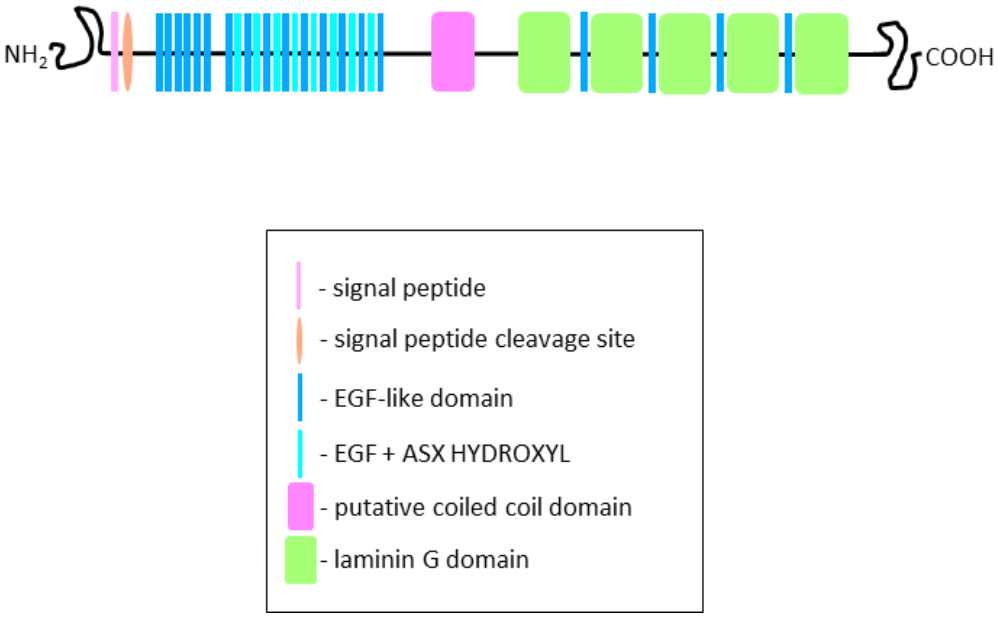

Figure 1.6 A schematic view of the predicted domain structure of EYS protein. EYS is composed of a signal peptide followed by 21 epidermal growth factor (EGF)-like domains, putative coiled-coil domain and five Laminin G-like domains that are interspersed by further EGF-like repeats.

Intriguingly, in the course of evolution the expression of *EYS* orthologues has been lost in the lineages of mammals including armadillo, little brown bat and ruminant lineages. The expression of *EYS* orthologues is also absent in rodent genomes, including the mouse, rat and guinea pig.

By performing RT-PCR analysis and immunohistochemistry experiments, it has been demonstrated that EYS is specifically expressed in the retina and it localises to the outer segments of porcine photoreceptor cells. Based on these observations and the data obtained from research on the *Drosophila* model, it has been suggested that EYS may play a structural role in the human photoreceptor cells (Abd El-Aziz *et al.*, 2008; Collin *et al.*, 2008; Nie *et al.*, 2012; Zelhof *et al.*, 2006).

1.5 Prominin-1

Mutations in *PROM1* gene cause clinically heterogeneous retinal degeneration (MIM 604365). To date, there have been 19 mutations identified in *PROM1* and the majority of the reported cases were diagnosed with autosomal recessive RP. Mutations in *PROM1* can also cause autosomal recessive macular degeneration, autosomal recessive cone-rod dystrophy and there has been one mutation reported to cause autosomal dominant macular degeneration (Appendix A). RT-PCR analysis of *PROM1* expression revealed that the gene is expressed in many tissues of the human body, including the retina, pancreas, placenta, kidney, liver, lung, brain and heart (Yu *et al.*, 2002). Nonetheless, in spite of the ubiquitous expression, individuals carrying mutations in *PROM1* have only been reported to exhibit an ocular phenotype. It has been proposed that this phenomenon is a result of the specific tissue distribution of Prominin-1 and its homolog, Prominin-2. Prominin-2 has similar topology to Prominin-1 but it is not present in the retina. Therefore, it has been hypothesised that rescue of the phenotype in tissues other than the eye comes from Prominin-2, which compensates for the lack or impairment of Prominin-1 (Fargeas *et al.*, 2003).

Prominin-1, also known as CD133, was identified in two independent studies as a microvilli specific protein expressed in murine neuroepithelial cells and as a plasma membrane marker of human hematopoietic stem and progenitor cells (Miraglia *et al.*, 1997; Weigmann *et al.*, 1997). The protein was described as a

cholesterol binding pentaspan membrane glycoprotein with a strong preference to plasma membrane protrusions. It has a unique membrane topology, containing five transmembrane domains, two large extracellular loops containing eight N-linked glycosylation sites, and a cytoplasmic tail (Figure 1.7) (Miraglia *et al.*, 1997; Roper *et al.*, 2000).

There have been at least nine different transcript variants and five alternative promoters identified for Prominin-1; however, only seven protein isoforms, ranging from 826 to 866 amino acids, seem to be produced in humans (Fargeas *et al.*, 2007). This discrepancy between number of transcripts and protein isoforms has been suggested to arise from differences at the untranslated regulatory regions. In the human retina, the most abundantly expressed isoforms are the s11 and s12 splice variants (47% and 43% respectively) (Permanyer *et al.*, 2010). The functional significance of this variability is not yet fully understood; however, the appearance of certain variants is thought to be tissue specific (Jaszai *et al.*, 2011). The differences between the seven human isoforms are presented in Table 1.3.

Isoform	Uniprot Identifier	Length [aa]	Variation
1 (s2)	O43490-1	865	canonical
2 (s1)	O43490-2	856	92-100: missing
3 (s3)	O43490-3	830	93-101: missing 831-839: VETIPMKNM → SSWVTSVQC 840-865: missing
4 (s10)	O43490-4	833	93-101: missing 839-861: missing
5 (s7)	O43490-5	825	93-101: missing 831-861: missing
6 (s11)	O43490-6	834	831-861: missing
7 (s12)	O43490-7	842	839-861: missing

Table 1.3 Summary of isoforms of Prominin-1 based on data derived from the UniProt database (www.uniprot.org).

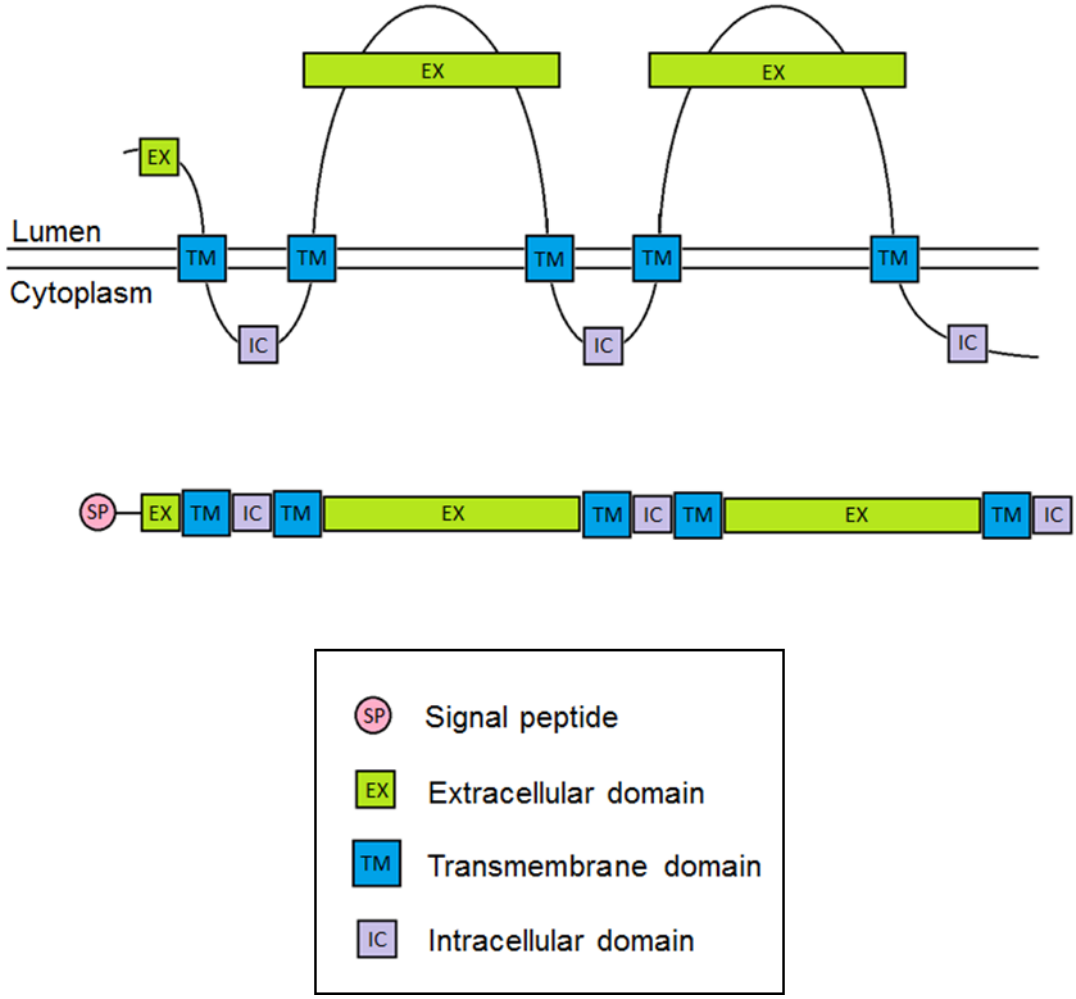

Figure 1.7 A schematic view of the predicted domain structure of Prominin-1. Prominin-1 is composed of five transmembrane domains, two large extracellular loops containing eight N-linked glycosylation sites, and a cytoplasmic tail.

The biology of Prominin-1 has been extensively studied and it has been argued that Prominin-1 is a key player in maintenance of the integrity of photoreceptors from insects to mammals, in spite of the significant differences in organization of their visual organs (Jaszai *et al.*, 2007). Supporting evidence was provided by Maw et al., who reported that mutations in *PROM1* cause retinal degeneration and demonstrated that Prominin-1 localises at the base of murine rod outer segments and more specifically, to the protrusions of plasma membrane that form the new basal lamellae destined to become membranous disks (Maw *et al.*, 2000).

In another study published by Zacchigna et al. in 2009 it was reported that knocking out expression of the orthologue of Prominin-1 in mice causes progressive degeneration of photoreceptors manifested by thinning of the outer nuclear layer and disruption of both rods and cones. The study provided further evidence that Prominin-1 is likely to be involved in morphogenesis of the photoreceptor membranous disks (Zacchigna *et al.*, 2009). Moreover, it has been shown via immunoprecipitation studies that Prominin-1 interacts with protocadherin 21 (PCDH21) and actin filaments; both of the interactions have been suggested to be critical to the disk membrane morphogenesis (Yang *et al.*, 2008).

Further studies performed in *Xenopus laevis* model demonstrated that the frog orthologue of Prominin-1 is present in both rods and cones. It has been shown that it localises to the basal disks of rod outer segments and at the outer rims of open disk lamellae of cone outer segments, where it may play a role in maintaining the structure and/or morphogenesis of the photoreceptor disk membranes (Han *et al.*, 2012).

Interestingly, an orthologue of Prominin-1 was also found in *Drosophila*, where it was demonstrated to be essential for defining the inter-rhabdomeral space in the compound eye through interaction with spam, the *Drosophila* orthologue of EYS (Zelhof *et al.*, 2006).

1.6 EYS and Prominin-1 as Potential Interacting Partners

The main feature of photoreceptor cells is the presence of a specialised compartment, whose role is to accommodate the millions of light sensing molecules required for efficient photon collection. In vertebrates, the light sensing compartments evolved as photoreceptor outer segment membranous disks whereas in insects there are microvilli rhabdomeres formed of the apical membrane (Kolb *et al.*, 1995).

Insects possess compound eyes that are formed of thousands of ommatidia (or facets), each of which houses photoreceptor cells and acts as a light sensing unit (Figure 1.8). Ommatidia can have two different inner architectures of the rhabdom, which is understood as all of the rhabdomeres taken together. Fruit flies *(Drosophila melanogaster)* and houseflies (*Musca domestica*) have an open rhabdom system, in which each ommatidium contains seven rhabdomeres that are separated from one another and function as independent light guides. In contrast, honey bees *(Apis mellifera)*, various mosquitoes and beetle species have a closed system, in which rhabdomeres are fused together and share the same visual axis (Figure 1.9). During ommatidium biogenesis the apical membranes of different photoreceptor cells separate from one another and produce the rhabdomeric structure needed for housing the phototransduction cascade. The process of production of microvilli requires coordination of membrane-membrane adhesion events and, in the open system, rhabdomeres partition from each other to form the inter-rhabdomeral space (IRS). Separation of rhabdomeres in the open rhabdom system improves vision resolution and allows detection of smaller moving objects (reviewed in Mishra & Knust, 2013; Moses, 2006).

The generation of the IRS is an essential event in the transition of compound eyes from a closed to an open system and the molecular mechanisms underlying this process have been extensively studied. Investigation was carried out using *Drosophila* mutants that had no IRS but had the rhabdomeres resembling the closed rhabdom system. The genetic screening of these mutant flies resulted in identification of two genes, products of which were thought to be implicated in formation of the IRS.

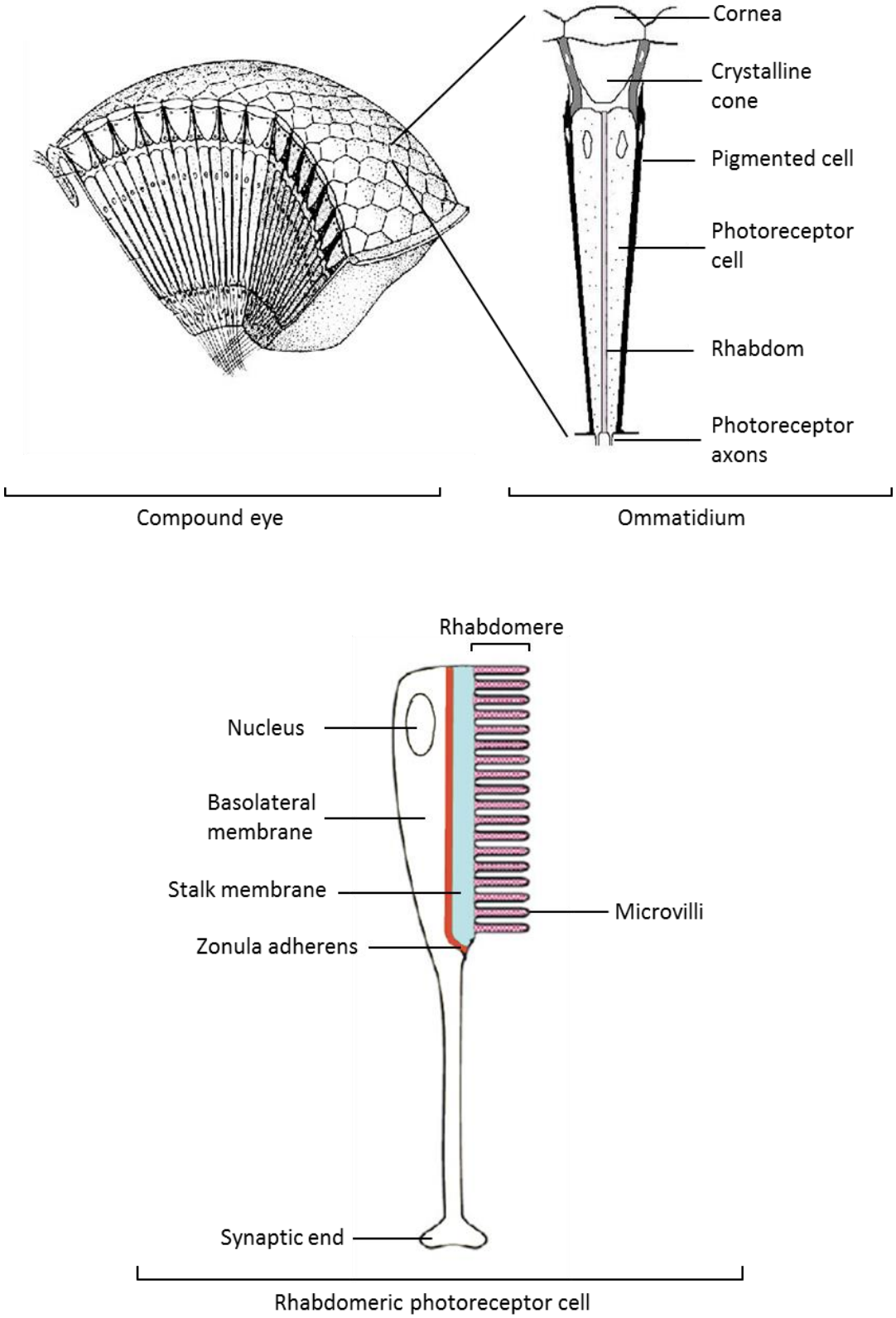

Figure 1.8 A schematic view of the structure of the *Drosophila* compund eye. The compound eye is formed of thousands of ommatidia (or facets), each of which houses photoreceptor cells and acts as a light sensing unit. Image modified from Wikmedia Commons ("Ommatidie" by Nono64; https://commons.wikimedia.org/wiki/File:Ommatidie.JPG#/media/File:Ommatidie.JPG, Kolb *et al.*, 1995 and (Duke-Elder, 1958).

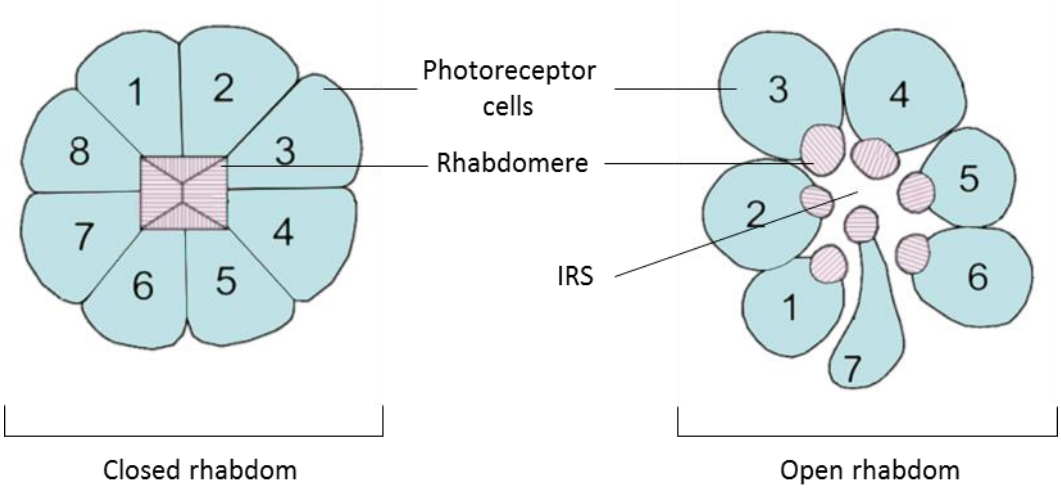

Figure 1.9 A schemtaic view of a cross-section through an ommatidium with a closed rhabdom system and an ommatidium with an open rhabdom system. Eys and prominin have been suggested to be key players in the morphogenesis of the IRS and the open rhabdom system (image modified from Karman *et al.*, 2012; open access journal).

The first identified gene was *spam* (or *spacemaker*), which was later discovered to be an orthologue of the human *EYS*. The second identified gene was *prom* (*prominin*), whose human orthologue is *PROM1* (Husain *et al.*, 2006; Zelhof *et al.*, 2006).

In *Drosophila, spam* encodes a polypeptide consisting of 2,165 amino acids. The protein comprises seven EGF-like domains followed by a linker region with multiple glycosylation sites and four alternating repeats of EGF-like and LamG domains. *Prom* encodes a 910 amino acid protein named prominin (prom) which belongs to a family of evolutionarily conserved transmembrane proteins associated with microvilli, whose function has not yet been fully understood (Husain *et al.*, 2006; Zelhof *et al.*, 2006).

It has been demonstrated that spam is a secreted extracellular protein specifically localising to the IRS. Furthermore, *spam* was shown to be expressed at 36-64 hours after puparium formation, a window of time coincident with the rhabdomere biogenesis. This suggests it plays a role in the development of the *Drosophila* visual system. Similarly, prominin is also expressed during rhabdomere biogenesis, at approximately 48 hours after puparium formation. Prominin was found to decorate the entire photoreceptor apical surface; however, by the time of eclosion it is selectively localised to the stalk membrane and tips of the microvilli.

The extensive analysis of *Drosophila* mutant prominin and spam phenotypes led to a conclusion that the two proteins act together in the architectural organisation of the *Drosophila* ommatidium. It has been hypothesised that the secretion of spam to the IRS forces the separation of the stalk membranes and pushes the rhabdomeres apart, and that spam is recruited to the microvillar surface by the binding with prominin. The interaction of spam and prominin was reasoned to act against the adhesive force of chaoptin, which is a membrane protein responsible for crosslinking of the microvilli by means of homophilic interactions. The published data have demonstrated that spam, prominin and chaoptin orchestrate the assembly of microvilli, ensure the structural integrity and the partitioning of rhabdomeres, and guarantee the construction of an open rhabdom system (Zelhof *et al.*, 2006).

Since both spam and prominin have orthologues expressed in humans, which are implicated in retinal degeneration, it has been suggested that the functional interaction between *Drosophila* spam and prominin may be

evolutionary conserved and be critical to the homeostasis of the human photoreceptor cells. This has been addressed by further studies performed using *Drosophila* models, where it was demonstrated that the human EYS and Prominin-1 can function in *Drosophila* photoreceptors and rescue the mutant phenotypes. The study has provided evidence strengthening the hypothesis that the functional link between EYS and Prominin-1 is conserved and the authors have suggested that it may be required for promoting structural integrity to the rhabdomeres and membrane disks by preventing contacts between adjacent membrane protrusions (Nie *et al.*, 2012).

Furthermore, the hypothesis that prominin binds spam was supported by experiments performed in cultured cell lines. *In vitro* experiments performed on a *Drosophila* Shneider-2 cell line showed that when cells are transfected with *spam*, the protein is secreted into the medium. However, if the same cells are instead co-transfected with both *spam* and *prom*, spam protein localizes selectively to the exterior surface of the plasma membrane. These results have indicated that prominin may function as a binding partner for spam (Zelhof *et al.*, 2006).

Interesting insights into the potential role of spam was provided by Cook et al., who demonstrated that *spam* is expressed in the *Drosophila* mechanosensory neurons, where it forms an extracellular shield that guards the cells from environmental insult. The hypothesis was supported by experiments performed *in vitro*, where it was demonstrated that spam decorates the external surface of the cell membrane surface only in the presence of prominin and it makes the cell membrane nearly ten times stiffer than uncoated controls; this has been shown to protect the cell shape in exposure to the osmotic, chemical and temperature stress (Cook *et al.*, 2008).

1.7 Protein-protein Interactions

Sequencing of the whole genome of many organisms has been an accomplishment with tremendous scientific impact; nonetheless, genomic information alone does not explain cellular functions. Most of the biological processes in living organisms are controlled by proteins, which rarely act alone but rather function in multiprotein assemblies. A critical step towards understanding the complex relationships between proteins in living organisms is mapping of the

protein-protein interactions (PPIs), a complete map of which is referred to as the interactome. Interactomic data is invaluable in studies aiming to elucidate the role of newly identified proteins (e.g. EYS). The function of a given protein can be hypothesised based on the interactions it is involved in, given that the function of an interacting partner has already been established (reviewed in De Las Rivas & Fontanillo, 2010).

By definition, PPI implies non-random physical contact between at least two proteins that intentionally occurs at a specific interface and time. PPIs depend on many factors such as cell type, developmental stage, cell cycle stage, post-translational modifications, external conditions etc. The protein assemblies are usually dynamic and they undergo a continuous turnover. The PPIs can be classified based on the strength of binding into transient and stable interactions. It needs to be noted, however, that sharing a 'functional contact' does not mean that the two proteins directly bind each other. It can be that they function in the same protein complex assembly but there are intermediate interactors between them, which together form a more elaborate network (reviewed in De Las Rivas & Fontanillo, 2010; Ngounou Wetie *et al.*, 2014).

Methodological approaches in interactomics are versatile and involve various scientific disciplines including molecular and cellular biology, genomics, biochemistry and biophysics. A very common experimental approach in researching PPIs is based on the principle compared to fishing. A known protein (a bait) is used in an experiment to fish out one or more interacting partners (preys) that are subsequently identified and validated by further experiments (reviewed in Ivanov *et al.*, 2011).

Experimental methods used to investigate PPIs can be divided into genomic and biochemical approaches. Genomic approaches utilise the expression of a reporter gene upon interaction of a bait and prey. An example of such a method is Yeast 2-hybrid (Y2H), which is widely used to screen cDNA libraries using a known bait protein. The approach is based on the possibility of separating some transcription factors into two domains: a DNA binding domain and a transcription activation domain. The conventional Y2H system was developed from the GAL4 transcription activator, DNA binding domain of which is usually fused with a bait protein whereas a prey is fused with the activation domain. When interaction between a bait and a prey occurs, the GAL4 moieties are brought in proximity,

reconstituting a functional transcription factor, which in turn activates transcription of the reporter gene (Fields & Song, 1989) (see Materials and Methods, section 3.2 for more detailed description of Y2H). There have been several modifications of Y2H system developed, e.g. LexA repressor based Y2H or the MYTH system, which enables investigation of membrane proteins (reviewed in Brückner *et al.*, 2009).

From a wide range of biochemical methods, co-immunoprecipitation is one of the most popular methods to identify PPIs between two or more proteins. The principle is based on 'fishing' from a cell lysate using an antibody directed against the protein of interest and subsequent isolation of immune complex using immobilised protein A or G. Such approach is usually followed by mass spectrometry (MS) for identification of the interacting partners. An alternative approach can be affinity purification (AP), which is based on purification of a tagged protein of interest (e.g. with His, GST or FLAG tags) followed by MS (AP-MS approach). AP-MS does not require the use of antibodies and it is a good alternative to Co-IP, especially when antibodies against a protein of interest are unavailable (reviewed in Ivanov *et al.*, 2011; Ngounou Wetie *et al.*, 2014).

Y2H method enables screening of species and tissue specific cDNA libraries and it identifies binary interactions. On the other hand, Co-IP and AP-MS approaches are used to determine components of the multiprotein complexes, which not necessarily all interact directly with one another (reviewed in Brückner *et al.*, 2009).

All experimental methods currently available to investigate PPIs have advantages as well as disadvantages and therefore, it is important to analyse novel PPIs using more than one approach for confirmation and validation of the results. This is particularly important when, for example, investigation of a human protein's interactome is carried out in simpler organisms such as yeast, whose protein biosynthesis machinery may differ, e.g. in terms of post-translational modifications. Therefore, results obtained from Y2H require validation using biochemical methods such as immunoprecipitation or immunofluorescence, which allow to investigate the potential interaction in more detail using mammalian systems (Ngounou Wetie *et al.*, 2014). Examples of methods that can be used for the purpose of Y2H validation are summarised in Table 1.4.

Method	Type	Description
Pull-down assay	*in vitro*	Tagged bait is immobilized on a resin and binds prey/s from lysates of eukaryotic cells or of *E.coli* expressing proteins of interest. After washing steps, prey is detected by SDS-PAGE/immunoblotting or Mass Spectrometry (MS)
Surface plasmon resonance	*in vitro*	Bait immobilised on the surface of a sensor chip is probed by injection of prey onto the surface. Protein interaction is detected by the use of the change in refractive index at the sensor surface. After elution, proteins are analysed by MS.
Co-immunoprecipitation	*ex vivo*	A specific antibody is used to precipitate the bait from cell lysates on a pull-down assay. After washing steps, co-immunoprecipitated prey is detected by SDS-PAGE/immunoblotting and MS
In situ hybridization	*in situ*	Hybridization of a labelled complementary DNA or RNA strand (i.e. probe) to a specific DNA or RNA sequence in a tissue section. Visualises expression of specific genes to evaluate potential co-expression of proteins of interest in the same cell of a given tissue.
Immunohistochemistry, immunocytochemistry	*in situ*	Proteins in fixed cells or tissue sections are detected by immuno-labelling with fluorescently tagged antibodies, e.g. using confocal microscopy. Visualises co-expression of proteins of interest in the same cell and potential subcellular co-localization.
Fluorescent detection in live cells	*in vivo*	Proteins in living cells are detected with fluorescently tagged antibodies or they are expressed with fluorescent tags. Visualises co-localization of proteins of interest.
Fluorescence resonance energy transfer (FRET)	*in vivo*	Bait and prey are fused to two different fluorescent tags with overlapping emission/excitation spectra. If both proteins are in close proximity, excitation of the first fluorophore (donor) leads to energy transfer to the second fluorophore (acceptor). Acceptor fluorescence can be observed in vitro (fluorimeter) or in living cells (confocal microscopy).
Bioluminescencer resonance energy transfer (BRET)	*in vivo*	Similar to FRET, but with bait fused to bioluminescent luciferase, thus avoiding the external excitation step susceptible to generate background. Detection as with FRET.

Table 1.4 Overview of methods that can be used to validate the results obtained from Y2H (adapted from Brückner *et al.*, 2009).

1.8 Aims and Objectives

The aim of this project is to investigate the molecular mechanisms underlying the phenotype of arRP associated with mutations in *EYS*. *EYS* is a major gene implicated in arRP; however, the function of the protein it encodes has not yet been fully understood.

The EYS protein has been found to localise to the photoreceptor outer segments of the porcine retina and it has been suggested that it may play a structural role (Abd El-Aziz *et al.*, 2008). Studies conducted in *Drosophila* have demonstrated that the *Drosophila* orthologue of EYS is a key player in the organisation of the open rhabdom system in the *Drosophila* ommatidium, where it interacts with prominin during the biogenesis of the inter-rhabdomeral space formation (Zelhof *et al.*, 2006). Furthermore, in the *Drosophila* mechanosensory neurons, EYS has been shown to provide protection from environmental stress by stiffening the cell membrane (Cook *et al.*, 2008).

Taken together data from the previous studies, it can be hypothesised that EYS is likely to be a structural protein which is necessary for stability of human photoreceptors and that it may be involved in morphogenesis of the photoreceptor outer segments via the interaction with Prominin-1.

The approach undertaken in this study will be to identify and characterise novel retinal interacting partners of EYS, which will be achieved by performing Yeast 2-hybrid screening against a human retinal cDNA library. This will be followed by in-depth analysis and validation of the identified interactions. Moreover, the putative interaction of EYS and Prominin-1 will be investigated in detail to verify whether it may be conserved in humans. Since mutations in human *PROM1* have been shown to be causative of retinal dystrophies, a cohort of 96 unrelated arRP patients will also be screened for novel mutations. Identified mutations may be used in the part of the project devoted to investigation of potential interaction of EYS and Prominin-1.

Chapter 2: Materials and Methods

2.1 General Methods

2.1.1 DNA Techniques

2.1.1.1 Polymerase Chain Reaction (PCR)

PCRs were carried out at several stages of the project, using two different polymerases depending on the purpose: Mango*Taq* DNA Polymerase (Bioline, UK) and KOD polymerase (Toyobo Novagen, Japan). Optimal annealing temperatures were established for each primer pair using control DNA. A negative control including no DNA template was included in every run to check for contamination of reagents. Conditions of reaction were polymerase specific and are summarised in Table 2.1.

Unless otherwise stated, PCR primers were designed using the relevant reference sequences, avoiding areas of high GC content and repeats. Primers were designed to be 18-28 nucleotides in length, with GC content between 50-60 %. Temperatures of annealing (Tm) were desired to be within a range of 50-65 ˚C. Specific primers used in the study will be described in the following, corresponding subsections.

2.1.1.2 Agarose Gel Electrophoresis

DNA molecules were separated on 1 % agarose gels for the purpose of visualisation, quantification or for subsequent gel extraction. Agarose gel was prepared by dissolving agarose powder in TAE buffer, to which GelRed Nucleic Acid Gel Stain (10 000X) was added. The solution was poured onto a sealed casting plate with a comb and allowed to set. Samples (0.5 – 5.0 µl) were loaded on the gel and run at 80-150 V until desired separation was achieved. For PCR products amplified with KOD polymerase, 1X DNA loading dye (Bioline, UK) was added for visualisation. For fragments amplified with Mango*Taq* it was not necessary since

the reaction buffer is pre-stained. Separated DNA was visualised on a UV transilluminator (UVP).

Reagent	Mango*Taq*	KOD
Mango*Taq* Reaction buffer	3 µl	-
KOD polymerase buffer	-	2.5 µl
50 mM $MgCl_2$	0.45 µl	
25 mM $MgSO_4$	-	1.5 µl (2.5 µl for baits 7 and full length)
100 mM dNTP Mix	0.15 µl	2.5 µl (5 µl for baits 7 and full length)
Template DNA	1 µl	1 µl
10 mM forward primer	0.4 µl	0.75 µl
10 mM reverse primer	0.4 µl	0.75 µl
Mango*Taq* Polymerase	0.1 µl	-
KOD polymerase	-	0.5µl
DMSO	-	2.5 µl (used where required)
Water (ddH_2O)	9.5 µl	15.5 µl (9.5 µl for baits 7 and full length)
TOTAL VOLUME	**15 µl**	**25 µl**
Step	**Mango*Taq***	**KOD**
Initial denaturation	96 ˚C, 5'	95 ˚C, 2'
Number of cycles	35	35
Denaturation	96 ˚C, 30''	95 ˚C, 20''
Annealing	as optimized, 30''	as optimized, 10''
Elongation	72 ˚C, 30''	70 ˚C, 25'' per 1 kb
Final elongation	72 ˚C, 5'	70 ˚C, 60'' per 1 kb
Final hold	4 ˚C,∞	4 ˚C,∞

Table 2.1 The summary of PCR conditions used throughout the project.

2.1.1.3 DNA Purification

Three different methods were used to purify DNA, depending on the purpose of further experiments:

1. For the purpose of sequencing: The ExoSAP-IT reagent (Affymetrix, USA) was used to remove excess dNTPs and primers that were not consumed in PCRs. The Exo-SAP-IT reagent includes two hydrolytic enzymes, Exonuclease I and Shrimp Alkaline Phosphatase. The Exonuclase I degrades residual primers and any other single-stranded DNA produced by PCR. The

Shrimp Alkaline Phosphatase hydrolyses dNTPs unused in the reaction that could interfere with the sequencing reaction. The clean-up reaction was optimized according to manufacturer's recommendations and comprised of 1-2 µl of PCR product, 0.5 µl of ExoSAP-IT and double-distilled water (ddH_20) added to a final volume of 15 µl. Reactions were carried out for 15 minutes at 37 °C and were followed by a 15 minute incubation period at 80 °C to inactivate both enzymes.

2. For the purpose of cloning and from agarose gel: PCR fragments were cleaned using the Wizard®SV Gel and PCR Clean-Up System (Promega, UK). A slice of excised gel containing DNA was placed in a 1.5 ml microcentrifuge tube and the Membrane Binding Solution was added (10 µl per 10 mg of gel). Tube was vortexed and incubated at 50-65 ˚C until the gel slice was completely dissolved. For PCR product processing, an equal volume of the Membrane Binding Solution was added to the reaction volume and mixed gently. Dissolved gel mixture or prepared PCR product were placed onto the Minicolumn assembly, incubated for 1 minute and centrifuged at 14 000 rpm for 1 minute. The collection tube was emptied and 700 µl of Membrane Wash Solution, previously diluted with absolute ethanol, was added onto the membrane. This step was followed by centrifugation at 14 000 rpm for 1 minute. The flow-through was discarded and the membrane was washed using 500 µl of Membrane Wash Solution. The column assembly was centrifuged at 14 000 rpm for 5 minutes and afterwards, the flow-through was discarded and the column was re-centrifuged for 1 minute with the microcentrifuge lid open to allow evaporation of residual ethanol. The column was later transferred to a clean 1.5 ml microcentrifuge tube. For elution of DNA, 50 µl of ultra-pure water was dropped on the membrane and allowed to stand at room temperature for 1 minute. This step was followed by final centrifugation at 14 000 rpm for 1 minute. The column was discarded and eluted DNA stored at 4 ˚C or at -20 ˚C (long term storage).

3. From *Escherichia coli*: A single colony of transformed *E.coli* was grown overnight at 37 ˚C in 5 ml of LB medium supplemented with the relevant

antibiotic for selection. Plasmid DNA was extracted from bacterial cells using the PureYield™ Plasmid Miniprep System (Promega, UK). Overnight bacterial culture (600 µl) was transferred to a 1.5 ml microcentrifuge and lysed by inverting with 100 µl of Cell Lysis Buffer. Cold Neutralisation Solution (350 µl) was then added to the tube and mixed thoroughly by invertion. This step was followed by centrifugation at 14 000 rpm for 3 minutes. Supernatant was transferred onto a PureYield™ Minicolumn, caring not to disturb the cell debris pellet. The Minicolumn was then placed on a collection tube and centrifuged at 14 000 rpm for 15 seconds. The flow-through was discarded and 200 µl of Endotoxin Removal Wash (ERB) was added to the assembly and then centrifuged at 14 000 rpm for 15 seconds. After removing the flow-through, 400 µl of Wash Buffer was added and the column was again centrifuged at 14 000 rpm for 30 seconds. The washed column was subsequently placed in the fresh 1.5 ml microcentrifuge tube and eluted using 30 µl of ultra-pure water. The column was allowed to stand at room temperature for 1 minute. This step was followed by final centrifugation at 14 000 rpm for 15 seconds to elute plasmid DNA. Concentration of obtained samples was checked on the spectrophotometer (NanoDrop) and they were stored at 4 ˚C or at -20 ˚C (long term storage). Plasmid DNA isolated with this method was used directly for sequencing and cloning.

4. From *Saccharomyces cerevisiae*

Plasmid DNA was isolated from yeast cells using Easy Yeast Plasmid Isolation Kit (Clontech, USA). To isolate plasmid DNA from yeast cells, it is first necessary to disrupt the cell wall, which is achieved by enzymatic treatment using Zymolyase (component of the kit). Fresh patches of transformed yeast (approximately 1 cm x 1 cm) were prepared each time prior to plasmid isolation and colonies no older than 3 days were used. Half of the patch was collected using a sterile inoculation loop and re-suspended in a 1.5 ml microcentrifuge tube containing 500 µl of the supplied 10 mM EDTA. The cells were then pelleted by centrifugation at 14 000 rpm for 1 minute and the supernatant was removed. The cell pellets were carefully re-suspended in 200 µl of ZYM buffer and 20 µl of the Zymolyase were

added. Samples were mixed by inverting the tubes 2-3 times to ensure a uniform suspension of Zymolyase and incubated with gentle shaking at 30 ˚C for 1 hour. Afterwards, the spheroplasts were pelleted by centrifugation at 4000 rpm for 1 minute and the supernatant was discarded. To lyse the spheroplasts, the pellets were re-suspended in 250 µl of Y1 Buffer/RNase A solution. Then, 250 µl of Y2 Lysis buffer were added and the tubes were gently mixed by inverting 6-8 times and incubated at room temperature for the maximum of 5 minutes. Following this, 300 µl of Y3 Neutralisation buffer were added and the solution was again mixed gently by inverting the tubes 6-8 times. This step was followed by centrifugation at 14 000 rpm for 5 minutes at room temperature. The supernatant was transferred to a fresh tube and the centrifugation was repeated. A Yeast Plasmid Spin Column was placed inside a 2 ml collection tube and the supernatant obtained in the previous step was loaded. The columns were centrifuged at 14 000 rpm for 1 minute and the flow-through was discarded. Then 450 µl of Y4 Wash Buffer were added and the columns were centrifuged at 14 000 rpm for 3 minutes. The flow-through was removed and the centrifugation step was repeated to completely remove any residual Wash Buffer. To elute plasmid DNA, the columns were placed inside sterile 1.5 ml microcentrifuge tubes and 50 µl of YE Elution Buffer was applied to the columns. This step was followed by 1 minute incubation at room temperature. The final centrifugation was carried out at 14 000 rpm for 1 minute and the concentration of eluted plasmid DNA was assessed using the NanoDrop. Samples were stored at 4 ˚C.

2.1.1.4 DNA Sequencing

DNA sequencing was performed using a BigDye™ Terminator v3.1 Cycle Sequencing Kit (Applied Biosystems, UK) and ABI PRISM® 3100 Genetic Analyzer. DNA samples (5-20 ng) were mixed with 1X BigDye™ v3.1 Cycle ready mix (containing ddNTPs, dNTPs, Amplitaq® DNA polymerase, pyrophosphatase and $MgCl_2$), 1X BigDye™ Sequencing Buffer, primer and dH_2O. The reaction mix and temperature cycling profile are summarised in Table 2.2.

In case of exon 25 of *PROM1*, which is flanked by poly-T tracks, it was necessary to supplement the reaction mix with a Hairpin DNA & GC Rich Sequencing Premix For BigDye™ 3.1. The reaction mix used is summarised in Table 2.3.

Reagent	Volume
BigDye ready mix	0.5 µl
Sequencing buffer	2.5 µl
Primer	0.5 µl
Template DNA	1-5 µl
dH_20	11.5-15.5 µl
Total volume	20µl
Step	**Conditions**
Initial denaturation	96 ˚C, 3'
Number of cycles	25
Denaturation	96 ˚C, 30''
Annealing	50 ˚C, 30''
Elongation	60 ˚C, 4'
Final hold	4 ˚C,∞

Table 2.2 Sequencing reaction mix and temperature cycling profile.

Reagent	Volume
BigDye ready mix	0.5 µl
Hairpin DNA Sequencing Premix	4 µl
Primer	0.5 µl
Template DNA	1-5 µl
dH_20	up to 10 µl
Total volume	**10 µl**

Table 2.3 Sequencing reaction for GC rich regions of DNA.

Sequencing reactions were purified using Sephadex® G-50 powder (Sigma-Aldrich, UK). Samples were transferred to the pre-washed Sephadex® G-50 Plate and cleaned by centrifugation of the plate at 910 rpm for 5 minutes; the cleaned PCR product was eluted into a clean 96-well plate, leaving any impurities in the Sephadex® gel.

2.1.1.5 Cloning

Cloning was performed at several stages of the project and two cloning system were utilised. First was based in ligation of the DNA fragments and the second was based on a recombination reaction between the compatible DNA sequences (Gateway system).

Cloning via Ligation

PCR products were prepared using primers containing a desired restriction site. The PCR products were purified using Wizard®SV Gel and PCR Clean-Up System (Promega, UK). Next, restriction enzyme digests were performed on the amplified insert and the desired vector, using approximately 1-5 µg of DNA per digest. The reactions were set using 1-2 units of a restriction enzyme, 1X of a corresponding restriction buffer and sterile water added to the total volume of 40 µl. The reactions were then incubated at a temperature indicated by the manufacturer of an enzyme for at least one hour per enzyme.

PCR insert fragments were cloned into the linearized vectors using the LigaFast Rapid DNA Ligation System (Promega, UK), according to the manufacturer's instructions. The recommended ratio of vector:insert was 1:2 and each reaction contained 3 units of T4 DNA Ligase, 2X Rapid Ligation Buffer and sterile water in the final volume of 10 µl. The reaction mix was incubated at room temperature for 2 hours and transformed into competent bacterial cells.

Gateway Cloning

The Gateway® Cloning Technology (Invitrogen, UK) is based on the bacteriophage-lambda site specific recombination system, which facilitates integration of the phage into *Escherichia coli* chromosome and switch between the lytic and lysogenic pathways. Lambda recombination occurs between site-specific attachment sites (*att*) (*att*B on *E.coli* chromosome and *att*P on the lambda chromosome) which serve as binding sites for recombination proteins. Upon integration, recombination occurs between *att*B and *att*P sites to give rise to *att*L and *att*R sites. The lysogenic pathway is catalysed by the bacteriophage λ Integrase (Int) and *E. coli* Integration Host Factor (IHF) proteins (in Gateway: BP Clonase™

enzyme mix catalysing BP reaction). The lytic pathway is catalysed by the bacteriophage λ Int and Excisionase (Xis) proteins, and the *E. coli* Integration Host Factor (IHF) protein (in Gateway: LR Clonase™ enzyme mix catalysing LR reaction).

In Gateway Technology, wild-type λ *att* recombination sites were modified to improve the efficiency and specificity of recombination reactions. Importantly, BP and LR reactions are conservative which means there is no gain or loss of nucleotides. It is also of prominent advantage that recombination can occur between DNAs of any topology (i.e. supercoiled, linear or relaxed), however the efficiency may vary. Schematic view of BP and LR reactions is depicted in Figure 2.1 and the recombination reactions are described as follows:

• **BP Reaction:** Facilitates recombination of an *att*B substrate (*att*B-PCR product or a linearized *att*B expression clone) with an *att*P substrate (donor vector) to create an *att*L-containing entry clone. This reaction is catalysed by BP Clonase™ enzyme mix.

• **LR Reaction:** Facilitates recombination of an *att*L substrate (entry clone) with an *att*R substrate (destination vector) to create an *att*B-containing expression clone. This reaction is catalysed by LR Clonase™ enzyme mix.

Presence of the *ccd*B gene in Gateway® vectors allows negative selection after transformation into *E.coli*. The CcdB protein interferes with *E.coli* gyrase and by that it inhibits growth of transformed bacteria. However, when recombination occurs, the *ccd*B gene is replaced by the gene of interest. Cells which take in non-recombined vectors carrying the *ccd*B gene or by-product molecules retaining the *ccd*B gene, will fail to grow.

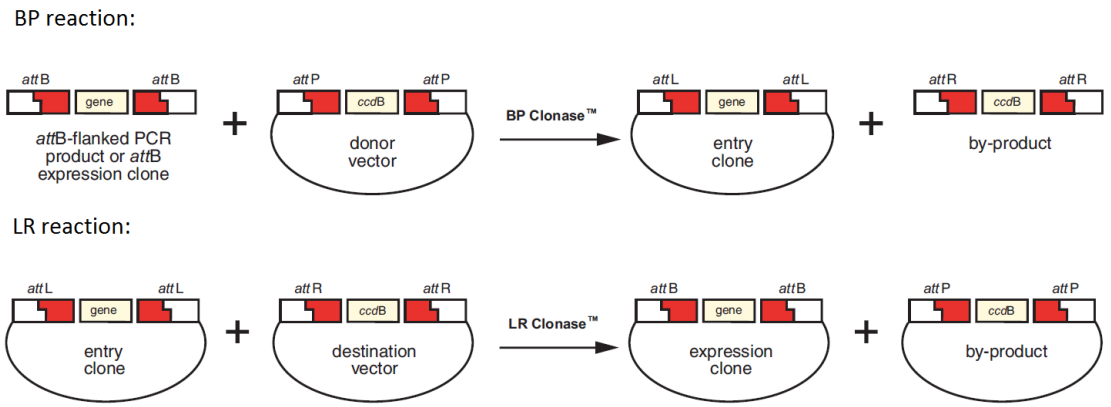

Figure 2.1 Schematic view of BP and LR recombination reactions (Image adapted from The Gateway® Technology Manual, 2010).

For the purpose of cloning, PCR fragments flanked by *att*B sites were generated by the use of *att*B primers and amplification with KOD polymerase. *Att*B-*PCR* products were purified using the Wizard®SV Gel and PCR Clean-Up System (Promega, UK). The purified PCRs were subsequently used for the BP reaction with pDONR-Zeo vector to generate the entry clones. The reaction mix is shown in Table 2.4. BP reaction mix was incubated at 25 ˚C for 1 hour and afterwards, terminated by addition of 1 µl proteinase K and incubation at 37 ˚C for 10 minutes. The reaction mix was then used for transformation of competent *E.coli*, strain DH5α (section 3.3.3). Transformed bacteria were plated on LB agar media supplemented with zeocin (40 µg/ml).

Reagent	Amount
*att*B-PCR	75 ng
pDONR-Zeo vecor	75 ng
BP Clonase™ mix II	1 µl
TE buffer (pH 8)	up to 5 µl

Table 2.4 BP recombination reaction mix.

Isolated and sequenced entry clones were subsequently used for the LR reaction with the relevant destination vectors to generate expression clones. The reaction mix is summarized in Table 2.5 and the reaction conditions were exactly the same as the BP reaction.

Ragent	Amount
pDONR-zeo/'bait'	75 ng
Destination vector	75 ng
LR Clonase™ mix II	1 µl
TE buffer (pH 8)	up to 5 µl

Table 2.5 LR recombination reaction mix.

2.1.1.6 Bacterial Transformation

In the project, two strains of competent *E.coli* cells were used: DH5α (Invitrogen, UK) and JM109 (Promega, UK) and the transformation was performed using an identical protocol.

The competent cells were thawed on ice and aliquoted (50-150 µl per transformation) into pre-chilled 1.5 ml microcentrifuge tubes. A range of 1-10 ng of plasmid DNA was used per transformation. DNA was added to the competent cells, gently mixed and incubated on ice for 30 minutes. Afterwards, samples were incubated at 42 ˚C for 45 seconds (heat-shock) and then immediately cooled on ice for 2 minutes. Cells were subsequently mixed with 900 µl of SOC medium (Invitrogen, UK) and incubated at 37 ˚C for an hour with shaking at 225 rpm. This step was followed by centrifugation at 10 000 rpm for 3 minutes. Supernatant was removed and the cell pellet was re-suspended in 100-200 µl of the LB medium. Transformed bacteria were spread on LB agar plates supplemented with the relevant antibiotic and incubated at 37 ˚C for 18-20 hours. On the next day, single colonies were picked and grown in LB-broth supplemented with the relevant antibiotic for 18-20 hours at 37 °C with shaking at 225 rpm. For long term storage, 30 % glycerol stocks were prepared and if needed, the plasmid DNA was isolated and subjected to further analysis. The antibiotics used in the project are summarised in Table 2.6.

Antibiotic	Final Concentration
Ampicilin (Amp)	100 µg/ml
Chloramphenicol (Cam)	170 µg/ml
Kanamycin (Kan)	100 µg/ml
Zeocin (Zeo)	40 µg/ml

Table 2.6 Summary of antibiotics used in the study.

2.1.2 RNA Techniques

2.1.2.1 Isolation of RNA from Cell Lines

In the project, RNA was isolated from mammalian cell lines using PureLink RNA Mini Kit (Life Technologies, UK) and the manufacturer's protocol was followed. The RNA extrication was carried out at the room temperature in an area cleaned with RNase removing detergents and RNase free tubes and pipette tips were used. Fresh amount of Lysis Buffer was prepared by adding 1 % 2-mercaptoethanol before each purification procedure.

For each of the isolations, $1x10^7$ cells were used and the cells were prepared depending on whether they grow in suspension or as a monolayer. In case of suspension cells, the relevant volume of the culture was transferred to an RNase free tube and centrifuged at 350 rpm for 10 minutes at 4 ˚C. The supernatant was discarded and the cells were rinsed with sterile PBS and centrifuged again at 350 rpm for 10 minutes at 4 ˚C. The PBS wash was repeated once. Following the last wash, the cell pellet was re-suspended in 1.2 ml of Lysis Buffer containing 2-mercaptoethanol.

For the monolayer of cells, the culture dishes were washed twice with PBS and the Lysis Buffer containing 2-mercaptoethanol was added. The cells were scraped off the culture dish and transferred to a 1.5 ml tube.

The tubes were then vortexed at high speed until the cell pellet was completely dispersed. The lysate was passed 5-10 times through an 18-gauge needle attached to a 2 ml syringe. Next, one volume of 70 % ethanol was added to each volume of cell homogenates. The tubes were vortexed thoroughly until any visible precipitate was dispersed. Then, the spin cartridge was assembled by placing the spin column in a collection tube and 700 µl of the sample were transferred to the spin column. The cartridges were then centrifuged at 14 000 rpm for 15 seconds at room temperature and the flow-through was removed. The two last steps were repeated until the entire sample was processed. Afterwards, 700 µl of Wash Buffer I was added to each of the columns which were then centrifuged at 14 000 rpm for 15 seconds at room temperature. The flow-through was discarded and the spin columns were placed into new collection tubes. The next wash was performed with 500 µl of Wash Buffer II and the

cartridges were centrifuged at 14 000 rpm for 15 seconds at room temperature. The wash with Wash Buffer II was repeated once. The flow-through was discarded after each wash and then, the cartridge was centrifuged at 14 000 rpm for 2 minutes at room temperature to dry the membrane with attached RNA. Following this, the collection tube was discarded and the column was placed into a fresh RNase free 1.5 ml tube. To elute RNA, 50 µl of RNase free water were added to the centre of the membrane and the column was incubated for 1 minute at room temperature and then centrifuged at 14 000 rpm for 15 seconds at room temperature. The eluted RNA was stored at -80 ˚C.

2.1.2.2 cDNA Synthesis via Reverse Transcription PCR (RT-PCR)

cDNA was synthesised using RNA isolated from cell lines available in the laboratory as well as a commercially available panel of RNA samples isolated from human tissues (Clontech, USA). In the project, QuantiTect Reverse Transcription Kit (Qiagen, The Netherlands) was used and the manufacturer's protocol was followed.

The first step was to purify the RNA samples by setting up a genomic DNA elimination reaction with gDNA Wipe-out Buffer. The reaction mix is summarised in Table 2.7. The samples were incubated for 2 minutes at 42 ˚C and then immediately placed on ice.

In the next step, the reverse transcription reaction was set up following the recipe shown in Table 2.8. The RNA template was added as the last component and the samples were incubated for 15 minutes at 42 ˚C. To inactivate the Quantiscript Reverse Transcriptase, the samples were incubated for 3 minutes at 90 ˚C. The samples were immediately used for further experiments or stored at -20 ˚C.

Component	Volume
gDNA Wipeout Buffer, 7X	2 µl
Template RNA, 1 µg	variable
RNase free water	variable
TOTAL	**14 µl**

Table 2.7 Summary of a genomic DNA elimination reaction mix.

Component	Volume
Quantiscript Reverse Transcriptase	1 µl
Quantiscript RT Buffer, 5X	4 µl
RT Primer Mix	1 µl
Template RNA (entire gDNA elimination reaction)	14 µl
TOTAL	**20 µl**

Table 2.8 Summary of components of reverse-transcription reaction.

2.1.3 Protein Techniques

2.1.3.1 Preparation of Protein Extracts from Mammalian Cells

Protein extracts were prepared from both suspension and monolayer cell lines. In the project, proteins were extracted on many occasions from both transfected and wild type cell lines. The optimised extraction protocol was uniform for all of the applications except the initial stages.

In case of suspension cell lines, the relevant volume of the culture was transferred to the test tube and centrifuged at 350 rpm for 10 minutes at room temperature. The supernatant was aspirated and the cell pellet was re-suspended in sterile PBS and centrifuged again at 350 rpm for 10 minutes at room temperature. The supernatant was discarded and the pelleted cells were re-suspended in the cell lysis buffer.

For cells growing as a monolayer, the culture media was aspirated and the cells were rinsed twice with sterile PBS. The cells were then scraped off the dish in PBS and transferred to a test tube. The tubes were centrifuged at 1000 rpm for 10 minutes at 4 ˚C, the supernatant was discarded and the pellet was re-suspended in the cell lysis buffer.

Prior to each extraction, the cell lysis buffer was supplemented with the mixture of protease inhibitors (ProeaseArrest 100X, Gbiosciences, USA) and 1 ml of the lysis buffer was used for approximately $5x10^7$ of cells. The tubes were placed on a tube rotator and mixed at 4 ˚C for 30 minutes. The homogenates were then passed through a 21-gauge needle attached to a 2 ml syringe and centrifuged at 14000 rpm for 15 minutes at 4 ˚C. The supernatants containing the total protein extracts were collected and subjected to further analysis or stored at -80 ˚C.

2.1.3.2 Preparation of Protein Extracts from Yeast Cells

Preparation of yeast culture for protein extraction

Protein extracts were prepared from liquid yeast cultures. Transformed yeast strains were cultured in appropriate liquid SDO selective media to keep selective pressure on the plasmid, whereas untransformed yeast strains were cultured in liquid YPDA medium. The growth rates differ between yeast strains and they may be affected by the presence of fusion proteins in certain transformants. Generally, the doubling time of most strains growing in SDO media is twice as long as in YPDA. In order to prepare a culture of a desired yeast strain, 1 colony (not older than 4 days) was inoculated in 5 ml of relevant media and incubated overnight at 30 ˚C with shaking (220-250 rpm). The next day, the cultures were centrifuged at 1200 rpm for 5 minutes and the media was removed. The pellets were re-suspended in 10 ml of YPDA and incubated for 3-5 hours at 30 ˚C with shaking (220-250 rpm) to obtain the mid-log phase cultures (OD600=0.4-0.6). Next, the cultures were pelleted at 1200 rpm for 5 minutes at 4 ˚C and the supernatants were discarded. The pellets were washed twice with ice-cold water, centrifuged as before and frozen at -70 ˚C or kept on ice if extractions were to be performed immediately after.

SDS/Urea Method

Complete cracking buffer was prepared just prior to protein extraction and pre-warmed to 60 ˚C; 100 µl of cracking buffer was used per 7.5 OD_{600} ($6x10^8$ cells/ml) of yeast cells. Previously prepared cell pellets were thawed by re-suspending in warm cracking buffer. The initial excess of PMSF in the cracking buffer degrades quickly and therefore, an additional aliquot (4.5 µl per 7.5 OD_{600} of cells) was added after 15 minutes and approximately every 7 minutes thereafter until the process was complete and extracts were ready to be frozen. Cell suspensions were transferred to 1.5 ml microcentrifuge tubes, containing 80 µl glass beads (425-600 µm) per 7.5 OD_{600} of yeast cells and incubated at 70 ˚C for 10 minutes. After incubation, samples were vigorously vortexed for 1 minute and centrifuged at 14 000 rpm for 5 minutes at 4 ˚C. The supernatant was transferred

to a fresh 1.5 ml microcentrifuge tube and placed on ice (first supernatant). Pellets were then boiled in a water bath for 5 minutes, vortexed vigorously for 1 minute and centrifuged at 14 000 rpm for 5 minutes at 4 ˚C. The second supernatant was combined with the first one. Prepared samples were subsequently briefly boiled and immediately used for SDS-PAGE or, frozen on dry ice and stored at -80 ˚C.

TCA Method

TCA buffer and TCA-Laemmli loading buffer were prepared just prior to use. Cell pellets were thawed on ice for 10-20 minutes, re-suspended in ice-cold TCA buffer (100 µl per 7.5 OD_{600} of yeast cells) and placed on ice. Cell suspensions were transferred to fresh 1.5 ml microcentrifuge tubes containing glass beads (425-600 µm) and ice-cold 20 % TCA buffer. A mixture of 100 µl of glass beads and 100 µl of ice-cold 20 % TCA buffer were used per 7.5 OD_{600} of yeast cells. To disrupt the cell wall, samples were vigorously vortexed for 10 minutes at 4 ˚C. Supernatant was then transferred to fresh 1.5 ml microcentrifuge tubes (first supernatant) and placed on ice. Afterwards, glass beads were washed with 500 µl of an ice-cold 1:1 mixture of 20 % TCA and TCA buffer and vortexed at 4 ˚C for 5 minutes. Any liquid from above the glass beads (second supernatant) was combined with the first supernatant. Tubes were kept on ice to allow any carry-over glass beads to settle and then supernatants were transferred to fresh 1.5 ml microcentrifuge tubes. Proteins were pelleted by centrifugation at 14 000 rpm for 10 minutes at 4 ˚C. Supernatants were discarded and pellets re-suspended in TCA-Laemmli buffer (10 µl of buffer per 1 OD_{600} of cells). Tubes were subsequently placed in a water bath at 100 ˚C for 10 minutes. After boiling, samples were centrifuged at 14 000 rpm for 10 minutes at room temperature. Supernatants were collected in 1.5 ml microcentrifuge tubes and immediately used for SDS-PAGE or frozen on dry-ice and stored at -80 ˚C.

Y-PER Plus Based Method

Y-Per Plus reagent (Thermo Scientific, USA) uses a mild detergent formulation for protein extraction and the procedure is carried out at room temperature. Prior to extraction, a desired volume of Y-Per was supplemented with DTT to final concentration of 0.1 M and 100X ProteaseArrest mix (G-Biosciences, USA). Pellets of yeast cells were weighed and 2.5 ml of the lysis buffer were used per 1 g of cell paste. The pellets were re-suspended in the buffer until the mixture was homogenous. The samples were then placed on a rotary shaker for 20 minutes at room temperature. Afterwards cell debris were collected by centrifugation at 14 000 rpm for 5 minutes and the supernatant were subjected to further analysis.

2.1.3.3 Bicinchoninic acid assay (BCA assay)

The concentration of protein in total cell lysates was assessed by performing BCA assay after each extraction. The BCA assay is based on a biuret reaction, in which bivalent copper ions are reduced to monovalent ions in the presence of protein in an alkaline solution. The monovalent copper ions chelate with bicinchoninic acid, a chromogenic reagent, producing a purple complex with strong absorbance at 562 nm (Smith *et al.*, 1985).

In the project, the BCA Protein Assay Kit (Novagen, UK) was used and the manufacturer's protocol was followed. The standards were prepared using BSA stock solution at 2 mg/ml and the cell lysis buffer. The concentration was measured using a Nanodrop spectrophotometer and a pre-set BCA programme.

2.1.3.4 Sodium Dodecyl Sulfate Polyacrylamide Gel Electrophoresis (SDS-PAGE)

Proteins were separated using sodium dodecyl sulfate polyacrylamide gel electrophoresis (SDS-PAGE) with a discontinuous, 1X TRIS–glycine–SDS buffered system. In this study, gels of various percentages were used depending on the size of the protein of interest (Table 2.9) and recipe for resolving gels of various

percentages are summarised in Table 2.10. The stacking gel had a common composition for every SDS-PAGE run and the recipe is summarised in Table 2.11. Alternatively, ready-made Mini-PROTEAN TGX Precast Gels (BioRad, USA) were used. Before loading, 6X Laemmli buffer (Alfa Aesar, UK) was added to each sample, which were then incubated at 70-100 ˚C for 5-10 minutes, depending on the experiment. Typically, 20-30 µg of a total protein extract was loaded to each well. Precision Plus Protein Dual Standards (BioRad, UK) and Hi-Mark Pre-Stained High Molecular Weight Protein Standard (Life Technologies, UK) were used as markers for protein band size estimation. Gels were subject to electrophoresis until suitable separation of the marker was achieved, typically at 100 V, 3 A, 30 W.

Protein Size	Percentage
Over 100 kDa	~7 %
50-100 kDa	~10 %
20-50 kDa	~12 %
<20 kDa	~15 %

Table 2.9 Percentage of the resolving polyacrylamide resolving gels.

Ingredient	5 %	7.50 %	10 %	12 %	15 %	17.50 %
dH_20	8.5 ml	7.25 ml	6 ml	5 ml	3.5 ml	2.25 ml
30 % acrylamide	2.5 ml	3.75 ml	5 ml	6 ml	7.5 ml	8.75 ml
1.5 M Tris, pH 8.8	3.75 ml	3.75 ml	3.75 ml	3.75 ml	3.75 ml	3.75 ml
10 % (w/v) SDS	150 µl	150 µl	150 µl	150 µl	150 µl	150 µl
10 % (w/v) APS	100 µl	100 µl	100 µl	100 µl	100 µl	100 µl
TEMED	25 µl	25 µl	25 µl	25 µl	25 µl	25 µl

Table 2.10 Composition of the resolving polyacrylamide gels.

Ingredient	Volume
H_20	3 ml
30 % acrylamide	625 µl
0.5M Tris, pH 6.8	1.25 ml
10 % (w/v) SDS	50 µl
10 % (w/v) APS	30 µl
TEMED	10 µl

Table 2.11 Composition of a polyacrylamide stacking gel.

2.1.3.5 Immunoblotting (Western blotting)

Separated proteins were transferred on to nitrocellulose membrane (45 µm, BioRad) using two methods, depending on size of the protein. Typically, a semi-dry transfer was used; however, for the purpose of transferring EYS isoform 1 (350 kDa) wet transferred was preferred. Semi-dry transfer was performed using a BioRad Trans-Blot Turbo system. The process was carried out at 25 V, 1 A for 30 minutes. Wet transfer was carried out in a Mini Trans-Blot Electrophoretic Transfer Cell (BioRad, USA) at 100 V, 0.35 A for 2 hours. When Mini-PROTEAN TGX Precast Gels were used, transfer was performed using Trans-Blot Turbo Mini PVDF Transfer Packs and the Trans-Blot Turbo system; pre-set programmes were used depending on the protein size.

To check whether proteins were transferred onto the membrane, Ponceau Red staining was performed using the ready-made Ponceau Red solution (Sigma, USA). The membrane was submerged in the solution for 5 minutes to visualise protein bands and then, the membrane was rinsed with TBS-T solution until the stain was completely removed. Blocking of the membrane was carried out using 5 % milk or 5 % BSA in dissolved in 1X TBS-T for 1 hour at room temperature with gentle agitation.

Immunolabelling was performed with the relevant primary antibodies at optimised dilutions, which were prepared in the blocking solution. Incubation with primary antibodies was performed overnight at 4 ˚C. Afterwards, membranes were washed 3 times 10 minutes in 1X TBS-T. HRP conjugated secondary antibodies were used, typically at 1:10000 dilutions prepared in 1X TBST-T, and the incubation was carried out for 1 hour at room temperature with gentle agitation. After the incubation, the membrane was washed 2 times 15 minutes in 1X TBS-T and then 2 times 10 minutes in 1X TBS. For the development, ECL solution (BioRad, USA) was prepared, spread on the membrane and incubated for 1 min. The visualisation was performed using the GelDoc XR+ System (BioRad, USA) and the images were processed using the Image Lab software (BioRad, USA).

2.1.4 Cell Culture Techniques

2.1.4.1 Mammalian Cell Lines

The cell lines used in the study were already available in the Bhattacharya laboratory. The cells were grown in plastic culture vessels and the incubation conditions were set to maintain the temperature at 37 ˚C, the level of CO_2 at 5 % and humidity at a minimum of 80 %.

The day-to-day maintenance of the cell cultures involved media changes and passaging the cells to maintain the desired confluence level. To detach adherent cells from the surface of the culture dishes, the media was aspirated, the cells were rinsed with sterile PBS and incubated with 1X 0.05% Trypsin-EDTA (Life Technologies, USA) for 5-10 minutes. The cultures were then split, usually at a ratio of 1:3. In case of suspension cells, the culture was transferred to a suitable size tube and centrifuged at 350 rpm for 10 minutes at room temperature. The supernatant was discarded, the cell pellet re-suspended in sterile PBS and the centrifugation step repeated. The cell pellet was suspended in the fresh volume of media and incubated as usually.

The cell stocks were prepared by collecting approximately $1x10^6$ cells and suspending them in 1 ml of the Recovery Cell Culture Freezing Medium (Life Technologies, USA). The mammalian cell stocks were kept at -80 ˚C.

<u>Y79 cell line</u>

Y79 cell line is a suspension cell line derived from human retinoblastoma. The cell line was maintained in RPMI 1640 medium (Life Technologies, USA) supplemented with 20 % FCS and 1 % penicillin/streptomycin antibiotic mixture.

<u>HeLa cell line</u>

HeLa cell line grows as an adherent monolayer and was derived from a human epitheloid cervix carcinoma. The cells were cultured in DMEM medium (Life Technologies, USA) supplemented with 10 % FCS and 1 % penicillin/streptomycin antibiotic mixture.

SK-N-SH cell line

SK-N-SH cell line was derived from human neuroblastoma and the cells grow as a monolayer. The cells were cultured in DMEM-F12 medium (Life Technologies, USA) supplemented with 10 % FCS and 1 % penicillin/streptomycin antibiotic mixture.

ARPE-19 cell line

ARPE-19 is a human retinal pigment epithelial cell line derived from a healthy tissue. The cells grow as a monolayer and were cultured in DMEM-F12 medium (Life Technologies, USA) supplemented with 10 % FCS and 1 % penicillin/streptomycin antibiotic mixture.

2.1.4.2 Cell Counting

When required, cells were counted using a hemacytometer (Cascade Biologicals, USA), following the protocol recommended by the manufacturer. The suspension of cells was prepared and carefully pipetted to disperse any clumps to obtain a uniform suspension of single cells. Next, 1:1 dilution of the cell suspension in trypan blue was prepared and 20 µl of the mixture were used to charge the chambers. Trypan blue allows for determination of viability of cells and it is excluded from viable cells. The cells were viewed under a microscope and the cell number overlying four 1 mm^2 areas was determined. The number of cells was calculated by the following the formula according to the manufacturer's protocol:

Number of cells counted in 4 mm^2/4/dilution factor=number of cells x 10^4/ml

2.1.4.3 Transfections

Two reagents for transfecting adherent cell lines were used in the study, Lipofectamine 2000 (Life Technologies, USA) and Effectene (Qiagen, The Netherlands).

For transfection with Lipofectamine 2000, cells were plated to be 90-95 % confluent on the day of transfection and the manufacturer's protocol was followed.

Briefly, on the day of transfection the cells were rinsed twice with sterile PBS and the culture media was changed to DMEM supplemented with 10 % FCS but lacking the antibiotic mixture. The dilutions of DNA and Lipofectamine 2000 were prepared in Opti-MEM media (Life Technologies, USA) according to the manufacturer's recommendations. The dilution of Lipofectamine 2000 was incubated for 5 minutes at room temperature before being mixed with the dilution of DNA. In all experiments, the ratio of DNA (μg):Lipofectamine 2000 (μl) was 1:2,5. The mixture was incubated at room temperature for 20 minutes to allow complex formation and then, it was added directly into the culture vessels. Media was changed 4 hours later to DMEM supplemented with 10 % FCS 1 % penicillin/streptomycin antibiotic mixture.

Effectene (Qiagen, The Netherlands) was used to transfect adherent cell lines with constructs carrying full sized EYS isoform 1 (9435 bp). The cells were plated to be 40-80 % confluent on the day of transfection. Prior to transfection, the media from above cells was aspirated and the cells were rinsed with sterile PBS. The volume of media added to the cells was split into two portions; one constituted 75 % and the second 25 % of the total volume. The first, 75 % portion of DMEM supplemented with 10 % FCS but lacking the antibiotic mixture was added to the cells. The desired amount of DNA was diluted in the provided TE buffer and incubated with an Enhancer for 5 minutes. Then, Effectene Transfection Reagent was added and the mixture was incubated at room temperature for 10 minutes to allow transfection complex formation. For all transfections performed with tagged EYS isoforms 1 constructs the ratio of DNA (μg):Enhancer (μl):Effectene Transfection Reagent (μl) was 1:8:25. The complex was mixed with the remainder of culture media and added directly to the culture vessel. Media was changed 4 hours later to DMEM supplemented with 10 % FCS 1 % penicillin/streptomycin antibiotic mixture.

Cell lines grown in suspension were first seeded onto to pre-treated coverslips (see section 2.1.4.4) and then transfected following the same protocol as described for adherent cell lines.

2.1.4.4 Y79 Cell Attachment and Differentiation

Since Y79 cells grow in suspension, it was necessary to optimise immobilisation protocols in order to be able to perform transfections followed by

immunocytochemistry experiments. A modified protocol for cell attachment and growth enhancement was used (Kyritsis *et al.*, 1984).

In this study, glass coverslips were coated with poly-L-lysine (Sigma, USA) at concentration 2 μg/cm^2. The glass coverslips were placed in a 24-well plate and 500 μl of poly-L-lysine were added. The plate was then incubated at 37 ˚C for 2 hours. Next, the glass coverslips were rinsed twice with sterile water and 500 μl of the cell suspension were added. Y79 cells typically grow in RPMI 1640 media; however, for the purpose of cell attachment they were suspended and seeded in complete DMEM media. More than 90 % of cells were attached to the coated glass coverslips after 2 hours post seeding.

In order to enhance the growth of Y79 cells, they were treated with dibutyryl cyclin AMP (dbcAMP) (Sigma, USA). Once the cells were attached to the coated coverslips, the media was aspirated, the cells were rinsed twice with sterile PBS and DMEM (serum and antibiotics free media) was added. dbcAMP was added to the media at the final concentration of 2 mM and was re-administered every 2 days with media changes. After 5 days of treatment the cells were fixed and immunolabelled.

2.2 Yeast 2-hybrid (Y2H)

In 1989, Fields and Song revolutionised analysis of PPIs by elaborating a genetic system to detect direct interactions between proteins in *Saccharomyces cerevisiae* (Fields & Song, 1989). They were inspired by results obtained by Keegan et al. who discovered the structure of GAL4, a transcriptional activator in yeast (Keegan *et al.*, 1986). The group demonstrated that GAL4 binds to a specific DNA sequence (UAS, upstream activation sequence) and activates transcription in the presence of galactose. Moreover, they showed that when separated into two fragments, the N-terminal fragment of GAL4 can bind to the DNA sequence but cannot activate transcription whereas the C-terminal fragment of the protein does not bind DNA but is capable of initiating transcription by recruitment of RNA polymerase II. Both fragments are, however, able to bind non-covalently to each other and reconstitute the structure of GAL4. As a result of this study, two functional domains of GAL4 were identified: an N-terminal DNA binding domain (GAL4 DBD) and C-terminal activation domain (GAL4 AD) (Keegan *et al.*, 1986)

(Figure 2.2 A). Fields and Song exploited these findings to create a system monitoring PPIs. The basic idea of the system was to fuse the bait protein to the GAL4 DNA BD and the prey protein to the GAL4 AD. Expression of both fusion proteins in yeast and interaction between them brings the GAL4 DBD and GAL4 AD domains in proximity and activates transcription of a reporter gene, e.g. *GAL1-LacZ.* This gene encodes the enzyme β-galactosidase which labels yeast cells when using a colorimetric substrate (Fields & Song, 1989) (Figure 2.2 B, C).

Y2H has become a popular tool for investigating PPIs due its cost-effectiveness, simplicity and suitability for high-throughput screening of cDNA libraries. It not only allows for identification of new binary interactions but also enables their further exploration by using protein fragments and mutated constructs of proteins of interest.

In spite of many advantages of Y2H, the method has some limitations. The main drawback of GAL4 based Y2H is that the interacting complex needs to be transported to the nucleus in order to activate transcription of the reporter genes. This makes it impossible to investigate integral membrane proteins or proteins with strong cytoplasm tropism. These issues have been addressed by creating modified Y2H system, e.g. development of split-ubiquitin Y2H systems (or membrane Y2H; MYTH) enabled detection of interacting partners of proteins bound to the cell membrane. Furthermore, Y2H is characterised by low reproducibility of the results, which was estimated to be approximately 20 %, and by a high number of false positive results. It can also happen that some bait protein fragments can be toxic to yeast cells or produce spontaneous transcription activation activity of the reporter gene. To address these issues, many control experiments preceding Y2H screening are required to ensure that a bait is suitable for the use in Y2H. Also, Y2H results always need to be subjected to validation experiments in order to provide additional evidence in their support (reviewed in Ivanov *et al.*, 2011; Ngounou Wetie *et al.*, 2014).

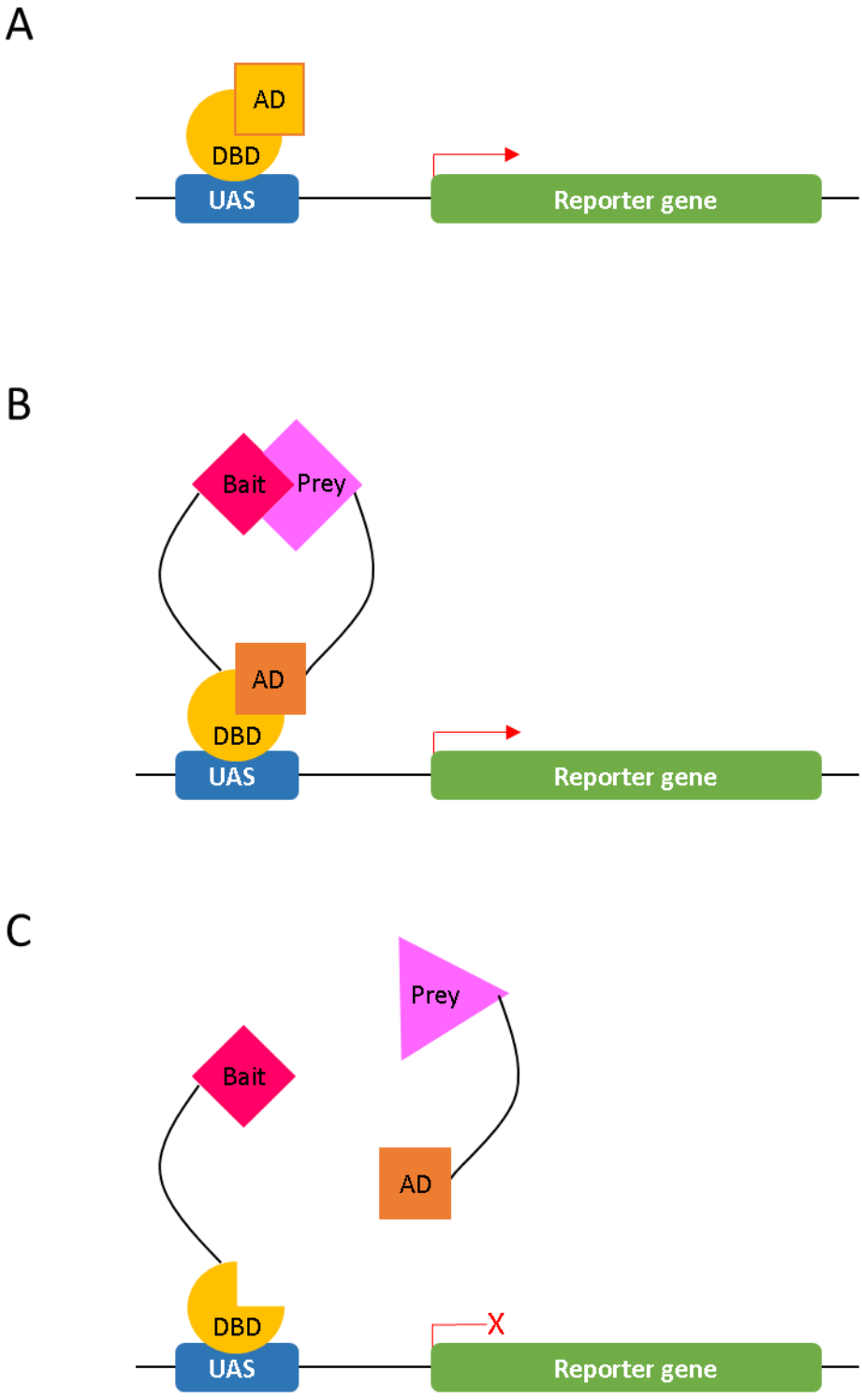

Figure 2.2 Overview of Y2H technology. Image **'A'** demonstrates the activity of GAL4 transcription activator in wild type conditions: GAL4 DBD binds to the UAS sequence and GAL4 AD initiates transcription by recruitment of RNA polymerase II. Image **'B'** illustrates events in Y2H when a bait fused to GAL4 DBD interacts with a prey fused to GAL4 AD and brings the two GAL4 moieties in proximity, thereby activating transcription of the reporter gene. Conversely, image **'C'** depicts the scenario when a bait fused to GAL4 DBD does not interact with a prey fused to GAL4 AD and the transcription is not activated. DBD – GAL4 DNA binding domain, AD – GAL4 activation domain, UAS – upstream activation sequence.

In this study, the Matchmaker Gold Yeast Two-Hybrid System (Clontech, USA) was used. This is a classic Y2H system exploiting the modular nature of the GAL4 transcription factor. Cloning of baits was performed using the Gateway cloning system (Life Technologies, USA) and the pBD-DEST vector (Stratagene, USA) was used as a destination vector, enabling expression of bait fusion proteins. The retinal cDNA library was previously constructed in the Bhattacharya laboratory, using the pGADT7-Rec vector (Clontech, USA). It was additionally confirmed that the vectors manufactured by Clontech and Stratagene are compatible and can be used together.

Yeast cells can grow as haploid organisms or they can mate and form diploid cells. Traditionally, bait and prey plasmids are co-transformed into a single yeast strain; however, it is also possible to transform them into two separate yeast strains of opposite sex type and mate them to enable the bait and prey to come together. The Matchmaker Gold Yeast Two-Hybrid System is based on the yeast mating procedure. Two strains of *Saccharomyces cerevisiae* are provided in the system: Y2HGold and Y187. Y2HGold cells are of mating type a (MATa) and are used for production of baits whereas preys are hosted in Y187 yeast strain of mating type α (MATα). Mating can occur only between yeast cells of opposite mating type and yeast strains provided by Clontech were modified so that cells are incapable of switching their sex type, as may happen in wild type strains.

When interaction between bait and prey occurs, expression of reporter genes is activated. The Y2HGold strain has four reporter genes and the Y187 strain incorporates two. The reporter genes have two main functions: firstly to distinguish transformed haploid cells, and secondly, to help identify mated diploid cells containing potential interactions. The number and/or combination of reporter genes can be used to moderate the stringency of the Y2H. Reporter genes used in the Matchmaker Gold Yeast Two-Hybrid System are summarised in Table 2.12. Promoters controlling four reporter genes in Y2HGold cells are unrelated except for the short protein binding sites in the upstream activating sequences (UAS) region that are specifically bound by GAL4 DNA BD. This means that prey proteins which can interact with sequences flanking or within UAS and cause false positive results, are screened out.

Yeast strain	Gene	Promoter	Description
Y2HGold	*AUR1-C*	M1	A dominant mutant version of the *AUR1* gene that encodes the enzyme inositol phosphoryl ceramide synthase. In *Saccharomyces cerevisiae*, its expression confers strong resistance (*AbA*^{r}) to the otherwise highly toxic drug Aureobasidin A (AbA). This drug reporter is preferable to nutritional reporters alone due to lower background activity.
Y2HGold	*MEL1*	M1	*MEL1* encodes α-galactosidase, an enzyme occurring naturally in many yeast strains. As a result of two-hybrid interactions, α-galactosidase is expressed and secreted by the yeast cells. Yeast colonies that express *MEL1* turn blue in the presence of the chromogenic substrate X-α-Gal.
Y2HGold	*HIS3*	G1	Y2HGold is unable to synthesize histidine and is therefore unable to grow on media that lack this essential amino acid. When bait and prey proteins interact, GAL4-responsive *HIS3* expression permits the cell to biosynthesize histidine and to grow on –His minimal medium.
Y2HGold	*ADE2*	G2	Y2HGold is also unable to grow on minimal media that does not contain adenine. However, when two proteins interact, *Ade2* expression is activated, allowing these cells to grow on –Ade minimal medium.
Y187	*lacZ*	G1	*LacZ* gene encodes for β-galactosidase. The presence of an active β-galactosidase is detected by X-gal, which produces a characteristic blue dye when cleaved by β-galactosidase. This reporter gene is not used in this project and may be used as an alternative to *MEL1*. The difference is that β-galactosidase is not secreted and therefore, a β-galactosidase assay needs to be performed to prove occurrence of an interaction.
Y187	*MEL1*	M1	as above

Table 2.12 Summary of reporter genes used in Matchmaker Gold Yeast Two-Hybrid System manufactured by Clontech.

2.2.1 Yeast Media

A wide range of media were used to culture yeast in this study depending on the purpose of an experiment. Wild type yeast strains were cultured in YPDA medium which contains all ingredients required for an optimal growth of *Saccharomyces cerevisiae*.

Single drop-out (SDO) media lack an amino acid which is used as a nutritional marker to select colonies that have been transformed with a vector encoding an enzyme required for the biosynthesis of the missing amino acid. Depending on the type of a vector used for transformation, SDO media lacking tryptophan or leucine were used (SDO/-Trp or SDO/-Leu respectively). Following the same principle, double drop-out (DDO) media lack two amino acids and select for yeast cells that carry two of the vectors encoding the missing nutrients (mated diploid cells or co-transformed haploid cells). Triple drop-out (TDO) and quadruple drop-out (QDO) lack three or four amino acids respectively and they additionally select for interaction between bait and prey which, if present, will activate biosynthesis of amino acids adenine and histidine. Yeast media can additionally be supplemented with X-α-Gal which is a chromogenic substrate which can be used to demonstrate α-galactosidase activity. Another supplement used in yeast media was Aureobasidin A (AbA) which is a highly toxic anti-fungal agent. Only yeast cells expressing AbA^r resistance gene are able to grow in presence AbA in the media. X-α-Gal and AbA were used as markers for detecting interaction between bait and prey.

All of the yeast media could have liquid or solid form and the latter was achieved by supplementing the media with agar. The recipes of media used in the study are summarised in section 2.9.

2.2.2 Yeast Cell Stock Maintenance

Untransformed Y2HGold and Y187 yeast strains were maintained in YPDA medium with 25 % glycerol at -80 ˚C. Additionally, both strains were maintained on solid media by re-streaking on fresh YPDA agar plates every 30 days. Transformed yeast cells were also stored as glycerol stocks at -80 ˚C in relevant selective media and on SDO agar media, being re-streaked onto fresh plates every

30 days. SDO media allow nutritional selection and were used to culture transformed yeast cells. Depending on the type of a vector used for transformation, SDO media lacking tryptophan or leucine were used (SDO/-Trp or SDO/-Leu respectively).

2.2.3 Determination of Yeast Cells Number in Liquid Culture

In order to evaluate the number of cells in liquid culture, the optical density of 1 ml of liquid culture was measured at 600 nm wavelength (OD_{600}). The result multiplied by the total volume of the culture to determine the total OD_{600}, as shown below:

$$\text{Total } OD_{600} = \text{obtained } OD_{600} \text{ x final culture volume}$$

The number of yeast cells is calculated following the below equation:

$$OD_{600} \text{ of } 1 = 8x10^7 \text{ cells/ml}$$

2.2.4 Designing Y2H Baits

Baits for Y2H screening were designed using the reference sequence of *EYS* gene, derived from Ensembl database (transcript ID: ENST00000503581). In this study, the cDNA of EYS isoform 1 was available, which comprises of 9435 bp. Altogether, nine fragments were designed, including the full length gene. Every bait spans a different part of the protein encompassing particular domains. Baits were constructed by PCR amplification of the desired fragments using KOD polymerase and primers compatible with the Gateway cloning system that are listed in Table 2.13. First the fragments were cloned into pDONR/Zeo to obtain entry clones and the expression clones were obtained by subsequent cloning into pBD-DEST vectors. Detailed information regarding baits is presented in

Table 2.14.

Fragment name	Forward primer (5'->3')	Reverse primer (5'->3')	Product size [bp]	Tm [°C]
Bait 1	ggggacaagtttgtacaaaaaagcaggcttc ATGACTGACAAATCAATCGTCATTC	ggggaccactttgtacaagaaagctgggtg TTACAAACCAGTGGTTGGGAGAAT	3994	75
Bait 2	ggggacaagtttgtacaaaaaagcaggcttc ACAGTTATGGCAAGTGGTCCATCAC	ggggaccactttgtacaagaaagctgggtg TTACAAACCAGTGGTTGGGAGAAT	3547	75
Bait 3	ggggacaagtttgtacaaaaaagcaggcttc ACAGTTATGGCAAGTGGTCCATCAC	ggggaccactttgtacaagaaagctgggtg TTAACTCTTTTTAGAAGGAAATAAA	4522	60
Bait 4	ggggacaagtttgtacaaaaaagcaggcttc AACATCTGTGAGATAGATACTGAAG	ggggaccactttgtacaagaaagctgggtg TTAACTCTTTTTAGAAGGAAATAAA	3058	60
Bait 5	ggggacaagtttgtacaaaaaagcaggcttc CAACGGCTGATGATTTCTGATTTCA	ggggaccactttgtacaagaaagctgggtg TTATGTAACCTCATTTTGTTCATCT	3874	70
Bait 6	ggggacaagtttgtacaaaaaagcaggcttc AAAGCCTTCAATCCCAGTGAATATC	ggggaccactttgtacaagaaagctgggtg TTATGTAACCTCATTTTGTTCATCT	4945	70
Bait 7	ggggacaagtttgtacaaaaaagcaggcttc ACAGTTATGGCAAGTGGTCCATCAC	ggggaccactttgtacaagaaagctgggtg TTATGTAACCTCATTTTGTTCATCT	9052	55
Bait 8	ggggacaagtttgtacaaaaaagcaggcttc AGACCTGGGTTTTCTGGATCTCTG	ggggaccactttgtacaagaaagctgggtg TTAACACTGGCCAACACTGCGTCC	5140	50
Bait - Full length	ggggacaagtttgtacaaaaaagcaggcttc ATGACTGACAAATCAATCGTCATTC	ggggaccactttgtacaagaaagctgggtg TTATGTAACCTCATTTTGTTCATCT	9699	55

Table 2.13 Summary of primers used for Gateway cloning of Y2H EYS bait fragments. *Att*B1 sequence is shown in green, *att*B2 sequence in blue and stop codon are in red. Expected amplicon sizes are indicated. Tm – melting temperature of the primer pair.

Bait	Size [bp]	Size [kDa]	Fragment [aa]	Domain structure
9	9435	346	1-3144	
1	3930	144	1-1310	
2	3483	127	149-1310	
3	4458	163	149-1635	
4	2994	110	637-1634	
5	3810	140	1875-3144	
6	4881	179	1518-3144	
7	8988	329	149-3144	
8	5079	186	916-2609	

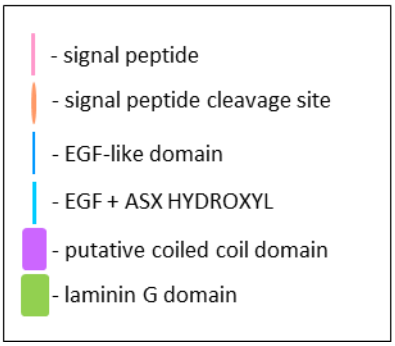

Table 2.14 Summary of EYS bait fragments designed for the purpose of Y2H screening.

2.2.5 Preparation of Competent Yeast Cells

Competent cells were prepared under sterile conditions using the Yeastmaker™ Yeast Transformation System 2 User Manual (Clontech, USA). A single colony of the relevant yeast strain was inoculated in 3 ml of YPDA medium in a sterile 50 ml tube and incubated for 8-12 hours at 30 ˚C with shaking at 225 rpm. An aliquot (500 µl) of the culture was subsequently transferred to 50 ml of YPDA medium in a sterile 250 ml flask and incubated at 30 ˚C with shaking at 225 rpm for 16-20 hours, until the OD_{600} reached 0.8-1.0. The culture was then equally divided into two sterile conical 50 ml tubes and centrifuged at 1700 rpm for 5 minutes at room temperature. The supernatant was discarded and pellets were re-suspended in 30 ml of sterile water. The centrifugation step was repeated, supernatant discarded and pellets re-suspended in 1.5 ml of 1.1 TE/LiAc solution. Each cell suspension was transferred to a 1.5 ml microcentrifuge tube and centrifuged at 14 000 rpm for 20 seconds. Supernatant was removed, pellets re-suspended in 600 µl of 1.1 X TE/LiAc solutions and placed on ice. Competent cells were used for transformation within 2 hours of preparation.

2.2.6 Transformation of Yeast Competent Cells

Prior to transformation of freshly prepared yeast competent cells, Yeastmaker Carrier DNA (provided in Yeastmaker™ Yeast Transformation System 2; 10 µg/µl) was denatured at 95 ˚C for 5 minutes. Denatured Yeastmaker Carrier DNA (5 µl) was combined with 100 ng of plasmid DNA, added to the 1.5 ml microcentrifuge tube containing 50 µl of yeast competent cells and gently mixed. PEG/LiAc (500 µl) was then added; suspensions were gently mixed and incubated at 30 ˚C for 30 minutes, mixed gently by tapping every 10 minutes. After incubation, 20 µl of DMSO was added to suspensions and tubes were incubated at 42 ˚C for 15 minutes, being gently mixed by tapping every 5 minutes. Cells were subsequently centrifuged at 14 000 rpm for 15 seconds, supernatant was discarded and pellets re-suspended in 1 ml of YPD Plus Medium provided in the kit. Cells were then incubated at 30 ˚C for 1 hour with shaking at 225 rpm. After incubation, cells were pelleted by centrifugation at 14 000 rpm for 15 seconds and re-suspended in 500 µl 0.9 % NaCl solution. Cell suspensions were diluted 1:10

and 1:100, and 100 µl of each dilution was spread using sterile glass beads (3 mm) onto single drop out (SDO) agar media supplemented with relevant drop-out solution (-Trp or -Leu depending on the vector used). Plates were incubated upside down at 30 °C for 3 to 5 days, until colonies appeared.

2.2.7 Determination of Transformation Efficiency

Transformation efficiency was determined after every transformation. The number of colonies grown (colony forming units; cfu) was evaluated and efficiency of transformation was calculated according to the equation below:

$$\text{Transformation efficiency } \left[\frac{\text{cfu}}{\mu\text{g}}\right] = \frac{\text{cfu x suspension volume [ml]}}{\text{volume plated [ml]x amount of DNA [µg]}} \text{ x dilution factor}$$

2.2.8 Small Scale Mating

Small scale mating was performed between Y2HGold and Y187 yeast strains carrying bait and prey vectors respectively. A single colony of each previously transformed yeast strain was picked up from SDO agar plates and both colonies were inoculated together in 500 µl of 2X YPDA in a 15 ml tube. The tube was then incubated for approximately 24 hours at 30 ˚C with shaking at 225 rpm. Afterwards, dilutions of mated culture were prepared (1:10, 1:100 and 1:1000) and 100 µl of each were plated on relevant selective 15 cm agar plates. Alternatively, wherever the number of colonies was not important for calculations, 10-20 µl of diluted cultures were dropped on the desired type of media plate.

2.2.9 Control Mating

Control mating was performed in order to confirm that the Y2H system used in our laboratory was working and that vectors used for cloning of bait and prey fragments are compatible. This was necessary as the vectors were

manufactured by two different companies (pBD-DEST vector from Stratagene and vectors supplied in the Clontech Y2H kit). Three control vectors were used in this study:

1. pBD-DEST-p53 encoding the GAL4 BD fused with p53 protein (bait).
2. pBD-DEST-pLc encoding GAL4 BD fused with human lamin C (bait).
3. pGADT7-T encoding the GAL4 AD fused with SV40 large T antigen (prey).

It is known that p53 protein interacts with SV40 large T antigen and therefore this interaction was used as a positive control. Conversely, pLc protein does not interact with SV40 large T antigen and this relationship was used as a negative control. The vectors were first transformed into the relevant yeast strains: pBD-DEST-p53 and pBD-DEST-pLc were transformed into Y2HGold strain whereas pGADT7-T was transformed into Y187 strain. Mated yeast cultures were afterwards plated on the following solid media:

- SDO/-Trp (Single drop-out medium lacking tryptophan)
- SDO/-Leu (Single drop-out medium lacking leucine)
- DDO (Double drop-out medium lacking tryptophan and leucine)
- DDO/X/A (Double drop-out medium lacking tryptophan and leucine, supplemented with X-α-gal and AbA)

Plated cultures were incubated for 3-5 days, until yeast colonies appeared. The experiment procedure and expected phenotypes are summarised in Table 2.15.

		Type of minimal agar medium	Selection for	Expected MEL1 phenotype
Positive control	Y2hGold[pBD-DEST/p53] x Y187[pGADT7-T]	SDO/-Leu	pGADT7-T	white
		SDO/-Trp	pBD-DEST/p53	white
		DDO (-Leu /-Trp)	Diploids containing pGBKT7-T and pBD-DEST-p53	white
		DDO/X/A (-Leu/-Trp/X-α-Gal, AbA)	Diploids that have also activated Aureobasidin A resistance and α-galactosidase through protein-protein interactions	blue
Negative control	Y2hGold[pBD-DEST/p53] x Y187[pGADT7-Lam]	SDO/-Leu	pGADT7-Lam	white
		SDO/-Trp	pBD-DEST/p53	white
		DDO (-Leu /-Trp)	Diploids containing pGBKT7-Lam and pBD-DEST-p53	white
		DDO/X/A (-Leu/-Trp/X-α-Gal, AbA)	Diploids that have also activated Aureobasidin A resistance and α-galactosidase through protein-protein interactions	no growth observed

Table 2.15 Overview of the control mating experiment conducted before Y2H screening. Vectors used, yeast strain and expected phenotype of yeast colonies are summarised. The experiment also tested whether the p-BD-DEST (Stratagene, USA) and pGADT7 (Clontech, USA) vectors, manufactured by two different companies, can be used together.

2.2.10 Testing Baits for Auto-Activation

Baits used in Y2H screening should not activate transcription of reporter genes on their own as it would cause obtaining false positive results. Therefore, every bait needs to be tested for auto-activation of reporter genes before it can be used in Y2H screening. In this experiment, bait constructs were transformed into Y2HGold yeast strain and serial dilutions of the cultures were prepared. Next, 10-20 µl of each dilution were dropped on relevant single drop-out selective media. The following types of solid media were used:

- SDO/-Trp (Single drop-out medium lacking tryptophan)
- SDO/-Trp/X (Single drop-out medium lacking tryptophan supplemented with X-α-gal)
- SDO/-Trp/X (Single drop-out medium lacking tryptophan supplemented with X-α-gal and AbA)

As a positive control, a mated culture of Y2HGold [pBD-DEST/p53] x Y187[pGADT7-T], obtained in the control mating experiments was used. Media plates were incubated at 30 ˚C for 3-5 days.

If a bait is able to activate transcription of reporter genes, it should form blue colonies on SDO/X and SDO/X/A agar media. Otherwise, colonies grown on SDO/X will be white and no growth will be observed on SDO/X/A agar plates.

2.2.11 Testing Baits for Toxicity

To ensure that baits do not have a toxic effect on the host strain of yeast, pBD-DEST-'baits' and pGBKT7-WT (encoding GAL4 DNA BD only) vectors were transformed into Y2HGold strain. After transformation, yeast cells were plated on SDO/-Trp solid media in 1:10 and 1:100 dilutions and incubated at 30 ˚C for 3-5 days. After colonies appeared, the agar plates were placed on a light box and the colonies were manually counted to determine the transformation efficiency. The colonies were also measured in diameter and the sizes of colonies carrying baits and wild type GAL4 DNA BD were compared. The average size of a healthy transformed colony was between 1-2 mm; if a bait is toxic to yeast cells, their growth will be slowed down (forming smaller colonies) or inhibited completely.

2.2.12 cDNA Library Screening Using Mating

The cDNA library screening was performed by mating an Y2HGold strain transformed with a particular bait and an aliquot of a cDNA library prepared in Y187 cells. To prepare a culture of the bait strain, one fresh colony was inoculated in 50 ml of SDO/-Trp liquid medium and incubated with shaking at 250-270 rpm at 30 ˚C for 16-20 hours, until the OD_{600} reached 0.8. Then, the culture was centrifuged to pellet cells (1200 rpm for 5 minutes) and the supernatant was discarded. The culture was re-suspended in SDO/-Trp medium to obtain a cell density of $>1x10^8$ cells per ml (4-5 ml). Next, an aliquot of a cDNA library was thawed and 10 µl were removed for library titering (section 2.2.15). The library was combined with the dilution of the bait strain and transferred to a 2 L sterile flask containing 45 ml of 2X YPDA medium supplemented with kanamycin (50 µg/ml). The library vial was rinsed twice with 1 ml of 2X YPDA which was added to the 2 L flask. The culture was incubated at 30 ˚C for 20-24 hours, slowly

shaking at 30-50 rpm. After the incubation, a drop of a culture was examined under a light microscope to see whether diploid cells are present. If so, the culture was collected and centrifuged at 1200 rpm for 10 minutes. The 2 L flask was rinsed twice with 50 ml of 0.5X YPDA (supplemented with 50 μg/ml kanamycin; 0.5X YPDA/Kan), the rinses were combined and used to re-suspend the pelleted cells. The cells were centrifuged again at 1000 g for 10 minutes and the supernatant was discarded. The cell pellet was re-suspended in 12 ml of 0.5X YPDA/Kan liquid medium and the total volume of the culture was measured. From the mated culture, 100 μl of 1/10, 1/100, 1/1000 and 1/10000 dilutions were spread on SDO/-Trp, SDO/-Leu and DDO media plates (selecting respectively for the presence of bait plasmids, prey plasmids or both). This was necessary for the purpose of evaluation of the mating efficiency and the number of screened clones. The remainder of the culture was plated pure/undiluted onto selective media plates; 100 μl were spread on one plate using sterile glass beads (3 mm) and the plates were incubated at 30 ˚C for 3-5 days. In initial screens, DDO/X/A media plates were used, however, the conditions were then modified and the mated cultures from further screens were spread on TDO/X media plates.

Following incubation, the plates were reviewed and any blue colonies grown were transferred onto increased stringency media plates (sequentially on TDO/X/A, QDO/X and QDO/X/A media plates). Blue colonies growing on the most stringent plates were subjected to further analysis.

The colonies grown on the control plates were counted and the numbers were used for calculating the mating efficiency and the number of screened clones.

2.2.13 Determination of Mating Efficiency

Each mating was followed by determination of mating efficiency which had to be no less than 2 %. It was calculated following the equation below:

$$\text{Mating efficiency [\% of diploids]} = \frac{\text{number of } \frac{\text{cfu}}{\text{ml}} \text{ of diploids}}{\text{number of } \frac{\text{cfu}}{\text{ml}} \text{ of limiting partner}} \text{ x } 100\ \%$$

The strain (bait or prey) with the lower viability, which is equal to the number of clones on SDO medium, is considered to be the “limiting partner”.

2.2.14 Determination of the Number of Screened Clones

The number of screened clones (diploid cells) was determined after each screen and it was imperative to screen at least 1 million of diploids. Screening less than 1 million of diploids would result in smaller chances of detecting interactions. To calculate the number of screened clones, DDO plates (selecting for the presence of both bait and prey plasmids) were placed on a light box and the grown colonies were manually counted. The equation given below was used to determine the number of screened clones:

Number of Screened Clones

$$= \text{number of } \frac{\text{cfu}}{\text{ml}} \text{ of diploids x resuspension volume [ml]}$$

2.2.15 cDNA Library Tittering

In each screen an aliquot of the library used was titered in order to verify its viability and it was a requirement that there are at least 2 x 10^7 cells per 1 ml of library. To check the titer, 10 µl were removed from the library aliquot, serial dilutions were prepared (1/100, 1/1000 and 1/10000) and 100 µl of each were plated on SDO/-Leu medium, selecting for prey plasmids. The colonies were then counted and the library titer was calculated using the equation below:

$$\text{Library titer } \left[\frac{\text{cfu}}{\text{ml}}\right] = \frac{\text{number of colonies}}{\text{plating volume x dilution factor}}$$

2.2.16 Yeast Colony PCR

Yeast colony PCR was performed to amplify prey fragments from yeast colonies able to grow on the highest stringency media. For this purpose, fresh patches of colonies were prepared to make sure that the yeast cells are not older than 4 days. A dab of yeast cell paste from each patch was collected with a 10 µl pipette tip and transferred to 20 µl of 20 mM NaOH solution. The samples were

incubated at 98 ˚C for 45 minutes in order to lyse the yeast cells; 1 µl was then taken from each sample and used as a template for PCR reaction. Mango*Taq* Polymerase (Bioline, USA) was used for the reaction, and 5 µl of each PCR reaction were separated using agarose gel electrophoresis to verify the size of the insert. The remainder was purified and used for sequencing of prey fragments with prey vector specific primers.

2.2.17 Human Retinal cDNA Library

The human retinal cDNA was constructed and characterised in the Bhattacharya laboratory by Dr Barbara Czub and Dr Amna Shah. The library was prepared directly in Y187 yeast strain using the Make Your Own "Mate & Plate™" Library System (Clontech, USA) which utilises the SMART™ cDNA synthesis technology.

Briefly, the first cDNA strand was transcribed from the total human retinal RNA purchased from Clontech using a 1:1 ratio of two types of primers: a modified oligo-dT primer (CDS III Primer) and a random primer (CDSIII/6 Primer). The former hybridises to the 3' end of poly A+ RNA, which results in sequences located towards the 5' end being under-represented. The CDS III/6 Primer is able to hybridise to a variety of sequences on the RNA template, making a library generated using this primer containing a wider range of sequences. In this study, a library prepared using both primers was used. The cDNA was then amplified using long distance PCR (LD-PCR) and double-stranded cDNA was purified using the CHROMA SPIN TE-400 Columns (Clontech). The columns allowed fractionation of the cDNA according to size and it selected for molecules larger than 200 bp. Next, large scale co-transformation of Y187 yeast strain was performed using the purified cDNA and pGADT7-Rec vector. The highly potent homologous recombination machinery of *Saccharomyces cerevisiae* allowed obtaining a cDNA library of prey vectors. Recombination process occurs between sequences introduced by primers used in LD-PCR and complementary fragments present in pGADT7-Rec vector. A total volume of approximately 500 ml of library was obtained and cell density was adjusted to yield at least $2x10^7$ per 1 ml. The library was aliquoted and stored at -80 ˚C.

2.3 Immunofluorescence (IF)

2.3.1 Immunocytochemistry (ICC)

2.3.1.1 Paraformaldehyde (PFA) Cell Fixation

In all experiments performed in the study, fixation of cells was performed with PFA, which forms cross-links between protein and thereby preserves the morphology of the cell. For the purpose of immunocytochemistry, cells were grown on glass coverslips placed in a 24-well plate. Before fixation, media was aspirated from the cells and two washes with sterile PBS were performed. Fixation was carried out using 300 µl of 4 % PFA for 20 minutes at room temperature. Next, to permeabilise the cell membrane, the cells were incubated for 5 minutes in the solution made up of 0.3 % Triton-X in 1X PBS. The cells were then washed twice with the solution of 20 mM glycine in 1X PBS and incubated for 15 minutes in the same solution. The cells were then used for subsequent experiments or stored in 0.5 % BSA solution at 4 ˚C.

2.3.1.2 Immunolabelling of Fixed Cells

The coverslips with fixed cells were transferred to a fresh 24-well plate and incubated in 300 µl of the blocking solution (6% BSA, 0.3% Tween 20 in 1X PBS) for 1 hour at room temperature. In the meantime, a humid chamber was prepared by placing a piece of wet 2 mm filter paper in a plastic dish. Next, a piece of parafilm was placed on the wet blotting paper and 10 µl of primary antibody dilutions were dropped on the surface of the parafilm. The blocked coverslips were transferred to the humid chamber and placed on the drops of antibody dilutions upside down, i.e. the side with fixed cells was facing down. The incubation with primary antibodies was carried out for 2 hours at room temperature or overnight at 4 ˚C. Next, the coverslips were transferred back to the 24-well plate, making sure that the side of the coverslip with attached cells is facing up. The coverslips were washed 3 times 10 minutes with 500 µl of PBS-T (0.1 % Tween 20 in 1X PBS) and gentle agitation. Afterwards, the dilutions of fluorophore conjugated secondary

antibodies were prepared in the blocking solution and 150 µl of the desired dilution were added per well. The incubation was carried out for 1 hour at room temperate with gentle agitation and was followed by three 10-minute washes with 500 µl of PBS-T and gentle agitation. To stain DNA, incubation with a solution of 4',6-Diamidino-2-Phenylindole (DAPI; Sigma) was carried out for 10 minutes at a working dilution of 1:5000. The cells were then washed 3 times 10 minutes in PBS with gentle agitation and mounted on glass slides using the Dako Mounting Fluorescence medium (Dako, Denmark). Visualisation of immuno-labelled cells was performed using the Zeiss LSM 700 confocal microscope.

2.3.2 Immunohistochemistry (IHC)

2.3.2.1 Retinal Cryosections

Retinal cryosections used in the project were kindly provided by Professor Glenn Jeffery, UCL. The sections were derived from two 2 year old *Macaca fascicularis* monkeys. The eyes were fixed in 4 % PFA for 2 days and stored in 30 % sucrose at 4 ˚C. Next, the retina and RPE were removed, embedded in OCT and sectioned at 10 microns. The slides were stored at -80 ˚C.

2.3.2.2 Immunolabelling of Retinal Cryosections

Before IHC was performed, retinal cryosections were taken out of the -80 ˚C freezer and kept at room temperature for 2 hours. Then, the slides were washed in PBS (3 times for 10 minutes) with gentle agitation. Antigen unmasking was performed by incubating the slides in 0.1 M citrate buffer (Antigen Unmasking Buffer, Vector Laboratories) and warming them up in a microwave in three steps: P100 for 3 minutes, P80 for 2 minutes and P10 for 10 minutes, where P stands for the microwave power. The slides were then washed in PBS (3 times for 10 minutes) with gentle agitation and incubated for 4 hours in a blocking reagent made up of 0.3 % Tween 20, 1 X PBS, 6 % BSA and 5 % normal donkey/goat serum.

The incubation with primary antibodies was carried out overnight at 4 ˚C and the antibody dilutions were prepared in the blocking solution. The incubation was followed by washes in PBS-T (3 times 10 for minutes) with gentle agitation and then, the slides were incubated for 1 hour with secondary antibodies diluted in

the blocking reagent. The slides were washed 3 times for 10 minutes in PBS-T, 2 times for 10 minutes in PBS and incubated for 10 minutes in DAPI (1:5000 dilution). Next, three 10 minute washes in PBS were carried out and the slides were mounted using the Dako Mounting Fluorescence medium (Dako, Denmark). Visualisation of immuno-labelled cells was performed using the Zeiss LSM 700 confocal microscope. Every assay was accompanied by control experiments aiming to confirm the specific binding of primary antibodies and to verify the strength of autofluorescence.

2.4 Immunoprecipitation (IP)

Immunoprecipitation (IP) was used in the project to test whether the two proteins of interest complex together and in such case the method was referred to as co-immunoprecipitation (Co-IP). The assays were performed using SureBeads Protein G Magnetic Beads (BioRad, USA) according to the manufacturer's recommendations. The interactions were tested in protein extracts obtained from transfected or non-transfected cells. To test the interaction, 100 µl of protein extract (at the concentration of total protein extract of 1-1.5 mg/ml) were transferred to a 2 ml microcentrifuge tube, which was then placed on a magnetic tube rack. Once the beads magnetised, the supernatant was discarded and the beads were washed three times with 1 ml of PBS-T (0.1 % Tween 20 in 1X PBS). Next, 10 µg of antibody were added in a final volume of 200 µl; the volumes were adjusted with PBS-T. The tubes were placed on a rotary shaker and mixed for 10 minutes at room temperature. The beads were then magnetised, the supernatant removed and three washes with PBS-T were performed. Antigen containing lysate was then added to the beads and typically, 100-150 µg of the total protein extract per sample were used. The tubes were mixed on a rotary shaker at room temperature for 1 hour. Afterwards, the beads were magnetised, the supernatant removed and three washes with PBS-T were performed. To elute the pulled down protein complexes, 40 µl of 1X Laemmli buffer were added and the tubes were incubated at 70 ˚C for 10 minutes. The eluted samples were immediately resolved by SDS-PAGE and analysed by immunoblotting.

2.5 Mutation Screening

2.5.1 Patients

Mutation screening was carried out on a panel of 96 unrelated autosomal recessive retinitis pigmentosa (arRP) patients. Informed consent was obtained from each patient, in accordance with guidelines established by the Declaration of Helsinki and was approved by the Moorfield's Eye Hospital Ethics Committee. Genomic DNA was provided by Dr Naushin Waseem and Ms Beverley Scott.

2.5.2 Primer Design and Mutation Screening

Primers for mutation screening were designed using the reference sequence derived from Enembl database (*PROM1*, Transcript ID: ENST00000510224). Primers were anchored in introns so that the full sequences of exons as well as splicing sites are covered. The primers used for mutation screening of *PROM1* are summarised in Table 2.16. It is necessary to mention that the primers shown in the table cover all of the coding exons in 7 isoforms of human *PROM1* but additional primer pairs had to be designed for exons 24 and 25 of isoform 3 (s3). This was necessary because isoform 3 differs from the canonical isoform of Prominin-1 in that it has an amino-acid change from VETIPMKNM to SSWVTSVQC at the position 831-839. This change localizes at the C-terminus of the protein and is not included in any of the conserved domains.

The DNA fragments were amplified using MangoTaq polymerase (Bioline, UK) and the sequencing was performed using BigDyeTM Terminator v3.1 Cycle Sequencing Kit (Applied Biosystems, UK), as described in section 2.1.1.

The sequencing electropherograms obtained were analysed using Lasergene DNASTAR® software (DNASTAR, Inc). Any variations found were annotated in accordance with recommendations by Human Genome Variation Society (www.hgvs.org/mutnomen). Nucleotide numbering reflects cDNA numbering with +1 corresponding to the A of the ATG translation initiation codon in the reference sequence. The initiation codon is codon 1 and there is no nucleotide or codon 0.

Potential pathogenicity of novel substitutions was assessed using Polyphen2 (http://genetics.bwh.harvard.edu/pph2/; Adzhubei *et al.*, 2010) and SIFT (http://sift.jcvi.org/; Ng & Henikoff, 2002) software.

Exon	Froward Primer (5'->3')	Reverse Primer (5'->3')	Product Size [bp]	Tm [˚C]
1	CGCGGTGAGTATGTTTAAGGA	CCTACTCCCGCTGTGG	890	51
2	CTGGAGCAGGTTGTGTG	CCTCGCAACCTATGTAACC	764	54
3	GGCTTCTGGCTAGAGGTC	GGTGGTTCAATATTCCATG	384	54
4	CACCCAATTTCCTCCTTG	GTACATTTGATAACACAGCCTTTC	495	54
5	AAAAGAACTTTGTACACCATGGAATG	CATTACAACGCTAATGTCTG	499	55
6	GAAGGATGTGGGAGGAG	CAGATAACACCAGTCTACGC	397	54
7	CTAGGAACTTGCTGGTTACC	GGCTAGATTCTAATCGCTG	359	54
8	CAGTTGGTGCGGAGAC	CCAAGCCAGCTCTCAG	369	54
9	CTAGCGATGCTCCTGTATTC	CTAACTGTTCTCCAAGTCAGG	495	54
10	CAGCAAGAGACCTCCAGAC	CATGCCACTTCACACATC	500	54
11	GACTCTTGATGACCATATAATG	GTCCGAATGACACAATTG	379	54
12	CGATGGTCTTGGCTATATTC	GCGAGCACTTCAAATTC	498	55
13	CACTCAACATTATTGTCCTCTG	GCAGGATCTCTCCTCCTC	450	57
14	CTCCTAGGTGGATGATCTG	GCAATCCACATTGAGC	548	55
15	GTTGGAAATCAACCAGAAAAATAATG	CCAGAGATTATTGGAGAGCGAGA	476	55
16	CAAGGCAAGAAGTCAGAAG	GAGGTGAAGGTTACACAGC	431	55
17	GAGATGCCAGTCAAGTGC	CCACCGAATTGCTCAC	580	55
18	GTTTCTGACCTCACATGATTAC	GACACACACAAGAGAGGTG	333	55
19	CATCATTGCATGCTTATGTC	GGCCAGCTCAACTTCTG	354	55
20	CACATTGTTAATTGTGTTGG	GATGAGGTCTGCACTTAGAG	400	52
21	CCTCTTAACTAGCAGGTCCAG	GTCTTGGTCCTGCACATC	552	55
22	CCTCTTAACTAGCAGGTCCAG	GTCTTGGTCCTGCACATC	552	55
23	CCTGTCTTAGAGGACATGG	GTCTATTAGCATCTCAATACACTG	369	55
24	GGTCCACATGACATTCTC	CGAGAGAGAGGAACTGC	541	54
25	CATTCTGTGTCTGGTGAATG	GCCTGTACAGATCTGCTG	331	55
26	GTCCTTTGGTCTTTGAAG	GAGCATGATTGGAGACTAG	392	55
27	GTCAAGGCCATTATCACAGAG	GAATCAATCGGTGGATGTG	763	55
28	GCTTTGCAACAAACATATTG	GGAGTTACGCAGGTTTCTC	825	55
24 (s3)	GGTCCACATGACATTCTC	CGAGAGAGAGGAACTGC	541	54
25 (s3)	GCATAAGACTTGATAACTCTTGG	CTGTGGACCGTTAAGGAAG	351	54

Table 2.16 Summary of primers used to perform mutation screening of *PROM1*. Tm – optimised melting temperatures of primers.

2.6 Summary of Vectors

Plasmid vectors used in the study were available in the Bhattacharya laboratory and were purchased directly from the manufactures, unless stated otherwise. The summary of vectors used in the study is presented in Table 2.17.

Vector	Purpose	Features
pDONR/Zeo (Life Technologies, USA)	Gateway donor vector used to generate entry clones	Resistance to zeocin, *ccdB* gene used as negative selection marker
pBD-DEST (Stratagene, USA)	Gateway entry vector used to generate expression clones, N-terminally tagged with GAL4 DBD	Resistance to chloramphenicol, *TRP1* nutritional reporter gene , *ccdB* gene used as negative selection marker; gift from Dr Ronald Roepman
pAD-DEST (Stratagene, USA)	Gateway entry vector used to generate expression clones, N-terminally tagged with GAL4 AD	Resistance to ampicillin, *LEU2* nutritional reporter gene, *ccdB* gene used as negative selection marker; gift from Dr Ronald Roepman
GBKT7 (Clontech, USA)	Vector encoding GAL4 DBD used to express wild type GAL4 DBD in yeast , it can be used to generate 'baits' as an alternative to pBD-DEST	Resistance to kanamycin, *TRP1* nutritional reporter gene
pBD-p53 (Stratagene, USA)	Destination vector encoding GAL4 DBD fused to p53 protein, used in Y2H control experiments	Resistance to chloramphenicol, *TRP1* nutritional reporter gene , *ccdB* gene used as negative selection marker
pGADT7 -T (Clontech, USA)	Vector encoding GAL4-AD fused to SV40 large T antigen protein, Used in Y2H control experiments	Resistance to ampicillin, *LEU2* nutritional reporter gene
pGBKT7 -Lam (Clontech, USA)	Vector encoding GAL4-BD fused to human lamin C protein, used in Y2H control experiments.	Resistance to kanamycin, *TRP1* nutritional reporter gene

pcDNA 3.2/V5-DEST (Life Technologies, USA)	Gateway destination vector to generate C-terminally V-5 tagged proteins	Resistance to ampicillin, ccdB gene used as negative selection marker
p3xFLAG-Myc-CMV (Sigma, USA)	Vector used to generate proteins tagged with 3xFLAG tag from N-terminus and/or c-myc tag from C-terminus	Resistance to ampicillin
pEGFP-C3 (Clontech, USA)	Vector used to generate proteins N-terminally tagged with eGFP	Resistance to kanamycin
pDsRed-Monomer-Hyg-N1 (Clontech, USA)	Vector used to generate proteins C-terminally tagged with DsRed	Resistance to ampicillin
pcDNA 3.1/EYS isoform 1	Vector carrying cDNA sequence of EYS isoform 1; used as template for amplification	Resistance to ampicillin
pcDNA 3.1/PROM1	Vector carrying cDNA sequence of PROM1; used as template for amplification	Resistance to ampicillin; gift from Prof Andrew Zelhof, Indiana University
pCMV-Tag3C/AIPL1	Vector encoding N-terminally c-myc tagged AIPL1	Resistance to kanamycin; gift from Dr Jacqueline van Der Spuy, UCL IoO
pCMV-Tag3B/NUB1	Vector encoding C-terminally c-myc tagged NUB1	Resistance to kanamycin; gift from Dr Jacqueline van Der Spuy, UCL IoO

Table 2.17 Summary of vectors used in the project.

2.7 Summary of Antibodies and Dyes

Primary antibodies used in the study are summarised in Table 2.18 whereas secondary antibodies used are listed in Table 2.19. Dyes that were applied in immunofluorescence are listed in Table 2.20. Concentrations of the antibodies and dyes used were experimentally optimised for every assay.

Antibody	Animal raised in	Manufacturer	Working Dilution
anti-GAL4 DBD	Rabbit	SantaCruz, USA	IB: 1:500
anti-acetylated alfa-tubulin	Mouse	Sigma, USA	ICC: 1:5000 IHC: 1:1000
anti-AIPL1*	Rabbit	Custom made	IB: 1:30000, ICC: 1:15 000
anti-alfa-tubulin	Mouse	Sigma, USA	ICC: 1:3500
anti-arrestin	Mouse	SantaCruz, USA	IHC: 1:500
anti-c-myc	Mouse	Genron, UK	ICC: 1:1000
anti-EYS1	Rabbit	Custom made	IB: 1:500 ICC: 1:300
anti-EYS2	Rabbit	Custom made	IHC: 1:50
anti-EYS3	Goat	SantaCruz, USA	ICC: 1:300
anti-GFP	Mouse	SantaCruz, USA	IB: 1:500
anti-giantin	Mouse	Abcam, UK	IB: 1:250
anti-Prominin-1	Mouse	Miltenyi Biotec, Germany	IB: 1:100 ICC: 1:10 ICH: 1:10
anti-s-opsin	Goat	SantaCruz, USA	ICH: 1:20
anti-V5	Goat	SantaCruz, USA	IB: 1:500 ICC: 1:300

Table 2.18 Summary of primary antibodies used in the study. *- anti-AIPL1 rabbit antibody was kindly provided by Dr Jacqueline van der Spuy, UCL Institute of Ophthalmology. IB – immunoblotting, ICC– immunocytochemistry, ICH - immunohistochemistry.

Antibody	Animal raised in	Manufacturer	Working Dilution
HRP anti-mouse	Goat	Jackson ImmunoResearch, USA	IB: 1:15000
HRP anti-rabbit	Goat	Jackson ImmunoResearch, USA	IB: 1:15000
HRP anti-goat	Rabbit	Jackson ImmunoResearch, USA	IB: 1:15000
Cyanine 3 anti-rabbit	Donkey	Jackson ImmunoResearch, USA	IF: 1:500
Cyanine 3 anti-goat	Donkey	Jackson ImmunoResearch, USA	IF: 1:500
Cyanine 3 anti-mouse	Donkey	Jackson ImmunoResearch, USA	IF: 1:500
Cyanine 3 anti-mouse	Goat	Jackson ImmunoResearch, USA	IF: 1:500
AlexaFluor 488 anti-rabbit	Donkey	LifeTechnologies, USA	IF: 1:500
AlexaFluor 488 anti-rabbit	Goat	LifeTechnologies, USA	IF: 1:500
AlexaFluor 488 anti-goat	Donkey	LifeTechnologies, USA	IF: 1:500
AlexaFluor 633 anti-mouse	Goat	LifeTechnologies, USA	IF: 1:500
AlexaFluor 633 anti-rabbit	Goat	LifeTechnologies, USA	IF: 1:500
AlexaFluor 594 anti-goat	Donkey	LifeTechnologies, USA	IF: 1:500

Table 2.19 Summary of secondary antibodies used in the study. IB – immunoblotting, IF – immunofluorescence.

Dye	Manufacturer	Working Dilution
DAPI	Sigma, USA	IF: 1:5000
AlexaFluor 594 Phalloidin	LifeTechnologies, USA	IF: 1:800
AlexaFluor 488 WGA	LifeTechnologies, USA	IF: 1:800
TexasRed-X WGA	LifeTechnologies, USA	IF: 1:800
TexasRed-X PNA	LifeTechnologies, USA	IF: 1:800

Table 2.20 Summary of dyes used in the study. IF – immunofluorescence.

2.8 Summary of Materials

Materials used in the projects are summarised in Table 2.21

Item	Company
1 M lithium acetate (10X) (LiAc (10X))	Clontech, USA
10X Loading Buffer, Bromophenol Blue	Sigma, USA
10X Tris-glycine-EDTA	Flowgene Bioscience, UK
2-Mercaptoethanol	Sigma, USA
50X TAE	VWR, USA
5-Bromo-4-chloro-3-indolyl alpha-D-galactopyranoside (X-alpha-gal)	Glycosynth, UK
6X Laemmli Bufer	Alfa Aesar, UK
Adenine hemisulphate	Sigma, USA
Agar	VWR, USA
Agarose	Sigma, USA
Antigen Unmasking Buffer	Vector Laboratories, UK
Aprotinin	Sigma, USA
Benzamidine	Sigma, USA
BigDye® Terminator v3.1 Cycle Sequencing Kit	Applied Biosystems, USA
Coomassie Brilliant Blue	Sigma, USA
Dako Mounting Fluorescence medium	Dako, Denmark
DAPI	Sigma, USA
Dibutyryl cyclin AMP (dbcAMP)	Sigma, USA
Dimethyl Sulfoxide, DMSO	Sigma, USA
DMEM	Life Technologies, USA
dNTPs	Bioline, USA
Ethanol	BDH Chemicals, UK
Ethylenediaminetetraacetic acid (EDTA)	Sigma, USA
ExoSAP-IT	Affymetrix, USA
GAL4 BD monoclonal antibody (mAb; raised in mouse)	Clontech, USA
GelRed	Biotium, USA
Glass beads (3 mm)	Merck, USA
Glass beads (425-600 µm)	Sigma, USA
Glycerol	BDH Chemicals, UK
Glycine	Sigma, USA
Hi-Mark Pre-Stained High Molecular Weight Protein Standard	Life Technologies, USA
Hi-Mark Pre-Stained High Molecular Weight Protein Standard	Life Technologies, USA
Horseradish peroxidise (HRP) anti-mouse antibody (raised in goat)	Jackson ImmunoResearch

Hydrochloric acid	VWR, USA
Hyper Ladder I	Bioline, USA
Instant Dried Skimmed Milk	The Co-operative Food, UK
KOD Hot Start DNA Polymerase Kit	Toyobo Novagen, Japan
Leupeptin hemisulfate salt	Sigma, USA
Lipofectamine 2000	Life Technologies, USA
*Mango*TAQ polymerase Kit	Bioline, USA
Opti-MEM media	Life Technologies, USA
Paraformaldehyde	EMS, UK
PBS tablets	Oxoid, UK
Pepstatin A	Sigma, USA
Phenylmethyl-sulfonyl fluoride (PMSF)	Sigma, USA
Poly-L-lysine	Sigma, USA
Ponceau-Red stock solution	Sigma, USA
Precision Plus Protein Dual Standards	BioRad, USA
Precision Plus Protein Standards, Dual Color	BioRad, USA
Primers	Sigma, USA
ProteaseArrest 100 X	G-Biosciences, USA
RPMI Media	Life Technologies, USA
S.O.C. Medium Liquid	Life Technologies, USA
Sodium Chloride (NaCl)	Sigma, USA
Sodium Chloride, NaCl	Fischer Scientific, USA
Sodium dodecylsulfate, SDS	Sigma, USA
SureBeads	BioRad, USA
TRIS base	Sigma, USA
Triton-X	Sigma, USA
Trypan Blue	Sigma, USA
Trypsin-EDTA	Life Technologies, USA
Tryptone	Merck, USA
Tween 20	Sigma, USA
Yeast Extract	Sigma, USA
Yeastmaker Carrier DNA	Clontech, USA
YPD Broth	Sigma, USA
YPD Plus Liquid Medium	Clontech, USA
Y-Per	ThermoScoentific, USA

Table 2.21 Summary of materials used in the project.

2.9 Summary of Solutions

Solutions used in the study are summarised in the following tables.

LB Agar Medium		LB Liquid Medium
4 g Tryptone		4 g Tryptone
2g Yeast Extract		2 g Yeast Extract
3.2 g NaCl		3.2 g NaCl
6 g Agar		-
400 ml dH_2O		400 ml dH_2O

Table 2.22 Recipe for LB media.

YPDA Agar Medium		1X YPDA Liquid Medium		2X YPDA Liquid Medium
25 g YPD		25 g YPD		50 g YPD
0.02g adenine hemisupfate		0.02g adenine hemisupfate		0.04g adenine hemisupfate
12.5g agar powder		-		-
500 ml dH2O		500 ml dH2O		500 ml dH2O

Table 2.23 Recipes for YPDA media**.**

SDS-PAGE running buffer
100 ml of 10X Tris+glycine+SDS
900 ml of dH2O

Table 2.24 Recipe for SDS-PAGE running buffer.

Transfer buffer for electroblotting
100 ml of 100 ml of 10X Tris+glycine+SDS
200 ml of methanol
800 ml of dH2O

Table 2.25 Recipe for transfer buffer used for electroblotting.

Blocking solution for immunoblotting
5 % of non-fat milk
0.1 % of Tween-20
1X TBS to the maximum volume

Table 2.26 Recipe for blocking solution used in immunoblotting.

TBS 10X:
24.23 g of Tris-HCl
80.06 g of NaCl
800 ml of ultra-pure H_2O, pH to 7.6
Top up to 1 L

Table 2.27 Recipe for 10X TBS.

1X TBS-T
100 ml of TBS 10X
1 ml of Tween-20
900 ml of ultra-pure H_2O

Table 2.28 Recipe for 1X TBS-T.

1X PBS-T
100 ml of PBS 10X
1 ml of Tween-20
900 ml of ultra-pure H_2O

Table 2.29 Recipe for 1X PBS-T.

Ponceau Red 10 %
1 ml of Ponceau Red stock solution
9 ml of dH_2O

Table 2.30 Recipe for 10 % Ponceau Red solution.

'Coomassie 1 mixture'
40 % of dH_2O
10 % of acetic acid
50 % methanol
'Coomassie staining mixture'
40 % of dH_2O
10 % of acetic acid
50 % methanol
0.25 % Coomassie brilliant blue R250
Coomassie destaining mixture'
67.5 % dH_2O
7.5 % acetic acid
25 % methanol

Table 2.31 Recipe for solutions used in Coomassie staining.

TAE
2 M TRIS-Acetate
0.05 M EDTA

Table 2.32 Recipe for TAE buffer.

Synthetic Minimal Media
3.35 g Yeast nitrogen base
91.1 g D-sorbitol
500 ml dH2O
pH 5.8
20 g agar
Autoclave-sterilised
0.37 g of relevent dropout solution
20 ml 50 % glucose

Table 2.33 Recipe for synthetic minimal media.

1.1X TE/LiAc Solution
1.1 ml 10X TE (supplied with the kit)
1.1 ml 1 M LiAc (10X) (supplied with the kit)
7.8 ml sterile dH2O

Table 2.34 Recipe for TE/LiAc solution.

PEG/LiAc Solution
8 ml 50 % PEG 3350 (supplied with the kit)
1 ml 10X TE Buffer (supplied with the kit)
1 ml 1 M LiAc (10X) (supplied with the kit)

Table 2.35 Recipe for PEG/LiAc Solution.

0.9 % (w/v) NaCl Solution
0.9 g NaCl
100 ml dH2O

Table 2.36 Recipe for 0.9 % NaCl solution.

Cracking Buffer Stock Solution
8 M Urea
5 % (w/v) SDS
40 mM Tris-HCl, pH 6.8
0.1 mM EDTA
0.4 mg/ ml bromophenol blue
dH_2O

Table 2.37 Recipe for cracking buffer stock solution.

Complete Cracking Buffer
1000 µl Cracking Buffer Stock Solution
10 µl β-mercaptoethanol
70 µl pre-chilled protease inhibitor solution
50 µl 100X PMSF stock solution
0.4 mg/ ml bromophenol blue
dH_2O

Table 2.38 Recipe for complete cracking buffer.

TCA Buffer (10 ml)
200 µl of 1M Tris-HCl (ph 8)
66.6 µl of 7.5M Amonium acetate
40 µl of 0.5M EDTA
9.7 H_2O

Table 2.39 Recipe for TCA buffer.

SDS/glycerol stock solution
3.5 ml of 25% SDS
3.5 of 100% glycerol
1 ml of 1M Tris-base
spatula tip-full of bromophenol blue
dH2O up to 12 ml

Table 2.40 Recipe for SDS/glycerol stock solution

Tris-EDTA solution
2 ml of 1M Tris-base
0.4 ml of 0.5M EDTA
7.6 ml of dH2O

Table 2.41 Recipe for Tris-EDTA solution.

TCA-Laem mli loading buffer
480 µl of SDS/glycerol stock solution
400 µl of Tris/EDTA solution
50 µl of β-mercaptoethanol
20 µl of PMSF stock solution
20 µl of protease inhibitor solution
30 µl of dH2O

Table 2.42 Recipe for TCA Laemmli loading buffer.

Bloking solution for ICC
6 % BSA
0.3 % Tween 20
1X PBS

Table 2.43 Recipe for blocking solution used in ICC.

Blocking solution of ICH
6 % BSA
0.3 % Tween 20
1X PBS
5% normal donkey/goat serum

Table 2.44 Recipe for blocking solution used in ICH.

Chapter 3: Identification of Novel Interacting Partners of EYS

A powerful approach to investigate the function of a newly discovered protein is to study its interactome. Identifying interacting partners of EYS could provide useful insights into the biological processes it is involved in and it could help hypothesise its role in the human retina. This in turn could help answer the question of why mutations in *EYS* cause arRP. Understanding the role of EYS would be invaluable to the clinical management of arRP patients and it would provide critical knowledge for the design of future therapies.

The method of identification of novel interacting partners used in this study was Yeast 2-hybrid (Y2H).

3.1 Construction of EYS Baits

The first step of preparation for Y2H screening was construction of baits. In the study, cDNA of EYS isoform 1 was available and the constructed baits included the full length sequence as well as shorter fragments. The shorter bait fragments were constructed not only to perform Y2H screening but also to characterise potential interactions, i.e. to map the region of EYS responsible for mediating the protein-protein interactions. A schematic view of baits constructed in the study is shown in Figure 3.1. DNA fragments of *EYS* were amplified using *attB*-primers and KOD Hot Start DNA Polymerase Kit (Toyobo Novagen, Japan). Amplification of all *EYS* amplicons was successful as confirmed by agarose gel electrophoresis separation (Figure 3.2). *AttB*-PCR products were purified and cloned into pBD-DEST vectors using Gateway technology and direct sequencing was used to verify the sequence integrity. Purified expression clones were transformed into Y2HGold yeast cells and the transformants were examined in control experiments.

Bait	Size [bp]	Size [kDa]	Fragment [aa]	Domain structure
9	9435	346	1-3144	
1	3930	144	1-1310	
2	3483	127	149-1310	
3	4458	163	149-1635	
4	2994	110	637-1634	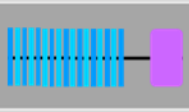
5	3810	140	1875-3144	
6	4881	179	1518-3144	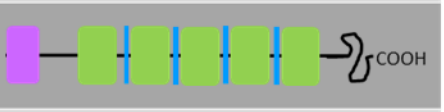
7	8988	329	149-3144	
8	5079	186	916-2609	

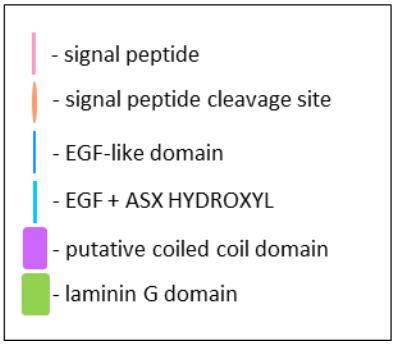

Figure 3.1 A schematic overview of bait fragments used in the study.

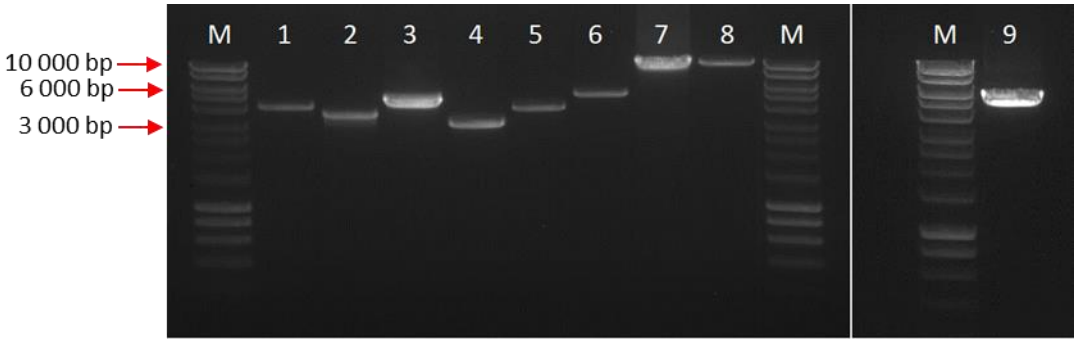

Figure 3.2 Bait fragments of EYS amplicons separated by electrophoresis on 1 % agarose gel. M- Hyperladder I molecular weight marker, 1 - bait 1 (3930 bp), 2 - bait 2 (3483 bp), 3 – bait 3 (4458 bp), 4 – bait 4 (2994 bp), 5 – bait 5 (3810 bp), 6 – bait 6 (4881 bp), 7 – bait 7 (8988 bp), 8- bait 9 FL (9435 bp), 9 – bait 8 (5079 bp).

3.2 Y2H Control Mating and Characterisation of the Baits

Before Y2H screening of a cDNA library can be performed, it is necessary to carry out a series of control experiments aiming to characterise baits and test the functionality of the system used. Characterisation of bait fragments includes verification of whether they possess features of an ideal Y2H bait, which should:

- not be toxic to yeast cells
- not activate transcription of the reporter genes
- be expressed in transformed yeast cells

It is important to note that not all of the bait fragments were used in Y2H screening and some of them were constructed with the aim to use them for characterisation and mapping of the putative interactions.

3.2.1 Y2H Control Mating

The control mating was performed in order to ensure that all components of the system used in our laboratory are functional and to obtain positive and negative controls for use later in the screen. In the first step, pBD-DEST-p53 (encoding p53 fused to GAL4 BD) and pBD-DEST-pLc (encoding Lamin C fused to GAL4 DBD) vectors were transformed into the Y2HGold yeast strain whereas pGADT7-T vector (encoding SV40 large T antigen fused to GAL4 AD) was transformed into Y187. Single colonies of each type of transformed yeast were mated as follows:

- Positive control: Y2HGold [pBD-DEST-p53] x Y187[pGADT7-T]
- Negative control: Y2HGold [pBD-DEST-pLc] x Y187[pGADT7-T]

Mated cultures were plated on relevant solid selective media as described in section 2.2.9. In the positive control, colonies of transformants grew on all types of selective solid media used (Figure 3.3). Growth on SDO/-Leu plate confirmed that pGADT7-T vector was successfully transformed into Y187 cells whereas colonies that grew on SDO/-Trp could only do so if they contained pBD-DEST-p53 plasmids. DDO medium selected for the presence of both plasmids, i.e. proper diploid cells, and DDO/X/A medium was used to additionally select for the interaction between

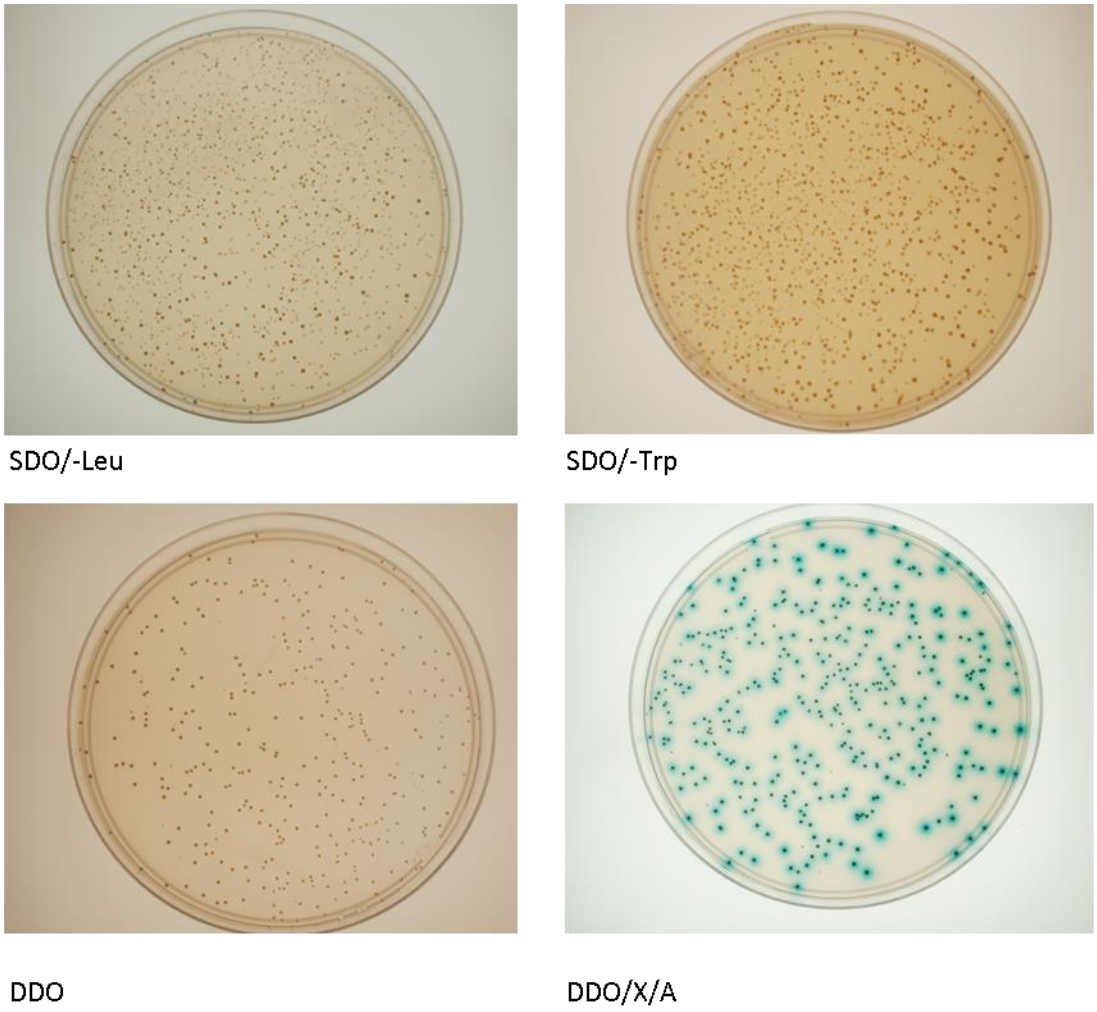

Figure 3.3 Control Y2H mating, positive control. Growth on selective media is only possible for yeast cells successfully transformed with a particular vector enabling synthesis of an amino acid absent in the medium. On media plates additionally supplemented with AbA, yeast cells need to activate the *AUR1-C* reporter gene in order to sustain growth. Activation of *MEL1* reporter genes results in yeast colonies turning blue on media supplemented with X-α-Gal. Colonies grown on selective media used in this experiment represent: **SDO/-Leu**: Y187 cells transformed with [pGADT7-T]; **SDO/-Trp:** Y2HGold [pBD-DEST-p53]; **DDO:** diploid cells carrying both pGADT7-T and pBD-DEST-p53 vectors. **DDO/X/A:** diploid cells carrying both pGADT7-T and pBD-DEST/p53 vectors this medium additionally selects for interaction between the bait and prey proteins, hence the blue colour of the colonies and the surrounding area.

the fusion proteins. Since p53 protein and SV40 large T antigen are known to interact, expression of the *AUR1-C* and *MEL1* reporter genes was activated. This resulted in diploid yeast cells being able to grow on media supplemented with Aureobasidin A (A; AbA), an antifungal agent which restricts yeast cells from growth unless the resistance is provided by the expression of *AUR1-C* reporter gene. The secretion of α-galactosidase was responsible for the hydrolysis of X-α-Gal (X) and the resulting blue colour of the colonies and the surrounding medium.

Results of the negative control mating of Y2HGold [pBD-DEST-pLc] with Y187 [pGADT7-T] cells are presented in Figure 3.4. Growth on SDO/-Leu and SDO/-Trp confirmed that transformation with the control vectors was successful and the growth of colonies on DDO medium was only possible for diploid cells containing both of the control plasmids. As there is no interaction between human Lamin C and SV40 large T antigen, reporter genes were not activated and therefore, no colonies were observed on DDO/X/A medium.

Results obtained from the control Y2H mating confirmed the functionality of the system and produced positive and negative controls. These were vital during subsequent stages of the project where it was necessary to assess putative interaction by the growth and colour of yeast colonies.

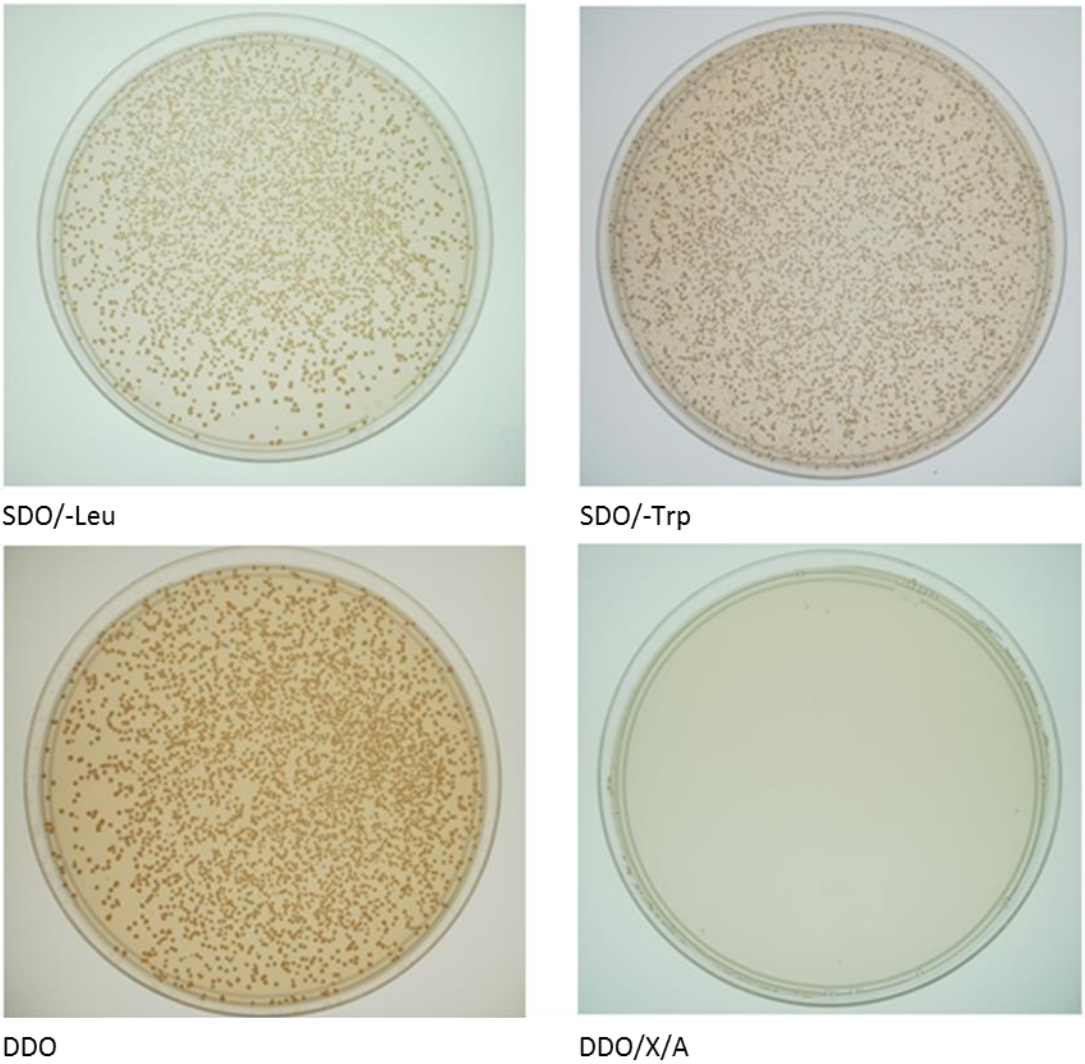

Figure 3.4 Control Y2H mating, negative control. Growth on selective media is only possible for yeast cells successfully transformed with a particular vector enabling synthesis of an amino acid absent in the medium. On media plates additionally supplemented with AbA, yeast cells need to activate the *AUR1-C* reporter gene in order to sustain growth. Activation of *MEL1* reporter genes results in yeast colonies turning blue on media supplemented with X-α-Gal. Colonies grown on selective media used in this experiment represent: **SDO/-Leu:** Y187 cells transformed with [pGADT7-T]; **SDO/-Trp:** Y2HGold cells transformed with pBD-DEST-pLc; **DDO:** diploid cells carrying both pGADT7-T and pBD-DEST/p53 vectors. **DDO/X/A:** diploid cells carrying both pGADT7-T and pBD-DEST-p53 vectors; this medium additionally selects for interaction between the bait and prey proteins, hence growth of yeast colonies is not observed.

3.2.2 Bait Toxicity Assay

To verify potential toxicity of EYS bait fragments, Y2HGold yeast cells were transformed with each of the bait constructs as well as the wild type GAL4 DBD control vector. Transformants were plated on solid SDO/-Trp medium and the growth and morphology of colonies were assessed after 5 days of incubation at 30 ˚C. The number of colonies grown on each plate is summarised in Table 3.1.

pBD-DEST/bait 7 and pBD-DEST/bait 9 (full length EYS) transformants formed fewer colonies compared with the positive control and other bait fragments. This could be due to the large size of these baits, which could reduce the efficiency of yeast transformation and/or protein translation. Nonetheless, as shown in Figure 3.5, all of the transformants formed healthy looking colonies that did not differ in size compared with the positive control. Based on these observations, it was concluded that none of the EYS bait constructs is toxic to the host Y2HGold yeast strain and therefore, they were considered suitable to be used in Y2H.

Construct	Number of colonies
pBD-DEST/bait 1	25
pBD-DEST/bait 2	56
pBD-DEST/bait 3	28
pBD-DEST/bait 4	45
pBD-DEST/bait 5	46
pBD-DEST/bait 6	41
pBD-DEST/bait 7	17
pBD-DEST/bait 8	33
pBD-DEST/bait 9 (full length EYS)	10
pGBKT7	34

Table 3.1 The number of transformed Y2HGold colonies grown on SDO/-Trp medium in a toxicity assay. pBD-DEST bait constructs encode respective EYS bait fragments fused to the GAL4 DNA binding domain; pGBKT7 control vector encodes the wild type GAL4 DBD only.

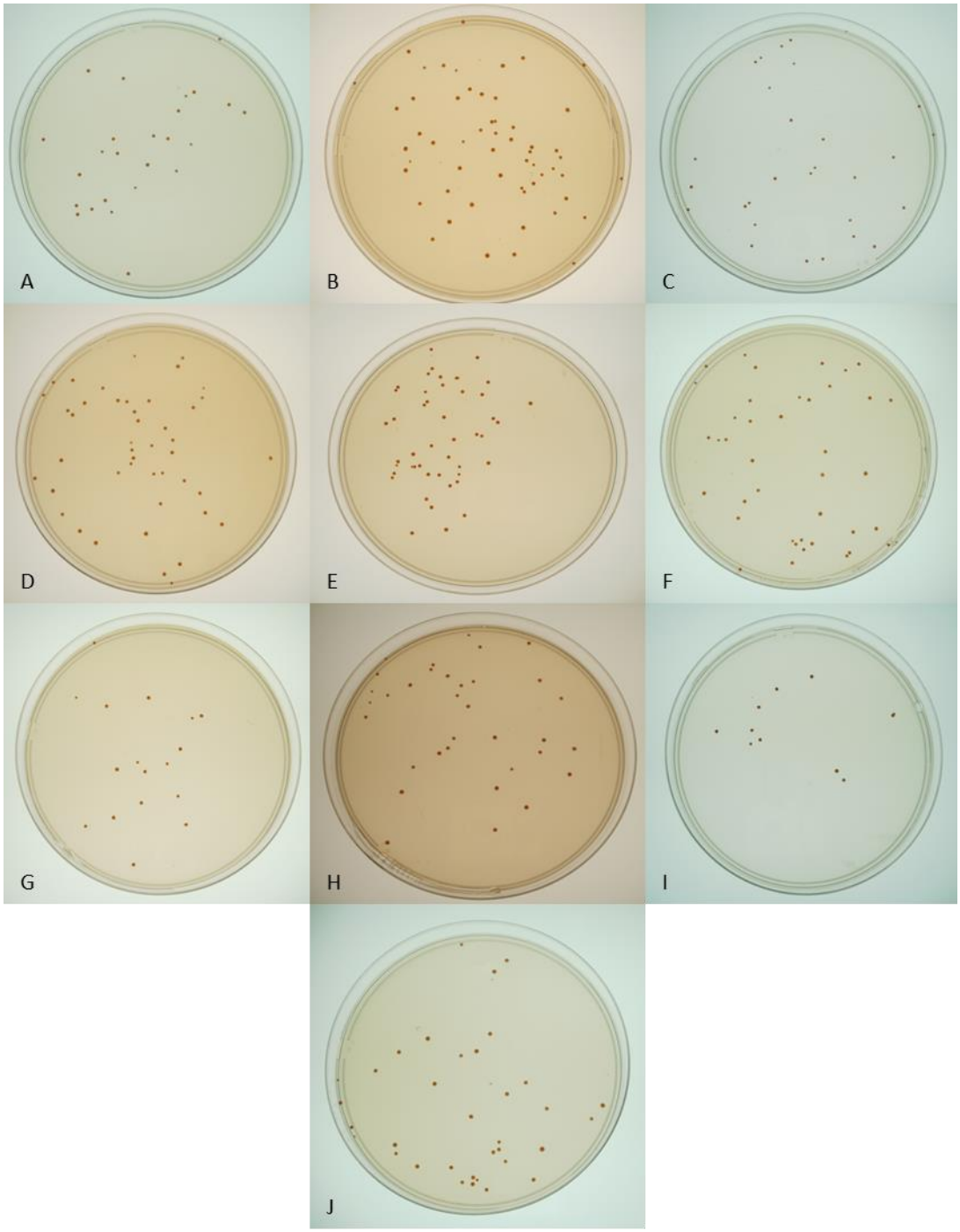

Figure 3.5 Bait toxicity assay. Snapshots of SDO/-Trp plates depict the number and size of colonies formed by transformed Y2HGold yeast cells. Each plate represents a different transformant: **A** - pBD-DEST/bait 1; **B** - pBD-DEST/bait 2; **C** - pBD-DEST/bait 3; **D** - pBD-DEST/bait 4; **E** - pBD-DEST/bait 5; **F** - pBD-DEST/bait 6; **G** - pBD-DEST/bait 7; **H** - pBD-DEST/bait 8; **I** - pBD-DEST/bait 9 (full length); **J** - control transformation with pGBKT7 encoding wild type GAL4 DNA binding domain.

3.2.3 Bait Auto-activation Assay

The Y2H system relies on a number of reporter genes that are activated when an interaction between the bait and prey occurs. Expression of the reporter genes is triggered by the GAL4 transcription regulator. As it was described in section 2.2, the GAL4 transcription regulator consists of a DNA binding domain (GAL4 DBD) and an activation domain (GAL4 AD). In Y2H, the GAL4 DBD is fused with a bait protein whereas the GAL4 AD is fused with a prey protein. When bait and prey interact, GAL4 moieties are brought in proximity (effectively reconstituting the transcriptional regulator) and the expression of reporter genes is activated. It could, however, happen that the expression of the reporter genes is not activated by the GAL4 transcription regulator but the bait itself. This would lead to obtaining false positive results and such a scenario must be excluded before a bait is used in Y2H.

To assess whether the EYS bait fragments have the ability to activate expression of the reporter genes, the bait auto-activation assay was performed. pBD-DEST/bait constructs as well as the wild type GAL4 DBD control vector (pGBKT7 wild type vector) were transformed into Y2HGold yeast cells and plated on a range of selective media at three different dilutions. Diploid cells carrying Y2HGold [pBD-DEST-p53] and Y187 [pGADT7-T] vectors were used as a positive control of interaction. As shown in Figure 3.6, all of the transformants formed white/pink colonies on SDO/-Trp medium, which confirms that the vectors were successfully transformed into Y2HGold. SDO/-Trp/X medium was supplemented with X-α-Gal, which is hydrolysed when the *MEL1* reporter gene is activated/expressed, resulting in blue yeast colonies. This was not the case for any of the baits, except for bait 4 transformants that formed pale blue colonies, suggesting that bait 4 could trigger low level expression of *MEL1*. SDO/-Trp/X/A medium was additionally supplemented with AbA and no transformant colonies were observed on SDO/-Trp/X/A medium, implying that the baits did not activate the expression of *AUR1-C* reporter gene and therefore, were unable to grow. Here, it was also shown that bait 4 could be used for Y2H screening as it was not able to activate the expression of two reporter genes simultaneously; nevertheless, it was considered as a bait of second choice.

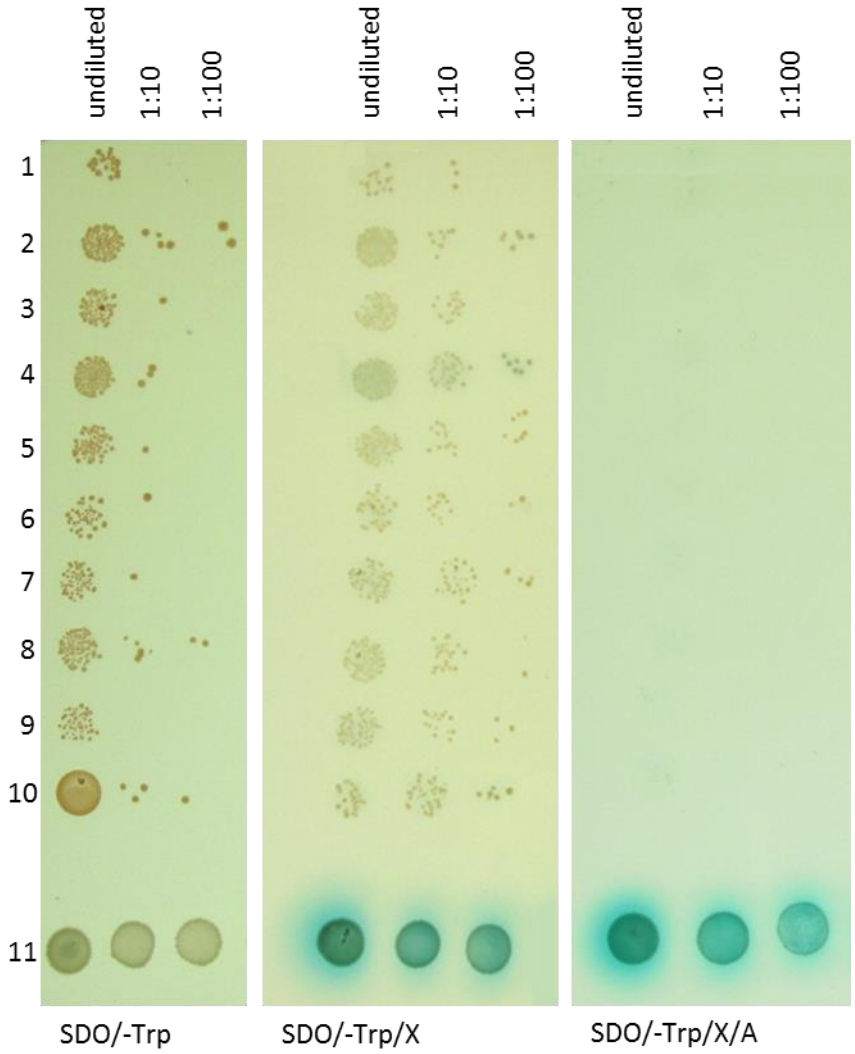

Figure 3.6 Bait auto-activation assay. Each of the transformants was plated in three dilutions (columns) on three different media plates. Each transformant was plated in a separate row: **1** - pBD-DEST/bait 1; **2** - pBD-DEST/bait 2; **3** - pBD-DEST/bait 3; **4** - pBD-DEST/bait 4; **5** - pBD-DEST/bait 5; **6** - pBD-DEST/bait 6; **7** - pBD-DEST/bait 7; **8** - pBD-DEST/bait 8; **9** - pBD-DEST/bait 9 (full length). **10** - pGBKT7 (wild type GAL 4 DNA binding domain); **11** – positive control formed of diploid cells : Y2HGold [pBD-DEST/p53] x Y187[pGADT7-T].

In summary, the auto-activation assay demonstrated that the baits were suitable to be used in Y2H since they were incapable of activating transcription of the reporter genes.

3.2.4 Bait Expression Assay

The last control experiment aimed to confirm whether EYS bait fragments were expressed in yeast cells. To do that, protein extracts were prepared from transformed Y2HGold strains and Western blot analysis was performed. In order to prepare the extracts, single colonies of transformed Y2HGold strains were inoculated in liquid selective medium (SDO/-W). Cultures transformed with wild type pGBKT7 and pBD-DEST-WT vectors were used as positive controls whereas wild type Y2HGold yeast strain was used as a negative control. Inoculated colonies were not older than four days, otherwise the extraction of proteins would have been hindered due to thickening of the yeast cell wall. The cultures were kept in the log phase of growth, which was necessary to enable expression of the bait fragments. In the late log phase, the expression of bait fragments could have been impeded by the increasing concentration of ethanol that accumulates in the culture medium as a by-product of yeast metabolism. The manual provided by Clontech recommends two extraction methods, Urea/SDS method and TCA method. Both of the methods were tested, however, bands corresponding to the bait fragments were not observed in Western blotting.

The methods recommend by Clontech involve many steps and disruption of yeast cells is achieved by vortexing the cultures with glass beads. These generally time consuming and rather harsh procedures could have had an impact on degradation of the proteins of interest during extraction. Therefore, another reagent enabling extraction of proteins from yeast, named Y-Per Plus (Thermo Scientific, USA) was used. Y-Per Plus is a detergent based lysis buffer allowing fast extraction of yeast proteins that is carried out at room temperature and the use of glass beads is not required. In order to obtain as high concentration of proteins as possible, only 40 µl of extract were prepared from each of the 5 ml overnight cultures. The concentrations obtained were checked using a BCA assay and the extracts were resolved by SDS-PAGE, transferred to PVDF membranes and probed with anti GAL4 DBD antibody. The developed membranes are shown in Figure 3.7.

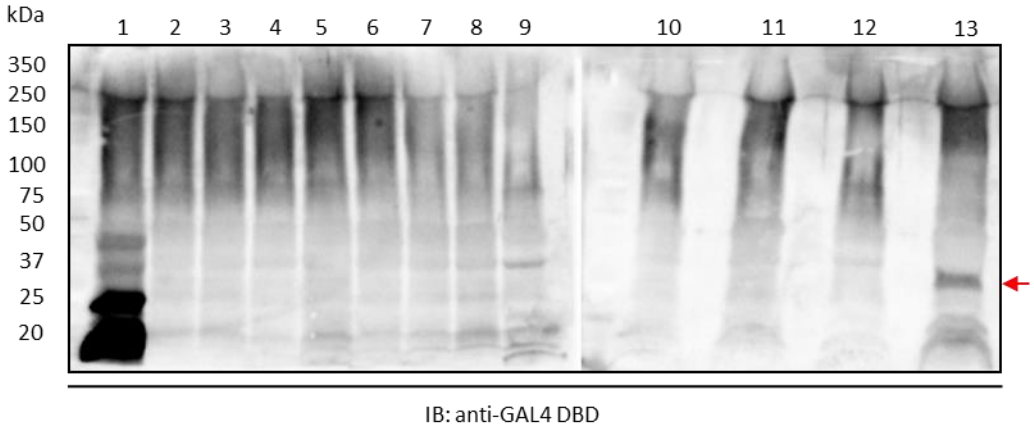

1. Y2HGold[pGBKT7-WT] (positive control 1) (22 kDa)
2. Y2HGold[pBD-DEST-bait 1] (141 kDa)
3. Y2HGold[pBD-DEST-bait 2] (127 kDa)
4. Y2HGold[pBD-DEST-bait 3] (163 kDa)
5. Y2HGold[pBD-DEST-bait 4] (110 kDa)
6. Y2HGold[pBD-DEST-bait 5] (140 kDa)
7. Y2HGold[pBD-DEST-bait 6] (179 kDa)
8. Y2HGold[pBD-DEST-bait 8] (186 kDa)
9. Y2HGold wild type (negative control)
10. Y2HGold[pBD-DEST-bait 7] (329 kDa)
11. Y2HGold[pBD-DEST-bait 9] (346 kDa)
12. Y2HGold wild type (negative control)
13. Y2HGold [pBD-DEST-WT] (positive control 2) (33 kDa)

Figure 3.7 Western blot analysis of the expression of EYS bait fragments in Y2HGold yeast cells. Extracts were prepared using Y-Per plus reagent and resolved on pre-cast 4-20 % gradient gels. Loading was optimised using BCA assay and approximately 40 µg of total protein extract were loaded in each well. Immunoblotting (IB) was performed with using anti-GAL4 DBD rabbit antibody and the secondary antibody was HRP-conjugated goat anti-rabbit. Bio-Rad Precision Plus Protein Standard was used to assess the size of protein bands. Samples 1-13 represent different samples run in the experiment and the expected size of each protein band is given in brackets. The red arrow indicates the band of wild type GAL4 DBD fused with 132-236 amino acids of wild type fragment C of lambda cI repressor (positive control 2).

There were two positive control samples, each of which contained GAL4 DBD wild type. In the first positive control GAL4 DBD wild type was expressed from the pGBKT7 wild type vector (lane 1) and in the second, a pBD-DEST-WT vector was used (lane 13). The band obtained from the latter appeared higher as this control vector encodes GAL4 DBD fused with 132-236 amino acids of wild type fragment C of lambda cI repressor. As it can be observed, there is a clear intense band in lane 1, but a weaker band was detected in lane 13 (marked with red asterisk). The presence of bands in the positive controls proves that the protein extraction was effective and that the conditions of SDS-PAGE and Western blotting were properly optimised. Clear bands were not, however, seen for any of the bait fragment proteins. Upon in-depth analysis of blots, it can be noticed that, in the lanes representing EYS bait fragments, there is a smeared signal in the range of approximately 75-350 kDa. The smeared signal suggests that the proteins in this range could have degraded during extraction, sample processing or gel separation. One could argue that degradation should not have been an issue since the wild type GAL4 DBD did not give a smeared signal. It should be pointed out, however, that there are two bands visible in lane 1, one at the size of wild type GAL4 DBD (~22 kDa) and the second one at about ~12 kDa. Even though the signal was not smeared, the presence of the second band implies that some level of degradation had happened and resulted in the appearance of two protein bands. Furthermore, it is necessary to highlight that the sizes of EYS bait fragments are relatively large and, therefore, the expected bands would have been detected at a lot higher molecular weights than wild type GAL4 DBD. It is also natural that the extraction of higher molecular weight proteins is more challenging and a lot more liable to potential sample degradation. The size of bait fragments may have had an impact on the efficiency of expression in yeast cells and another scenario could be that the expression level of bait fragments was not sufficient enough for the Western blotting to detect the protein.

Distinctly visible protein bands of the bait fragments were not detected and therefore, the important question of whether the baits were expressed in Y2HGold yeast cells could not be clearly answered. However, the baits passed the previous control experiments proving that the expression of proteins from the bait vectors was taking place – otherwise cultures would not have been able to grow on selective media lacking crucial amino acids that were encoded on the bait vectors

for the purpose of selection. Based on that, it was concluded that the EYS bait fragments were suitable for Y2H screening.

3.3 Y2H cDNA Library Screening

Y2H screens were performed using a human retinal cDNA Y2H library, which had previously been prepared in the Y187 yeast strain by members of the Bhattacharya laboratory at UCL. The library was screened by mating the Y2HGold yeast strains carrying the bait of interest with an aliquot of a human retinal cDNA library.

The use of bait fragments for screening was prioritised according to their size and domain structure. The aim was to use as long bait fragment as possible to replicate the natural three-dimensional structure of EYS protein. Following such a strategy was important for ensuring that the identified interactions were genuine.

Before each mating, an aliquot (10 µl) of the library culture was removed for the purpose of library titering. Also, an aliquot of the mated culture was taken each time and plated in relevant serial dilutions on control solid media plates for the purpose of assessing the efficiency of mating and the number of screened clones. The presence of zygotes in the mated culture was established in each screen prior to plating on selective solid media; an image shown in Figure 3.8 depicts an example of a mated culture seen under a light microscope (zygotes are indicated by red arrows). Plating of the mated culture on relevant selective media allowed identification of clones in which an interaction of bait and prey had occurred.

The first Y2H screen was performed using Y2HGold [pBD-DEST/bait 9] strain, which carried the full length EYS protein. As recommended by the manufacturer of the Y2H system, the mated culture was plated on DDO/X/A media plates and incubated for five days at 30 °C; however, no yeast colonies were observed upon examination of the media plates. Since the control experiments showed that the conditions of mating were in line with recommendations of the manufacturer (Table 3.2), it was concluded that the failure of the screen was due to some features of the bait. Full length EYS contains a signal peptide the role of which has not yet been fully investigated but it has been speculated that it might direct EYS protein to a secretory pathway.

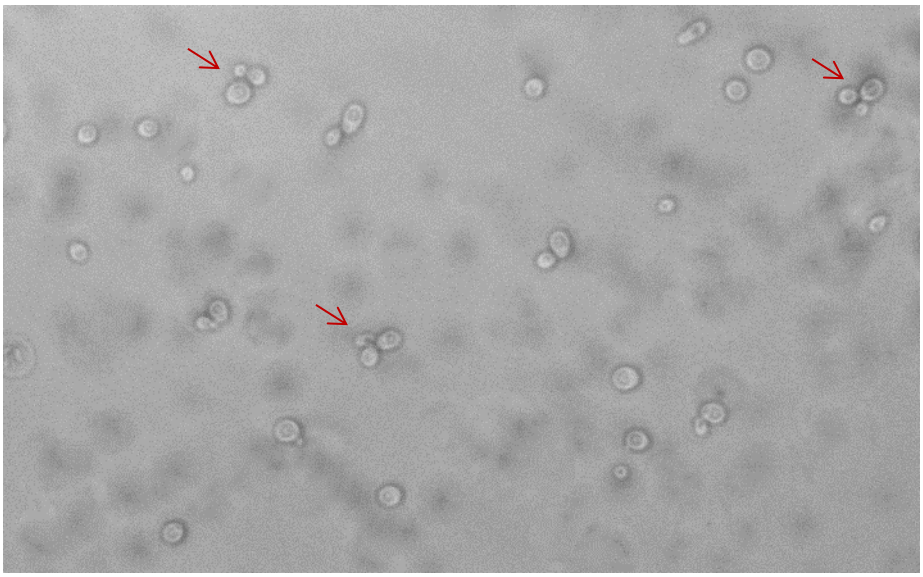

Figure 3.8 A micrograph showing a sample of a mated yeast culture. Red arrows indicate zygotes, which typically have a 3-lobed structure. The lobes represent the two haploid parental cells and the budding diploid cell.

Y2H screen	1	2	3
Primary selective media	DDO/X/A	DDO/X/A	DDO/X/A
Bait	Bait 9	Bait 7	Bait 8
Cell density of bait culture (recommended minimum = $1x10^8$ cells/ml)	$1.24x10^8$ cell/ml	$2.61x10^8$ cell/ml	$1.43x10^8$ cell/ml
Library titre (recommended minimum = $2x10^7$ cells/ml)	$3x10^6$ cell/ml	$1.04x10^7$ cell/ml	$1.12x10^7$ cell/ml
Mating efficiency (required minimum 2% required)	2.40 %	6.75 %	6.50 %
Number of screened clones (minimum $1x10^6$ required)	$9x10^6$	$1.012x10^6$	$1.087x10^6$

Table 3.2 Summary of the conditions of Y2H screens performed with bait 9, 7 and 8. DDO/X/A media plates were used to seed the mated cultures for the purpose of screening.

It could, therefore, happen that yeast cells secreted the bait, which in turn impeded possibility of identifying potential interacting partners, and subsequently, did not allow for the activation of the reporter genes.

In order to verify whether this might be the case, it was decided to use the Y2HGold [pBD-DEST/bait 7] strain, containing full size EYS protein lacking the sequence encoding the signal peptide. The mated culture was plated on DDO/X/A media plates as previously, but once more no growth of colonies was observed. Even though bait 7 does not contain the signal peptide, it constitutes approximately 95 % of the full-length protein, which is around 345 kDa including the GAL4 DBD. Therefore, it may have happened that it was the size of the bait protein that prevented the Y2H system from working. Another issue may have been the size or folding of the bait that prevented the complex of bait and prey to enter the nucleus and activate the expression of the reporter genes. In order to reduce this risk in the next screen, the Y2HGold [pBD-DEST/bait 8] strain was used. Bait 8 comprises of nine N-terminal EGF domains, a putative coiled-coil and three LamG domains; it reflects the domain structure of the full length EYS protein in its diminished form and constitutes around 53 % of the full size molecule. The mating procedure was performed as previously described and the culture of diploids was plated on DDO/X/A. The growth of positive diploid colonies was not observed.

Parameters of the screens performed to this point did not deviate from the protocol described by the manufacturer of the system used (Table 3.2). Also, colonies grown on the control media plates looked healthy and did not differ in any way from the colonies observed during pre-screening control experiments. This suggested that the failure of the screens may have been caused by some specific features of the bait fragments such as size, conformation, localisation or expression level. Another possible scenario was that the interaction of bait and preys were transient or not strong enough to overcome restrictive conditions imposed by DDO/X/A media. The Y2H system used in this study incorporates *AUR1-C* gene as one of the interaction reporters. *AUR1-C* confers strong resistance to the otherwise highly toxic Aureobasidin A (AbA), which provides high stringency of the screening conditions but it may at the same time cause weaker interactions to be missed. The workflow recommended by the manufacturer states that in the first instance a mated culture should be plated on DDO/X/A media and blue colonies should be re-patched to higher stringency QDO/X/A, which additionally lack adenine and histidine. These two amino acids are used as nutritional markers and diploids can grow on them only when a bait protein interacts with a prey protein, and activates their respective promoters. Such a procedure ensures high stringency of screening and reduces possible background and false positive results. In order to assess whether such stringent screening conditions are appropriate for EYS protein and its fragments, the strategy of Y2H screening was amended and less stringent conditions were allowed in the first place, and any colonies obtained were then re-patched onto media plates of increasing stringency. In more detail, mated cultures were initially plated on triple drop-out media (TDO) lacking tryptophan, leucine and histidine. Such media plates were able to select for diploid cells and a potential interaction using one nutritional marker (hisitidine). Any colonies grown on TDO plates were re-patched onto more stringent TDO/X media plates and any blue colonies grown here were subsequently re-patched on QDO/X. Yeast colonies that grew blue on QDO/X media where transferred onto QDO/X/A media plates which were the ultimate and most stringent media used in the screening. Furthermore, it was decided to use shorter bait fragments in order to lower the risk of the system not working due to the bait size. To allow comprehensive screening of the library, bait fragments needed to cover the full sequence of EYS proteins. The fourth screen was performed using bait 3, which encompasses the N-terminal part of EYS

including all of the N-terminal EGF domains and the putative coiled-coil domain (Figure 3.1). The fifth screen was carried out using bait 6, which begins with a coiled-coil domain at the N-terminus and covers the entire C-terminal fragment comprising of EGF and LamG domains. Next, bait 8 was used as it mimics the domain structure of the full sized EYS and bait 7 was utilised to verify whether any interaction can be identified using the full sequence of EYS and less stringent screening conditions. The parameters of Y2H screens performed in the modified conditions are summarised in Table 3.3. In the fourth screen performed using Y2HGold [pBD-DEST/bait 3], a total number of 37 white colonies grew on TDO media plates. These colonies were transferred onto TDO/X media plates and 28 colonies re-grew, 24 of which grew blue and four grew white. All of the colonies were re-patched onto QDO/X media plates and only the blue colonies were able to grow, meaning that the interaction between the bait and prey in the white colonies was not strong or abundant enough to activate the expression of more than one reporter gene. Blue colonies were eventually re-patched from QDO/X onto QDO/X/A and all of them were able to grow. The phenotypes of the colonies grown in this screen are summarised in Table 3.4 and the QDO/X/A is shown in Figure 3.9.

Y2H screen	4	5	6	7
Primary selective media	TDO	TDO	TDO	TDO
Bait	Bait 3	Bait 6	Bait 8	Bait 7
Cell density of bait culture (recommended minimum = $1x10^8$ cells/ml)	$1.25x10^8$ cells/ml	$1.20x10^8$ cells/ml	$1.50x10^8$ cells/ml	$1.43x10^8$ cells/ml
Library titer (recommended minimum = $2x10^7$ cells/ml)	$1.19x10^7$ cells/ml	$8.50x10^6$ cells/ml	$1.23x10^7$ cells/ml	$7.6x10^6$ cells/ml
Mating efficiency (required minimum 2% required)	11.13%	19.91%	13.04%	11.32%
Number of screened clones (minimum $1x10^6$ required)	$1.18x10^6$	$2.47x10^6$	$1.84x10^6$	$1.72x10^6$

Table 3.3 Summary of the Y2H screens performed with bait 3, 6, 8 and 7. The mated cultures were spread on TDO media plates for the purpose of screening.

Colony number	Medium type		
	TDO/X	QDO/X	QDO/X/A
1	blue	blue	blue
2	blue	blue	blue
3	blue	blue	blue
4	blue	blue	blue
5	blue	blue	blue
6	blue	blue	blue
7	blue	blue	blue
8	blue	blue	blue
9	blue	blue	blue
10	blue	blue	blue
11	blue	blue	blue
12	blue	blue	blue
13	white	x	x
14	blue	blue	blue
15	blue	blue	blue
16	blue	blue	blue
17	blue	blue	blue
18	white	x	x
19	blue	blue	blue
20	blue	blue	blue
21	blue	blue	blue
22	blue	blue	blue
23	blue	blue	blue
24	blue	blue	blue
25	blue	blue	blue
26	blue	blue	blue
27	white	x	x
28	white	x	x

Table 3.4 Summary of phenotypes of colonies grown in Y2H screen 4, which was performed using the Y2HGold [pBD-DEST/bait 3] strain. Out of 28 colonies grown altogether, 24 grew blue and 4 grew white on TDO media plates. Only the blue colonies were able to grow on QDO/X and QDO/X/A media plates. 'x' denotes no growth of yeast colonies.

Figure 3.9 QDO/X/A media plate with patches of colonies grown in Y2H screen 4, which was performed using the Y2HGold [pBD-DEST/bait 3] strain. Yeast colonies numbered 13, 18, 27 and 28 grew white on the TDO plate and did not grow in the most stringent conditions on the QDO/X/A plate, which indicates the interaction in those colonies was not strong or abundant enough to activate all of the reporter genes. The blue colour of the colonies grown on the QDO/X/A indicates activation of four reporter genes and only these results should be considered true positive.

In the fifth Y2H screen performed in the project, it was attempted to identify proteins interacting with the C-terminal part of EYS protein and the Y2HGold [pBD-DEST/bait 6] strain was used. Upon examination of TDO media plates, 14 white colonies were observed and re-patched onto TDO/X media plates. Of these, only three white colonies regrew and were subsequently re-patched onto QDO/X and QDO/X/A media plates (Table 3.5). One of the colonies remained consistently white regardless of the media plate, but the two other initially white colonies re-grew pale blue (Figure 3.10).

In order to survive the restrictive environment of selective media, yeast diploids had to express reporter genes encoding missing amino acids and the enzyme protecting them from the toxicity of AbA. In this screen only three colonies of yeast were able to grow on the selective media but they were unable to efficiently activate the expression of *MEL1* gene encoding α-galactosidase. This may raise concerns over reliability of the results obtained in this screen; however, since there were only three colonies grown altogether, they were all subjected to further analysis to verify credibility of the results.

	Medium type		
Colony number	TDO/X	QDO/X	QDO/X/A
1	white	white	white
2	white	pale blue	pale blue
3	white	pale blue	pale blue

Table 3.5 Summary of phenotypes of colonies grown in Y2H screen 5, which was performed using the Y2HGold [pBD-DEST/bait 6] strain. Out of 14 colonies grown on TDO media plates, only 3 were able to grow on TDO/X, QDO/X and QDO/X/A media plates. One of the colonies grew white on all of the media plates used and two re-grew pale blue on QDO/X and QDO/X/A media plates.

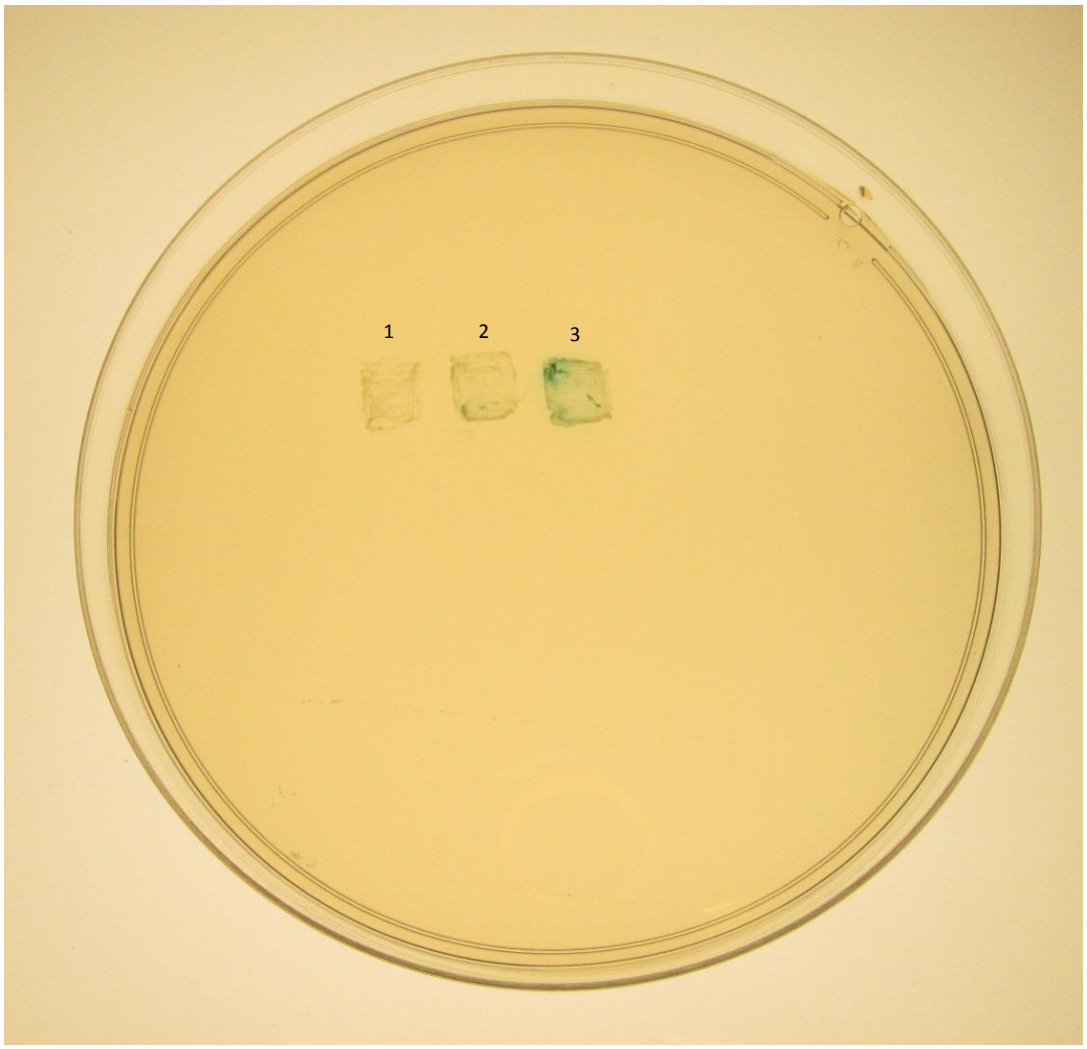

Figure 3.10 QDO/X/A media plate with patches of colonies grown in Y2H screen 5, which was performed using the Y2HGold [pBD-DEST/bait 6] strain. Three yeast colonies were able to grow on the most stringent QDO/X/A media plate. Colony 1 grew white whereas colonies 2 and 3 grew very pale blue, which means that none of the interactions was strong or abundant enough to activate all of the reporter genes.

The next Y2H screen (screen 6) was performed using Y2HGold [pBD-DEST/bait 8] strain. As previously, the mated culture was plated on TDO media plates in the first instance, resulting in growth of nine white colonies, which were subsequently re-patched onto TDO/X media plates. Out of nine white colonies grown on TDO/X, five were blue and four grew white. In the next stage of the screen, two of the white colonies were unable to regrow on QDO/X media plates and the other two regrew blue or pale blue. All five blue colonies were consistently growing blue on all selective media supplemented with X-α-gal. Table 3.6 summarises the phenotypes of colonies obtained in Y2H screen and the QDO/X/A plate showing the yeast patches is presented in Figure 3.11.

	Medium type		
Colony number	**TDO/X**	**QDO/X**	**QDO/X/A**
1	blue	blue	blue
2	blue	blue	blue
3	white	pale blue	pale blue
4	blue	blue	blue
5	white	x	x
6	blue	blue	blue
7	white	x	x
8	blue	blue	blue
9	white	blue	blue

Table 3.6 Summary of phenotypes of colonies grown in Y2H screen 6, which was performed using the Y2HGold [pBD-DEST/bait 8] strain. Nine white colonies were patched on TDO/X media plates, five of which grew blue and four were white. The blue colonies were also able to grow on more stringent media as well as two of the white colonies, which re-grew blue on QDO/X and QDO/X/A media plates. Two of the white colonies were unable to grow in more stringent conditions.

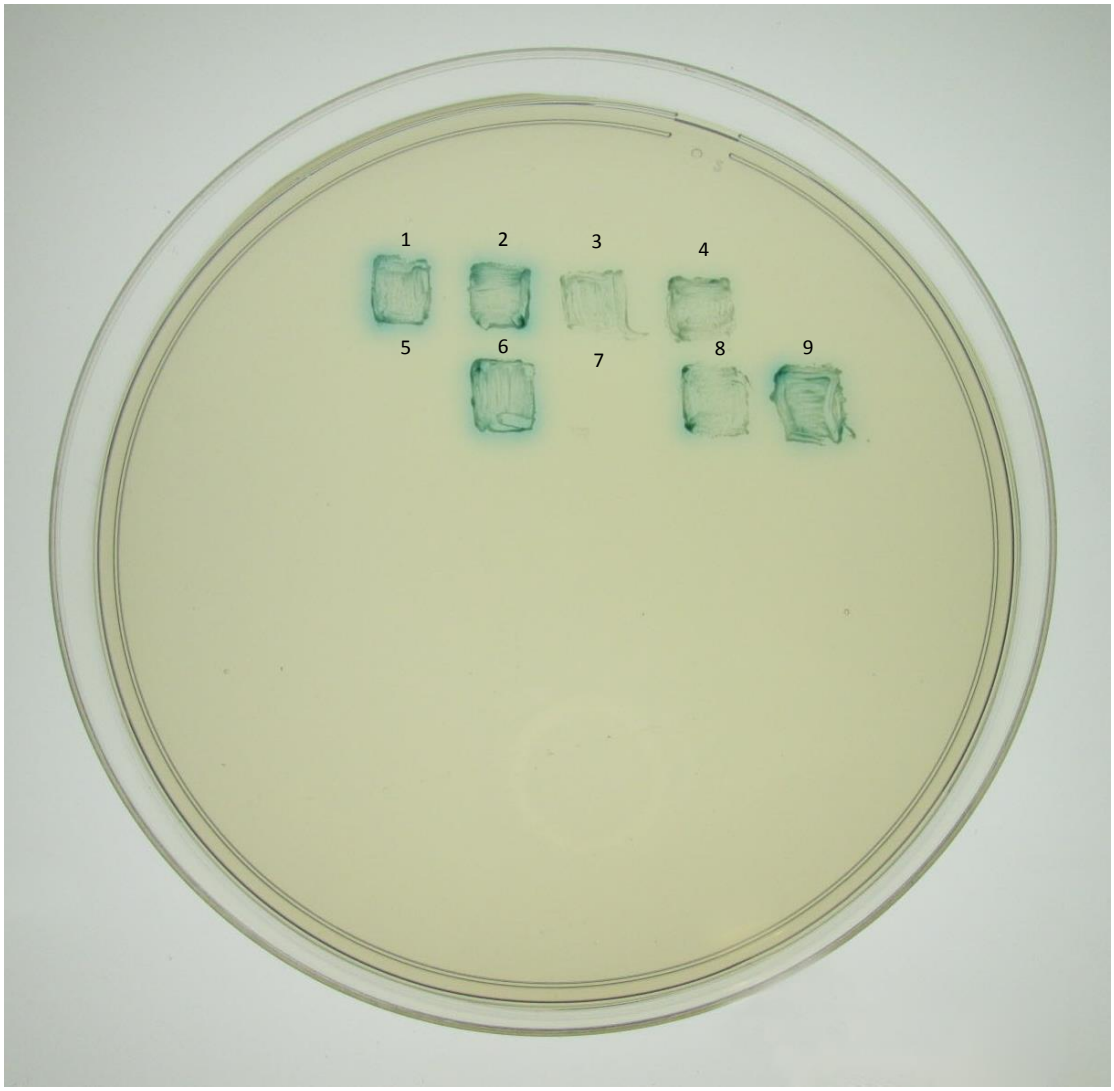

Figure 3.11 QDO/X/A media plate with patches of colonies grown in Y2H screen 6. Seven out of nine initially obtained colonies were able to grow blue or pale blue; two of the colonies were unable to survive the restrictive conditions of QDO/X/A media, which means that the interaction in these colonies were not strong or abundant enough to activate all of the reporter genes.

The final Y2H screen was carried out using the Y2HGold [pBD-DEST/bait 7] strain and the screen resulted in the growth of only one colony on TDO media. The colony was re-patched onto TDO/X, QDO/X and QDO/X/A media plates and grew blue on all of them (Table 3.1, Figure 3.12)

Altogether, seven Y2H screens were performed in the study resulting in 41 yeast colonies obtained on the low stringency media plates (TDO/X). Out of these, 35 colonies were able to survive more stringent conditions and re-grew on media additionally supplemented with AbA and X-α-gal, and lacking one more amino acid (QDO/X and QDO/X/A). Interestingly, some of the colonies initially grew white and became blue or pale blue when re-patched to more stringent conditions. This may be due to the interaction of bait and prey becoming more abundant over time or the yeast colonies overcoming restrictive conditions by adjusting their metabolism (revertant colonies). The latter scenario could shed negative light on the results obtained from colonies that changed colour from white to blue and these interactors would have to be disregarded based on such an assumption, following a general belief that the most genuine positive clones activate all of the reporter genes simultaneously.

	Medium type		
Colony number	**TDO/X**	**QDO/X**	**QDO/X/A**
1	blue	blue	blue

Table 3.7 Summary of the phenotype of the only colony grown in Y2H screen 7, which was performed using Y2HGold [pBD-DEST/bait 7]. The colony was able to grow blue on all of the selective media used.

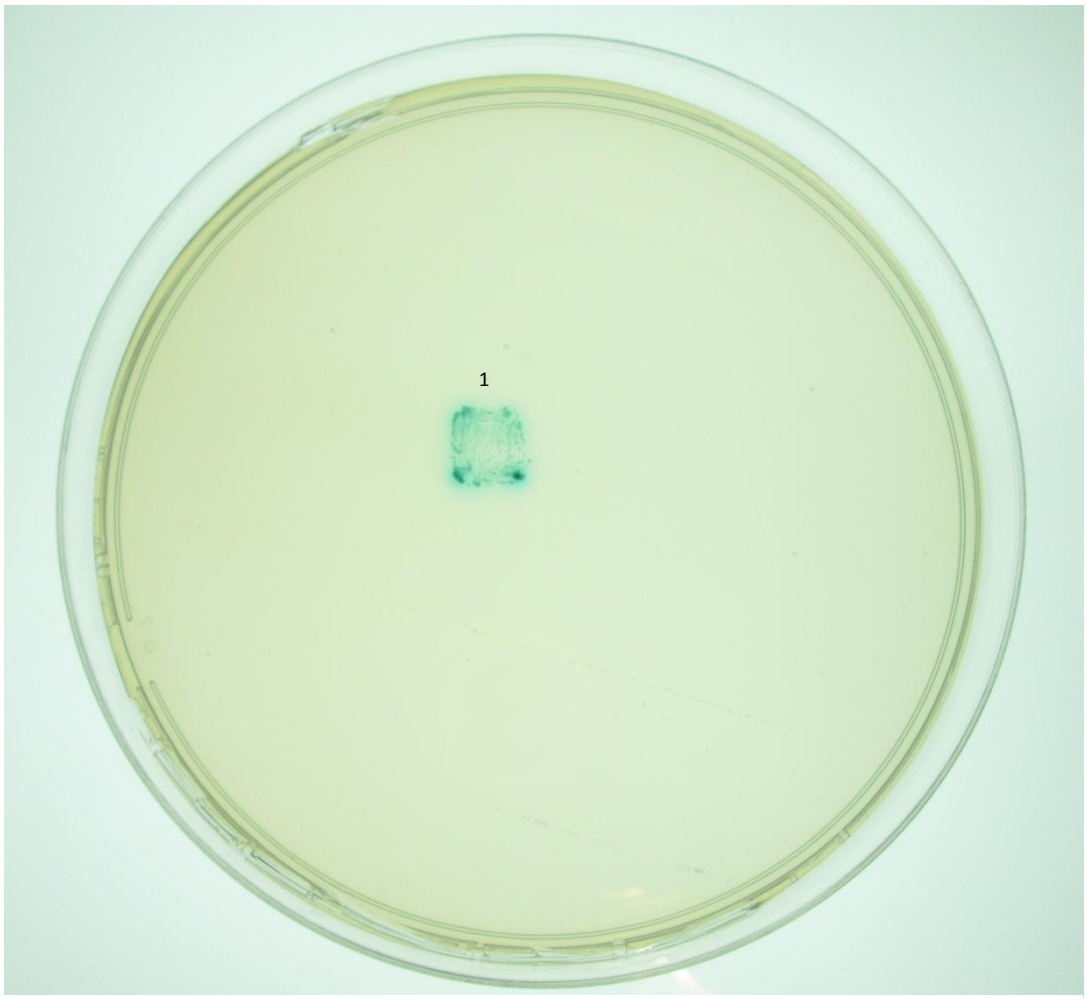

Figure 3.12 QDO/X/A media plate with a patch of the only yeast colony obtained in Y2H screen 7. The colony grew on all selective media used in the screen.

3.4 Identification of Putative Interacting Partners of EYS

The next step of the Y2H protocol was to identify the preys pulled out in screening. Since there were relatively few positive colonies obtained altogether, all colonies grown on TDO/X media were subjected to the analysis. The prey library inserts were amplified by yeast colony PCR and the products were run on an agarose gel. Following the Matchmaker™ Gold Yeast Two-Hybrid System User Manual, amplicons smaller than 200 bp were disregarded from further analysis as the peptides synthesised from them would be too short to provide reliable results. The PCR products larger than 200 bp were purified and sequenced using vector specific primers. The output sequences where afterwards analysed using online alignment tools (NCBI BLAST and UCSC Blat) in order to identify putative interacting partners of EYS. The information obtained from the online databases was used to identify genes encoding the preys that interacted with the bait and to check whether these gene fragments overlapped with the coding sequence. This was an important aspect of the analysis since the cDNA library used in the study was constructed using total retinal RNA, meaning that the prey inserts could also contain intronic sequences as well as fragments of ribosomal RNA and transfer RNA. Such preys had to be disregarded since the prey proteins translated from these sequences were artefacts. Another important aspect was to verify whether the prey inserts had been cloned in frame with the GAL4 AD; however, it is necessary to mention that it is a known fact that yeast can tolerate frameshifts, skip stop codons and continue with translation. It means that prey fragments which had not been cloned in frame, should not be completely disregarded but, as recommended by the system manufacturer, they should be re-cloned in frame and analysed further.

In the Y2H screen 4, growth of 28 yeast colonies was observed on TDO/X media plates; seven of these colonies contained a prey fragment smaller than 200 bp and were disregarded from further analysis. Interestingly, among these colonies there were the four colonies which grew white on TDO/X media and were unable to regrow in more stringent conditions. The remaining 21 prey fragments were sequenced and the outputs were analysed using online alignment tools. Out of 21 prey fragments, 13 contained sequences which aligned with protein coding fragments of genes (summarised in Table 3.8) whereas 8 of them aligned to either

intronic fragments or untranslated regions. The sequences of preys carrying coding sequences are summaries in Appendix G.

Colony number	Identified protein	Expression	Localisarion
1	Homo sapiens nuclear factor I/A (NFIA)	ubiquitous	nucleus
2	Homo sapiens small EDRK-rich factor 2 (SERF2)	ubiquitous	cytosol/nucleus
4	Homo sapiens eukaryotic translation initiation factor 3, subunit L (EIF3L)	ubiquitous	cytosol
5	Homo sapiens eukaryotic translation initiation factor 3, subunit L (EIF3L)	ubiquitous	cytosol
9	Homo sapiens nuclear factor I/A (NFIA)	ubiquitous	cytosol/nucleus
11	Homo sapiens aryl hydrocarbon receptor interacting protein-like 1 (AIPL1)	ubiquitous	cytosol/nucleus
12	Homo sapiens nuclear factor I/A (NFIA)	ubiquitous	cytosol/nucleus
15	Palmitoyl-protein thioesterase 2 (PPT2)	ubiquitous	cytosol
16	Homo sapiens fibulin 1 (FBLN1)	ubiquitous	extracellular matirx
19	Homo sapiens small EDRK-rich factor 2 (SERF2)	ubiquitous	cytosol/nucleus
22	Homo sapiens eukaryotic translation initiation factor 3	ubiquitous	cytosol
24	Homo sapiens ubiquitin A-52 residue ribosomal protein fusion product 1 (UBA52)	ubiquitous	cytosol/nucleus
26	Homo sapiens cytochrome c oxidase subunit VIIc (COX7C), nuclear gene encoding mitochondrial protein	ubiquitous	mitochondrial inner membrane

Table 3.8 Summary of prey fragments identified with bait 3. The table includes only prey fragments, which aligned to coding parts of the genome.

All of the three colonies grown in screen 5 (using bait 6) carried prey fragments shorter than 200 bp and/or were identified within non-coding genomic sequences. A similar finding was made when analysing prey fragments identified in Y2H screens 6 and 7 (baits 8 and 7 respectively), all of which aligned to non-coding genomic sequences (summarised in Appendix H).

The analysis of prey fragments identified in the Y2H screening revealed that only bait 3 was able to pull out genuine potential interactants. However, not all of the identified proteins seemed to be likely to interact with EYS. It has been shown that the porcine orthologue of EYS localises to the photoreceptor outer segments and the *Drosophila* orthologue of EYS plays a role in the organisation of the

compound eye. Based on these findings, proteins such as nuclear factors or translation initiation factors were excluded from further analysis at this stage and a shortlist of preys subjected to post-screening control experiments is presented in Table 3.9.

It is necessary to mention that none of the identified preys were cloned in frame with GAL4 activation domain and preys of interest would have to be re-cloned in frame and re-examined using bait 3.

Colony number	Prey identified	Prey length (Full length)	Expression	Localisation
2	Homo sapiens small EDRK-rich factor 2 (SERF2)	442 bp (643 bp)	ubiquitous	cytosol/nucleus
11	Homo sapiens aryl hydrocarbon receptor interacting protein-like 1 (AIPL1)	595 bp (2959 bp)	ubiquitous	cytosol/nucleus
15	Palmitoyl-protein thioesterase 2 (PPT2)	327 bp (1759 bp)	ubiquitous	cytosol
16	Homo sapiens fibulin 1 (FBLN1)	253 bp (11756 bp)	ubiquitous	extracellular matrix
24	Homo sapiens ubiquitin A-52 residue ribosomal protein fusion product 1 (UBA52)	252 bp (508 bp)	ubiquitous	cytosol/nucleus
26	Homo sapiens cytochrome c oxidase subunit VIIc (COX7C)	471 bp (1584 bp)	ubiquitous	mitochondrial inner membrane

Table 3.9 A shortlist of prey fragments identified with bait 3 and selected for analysis in post Y2H screening control experiments.

3.5 Confirmation of Positive Interaction

The next stage of the data analysis was devoted to confirming whether the interactions identified by the Y2H screens are genuine and not false-positives. It could be that the preys identified interact with GAL4 DBD, which would result in expression of the reporter genes and obtaining false positive results and such a scenario needed to be excluded. Moreover, the Y2H results need to be reproducible in order to be considered genuine. In order to verify these two aspects, prey plasmids were isolated from yeast cells, amplified in competent bacteria and purified. The purified vectors were sequenced to confirm their integrity and transformed into Y187 yeast strain.

In the first experiment it was established whether the identified interactions could be reproduced using freshly transformed yeast strains. To do that, small scale mating was performed using Y2HGold [pBD-DEST/bait 3] and Y187 yeast strain transformed with each of the tested prey constructs. Mated cultures were plated on a range of selective media allowing examination of whether the transformation and mating were successful, and if the reporter genes were activated. The results obtained are presented in Figure 3.13. As it can be observed, 2 out of 6 colonies were able to grow on the most restrictive media and activated all 4 of the reporter genes. The successful preys carried fragments of *AIPL1* and *FBLN1* genes and according to this experiment only these two interactants were genuine. The difference between the control experiment and a screen lies in the order of plating and exposing yeast colonies to different selective conditions. When screening, positive colonies were re-patched onto increasingly restrictive media in a sequential manner, i.e. colonies grown on one type of media were re-patched onto more stringent media once they were fully-grown. In contrast, for the post-screening control experiments, dilutions of mated culture were plated on the full-range of selective media simultaneously. This means that the positive diploid cells were required to activate the reporter genes immediately to be able to survive; in screening they would have had time to adjust to increasingly stringent conditions, which makes it easier for the revertant colonies to develop. In conclusion, only the interactions which were able to be reproduced in the post-screen control experiments can be considered genuine.

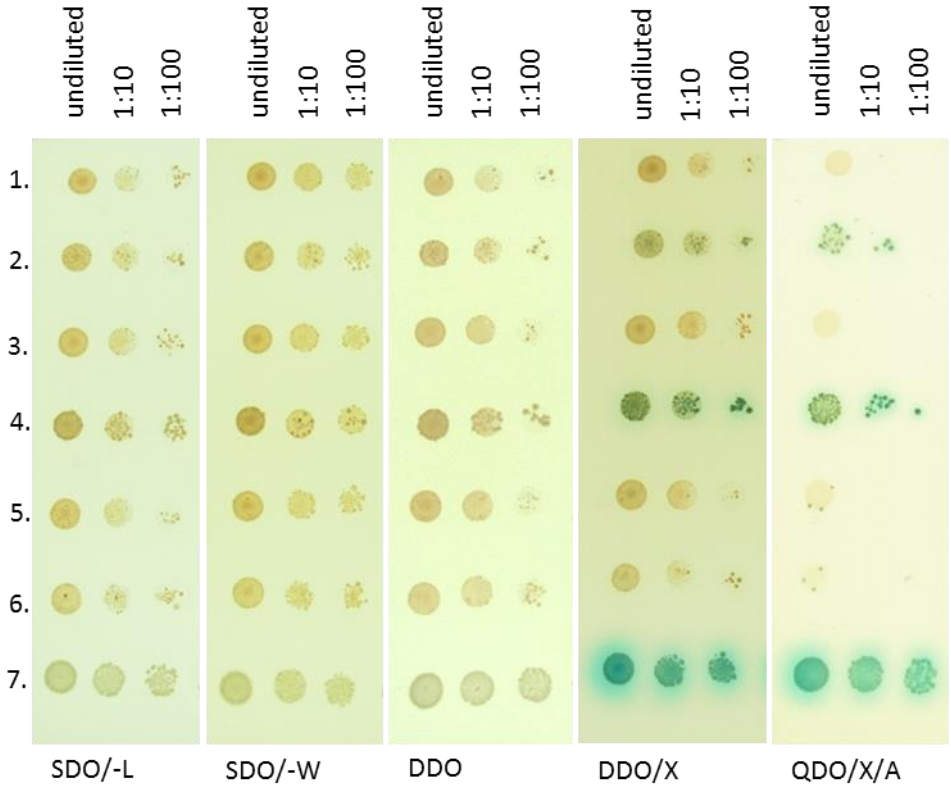

1. Y2HGold[pGBKT7-bait 3] vs. Y187[pGADT7-SERF2]
2. Y2HGold[pGBKT7- bait 3] vs. Y187[pGADT7-AIPL1]
3. Y2HGold[pGBKT7- bait 3] vs. Y187[pGADT7-PPT2]
4. Y2HGold[pGBKT7- bait 3] vs. Y187[pGADT7-FBLN1]
5. Y2HGold[pGBKT7- bait 3] vs. Y187[pGADT7-UBA52]
6. Y2HGold[pGBKT7- bait 3] vs. Y187[pGADT7-COX7C]
7. Y2HGold[pGBKT7-p53] vs. Y187[pGADT7-T] (positive control)

Figure 3.13 Post-screening control experiment aiming to reproduce the interactions identified in screen 4 performed with bait 3. Numbers 1-7 represent different mated cultures. Each of the cultures was plated in three dilutions on a range of selective media. Only cultures 2 and 4, containing prey fragments of *AIPL1* and *FBLN1*, were able to grow on all the media, which demonstrates that they are positive interactions. In this figure, prey gene names represent prey fragments of the genes and not full gene sequences.

In order to verify whether the prey fragments are able to interact with GAL4 DBD on its own, transformed Y187 yeast strains were mated with Y2HGold [pGBKT7-WT] that carried wild type GAL4 DBD. Serial dilutions of mated cultures were plated on a range of selective media, as shown in Figure 3.14. According to this experiment, the prey containing a fragment of *FBLN1* gene was able to interact with GAL4 DBD and activate the expression of all reporter genes. This interaction had to be considered a false positive result and excluded from further analysis.

In summary, out of the six putative interacting partners of EYS protein identified with bait 3, only one turned out to be genuine and the prey was found to be a fragment of *AIPL1* gene. The remaining five candidate preys had to be disregarded as they were unable to reproduce the interaction or they showed interaction with GAL4 DBD rather than the bait fragment of EYS protein.

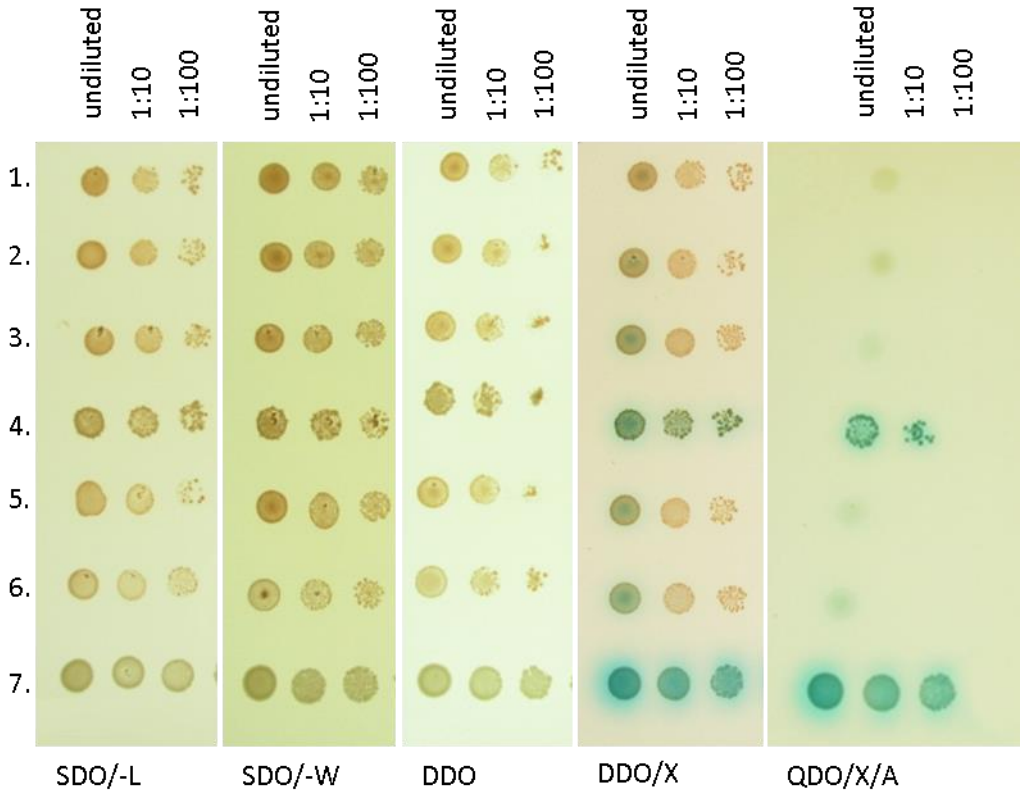

1. Y2HGold[pGBKT7-WT] vs. Y187[pGADT7-SERF2]
2. Y2HGold[pGBKT7-WT] vs. Y187[pGADT7-AIPL1]
3. Y2HGold[pGBKT7-WT] vs. Y187[pGADT7-PPT2]
4. Y2HGold[pGBKT7-WT] vs. Y187[pGADT7-FBLN1]
5. Y2HGold[pGBKT7-WT] vs. Y187[pGADT7-UBA52]
6. Y2HGold[pGBKT7-WT] vs. Y187[pGADT7-COX7C]
7. Y2HGold[pGBKT7-p53] vs. Y187[pGADT7-T] (positive control)

Figure 3.14 Post-screening control experiment aiming to verify whether the preys could interact with GAL4 DBD. Numbers 1-7 represent different mated cultures. Each of the cultures was plated in three dilutions on a range of selective media. The culture number 4, containing a prey fragment of FBLN1 gene grew blue which indicates that it interacted with the GAL4 DBD. For that reason, this interaction had to be regarded as false positive. In this figure, prey gene names represent prey fragments of the genes and not full gene sequences.

3.6 AIPL1

Mutations in *AIPL1* cause severe early-onset retinal degeneration called Leber's congenital amaurosis (LCA), which is characterized by the loss of vision diagnosed at birth or within first months of life (LCA4; MIM 604393)(Sohocki *et al.*, 2000). In humans, *AIPL1* is specifically expressed in the pineal gland and the photoreceptor cells, where it localises to the region spanning from the synapse to the inner segment with enrichment at the connecting cilium (Sohocki *et al.*, 2000; van der Spuy *et al.*, 2002). Moreover, AIPL1 is not only expressed in the adult photoreceptors but its expression has also been demonstrated to coincide with the development of both rods and cones (van der Spuy *et al.*, 2003).

The AIPL1 protein is composed of an N-terminal FKBP-like domain followed by three tetratricopeptide (TPR) repeats and a C-terminal proline-rich region (Figure 3.15) (Majumder *et al.*, 2013; Sohocki *et al.*, 2000). The FKBP-like domain of AIPL1 has been suggested to modulate interactions with farnesyl residues whereas the TPR domains can function as molecular scaffolds facilitating protein-protein interactions and assembly of higher order protein complexes. The role of the proline-rich C-terminal region has not been fully understood; however, it could participate in regulation of rapid protein exchange or recruitment in protein complexes (Majumder *et al.*, 2013; van der Spuy, 2006). The domains which AIPL1 is composed of are commonly found in proteins with chaperoning activity and in fact, AIPL1 shares homology with AIP (aryl hydrocarbon receptor interacting protein) and FKBP51 and FKBP52 proteins, all of which belong to a group of co-chaperones interacting with chaperone Hsp90 via a TPR repeat domain (Scheufler *et al.*, 2000; Sohocki *et al.*, 2000).

The function of AIPL1 in the human retina has been widely studied and a significant amount of knowledge of the biology of AIPL1 comes from studying its interactome. The first identified interacting partner of AIPL1 was NUB1 (NEDD8 Ultimate Buster 1), which is a negative regulator of NEDD8 and recruits NEDD8 and its conjugates to the proteasome for degradation (Akey *et al.*, 2002; Kamitani *et al.*, 2001; Kito *et al.*, 2001). Further research demonstrated that AIPL1 modulates the translocation of NUB1 from the nucleus to the cytoplasm and acts in a chaperone-like manner to suppress formation of inclusions by NUB1 fragments (van der Spuy & Cheetham, 2004).

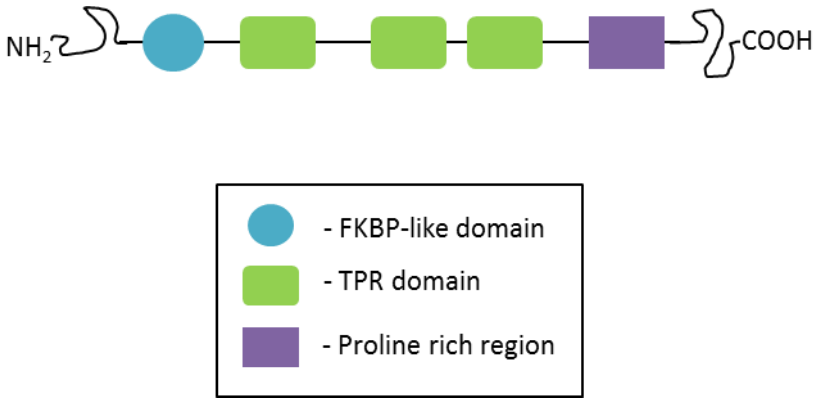

Figure 3.15 A schematic view of the predicted domain structure of AIPL1. The AIPL1 protein is composed of an N-terminal FKBP-like domain followed by three tetratricopeptide (TPR) repeats and a C-terminal proline-rich region.

Moreover, AIPL1 can also interact with FAT10 and FAT10-modified proteins, and form ternary complexes with NUB1. FAT10 is a ubiquitin independent signal for degradation, which is promoted by binding with NUB1; it has been demonstrated that binding with AIPL1 has an inhibitory effect on the NUB1-mediated degradation of a FAT10-modified substrates (Bett *et al.*, 2012). AIPL1 has also been shown to form heterocomplexes with Hsp70 and Hsp90 molecular chaperones that play essential role in photoreceptor proteostasis. Furthermore, it has been demonstrated that the cooperation of AIPL1 and Hsp70 supresses formation of NUB1 inclusions in a chaperone-like manner (Hidalgo-de-Quintana *et al.*, 2008).

Furthermore, Yeast 2-hybrid analysis has demonstrated that AIPL1 interacts with and aids in farnesylation of proteins (Majumder *et al.*, 2013; Ramamurthy *et al.*, 2003). Protein farnesylation, a type of prenylation, is a lipid post-translational modification of proteins which have a C-terminal CaaX motif recognised by farnesyltransferase enzyme. Farnesylation of proteins enhances protein-membrane interactions and protein-protein interactions (Zhang & Casey, 1996).

The analysis of AIPL1 hypomorphic mouse models revealed decreased levels of rod cGMP phosphodiesterase (PDE), which is one of the major components of the phototransduction cascade. PDE has been shown to be a client protein of AIPL1, chaperoning activity of which is required for localisation of PDE in the photoreceptor outer segments (Liu *et al.*, 2004b). Interestingly, PDE is a farnesylated protein and further studies have shown that AIPL1 interacts with the catalytic α-subunit of PDE and the interaction is essential for proper assembly of PDE (Kolandaivelu *et al.*, 2009).

In the most recent report, AIPL1 was demonstrated to interact and co-localise with EB proteins, which are microtubule plus-end tracking proteins that have an important function in microtubule dynamics. Co-localisation was detected at the photoreceptor connecting cilium but not in the cellular microtubule network or cilia of non-retinal cells, suggesting that the association of AIPL1 and EB proteins may have a specific function at the photoreceptor connecting cilium (Hidalgo-de-Quintana *et al.*, 2015).

The biology of AIPL1 has been extensively studied and there has been evidence provided that its disruption has significant implications for the

homeostasis of photoreceptor cells. Attempts of gene replacement therapy have been undertaken in murine models using AAV vectors. The rescue of a disease phenotype has been achieved, giving hope for the future clinical trials in humans (Sun *et al.*, 2010; Tan *et al.*, 2009).

3.7 Analysis of AIPL1 as an Interacting Partner of EYS Using Y2H

The prey fragment identified in Y2H screen performed with bait 3 aligned to the sequence of a human *AIPL1* gene. The prey fragment of AIPL1 identified by the Y2H screen comprised of 103 amino acids, which constitutes approximately 27 % of full length AIPL1, and covered a part of the third TPR domain and the C-terminal proline-rich region (Figure 3.16).

The Y2H system provides not only a powerful tool for identifying novel interacting partners of a protein of interest but it is also useful for investigation of already known or putative interactions. In order to further analyse the interaction of EYS and AIPL1 using the Y2H system, the interaction of bait 3 and AIPL1 prey fragment was reproduced and compared to a number of controls. In the first instance, it was tested whether bait 3 is able to interact with the full length AIPL1 prey. In addition to the positive and negative controls provided by the system manufacturer, a published and well characterised interaction of AIPL1 and NUB1 was used as a further control (Akey *et al.*, 2002). In this experiment NUB1 was cloned with GAL4 DBD and AIPL1 was fused with GAL4 AD. As it can be observed in Figure 3.17, the interaction of bait 3 and AIPL1 prey fragment could be reproduced (row 1); however, the bait was unable to interact with the full length AIPL1 (row 3). Furthermore, no blue colonies grew in the additional positive control culture containing NUB1 bait and AIPL1 prey (row 2). The interaction of AIPL1 and NUB1 was identified using the Y2H system, and well characterised in yeast as well as mammalian systems. It is, however, important to note that in the study, in which the interaction was discovered, a bovine sequence of AIPL1 was used as bait to screen a bovine retinal cDNA library. This means that, even though the interaction was proven to occur between human proteins, their bovine orthologues seem to be more likely to interact in yeast cells. This is an example of how complex the analysis of interactomes can be, especially when different species and systems are involved and mixed together.

A

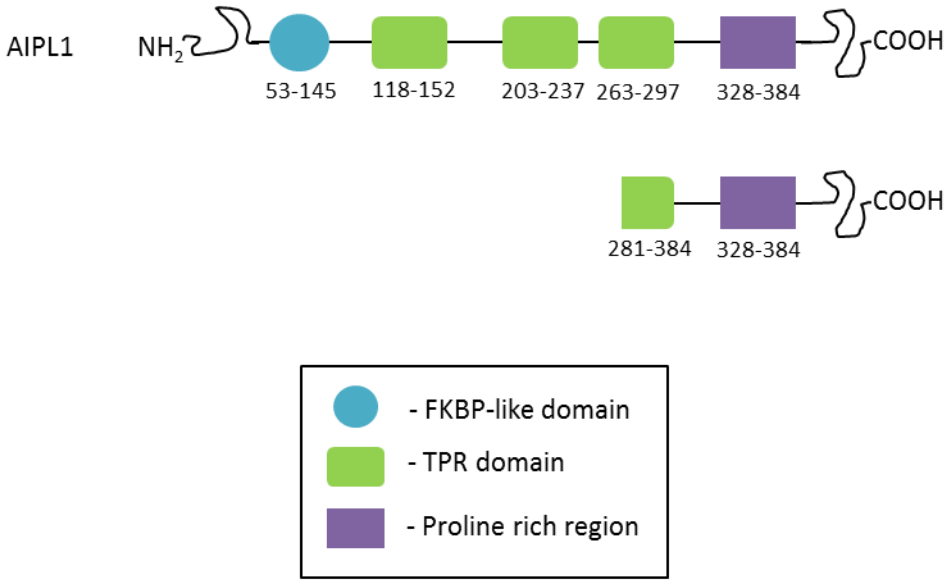

B

MDAALLLNVEGVKKTILHGGTGELPNFITGSRVIFHFRTMKCDEERTVIDDSRQVGQPMHIII
GNMFKLEVWEILLTSMRVHEVAEFWCDTIHTGVYPILSRSLRQMAQGKDPTEWHVHTCGL
ANMFAYHTLGYEDLDELQKEPQPLVFVIELLQVDAPSDYQRETWNLSNHEKMKAVPVLHGE
GNRLFKLGRYEEASSKYQEAIICLRNLQTKEKPWEVQWLKLEKMINTLILNYCQCLLKKEEYYE
VLEHTSDILRHHPGIVKAYYVRARAHAEVWNEAEAKADLQKVLELEPSMQKAVRRELRLLEN
RMAEKQEEERLRCRNMLSQGATQPPAEPPTEPPAQSSTEPPAEPPTAPSAELSAGPPAEPATE
PPPSPGHSLQH

Figure 3.16 Analysis of the prey fragment of AIPL1. **(A)** Alignment of full-length AIPL1 with AIPL1 prey fragment identified in Y2H screen 4. The domain structure should be read as follows: the blue oval: FKBP-like domain, the green boxes: TPR domains and the purple box: primate-specific proline rich region. AIPL1 prey fragment overlapped a part of the third TPR domain and the proline-rich region of AIPL1. Numbers below the domains correspond to the amino acid residues of AIPL1 **(B)** Protein sequence of full length AIPL1 (derived from Ensemble database, accessed on 12.03.2015). Amino acids in red font represent the sequence of the AIPL1 prey fragment.

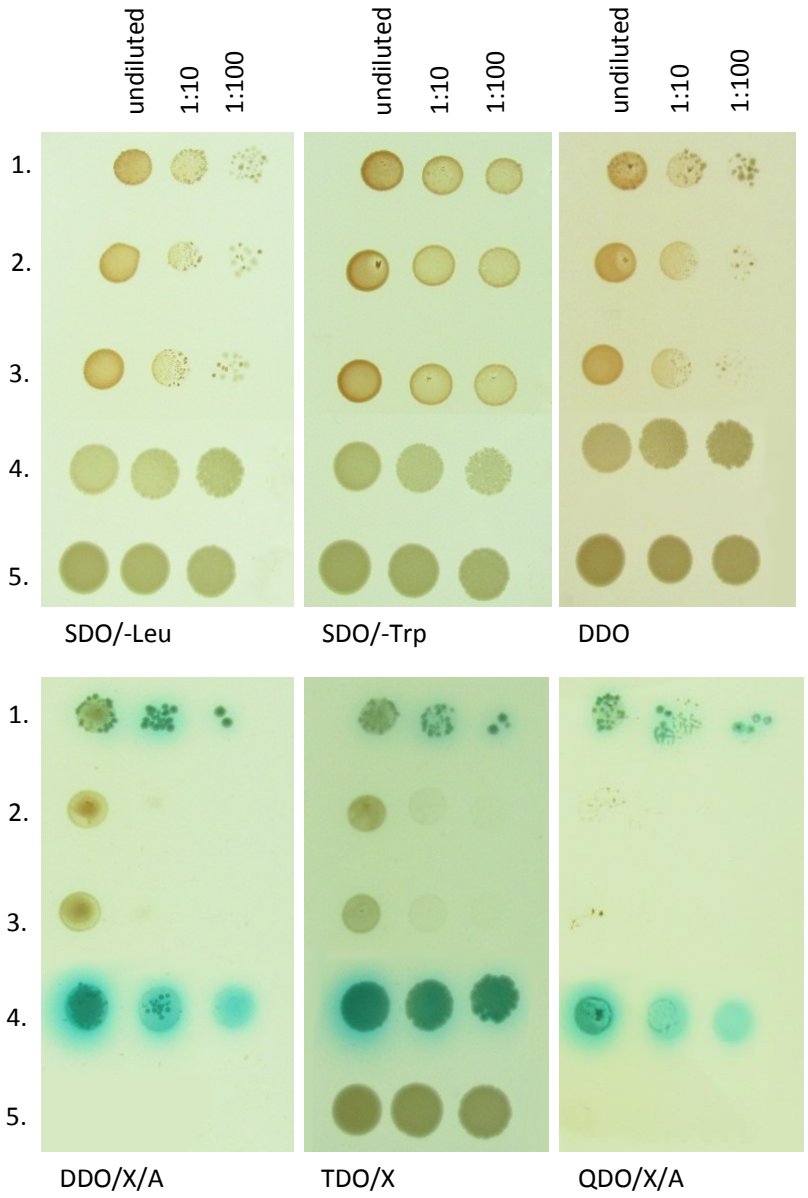

1. Y2HGold[pBD-DEST-bait 3] vs. Y187[pGADT7-prey AIPL1]
2. Y2HGold[pBD-DEST-NUB1] vs. Y187[pAD-DEST-AIPL1]
3. Y2HGold[pBD-DEST-bait 3] vs. Y187[pAD-DEST-AIPL1]
4. Y2HGold[pBD-DEST-p53] vs. Y187[pGADT7-T] (positive control)
5. Y2HGold[pBD-DEST-Lam] vs. Y187[pGADT7-T] (negative control)

Figure 3.17 Control experiment validating whether bait 3 can interact with full length AIPL1. An additional control using a known interaction between AIPL1 and NUB1 was used. Numbers 1-5 represent different cultures, each of which was plated on a range of selective media in three dilutions. Blue colour of the colonies indicates activation of reporter gene and digestion of X-α-gal added to the media. The interaction was demonstrated only for culture 1, which contained bait 3 and AIPL1 prey fragment.

Furthermore, one of the well-known drawbacks of Y2H is its low reproducibility between experiments and this could also explain why the interaction of AIPL1 and NUB1 was not reproduced (reviewed in Caufield *et al.*, 2012).

Another possible scenario could be that the assembly of fully functional GAL4 was impossible due to the incorrect conformation of the fusion proteins. To address that, in the next experiment the GAL4 tags were switched and AIPL1 was cloned with GAL4 DBD whereas NUB1 was cloned with GAL4 AD.

Moreover, it must not be overlooked that the AIPL1 prey fragment, as well as the other prey fragments fished out in the Y2H screening, was not in frame with GAL4 AD. In spite of the fact that the nature of yeast cells allows them to tolerate frameshifts, skip stop codons and continue with translation, it was essential to verify whether the interaction of bait 3 and AIPL1 prey fragment can be reproduced when the prey fragment is cloned in frame with the GAL4 AD.

Therefore, the next experiment addressed the aforementioned issues and the results are presented Figure 3.18. The interaction of bait 3 and AIPL1 prey fragment was consistently reproduced (row 1); however, when AIPL1 prey fragment was cloned in frame with GAL4 AD, no growth of colonies was observed on QDO/X/A media plate. Very little growth and very slightly blue colonies could be observed in undiluted culture on TDO/X media plates (row 2); nonetheless, it would be misleading to consider these colonies positive when compared to the original interaction and the controls. The interaction between AIPL1 and NUB1 could not be reproduced in this experiment either, suggesting that human orthologues of the two proteins do not interact in yeasts equally abundantly to their bovine counterparts.

In summary, the interaction of bait 3 and AIPL1 prey fragment was consistently reproduced in each of the control experiments. However, it was not possible to confirm whether the proteins interact when AIPL1 prey fragment was re-cloned in frame with the GAL4 AD domain. This observation could suggest that the result obtained in Y2H screening was a false positive interaction, occurring between bait 3 and the artefact protein synthesised on the template of the fragment of the *AIPL1* gene, which had not been cloned in frame with the GAL4 AD. Nonetheless, due to the specific biology of yeast cells (they can tolerate frameshifts, skip stop codons and continue with translation) the interaction of

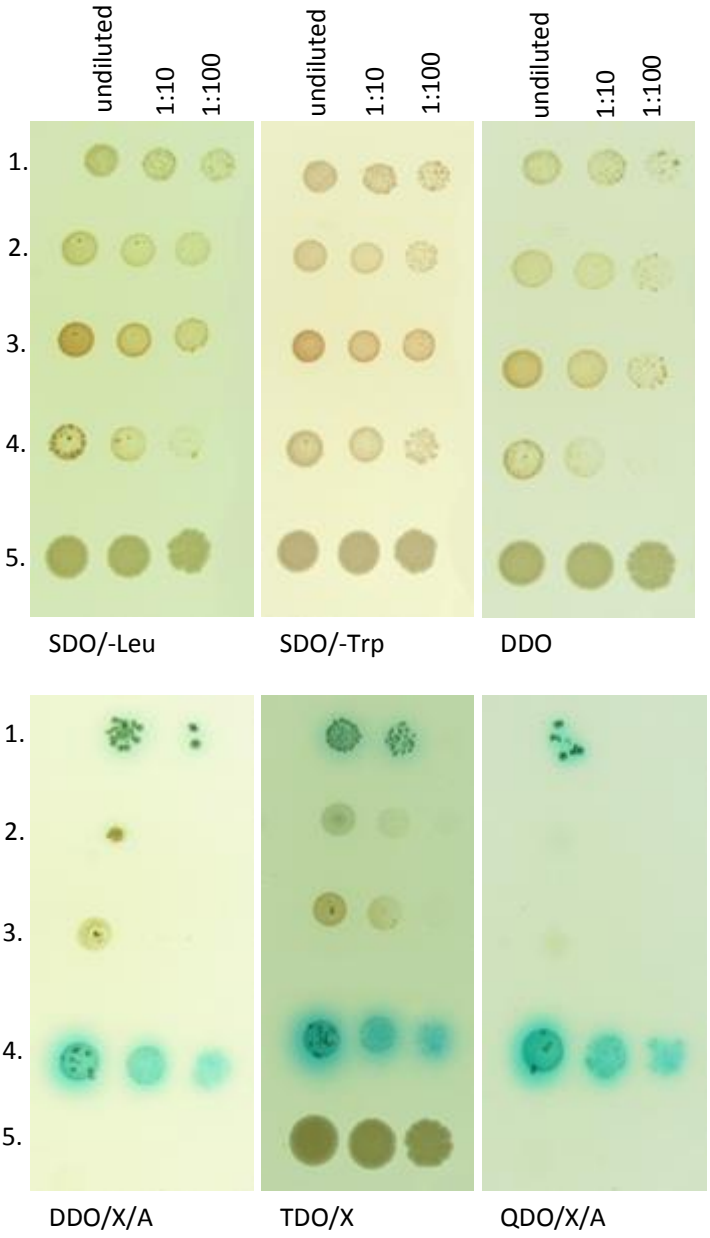

1. Y2HGold[pBD-DEST-bait 3] vs. Y187[pGADT7-prey AIPL1]
2. Y2HGold[pBD-DEST-bait 3] vs. Y187[pAD-DEST- prey AIPL1 in frame]
3. Y2HGold[pBD-DEST-AIPL1] vs. Y187[pAD-DEST NUB1]
4. Y2HGold[pBD-DEST-p53] vs. Y187[pGADT7-T] (positive control)
5. Y2HGold[pBD-DEST-Lam] vs. Y187[pGADT7-T] (negative control)

Figure 3.18 Control experiment verifying whether bait 3 is able to interact with AIPL1 prey fragment when the latter is cloned in frame with GAL4 AD. The known interaction of AIPL1 and NUB1 was used as a control in addition to the controls provided in the Y2H kit. Numbers 1-5 represent different cultures, each of which was plated on a range of selective media in three dilutions. Apart from the positive control, only culture 1 was able to grow blue on all of the selective media, which was indicative of an interaction.

bait 3 and AIPL1 cannot be categorically disproved without provision of additional evidence.

Furthermore, AIPL1 has been suggested to be a component of a chaperoning macromolecular heterocomplex that participates in protein biosynthesis and cellular translocation. It is, therefore, likely that EYS could be a client protein of AIPL1 and the interaction of EYS and AIPL1 could be essential for its proper folding and localisation. This purely theoretical assumption could be true but would require a significant amount of additional experimental data in its support.

In light of the above, further analysis of the putative interaction of EYS and AIPL1 was carried out in spite of the ambiguous results of Y2H. This was necessary for completeness of the study and thorough validation of Y2H data.

3.8 Validation of Y2H Results in Mammalian Systems

Any interaction identified by Y2H requires further experimental evidence confirming its authenticity. In this study, two validation methods were employed to verify the interaction of EYS and AIPL1: immunocytochemistry (ICC) and co-immunoprecipitation (Co-IP). ICC was performed in cultured mammalian cell lines and verified co-localisation of the two proteins of interest whereas Co-IP assays were conducted to establish whether the two proteins exist in one protein complex.

For better understanding of the results presented in this section, it should be noted that the results obtained in the project are not chronologically presented in the thesis. Some of the knowledge used to conduct and improve experiments described in this chapter was gained from experiments described further in the thesis. First of all, it should be taken into account that EYS is one of the largest genes discovered in the human retina thus far. The size of the gene has implications for feasibility of many standard procedures used in molecular biology such as cloning or transfections. Gateway technology used in the study allowed trouble-free cloning, however, transfection of the full length EYS vectors turned out to be extraordinarily challenging and successful only in very few attempts, as it will be described in more detail in the following Chapters 4 and 5.

Furthermore, detailed analysis of the genetic structure of *EYS* resulted in identification of two novel short isoforms of EYS expressed in the retina, annotated in UniProt as isoform 2 and isoform 3. This topic will be elaborated on in Chapter 4 but it is necessary to explain here that the isoforms map to the N-terminal fragment of full length EYS isoform 1 and overlap with bait 3, constituting around 40 % of its length. Therefore, these isoforms were included in the study for validation of the potential interaction with AIPL1 since they as well may interact with this putative binding partner.

3.8.1 Co-localisation Studies of Putative EYS-AIPL1 Interaction

Co-localisation studies of EYS and AIPL1 were performed in secondary cells lines. Both EYS and AIPL1 are photoreceptor specific proteins and the availability of cell lines endogenously expressing the two proteins is limited. In fact, there was

only one cell line available meeting this criterion, which was Y79 human retinoblastoma cell line. Y79 cells grow in suspension, are round in shape and have very little cytoplasm and membrane, which makes it challenging to properly distinguish their organelles under a light or confocal microscope. Therefore, protocols enabling attachment of Y79 cells to glass coverslips and outgrowth of protrusions had to be optimised prior to further experiments (see section 2.14.4 Y79 Cell Attachment and Differentiation). When overexpressing the proteins of interest, a human epitheloid cervix carcinoma (HeLa) cell line was used. HeLa cells were chosen because the efficiency of transfections was higher than in other tested cell lines.

3.8.1.1 Immunolabelling of EYS and AIPL1 in Y79 cells

In the first instance, endogenous expression patterns of EYS and AIPL1 were investigated. Y79 cells were seeded on poly-L-lysine pre-coated coverslips, fixed and stained with anti-EYS3 goat and anti-AIPL1 rabbit antibodies. A confocal micrograph shown in Figure 3.19 depicts a cluster of immunolabelled Y79 cells in which a potential co-localisation of EYS and AIPL1 can be observed (yellow signal). It has previously been demonstrated that AIPL1 localises to the cytoplasm and to the nucleus (van der Spuy *et al.*, 2002), and that expression pattern could be observed in this experiment. Nonetheless, the specific morphology of Y79 cells makes it difficult to assess whether the green signal coming from the anti-EYS3 antibody is localised in the cytoplasm, cell membrane or both. In order to be able to look into this matter more deeply, overexpression of the proteins of interest was attempted. As it was mentioned previously, it was not possible to successfully transfect Y79 cells with tagged EYS construct due its size and therefore, Y79 cells were transfected only with myc-tagged AIPL1 and the proteins of interest were detected using anti-EYS1 rabbit and anti-myc mouse antibodies. A cluster of two Y79 cells overexpressing myc-AIPL1 is shown in Figure 3.20. As it can be seen in the micrograph, AIPL1 is characteristically localised to the cytoplasm and the nucleus. The green signal coming from anti-EYS1 antibody forms a ring around the nucleus, which overlaps with AIPL1. This suggests that EYS is localised to the cytoplasm; nonetheless, some of the signal could also be associated with the cell membrane.

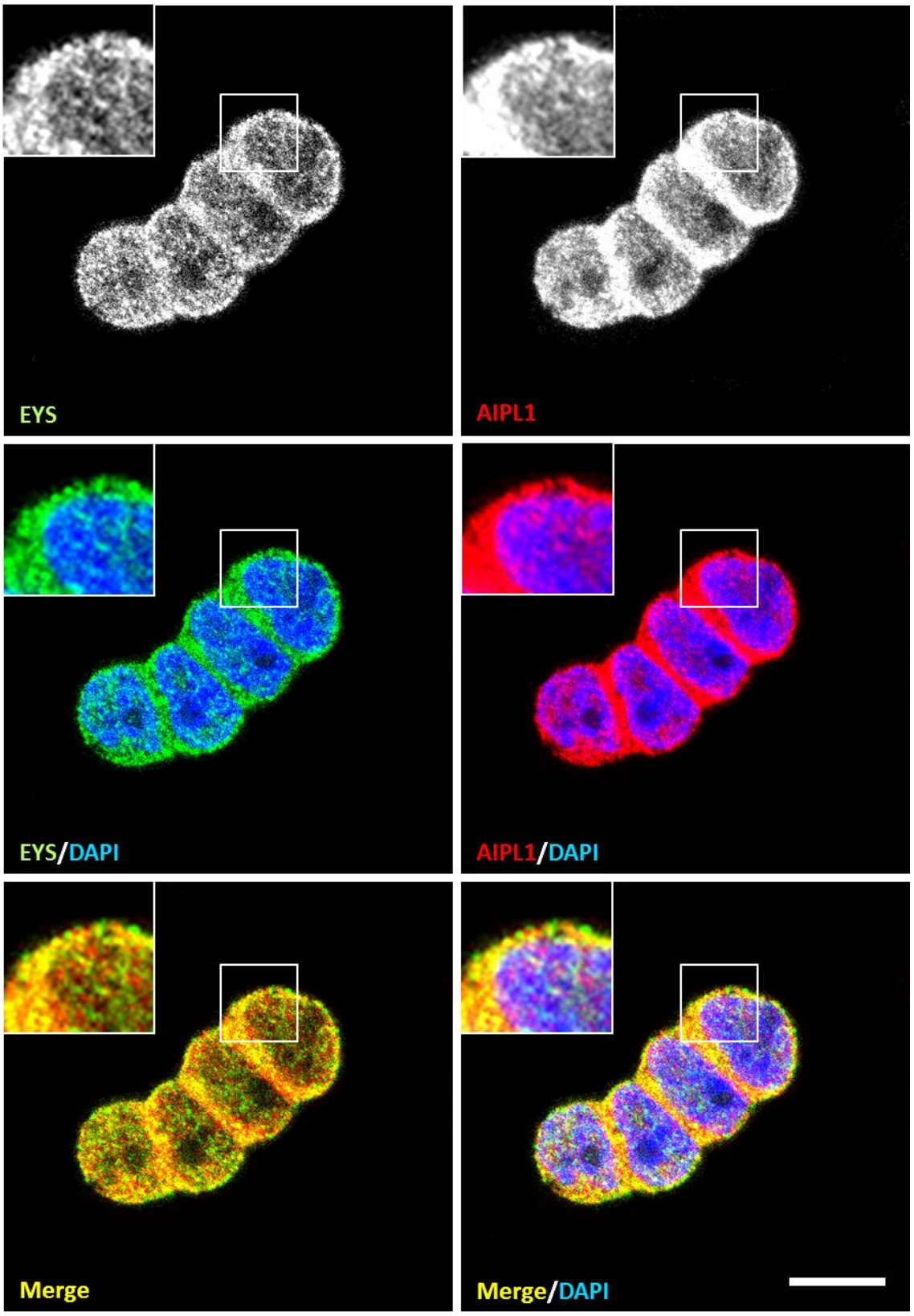

Figure 3.19 Localisation of EYS and AIPL1 in a cluster of Y79 cells. AIPL1 (red) localises to the cell cytoplasm and cell nucleus and EYS (green) overlaps with the cytoplasmic portion of the signal; co-localisation is indicated by yellow signal. The zoomed inserts represent the area demarcated by the white square in the images. The cells were immunolabelled with goat anti-EYS3 and rabbit anti-AIPL1 antibodies. Secondary antibodies were AlexaFluor 488 conjugated donkey anti-goat and Cyanine-3 conjugated donkey anti-rabbit antibodies. Nuclei are stained using DAPI (blue). Scale bar: 10 μm.

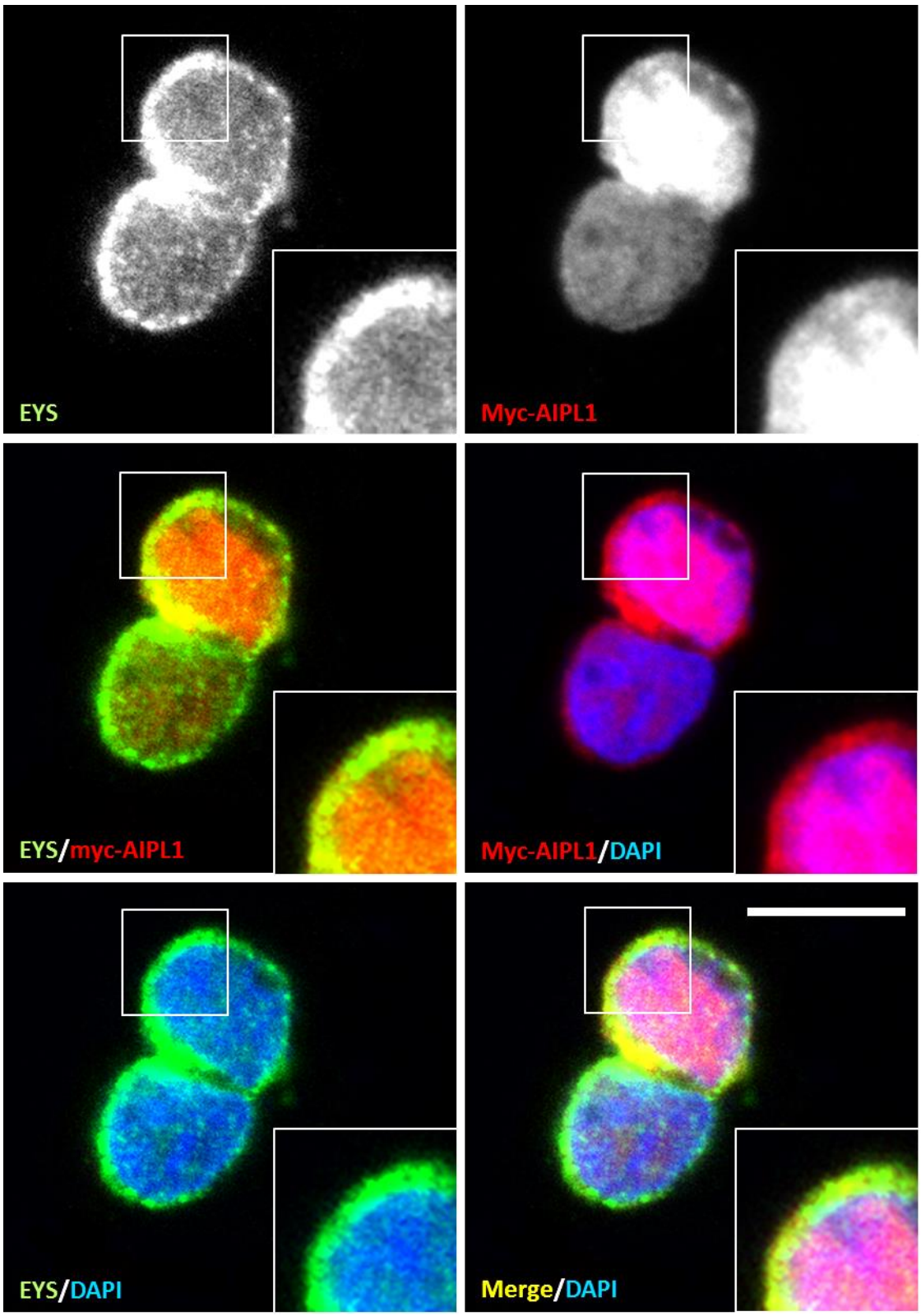

Figure 3.20 Localisation of EYS and myc-AIPL1 in a cluster of two Y79 cells. Myc-AIPL1 (red) was detected in the nucleus and the cell cytoplasm and EYS (green) overlaps with the cytoplasmic portion of the signal; co-localisation is indicated by yellow signal. The zoomed inserts represent the area demarcated by the white square in the images. Rabbit anti-EYS1 and mouse anti-myc primary antibodies were used. Secondary antibodies included AlexaFluor 488 conjugated goat anti-rabbit and AlexaFluor 633 conjugated goat anti-mouse antibodies. Nuclei are stained using DAPI (blue). Scale bar: 10 μm.

The merged signal in Figure 3.20 is only slightly yellow; however, it should be taken into account that the intensities of green and red signals differ depending on many factors, such as expression levels and affinity of the antibodies. It means that the strength of the yellow signal is variable and might not be equally apparent in all experiments. From the experiments performed on Y79 cells it could be concluded that EYS could co-localise with AIPL1, however, more detailed analysis would be required to fully validate this hypothesis. Notably, the existence of EYS short isoforms 2 and 3 came to our knowledge later in the project and this finding complicated the analysis of the Y2H results as these could also interact with AIPL1. As it will be described in the next chapter, anti-EYS1 antibody is only able to detect EYS isoforms 1 and 4 and therefore, the results obtained in Y79 cells presented in this section can only be related to the large EYS isoforms 1 and 4.

3.8.1.2 Analysis of Exogenously Expressed AIPL1 and EYS

Investigation of exogenous expression patterns of the proteins of interest was performed in HeLa cells and the vector constructs were introduced into the cells using transfection. The large size of full length EYS isoform 1 made it impossible to successfully transfect HeLa cells and therefore, tagged AIPL1 constructs were co-transfected with tagged constructs of shorter fragments of EYS. The fragments used in this set of experiments included V5 tagged AIPL1, GFP tagged N-terminal fragment EYS (1-1635 aa), GFP tagged EYS isoform 2 and GFP tagged EYS isoform 3; GFP empty vector was used as a control. The N-terminal fragment of EYS was chosen because it encompasses the sequence of bait 3 used in Y2H and it contains EYS signal peptide which may be necessary for its proper localisation. The schematic overview of the fragments is presented in Figure 3.21.

Figure 3.22-Figure 3.25 depict the expression patterns of the analysed proteins. V5 tagged AIPL1 characteristically localised to the cytoplasm and to the nucleus in all of the experiments. EYS N-terminal fragment and EYS isoforms 2 and 3 localised mainly to the cytoplasm. In some context, this observation could relate to Y2H in that the complexes of bait and prey need to be transported back to nucleus in order to activate the expression of reporter genes. As it can be seen in the micrographs presented here, EYS N-terminal fragment localised almost exclusively to the cytoplasm, which could explain the low efficiency of Y2H screens.

Upon examination of the confocal micrographs, it can be concluded that AIPL1 co-localises with EYS N-terminal fragment as well as isoform 2 and 3, which is indicative of a potential interaction. To validate these interactions, further analysis by Co-IP was performed.

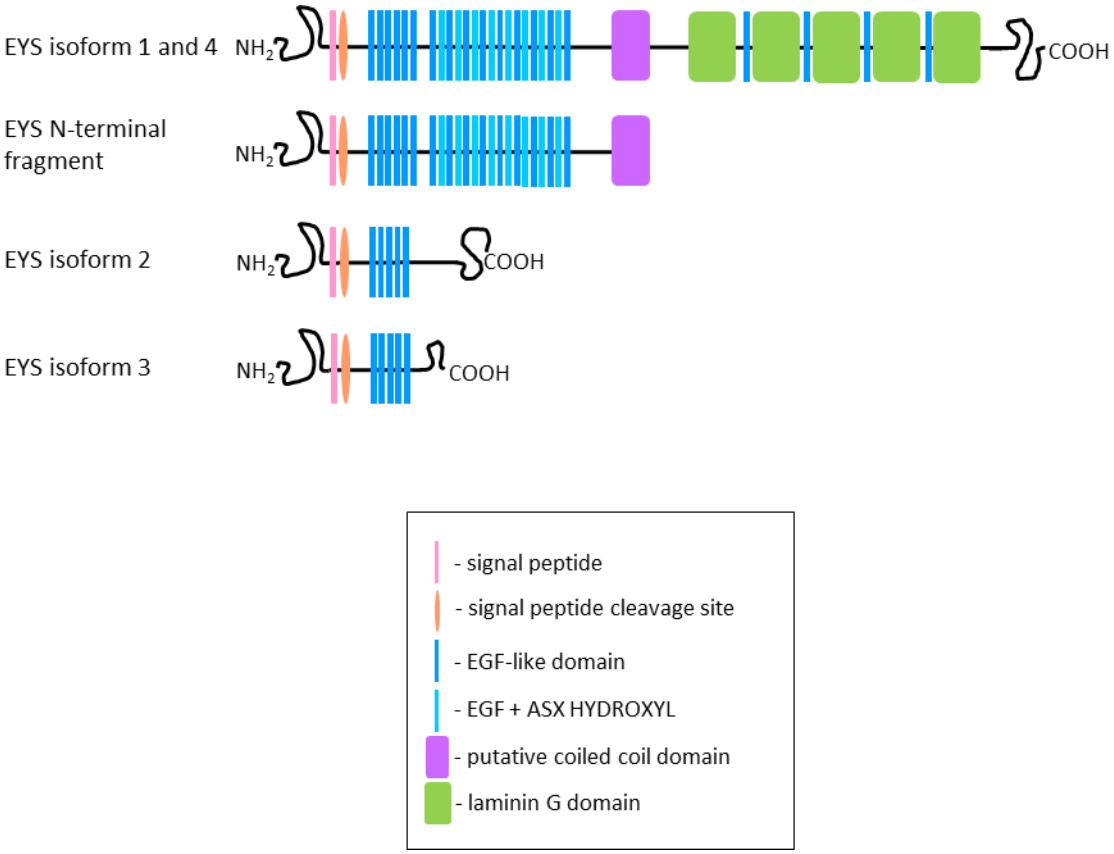

Figure 3.21 Schematic overview of protein fragments used in the localisation studies of EYS N-terminal fragment and EYS isoforms 2 and 3. In the experiment the fragments were tagged with GFP at the N-terminus and their expression patterns were compared to the expression pattern of V5 tagged AIPL1.

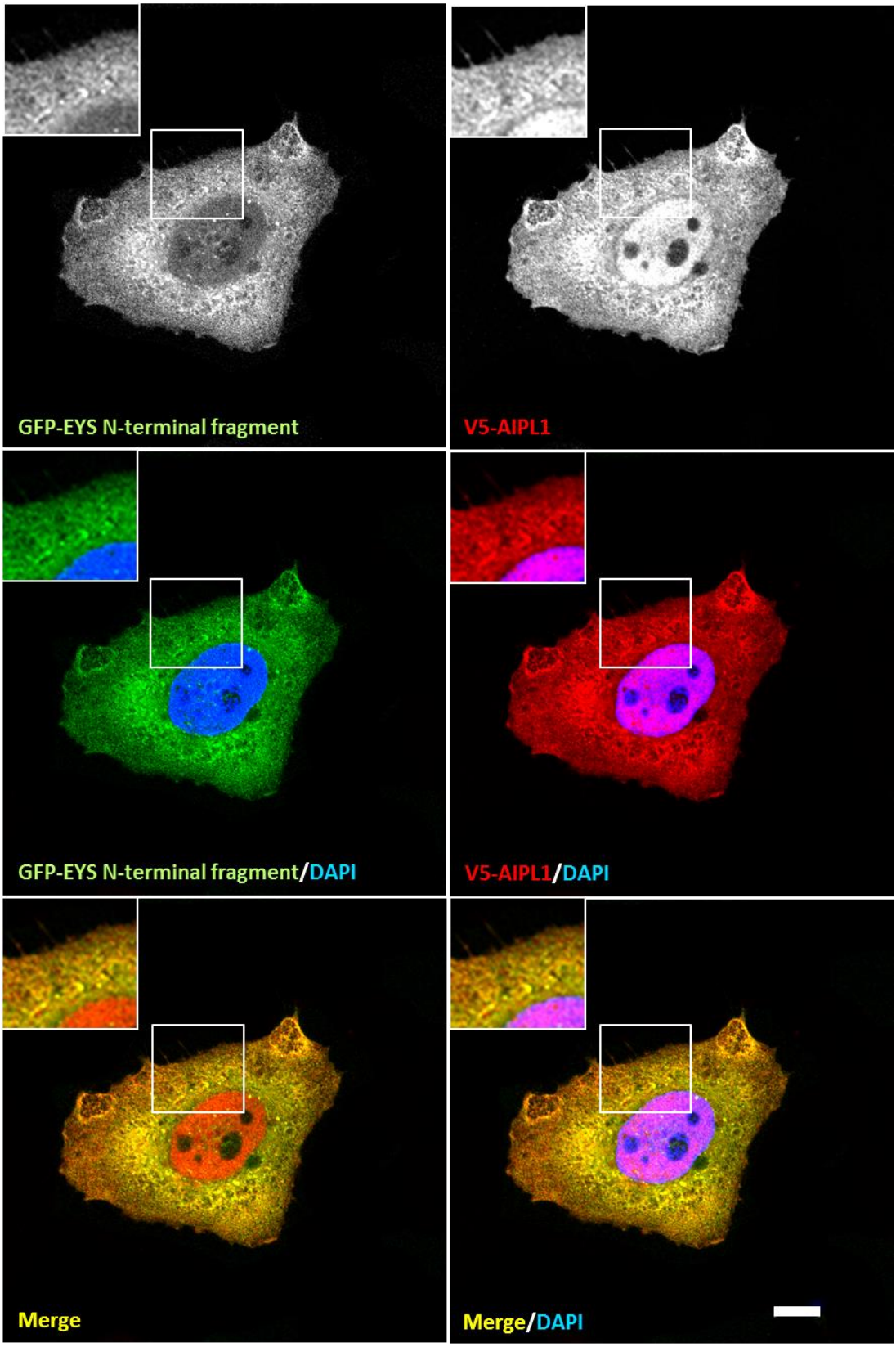

Figure 3.22 Localisation of GFP tagged EYS N-terminal fragment and V5 tagged AIPL1 in co-transfected HeLa cells. GFP tagged EYS N-terminal fragment localises to the cytoplasm whereas V5 tagged AIPL1 resides in the cytoplasm and the nucleus. Any co-localisation is indicated by the yellow/orange signal. The zoomed inserts represent the area demarcated by the white square in the images. Anti-V5 primary and Cyanine 3 conjugated donkey anti-goat secondary antibodies were used. Nuclei are stained using DAPI (blue). Scale bar: 10 μm.

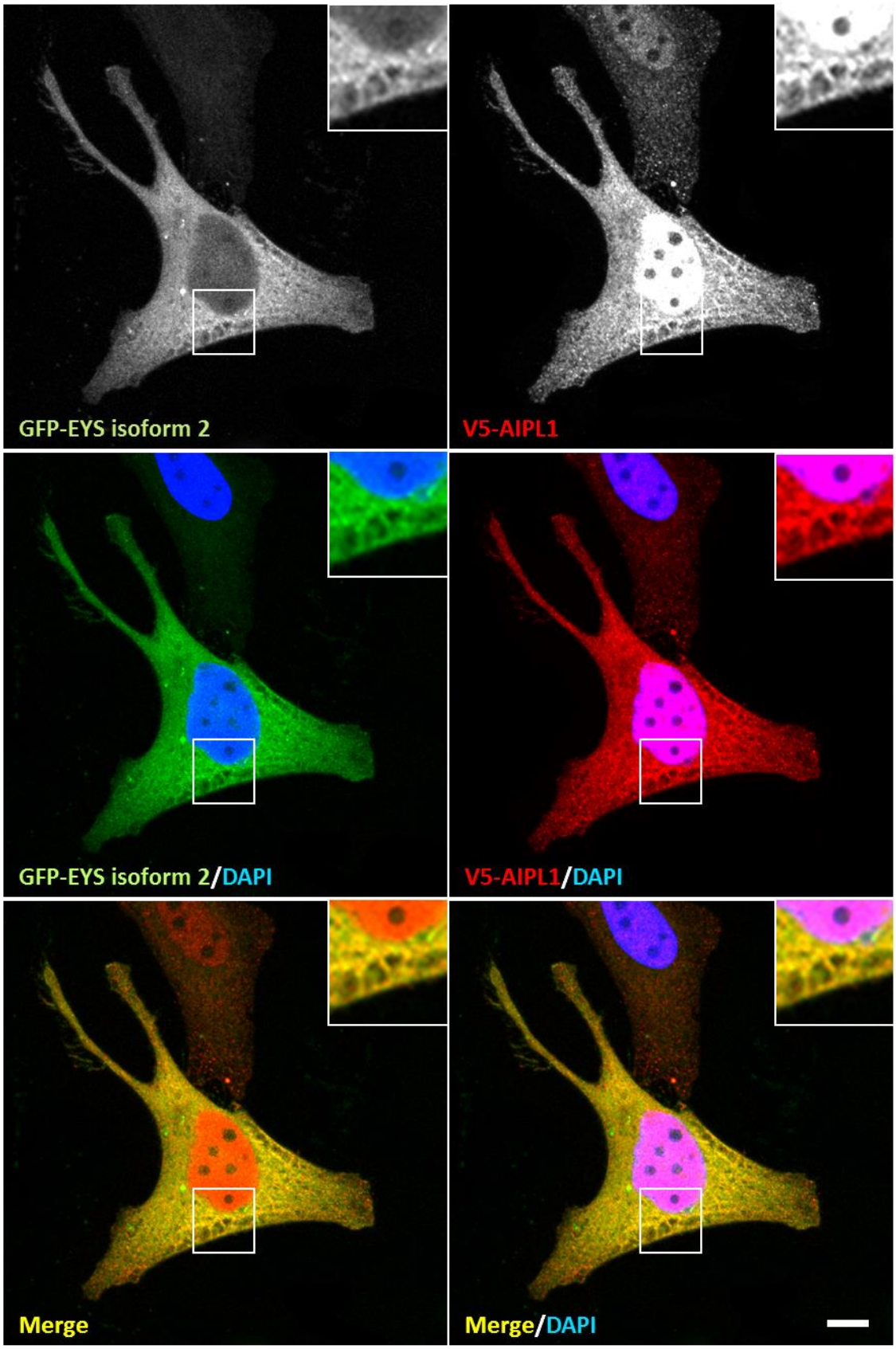

Figure 3.23 Localisation of GFP tagged EYS isoform 2 and V5 tagged AIPL1 in co-transfected HeLa cells. GFP tagged EYS isoform 2 localises to the cytoplasm whereas V5 tagged AIPL1 resides in the cytoplasm and the nucleus. Any co-localisation is indicated by the yellow/orange signal. The zoomed inserts represent the area demarcated by the white square in the images. Anti-V5 primary and Cyanine 3 conjugated donkey anti-goat secondary antibodies were used. Nuclei are stained using DAPI (blue). Scale bar: 10 µm.

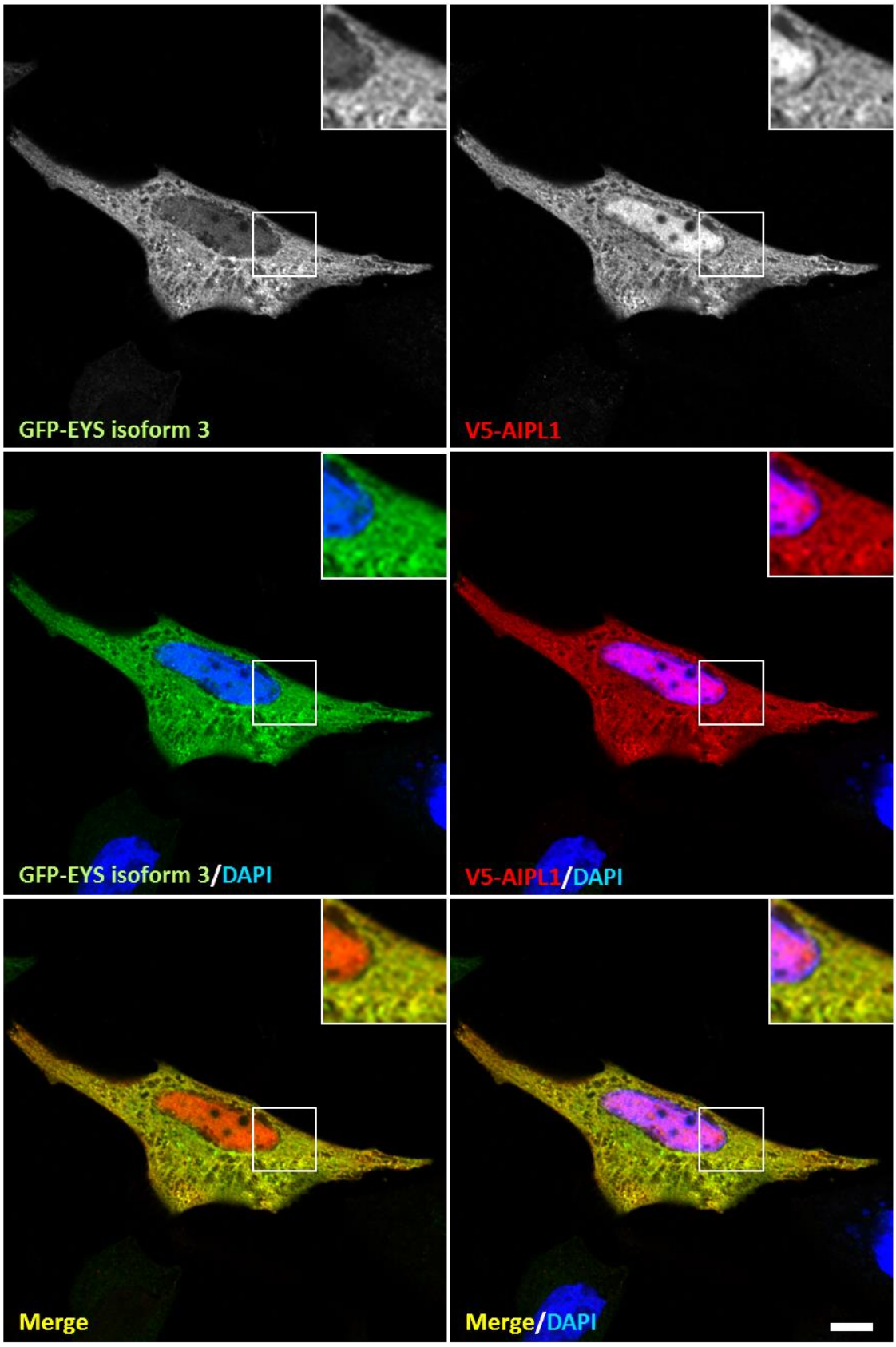

Figure 3.24 Localisation of GFP tagged EYS isoform 3 and V5 tagged AIPL1 in co-transfected HeLa cells. GFP tagged EYS isoform 3 localises to the cytoplasm whereas V5 tagged AIPL1 resides in the cytoplasm and the nucleus. Any co-localisation is indicated by the yellow/orange signal. The zoomed inserts represent the area demarcated by the white square in the images. Anti-V5 primary and Cyanine 3 conjugated donkey anti-goat secondary antibodies were used. Nuclei are stained using DAPI (blue). Scale bar: 10 μm.

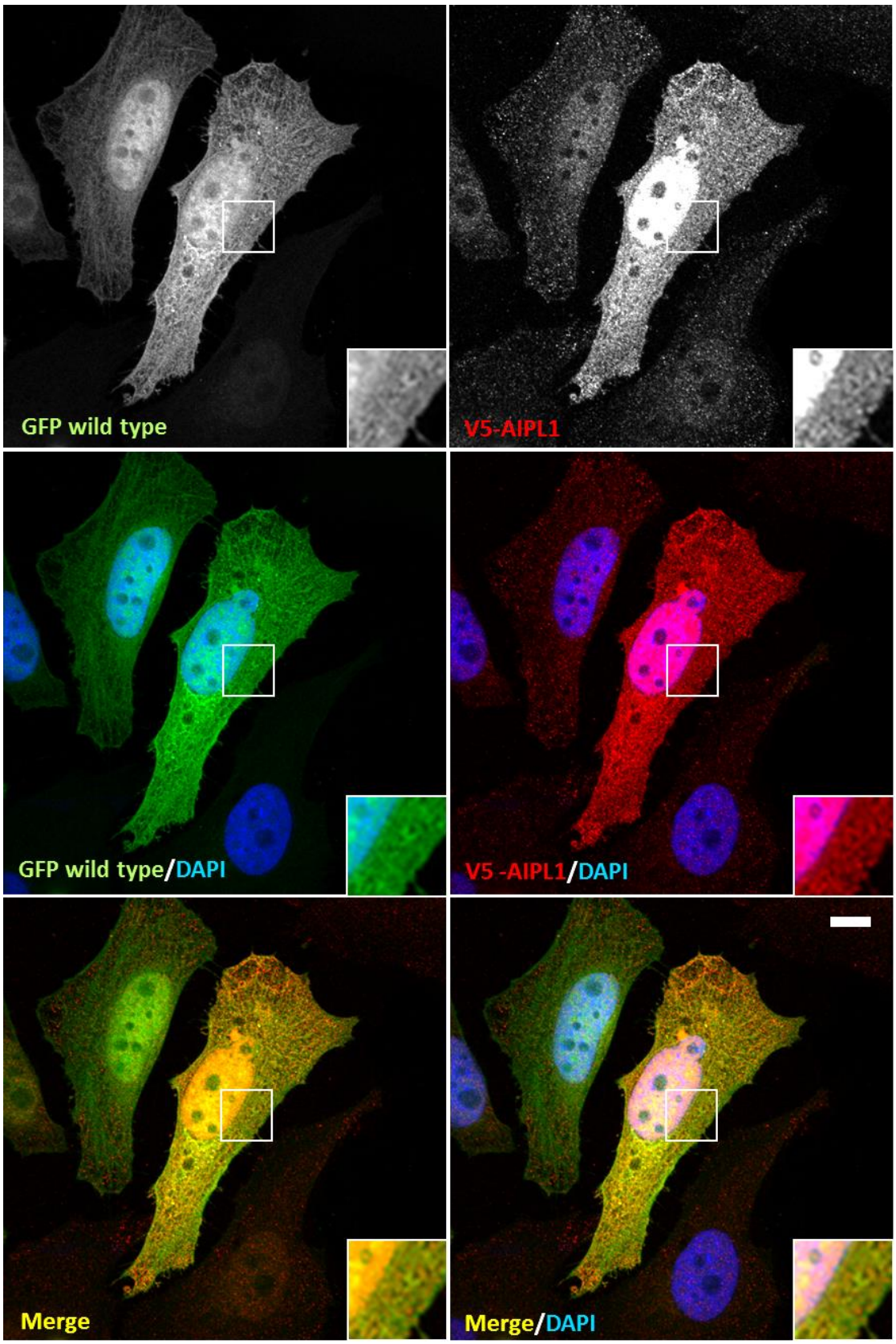

Figure 3.25 Localisation of GFP wild type and V5 tagged AIPL1 in co-transfected HeLa cells. GFP wild type as well as V5 tagged AIPL1 localises to the cytoplasm and the nucleus. Any co-localisation is indicated by the yellow/orange signal. The zoomed inserts represent the area demarcated by the white square in the images. Anti-V5 primary and Cyanine 3 conjugated donkey anti-goat secondary antibodies were used. Nuclei are stained using DAPI (blue). Scale bar: 10 µm.

3.8.2 Validation of Y2H Data by Co-Immunoprecipitation

Co-IP is one of the methods used to authenticate Y2H data by verifying whether the two proteins of interest form complexes together. In order to perform a successful Co-IP it is necessary to possess antibodies raised against the desired epitopes. One antibody is used to pull down the complex of proteins from the cell lysate and another is used in immunoblotting to verify the presence of a potential interacting partner. In this project, there were bespoke antibodies available raised against EYS and AIPL1, and both of them were produced in rabbit. In principle, the two antibodies used for Co-IP assay should be obtained in two different animals in order to avoid false positive results. This made it impossible to perform Co-IP assays using the custom made anti-EYS and anti-AIPL1 antibodies and wild type protein extract from Y79 cells. The correct selection of antibodies was especially important in this project since the size of AIPL1, which is approximately 50 kDa, is the same as that of the heavy chains of most antibodies. This means that if the anti-EYS rabbit antibody was used for pulling down the complex and anti-AIPL1 rabbit is used for immunoblotting, the band appearing at the size of 50 kDa could come from AIPL1 or the heavy chains of the anti-EYS rabbit antibody – anti rabbit HRP conjugated antibody could bind to both of them. In light of this, attempts to examine the potential interaction of full length EYS and AIPL1 in Y79 cells were not undertaken.

Instead, it was decided to carry out Co-IPs using tagged AIPL1 and EYS isoforms 2 and 3 as well as EYS N-terminal fragment corresponding to 1-1635 aa. Using tagged proteins resolved issues concerning protein specific antibodies; AIPL1 was cloned with a V5 tag whereas EYS proteins were fused with a 3XFLAG tag. For each of the experiments, the constructs were co-transfected into HeLa cells and cell lysates were freshly prepared before each Co-IP assay to avoid protein degradation during freeze-thaw cycles.

Co-IP experiments require a number of controls to confirm the specificity of the method and such controls were performed along with each Co-IP assay. Controls marked as ‘Input’ were total protein extracts prepared from cells co-transfected and single transfected with the used constructs. Since the same extracts were used in IP experiments, it was an important quality control demonstrating that the desired tagged proteins were present in the samples. As a

negative control, cell lysate from untransfected HeLa cells was used. Protein extracts from co-transfected cells were used to perform Co-IP verifying whether the two proteins of interest interact. It was also used in the negative control for IP, which was performed with goat unspecific IgG antibody (isotype control; marked as 'IgG') and it checked whether the antibodies raised in goat non-specifically bind any proteins present in the extract from co-transfected HeLa cells. Control IPs were performed using extracts form cells transfected with either 3XFLAG tagged construct or V5 tagged AIPL1. These samples aimed to control whether the V5 antibody used pulls down the V5 tagged protein only or whether it is also able to non-specifically bind overexpressed 3XFLAG tagged constructs. The presence of a tagged protein in a cell lysate used for preparation of a given sample is indicated at the bottom of each Co-IP figure, where '+' indicates the presence and '-' the absence of the fusion protein in the lysate.

In the first Co-IP experiment it was examined whether V5-AIPL1 interacts with EYS isoforms 2. Protein complexes were precipitated from the cell extract using anti-V5 antibody and immunoblotting was performed using anti-FLAG and anti-AIPL1 antibodies. The results are shown in Figure 3.26, where blot 'A' represents the membrane immunolabelled with anti-FLAG antibody and blot 'B' is a control blot immunolabelled with anti-AIPL1 antibody.

In the input lanes of blot 'A', there can be bands observed corresponding to the size of FLAG-EYS isoform 2 (~72 kDa; green asterisks) and no band is visible in the negative control (extract from untransfected HeLa cells). The bands were detected in lanes corresponding to co-transfected and single transfected cells, confirming that the fusion proteins were synthesised in the transfected cells. The negative IP control was free of any protein bands, demonstrating the specificity of the anti-V5 antibody used. The positive IP samples were performed using anti-V5 antibody and extracts from co-transfected and single transfected cells. The band marked with the red asterisk corresponds to the size of 3XFLAG-EYS isoform 2 and it confirms that it interacts with V5-AIPL1 as the extracts used in this sample contained both of the proteins. The specificity of IP is confirmed by the lack of protein band in the next lane which represents the IP performed with anti-V5 antibody and extract containing 3XFLAG-EYS isoform 2.

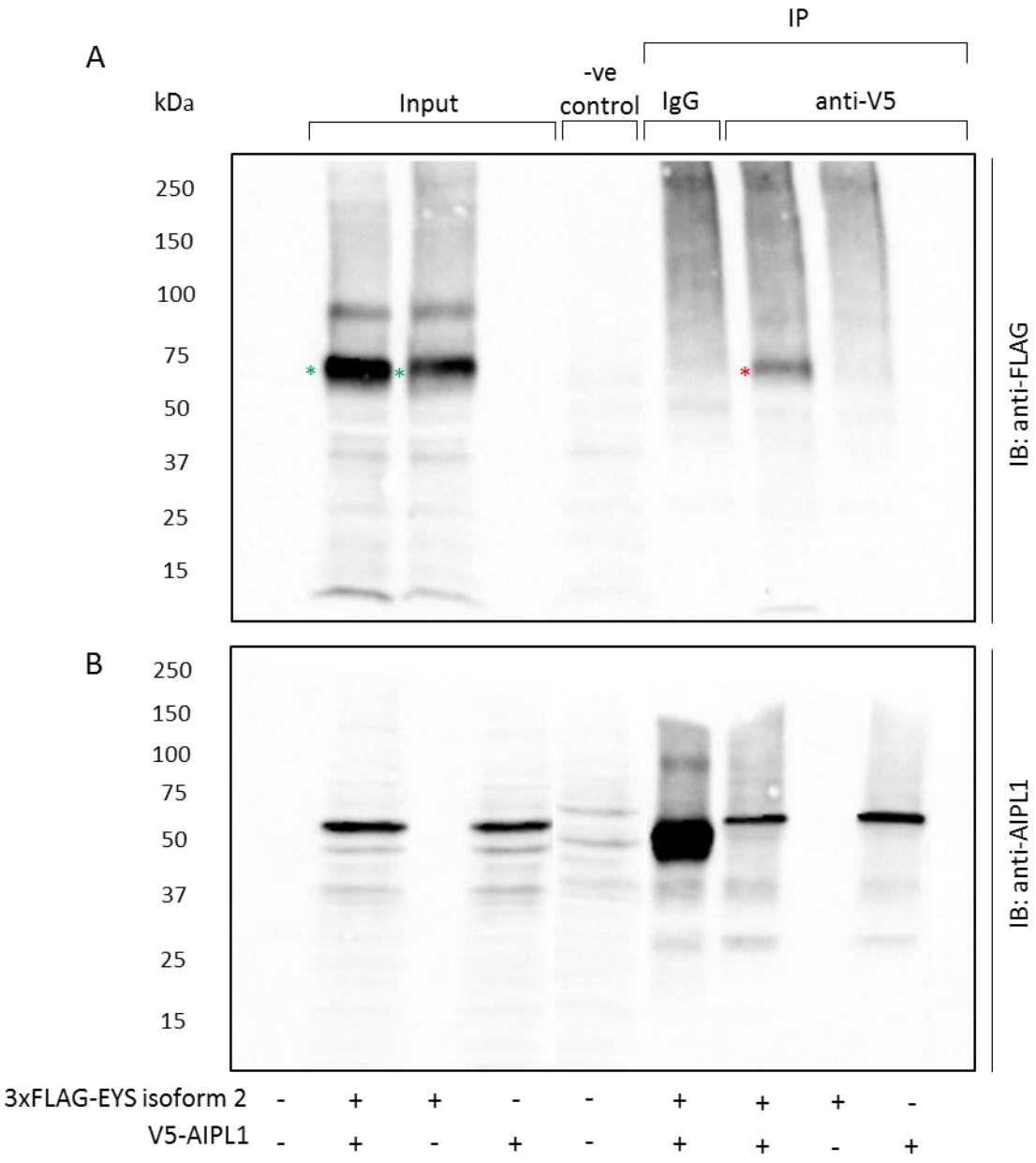

Figure 3.26 Co-immunoprecipitation assay demonstrating interaction between 3xFLAG tagged EYS isoform 2 and V5 tagged AIPL1. Blot **'A'** represents membrane probed with anti-FLAG antibody. The presence of a protein band in the Co-IP lane (red asterisk) confirms the interaction. IP performed with non-specific goat IgG was used as an IP negative control (IgG). Input refers to extracts from co-transfected and single transfected HeLa cells. The IB negative control (-ve control) was protein extract from untransfected HeLa cells. Blot **'B'** is a control blot probed with anti-AIPL1 antibody and it demonstrates specificity of the assay. Loading was normalised using a BCA assay and the samples were resolved by denaturing SDS-PAGE. Secondary antibodies were HRP conjugated goat anti-mouse and goat anti-rabbit antibodies. The presence of each construct in the loaded sample is denoted by '+' and the absence by '-'. Expected band sizes: 3xFLAG-EYS isoform 2 – ~72 kDa, V5-AIPL1 - ~50 kDa. IB – immunoblotting, IP – immunoprecipitation.

The control blot 'B' is a replica of blot 'A' but instead, it was immuno-labelled with anti-AIPL1 antibody. As expected, V5-AIPL1 was detected in the input lanes as well as IP lanes at the size of approximately ~50 kDa, confirming that the Co-IP assay was specific. However, the IP negative control performed with non-specific goat IgG antibody resulted in detection of a band at the size of around 50 kDa. As it can be seen, this band has slightly lower molecular mass than V5-AIPL1 and it most likely corresponds to the IgG antibody heavy chains which were non-specifically detected by the HRP conjugated goat anti-rabbit secondary antibody. The non-specific band is a lot more abundant than bands corresponding to V5-AIPL1 and the same amounts of extracts were used for each sample; if that band corresponded to V5-AIPL1, it would be expected that it is of the same intensity as other V5-AIPL1. Furthermore, since the same control was clean in blot 'A', the presence of this band does not question the obtained results and it can be considered as an artefact, which resulted from the limitations of the method. In the Co-IP protocol, magnetic beads are incubated with the desired antibody, rinsed and incubated with the cell lysate. Even though stringent washes were a routine procedure, some contamination with the unbound antibody might have happened. Also, in order to elute the complex from the magnetic beads, the sample was incubated at 70 ˚C and during that time some of the antibodies bound to the beads could have detached. Immunoglobulins are composed of heavy and light chains connected via disulphide bonds, which are broken when exposed to reducing agents. Therefore, any antibodies present in the Co-IP eluate may appear on the blot at the size of either ~50 kDa (heavy chains) or ~25 kDa (light chains). In practice, however, it happens that secondary antibodies raised against a particular animal non-specifically detect antibodies raised in another animal and this is what probably occurred in the experiments presented herein.

In the next experiment, the interaction between 3XFLAG-EYS isoform 3 and V5-AIPL1 was tested. The obtained results are presented in Figure 3.27 and the order of samples is the same as for the previous experiment. As it can be seen in blot 'A', protein bands corresponding 3XFLAG-EYS isoform 3 are observed in the input lanes (~69 kDa; green asterisks) and the IP lane (red asterisk) demonstrating that the interaction between the two tested took place.

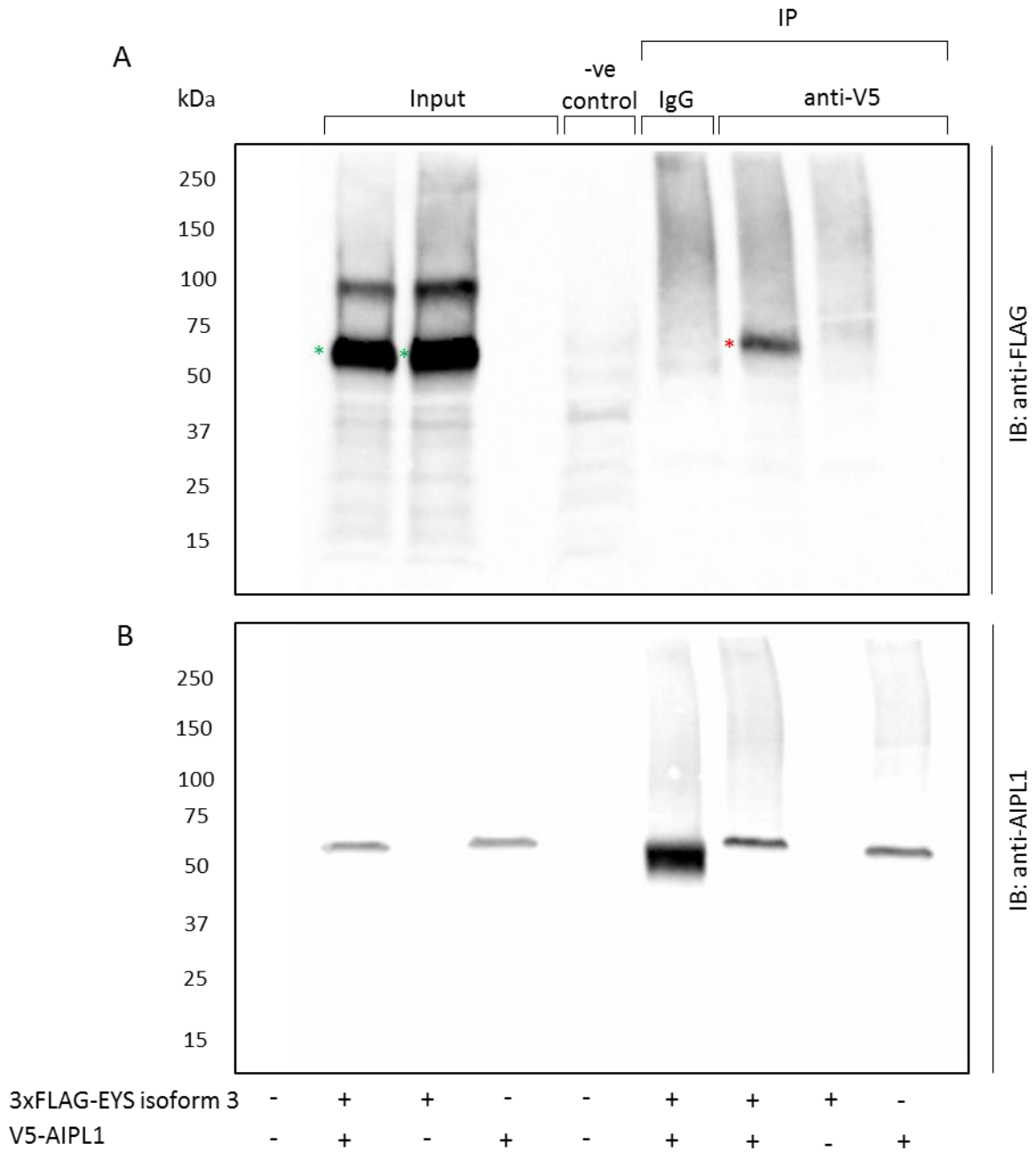

Figure 3.27 Co-immunoprecipitation assay demonstrating interaction between 3xFLAG tagged EYS isoform 3 and V5 tagged AIPL1. Blot **'A'** represents membrane probed with anti-FLAG antibody. The presence of a protein band in the Co-IP lane (red asterisk) confirms the interaction. IP performed with non-specific goat IgG was used as an IP negative control (IgG). Input refers to extracts from co-transfected and single transfected HeLa cells. The IB negative control (-ve control) was protein extract from untransfected HeLa cells. Blot **'B'** is a control blot probed with anti-AIPL1 antibody and it demonstrates specificity of the assay. Loading was normalised using a BCA assay and the samples were resolved by denaturing SDS-PAGE. Secondary antibodies were HRP conjugated goat anti-mouse and goat anti-rabbit antibodies. The presence of each construct in the loaded sample is denoted by '+' and the absence by '-'.Expected band sizes: 3xFLAG-EYS isoform 3 – ~69 kDa, V5-AIPL1 - ~50 kDa. IB – immunoblotting, IP – immunoprecipitation.

The negative control lanes on blot 'A' were clean and the control blot 'B' confirmed that the assay was properly conducted.

Interestingly, overexpressed EYS isoforms 2 and 3 were consistently detected with an accompanying band detected at around 100 kDa. It suggests that some portions of the protein is either more heavily modified, e.g. glycosylated, or it could be a result of EYS isoforms 2 and 3 forming dimers. This observation would need to be addressed experimentally in the future to fully understand it.

In the next Co-IP assay it was verified whether 3XFLAG-EYS N-terminal fragment (1-1635 aa), overlapping Y2H EYS bait 3, can interact with V5-AIPL1 (Figure 3.28). As shown in blot 'A', the interaction did occur, which is indicated by the band detected in the IP lane at approximately 180 kDa (red asterisks). Bands of the expected size were also seen in the input lanes (green asterisks) and the control samples as well the control blot worked as expected, confirming the specificity of the assay.

Altogether, Co-IP assays performed to validate the Y2H results demonstrated that EYS isoforms 2 and 3 as well as EYS N-terminal fragment (1-1635 aa) can physically bind AIPL1. These experiments enhance the data obtained from ICC experiments and complete the validation of Y2H results, making AIPL1 a true binding partner of the tested EYS proteins.

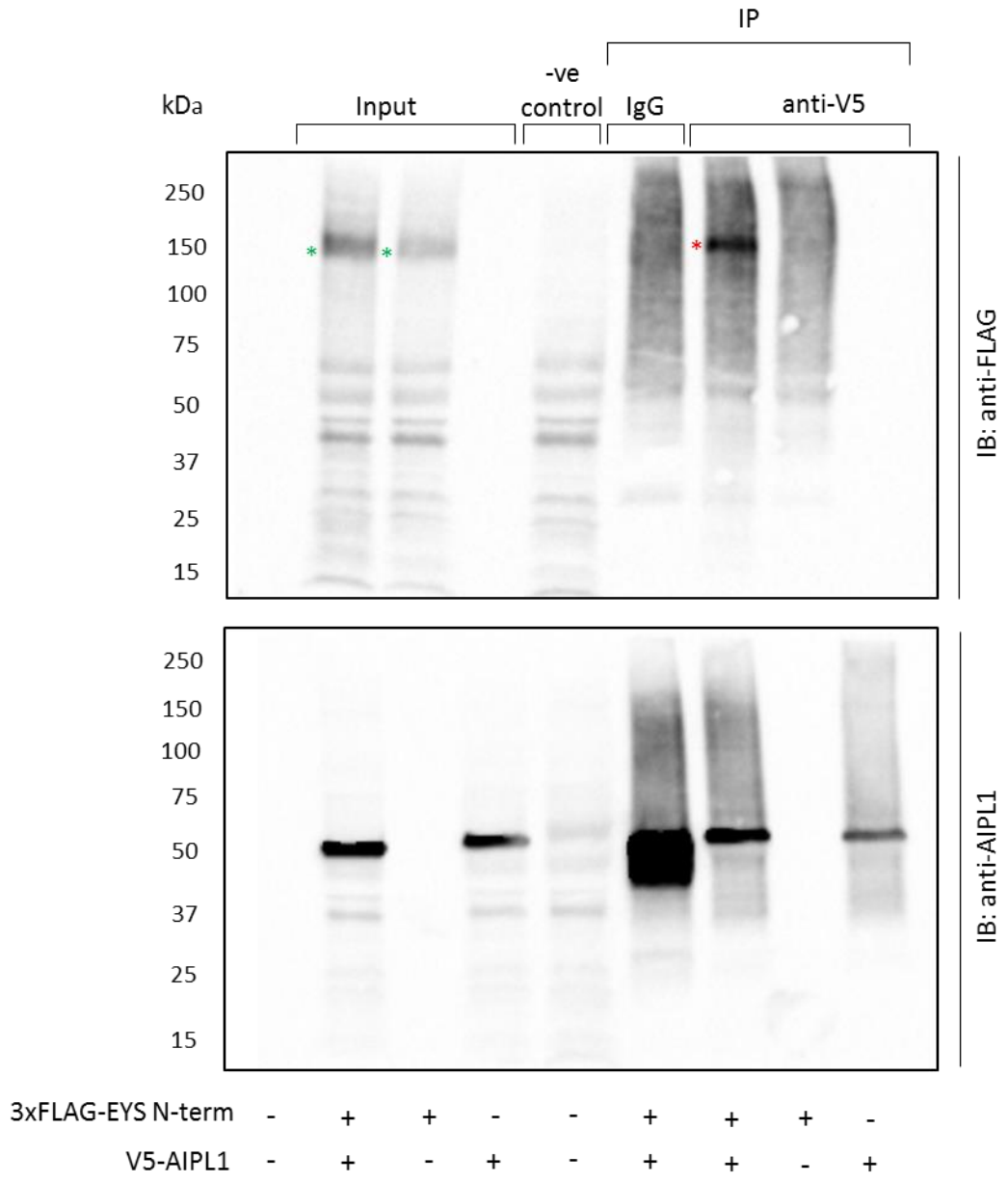

Figure 3.28 Co-immunoprecipitation assay demonstrating interaction between 3xFLAG tagged EYS N-terminal fragment (1-1635 aa) and V5 tagged AIPL1. Blot **'A'** represents membrane probed with anti-FLAG antibody. The presence of a protein band in the Co-IP lane (red asterisk) confirms the interaction. IP performed with non-specific goat IgG was used as an IP negative control (IgG). Input refers to extracts from co-transfected and single transfected HeLa cells. The IB negative control (-ve control) was protein extract from untransfected HeLa cells. Blot **'B'** is a control blot probed with anti-AIPL1 antibody and it demonstrates specificity of the assay. Loading was normalised using a BCA assay and the samples were resolved by denaturing SDS-PAGE. Secondary antibodies were HRP conjugated goat anti-mouse and goat anti-rabbit antibodies. The presence of each construct in the loaded sample is denoted by '+' and the absence by '-'. Expected band sizes: 3xFLAG-N-terminal fragment (1-1635 aa) – ~182 kDa, V5-AIPL1 - ~50 kDa. IB – immunoblotting, IP – immunoprecipitation.

3.9 Discussion of Chapter 3

The *EYS* gene was identified at the *RP25* locus and it was described as the largest gene known to be expressed in the retina (Abd El-Aziz *et al.*, 2008; Collin *et al.*, 2008). Mutations in *EYS* have been demonstrated to cause autosomal recessive retinitis pigmentosa (arRP) with the prevalence ranging from 5-23.5 % depending on population, making it a major gene for arRP (Abd El-Aziz *et al.*, 2010; Arai *et al.*, 2015; Audo *et al.*, 2010; Bandah-Rozenfeld *et al.*, 2010; Hosono *et al.*, 2012; Iwanami *et al.*, 2012). EYS has been demonstrated to localise to the photoreceptor outer segments in the porcine retina (Abd El-Aziz *et al.*, 2008) and to play a role in the organisation of *Drosophila* rhabdomeric photoreceptors (Zelhof *et al.*, 2006). Nevertheless, little is known about the role of EYS in the human retina and broadening that knowledge would be undoubtedly advantageous for understanding the molecular basis of arRP and for the development of potential therapeutic approaches.

A common approach to study a function of a newly discovered protein is to investigate its interactome. Proteins do not function as single entities; they form stable or transient complexes and are part of dynamic and carefully regulated machinery. By looking into interacting partners of a given protein, it is possible to determine what processes it is involved in and what role it might play in the network of interactions (Ngounou Wetie *et al.*, 2014). In the case of EYS, knowledge of its binding partners would provide vital clues to what function it may have in human photoreceptors and why its role is required for the homeostasis of the retina.

In this project, the Y2H system was chosen due to its relative simplicity and low cost. Another advantage was that Y2H is well adapted to high throughput screening aimed at identification of binary protein-protein interactions in a certain type of tissue, here the human retina. Furthermore, Y2H can not only be used for screening of DNA or cDNA libraries, but also for exploration of known interactions between two putative binding partners such as mapping interaction sites (Ivanov *et al.*, 2011).

EYS full-length isoform 1 protein comprises 3144 aa and has a complex domain structure. To allow more comprehensive Y2H screening, nine bait fragments were designed including the full-length EYS protein. The main purpose

of using protein fragments in addition to full-length EYS was to further characterise and map any interactions identified with the full length protein. However, using full length EYS did not yield positive results and the failure could have been caused by a number of factors. The most striking feature of EYS is its size and its impact on Y2H performance is not without significance. The expression level of such a large bait may have been low and not efficient enough to for detection by Western blot analysis, let alone activation of the reporter genes. Moreover, in Y2H the interacting bait and prey need to translocate to the nucleus in order to activate reporters and this may not be possible for large proteins that do not naturally reside in the nucleus. Consideration should also be given to the signal peptide present at the N-terminus of EYS, which could have caused the protein to be secreted out of the yeast cells or to localise to the membranous organelles of the cell. To verify if this might be the case, the next screen was performed with bait 7, which encompasses the full length of EYS apart from the signal peptide. The failure of this screen suggested that the signal peptide was not the main factor preventing the system from working.

To reduce the bait size but retain the natural domain order of EYS, bait 8 was used; however, this screen did not yield positive results either. The Y2H system manufactured by Clontech is characterised by its high stringency enforced by the use of AbA as one of the reporters. It is an advantageous modification of the system; however, it may cause weaker or transient interactions to be missed. In order to test whether this was the limitation in the previous Y2H screens, the conditions of screening were modified and the stringency was lowered by replacing the AbA reporter with the nutritional reporter (*HIS3*; histidine) in the media used for the initial plating of the mated culture. Indeed, this modification made a difference and positive colonies were observed in some of the screens. It was still not possible to screen the library using the full-length EYS; however, screens performed with bait 3, 6, 7 and 8 resulted in obtaining positive colonies.

This result addressed another very important question of whether the bait fragments were truly expressed in yeast cells. The control bait expression experiment did not decisively confirm the presence of bait proteins in the yeast protein extracts, although, the lack of protein bands may have been caused by protein degradation or low expression levels. Successful screening, resulting in

obtaining positive blue yeast colonies, supported this hypothesis and suggested that the bait constructs were expressed in yeast.

In all of the Y2H screens performed altogether, 41 colonies were obtained on the lowest stringency media (TDO/X) and out of these 35 colonies were able to grow on the highest stringency media (QDO/X/A). The sequence analysis of the prey fragments revealed that only 13 contained sequenced aligning with exonic sequences of the human genome. Interestingly, all 13 prey fragments were identified using bait 3, corresponding to the N-terminal part of EYS protein (23 - 1635 aa). This group of 13 prey fragments included nuclear and translation initiation factors which were excluded from further analysis. These could be returned to at later stages of the project; nevertheless, from what is known about the domain structure of human EYS and the role of the *Drosophila* orthologue of EYS in the rhabdomeric photoreceptors, it is unlikely that the excluded proteins interact with EYS *in vivo*. The final shortlist of prey fragments included six potential interacting partners that were subjected to further analysis using the Y2H system. The post-screening control experiments revealed that only one prey fragment provided reproducible results and the remaining five had to be classified as false positive results; four of them were most likely the result of revertant colonies formation and one was demonstrated to non-specifically activate expression of the reporter genes.

The remaining prey was identified to be a fragment of the *AIPL1* gene, implicated in Leber congenital amaurosis, a severe early onset retinal degeneration (Sohocki *et al.*, 2000). Importantly, the *AIPL1* fragment identified in the screening was not cloned in frame with the GAL4 AD and the interaction could not be reproduced when the frame was reinstated. The presence of such prey fragments in the cDNA library was a serious limitation of the system; however, the result was not categorically disregarded as AIPL1 appeared to be a strong candidate for a true interacting partner of EYS.

Furthermore, from the previous experience in the Bhattacharya laboratory, it was known that prey fragments with disrupted frame could provide true interacting partners of the protein of interest (personal communication). In light of this, further validation of the potential interaction of EYS and AIPL1 was pursued using mammalian cell lines employing ICC and Co-IP methods.

ICC was performed in Y79 and HeLa cell lines. Y79 cells were chosen since they endogenously express both EYS and AIPL1; however, these cells grow in suspension and so they have moderately developed morphology, which makes it challenging to perform accurate analyses of subcellular localisation of the proteins of interest. Even though yellow signal indicating co-localisation was observed, it was not possible to verify whether the signal comes from the cytoplasm, cell membrane or both, due to the characteristic large nucleus and little surrounding cytoplasm of Y79 cells. Transfection of suspension cell lines is challenging and Y79 cells are not an exception, therefore, overexpression studies of EYS were not possible using Y79 cells. Even though transfection with tagged AIPL1 was successful, the results did not provide sufficient clarity to substantiate whether the two proteins co-localise. Therefore, the analysis of exogenous expression patterns of tagged protein constructs was conducted in HeLa cells, which were chosen for their ease of transfection. The large size of EYS full-length protein made it impossible to successfully co-transfect HeLa cells with tagged constructs of EYS and AIPL1; however, a thorough analysis using EYS short isoforms and fragments was carried out. The results of immunolabelling experiments clearly showed that AIPL1 co-localizes in the cytoplasm with EYS isoforms 2 and 3 as well as N-terminal fragment of the protein, which is indicative of a potential interaction.

One of the biggest limitations in the project was the difficulty of overexpressing EYS in cell lines, which hindered much of the analysis of the expression patterns. The issue could be resolved by employing induced pluripotent stem cells (iPSC) which increasingly gain popularity as disease models and potential cell therapy tools (Ross & Akimov, 2014; Tucker *et al.*, 2014) . iPSCs could be differentiated into a cell line endogenously expressing EYS and AIPL1 and such a strategy would allow for greater accuracy when performing co-localization studies of EYS and AIPL1. It would also be invaluable to obtain iPSCs from patients carrying mutations in *EYS* and/or *AIPL1* and look into the differences in localisation of the two proteins of interest.

ICC provided useful insights into the subcellular localisation in which the proteins of interest function; however, the method did not validate whether they are able to bind each other. Therefore, immunofluorescence experiments were supplemented with Co-IP, which aimed to test if AIPL1 and EYS proteins form complexes together. Once more, the interaction between EYS isoform 1 and AIPL1

could not have been verified due to the lack of suitable reagents, i.e. antibodies raised in two different animals. The experiments were conducted using 3XFLAG tagged EYS isoforms 2 and 3 and EYS N-terminal fragment (1-1635 aa), and V5 tagged AIPL1. The experiments confirmed that the interaction between AIPL1 and tested EYS proteins does occur.

The Co-IP results provided additional evidence in support of the hypothesis that EYS proteins interact with AIPL1. The fact that EYS N-terminal fragment, which overlaps with the sequence of Y2H bait 3, interacted with AIPL1 in mammalian cells confirms that Y2H results were genuine. Moreover, the interaction with EYS isoforms 2 and 3 could suggest that the binding site maps to the portion of EYS encompassing the first five EGF-like domains, which are uniform in all of the tested EYS proteins. Further research would be required to narrow down and characterise the binding site. It would also be interesting to verify whether AIPL1 can interact with any of the C-terminal domains of EYS and whether disease causing mutations in *EYS* and *AIPL1* disrupt the interaction; such analysis was not undertaken in this project due to time constrictions.

AIPL1 is a multifunctional photoreceptor specific protein; it has been demonstrated to be a part of a chaperoning heterocomplex and to be able to interact with and aid in processing of farnesylated proteins such as PDE6 (Hidalgo-de-Quintana *et al.*, 2008; Ramamurthy *et al.*, 2003). Since AIPL1 is a molecular chaperone, it is within its nature to bind to many proteins that require its assistance in biosynthesis. The identified interaction does not provide information on what the role of EYS may be; however, it is still an exciting and novel discovery. Both AIPL1 and EYS are important for the homeostasis of the retina and the molecular mechanisms they are involved in may be interconnected. EYS lacks a C-terminal CaaX box required for farnesylation; however, AIPL1 could still be necessary for its folding and/or trafficking to the final subcellular localisation. These processes occur to be important enough to cause degeneration of photoreceptor cells when disrupted. Further research will be required to investigate whether AIPL1 can also interact with full length EYS isoform 1. To do this, it would be necessary to obtain anti-EYS or anti-AIPL1 antibodies raised in an animal other than rabbit or to elaborate an efficient method of introducing EYS isoform 1 cDNA into the cell lines. It should be noted that the goat anti-EYS

antibody (named anti-EYS3 in this study) did not work in immunoblotting and, therefore, it could not have been used for Co-IP (Appendix I).

Investigation of the EYS interactome turned out to be a lot more challenging than expected. Y2H screening resulted in identification of only one potential binding partner. The low yield of results provided by Y2H is not meaningless and suggests that something must have had a disadvantageous effect on the screening. Numerous controls were performed in the Y2H screening and all of them proved that the system was functional and was used properly. Also, the experiments in mammalian cells using EYS proteins were not straightforward to perform and the analysis of the obtained results was similarly complicated.

In light of this, it was concluded that difficulties in experimental procedures must have been related to some features of EYS and/or EYS bait fragments. Domain structure of EYS would suggest that it could be protein associated with the cell membrane or secreted to the extracellular matrix. If that is the issue for EYS, many interactions could have been missed due to bait and/or prey proteins being unable to enter the nucleus and activate expression of reporters (false negatives). Another possibility is that EYS is post-translationally modified in a manner that is crucial for its interactions and cannot be replicated in yeast cells. Further fundamental information regarding EYS would be crucial to redesigning the project: if EYS was a known membrane associated protein, it would be possible to use a Y2H system especially designed for detection of membrane proteins, e.g. Split-Ubiquitin Based Membrane Yeast Two-Hybrid (MYTH). If, on the other hand, EYS was known to be an extracellular protein, a SCINEX-P (screening for interactions between extracellular proteins) system could be employed (reviewed in Brückner *et al.*, 2009). One could argue that a different system examining protein-protein interactions could have been chosen for investigating of the interactome of EYS; however, there was no experimental data available to support the choice of one system over another. The likelihood that a modification of the Y2H system would have worked better was unpredictable, especially for a protein of unknown function that is as large as EYS.

Another option could be employing mass spectrometry (MS), which is a powerful method in proteomic research enabling investigation of the whole protein complexes that the protein of interest in incorporated in. To perform MS, a good source of protein extract, coming from either a cell line or a tissue, would be a

major requirement. Y79 cells are the only cells endogenously expressing EYS and they could be used, although, practically they are challenging to work with and the majority of the cell volume is due to the nucleus, where EYS is unlikely to reside. Proteins extracts could also be obtained from retinal tissue, however, it needs to be noted that EYS is not expressed in rodents which would make it more complicated to obtain a desired amount of tissue that would come from an animal closely related to human or form human directly. MS could be preceded by affinity purification (AP/MS); however, any method requiring transfection with tagged EYS is, at the current state of art, prone to failure.

In conclusion, the interactome of EYS could be analysed using alternative methods; however, an informed decision about the correct methodology to employ will not be possible until more is known about EYS localisation and/or function. This knowledge would greatly improve the relevance of methods chosen to study EYS and, therefore, the next stage of the thesis will be devoted to further investigating the nature of EYS.

Chapter 4: Characterisation of EYS

The *EYS* gene is one of the largest genes known to be expressed in the human retina and since its discovery more than one hundred fifty disease causing mutations have been identified in individuals suffering from arRP. In spite of an extensive knowledge of the clinical phenotype of affected individuals, little is known about EYS protein and its role in the human retina. Upon commencement of the project, it was recognised that EYS localises to the photoreceptor outer segments of porcine retina and that it is involved in the organisation of the *Drosophila* rhabdomeric photoreceptors. One approach to investigate the role of EYS was to perform Y2H screening and identify its interacting partners, which would provide an invaluable source of information regarding the molecular processes that EYS is involved in. As described in Chapter 3, Y2H screening identified only one potential interacting partner of EYS which did not provide enough data to make compelling conclusions regarding the putative function of the protein of interest. Reasons for such an outcome may have been many but most likely they were related to some characteristics of EYS such as size and/or localisation. Results obtained in Y2H screening highlighted the need for broadening the knowledge of EYS localisation, which would be crucial to redesigning the strategy and improving the methodology used to identify retinal interacting partners of EYS. Characterisation of EYS was the objective of the experimental work presented in this chapter.

4.1 EYS and Its Isoforms

The *EYS* gene was identified at the *RP25* locus by two research groups independently (Abd El-Aziz *et al.*, 2008; Collin *et al.*, 2008). In the study published by Abd El-Aziz and colleagues, *EYS* was reported to be composed of 43 exons whereas Collin et al. identified a 44 exon gene. The facultative 42nd exon comprises 63 bp and lies just prior to the sequence encoding the fourth LamG domain. By performing RT-PCR analysis and immunohistochemistry studies, both groups demonstrated that EYS has a retina specific expression pattern. When browsing online genomic databases, it cannot be overlooked that there have been

more than two EYS isoforms annotated. GenBank database reports the existence of four EYS isoforms which is consistent with the data annotated in Ensembl and UCSC genome browsers as well as UniProt protein database. UniProt database, however, provides nomenclature of EYS isoforms which is different to the nomenclature provided in NCBI and UCSC databases. In this study, nomenclature from the latter was followed and, for clarity, details of EYS isoforms are summarised in Table 4.1.

Isoform	cDNA [bp]	Protein [aa]	RefSeq (GenBank)	Variation with respect to the canonical isoform 4
Isoform 1	10589	3144	NM_001142800.1, NP_001136272	2691-2711 aa: Missing
Isoform 2	5450	619	NM_001142801.1, NP_001136273	595-3165 aa: Missing 590-594 aa: CSCSL → RILNTVIPHQIQQHIERFIQHDQVGFIVRI
Isoform 3	2168	594	NM_198283.1, NP_938024	595-3165 aa: Missing 590-594 aa: CSCSL → YLCII
Isoform 4	10485	3165	NM_001292009.1, NP_001278938	canonical

Table 4.1 An overview of human EYS isoforms based on the information derived from the GenBank and UniProt databases (accessed on 14.04.2015). NM numbers refer to transcript whereas NP numbers to protein variants.

EYS isoform 4 was described as canonical by UniProt as it is the longest of all the variants. EYS isoform 1 lacks the 42nd exon; however, this change does not seem to affect the domain structure of the protein as both of the groups who identified EYS reported identical order of domains. This was also confirmed by scanning the sequence of EYS isoforms 1 and 4 using the Prosite database of protein domains (http://prosite.expasy.org/**;** de Castro *et al.*, 2006). The domain structure of EYS isoforms 2 and 3 had not been examined before and therefore, the same tool was used to investigate the potential structure of the short variants of EYS. Both of the isoforms were predicted to be composed of five EGF-like domains, with a variable length and amino acid composition of the C-terminal ends of the protein. Since the first 589 aa of all of the EYS isoforms are identical, it is expected that EYS isoforms 2 and 3 also possess the N-terminal signal peptide which may be essential for their final localisation. The genetic and protein domain structure of EYS isoforms is shown in Figure 4.1.

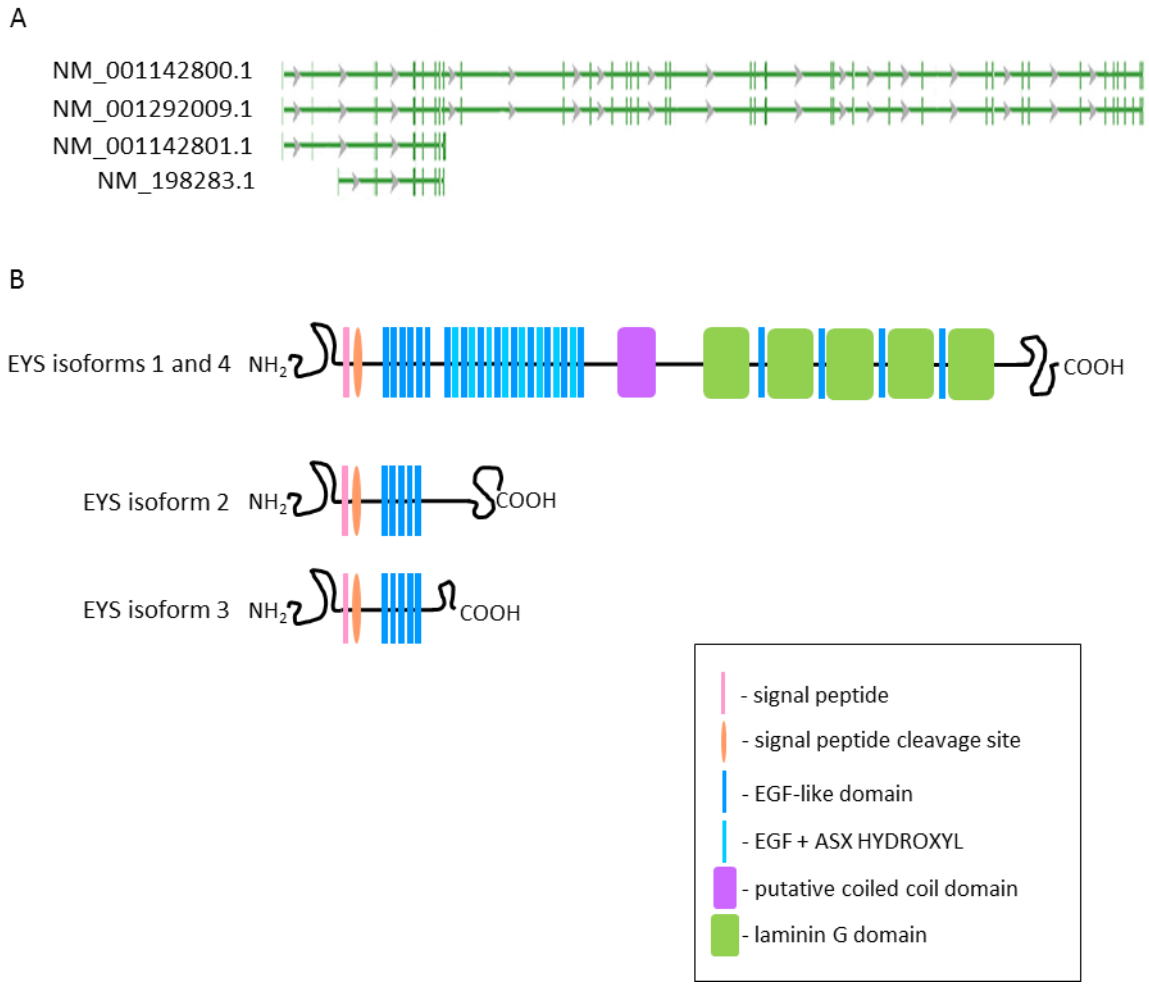

Figure 4.1 An overview of human EYS transcripts variants. **A:** a schematic view of EYS transcript variants; green perpendicular bars represent protein coding exons, lanes represent introns and arrows indicate the transcriptional direction (data from NCBI Gene database accessed on 14.04.2015; http://www.ncbi.nlm.nih.gov/gene/346007) **B:** Predicted protein domain structure of EYS isoforms; domain order of EYS isoforms 1 and 4 is presented as previously published (Barragan *et al.*, 2010) whereas the domain structure of EYS isoforms 2 and 3 were predicated using the Prosite ExPasy database (http://prosite.expasy.org/, accessed on 14.04.2015).

4.1.1 Characterisation of EYS Isoforms 1 and 4

Many of the disease-causing mutations in *EYS* affect the sequence encoding EYS isoforms 1 and 4. It is, therefore, of paramount importance to understand the role of these isoforms in the retina. To better characterise the EYS long variants, a set of experiments was performed aiming to investigate their localisation and expression patterns. EYS isoforms 1 and 4 seem to have an identical domain structure and in this study, the cDNA of EYS isoform 1 was available and used for experiments. Also, the difference in size between EYS isoforms 1 and 4 is undistinguishable via immunoblotting and therefore, some of the data presented in this section can concern both of the variants.

In the first instance, immunoblotting was performed in order to verify the presence of EYS isoforms 1 and 4 in the protein extracts prepared form cell lines available in the project, which were Y79, SK-N-SH, ARPE-19 and HeLa cell lines. The result of immunoblotting with anti-EYS1 antibody is shown in Figure 4.2, where it can be observed that there is a thin band visible in the Y79 lane at the size of approximately 350 kDa (indicated by a red asterisk). This band corresponds to EYS isoforms 1 and 4 and it was only detected protein extract from Y79 cells; this result is consistent with published RT-PCR analyses (Abd El-Aziz *et al.*, 2008).

Apart from the band at ~350 kDa, there are also multiple bands visible at lower molecular weights in all of the lanes. The protein bands detected between the sizes of 55 – 71 kDa in all lanes could correspond to EYS isoforms 2 and 3; especially that the anti-EYS1 antibody was raised against an epitope common for all four of EYS isoforms. The immunoblotting control experiments, however, demonstrated that anti-EYS1 antibody is unable to detect EYS isoforms 2 and 3 (Appendix I); this means that the bands were most probably non-specifically detected by either the primary or secondary antibodies used. Since EYS isoforms 1 and 4 are large proteins, they are prone to degradation when performing experiments and it is also plausible that bands visible in Y79 lane at lower sizes were degradation products.

Together, these observations suggest that bands detected below 350 kDa are most likely proteins non-specifically detected by the primary or secondary antibodies.

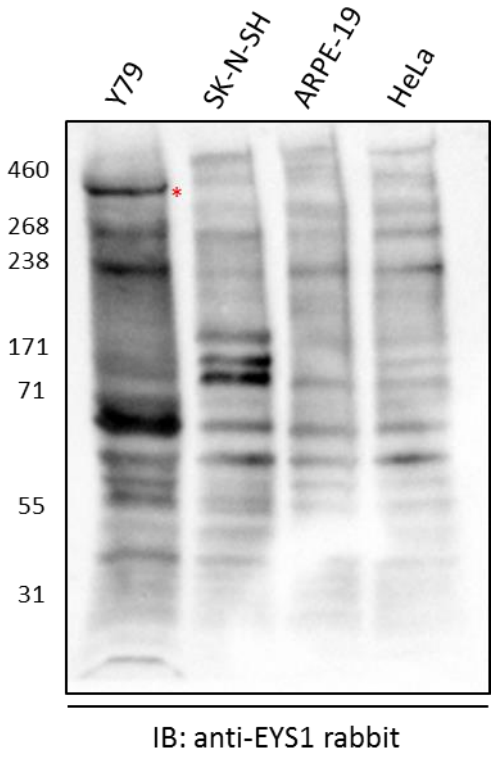

Figure 4.2 Western blot analysis of expression of EYS isoforms 1 and 4 in selected cell lines. The expected size of EYS isoform 1/4 is 350 kDa. A positive band was detected in protein extracts from wild type Y79 cells and is marked with a red asterisk. HiMark Protein standard was used to assess the size of protein bands. Loading was normalised using BCA assay; approximately 30 µg of protein was loaded in each lane. Immunoblotting was performed with anti-EYS1 rabbit and HRP conjugated goat anti-rabbit antibodies. Y79 – a human retinoblastoma cell line; SK-N-SH – a human neuroblastoma cell line; ARPE-19 – a human retinal pigment epithelial cell line; HeLa – a human epitheloid cervix carcinoma cell line.

The next stage of the analysis was to investigate the subcellular localisation of EYS isoforms 1 and 4. In order to look at the endogenous expression patterns, immunofluorescence experiments were performed on Y79 cells, which had been grown on poly-L-lysine coated coverslips. A cluster of Y79 cells stained with anti-EYS1 antibody is shown in Figure 4.3. As it can be observed, EYS is concentrated in the area most likely corresponding to the cytoplasm; however, it is also possible that some of the protein localises to the cell membrane.

To better understand the subcellular localisation of EYS in Y79 cells, immunofluorescence experiments were performed using a range of cellular markers allowing visualisation of certain structures of the cells. The first marker used was acetylated α-tubulin, which is a component of microtubules and allows visualisation of acetylated cytoskeletal structures present in the cytoplasm. A cell co-stained with anti-acetylated-α-tubulin and anti-EYS1 antibodies is shown in Figure 4.4. The signal generated by anti-EYS1 antibody forms a ring around the nucleus and is surrounding the cytoplasm highlighted by staining of acetylated-α-tubulin. This suggests that EYS could be associated with the plasma membrane; nevertheless, the signal was also detected in the cytoplasm.

To look into the membrane localisation of EYS, a fluorophore-conjugated wheat germ agglutinin (WGA) stain was used. WGA is a lectin that binds to N-acetyl-D-glucosamine and sialic acid residues found on the surface of cell membranes. The co-staining performed with fluorophore-conjugated WGA and anti-EYS1 antibody is shown in Figure 4.5; some co-localisation of EYS with WGA is visible, however, the overlap of signals is not thorough and some EYS signal could still come from the cytoplasm. As Y79 cells grow in suspension, they are spherical in shape and have low volume of the cytoplasm. These features make it challenging to make accurate observations regarding subcellular localisation of EYS, and therefore the yellow signal observed in co-staining with WGA could be random, especially in such a small and round cell body.

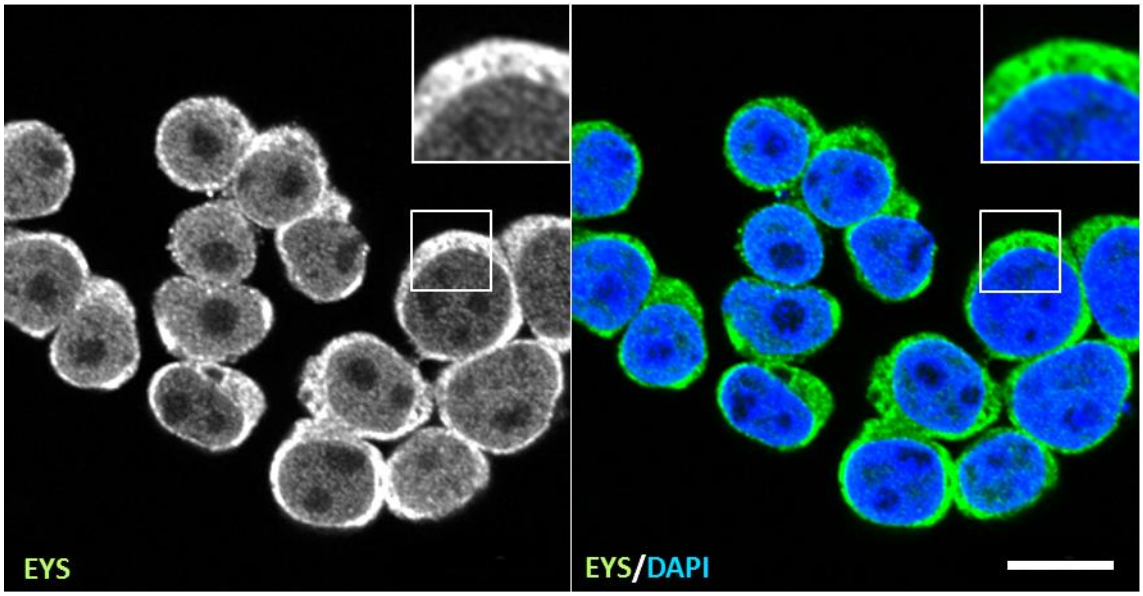

Figure 4.3 Localisation of EYS in a cluster of wild type Y79 cells. EYS (green) is concentrated in the area corresponding to the cytoplasm; however, it is also possible that some of the protein localises to the cell membrane. The zoomed inserts represent the areas demarcated by the white squares in the images. Immunostaining was performed with anti-EYS1 rabbit antibody. Secondary antibody was Alexa Fluor 488 conjugated goat anti-rabbit. Nuclei were stained with DAPI (blue). Scale bar: 10 μm.

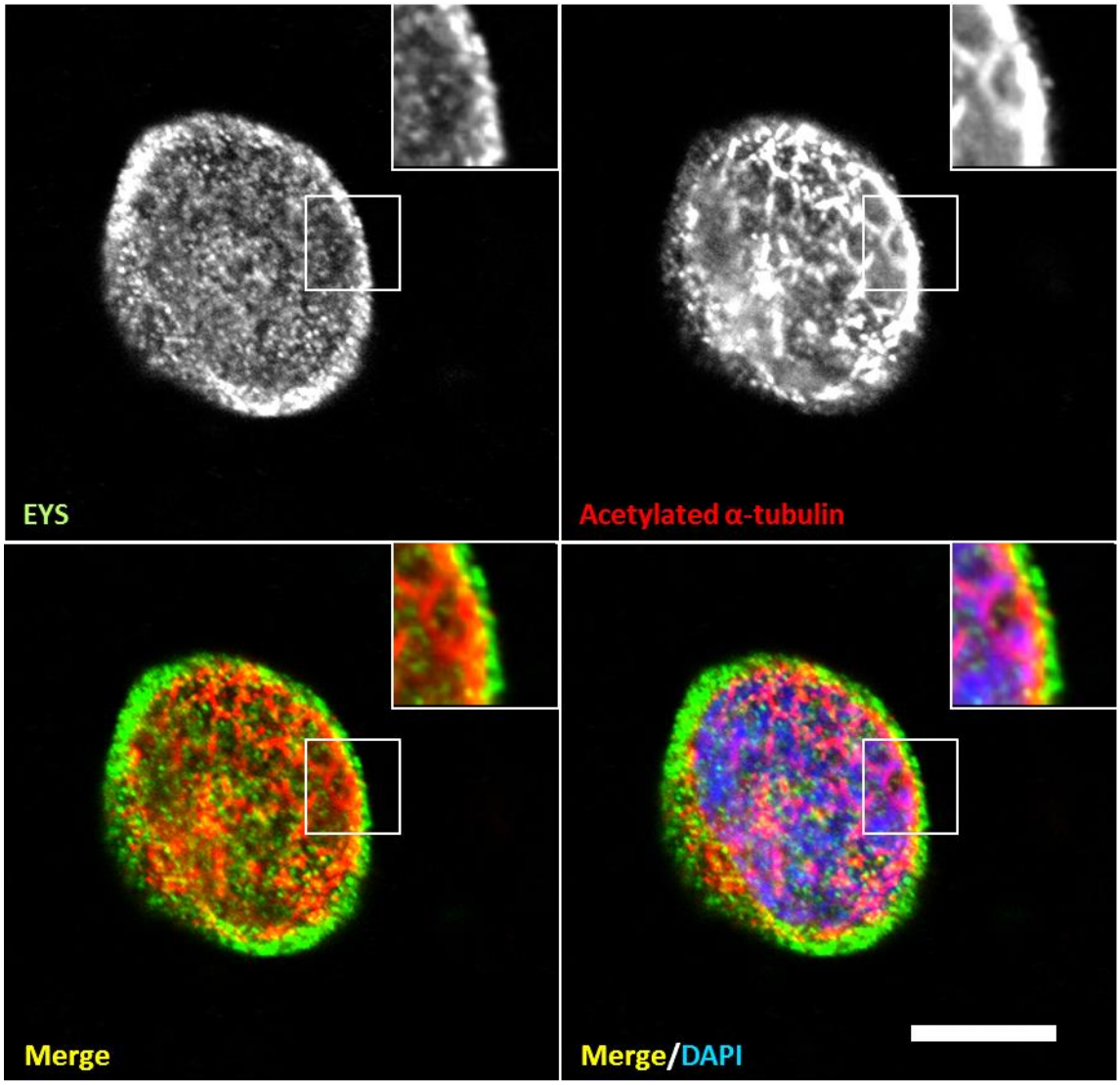

Figure 4.4 Localisation of EYS and α-tubulin in Y79 cell line. EYS (green) forms a ring around the nucleus and is surrounding the cytoplasm highlighted by staining of acetylated-α-tubulin (red). The zoomed inserts represent the areas demarcated by the white squares in the images. Immunolabelling was performed with anti-EYS1 rabbit and anti-acetylated-α-tubulin mouse antibodies. Secondary antibodies were Alexa Fluor 488 conjugated goat anti-rabbit and Cyanine 3 conjugated goat anti-mouse. Nuclei were stained with DAPI (blue). Scale bar: 10 μm.

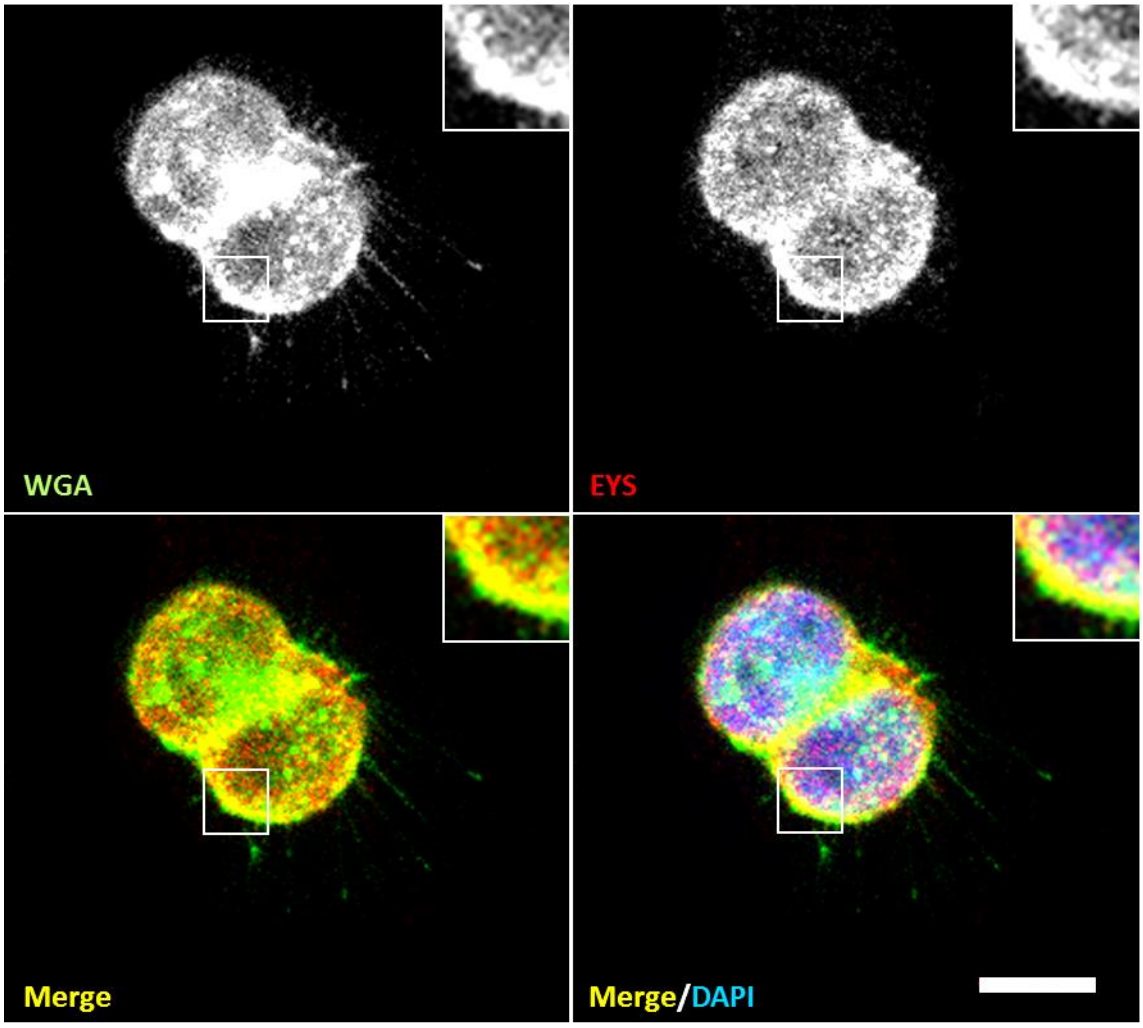

Figure 4.5 Localisation of EYS in Y79 cell s stained with a membrane marker, WGA. EYS (green) is present in the cell cytoplasm and some portion of the signal overlaps with the cell membrane stained with WGA (red). Co-localisation is indicated by a yellow signal. The zoomed inserts represent the areas demarcated by the white squares in the images. Immunolabelling was performed with anti-EYS1 rabbit antibody and AlexaFluor 488-conjugated wheat germ agglutinin (WGA) stain. Secondary antibody was Alexa Fluor 633 conjugated goat anti-rabbit. Nuclei were stained with DAPI (blue). Scale bar: 10 µm.

In order to encourage morphological differentiation, Y79 cells were seeded on coated coverslips and treated with dibutyryl-cAMP, according to a protocol optimised for the needs of the project. Figure 4.6 depicts a cluster of Y79 cells treated with dibutyryl-cAMP and stained with anti-EYS1 and anti acetylated-α-tubulin antibodies. Microtubules can be seen throughout the cytoplasm and one long membrane protrusion is visible, which most likely corresponds to the primary cilium. EYS was detected as speckled signal distributed in the areas that could correspond to the cytoplasm or the cell membrane.

To further analyse the subcellular localisation of EYS, the cells were stained with phalloidin conjugated with a fluorescent dye. Phalloidin specifically binds filamentous actin (F-actin) molecules which form actin filaments that are abundant throughout the cell but also present beneath the plasma membrane and in actin-based microvilli. As shown in Figure 4.7, F-actin is concentrated under the cell membrane and present in the membrane protrusions whereas EYS is mostly concentrated in the main cell body, in the areas that most likely represent the cytoplasm; very little signal is present in the protrusions and the two proteins seem to have distinctly separate localisation patterns.

Y79 cells are not the most convenient tool for studying localisation of proteins and it would have been undoubtedly advantageous to investigate the exogenous expression patterns of EYS isoform 1 and 4 in adherent cell lines. The size of vector constructs made it extraordinarily challenging to transfect full sized EYS isoform 1 constructs into cell lines and it was successful only on a few occasions, which will be referred to further in Chapter 5. To gain a better idea of how full length EYS could localise in adherent cell lines, N-terminal (1-1635 aa) and C-terminal (1880-3144 aa) fragments of EYS isoform 1 were cloned with a GFP tag and transfected into HeLa cells. This particular cell line was chosen as it was found at many stages of the project that it transfects with the highest efficiency. Transfected cells were afterwards stained with fluorophore-conjugated WGA stain to visualise the cell membrane and the result is presented in Figure 4.8. As shown, both N-terminal and C-terminal fragments of EYS isoform 1 appear to localise to the cytoplasm and no co-localisation was observed at the cell membrane or microvilli. This would suggest that EYS isoform 1 has a cytoplasmic localisation; however, the full length protein would need to be examined to verify this hypothesis.

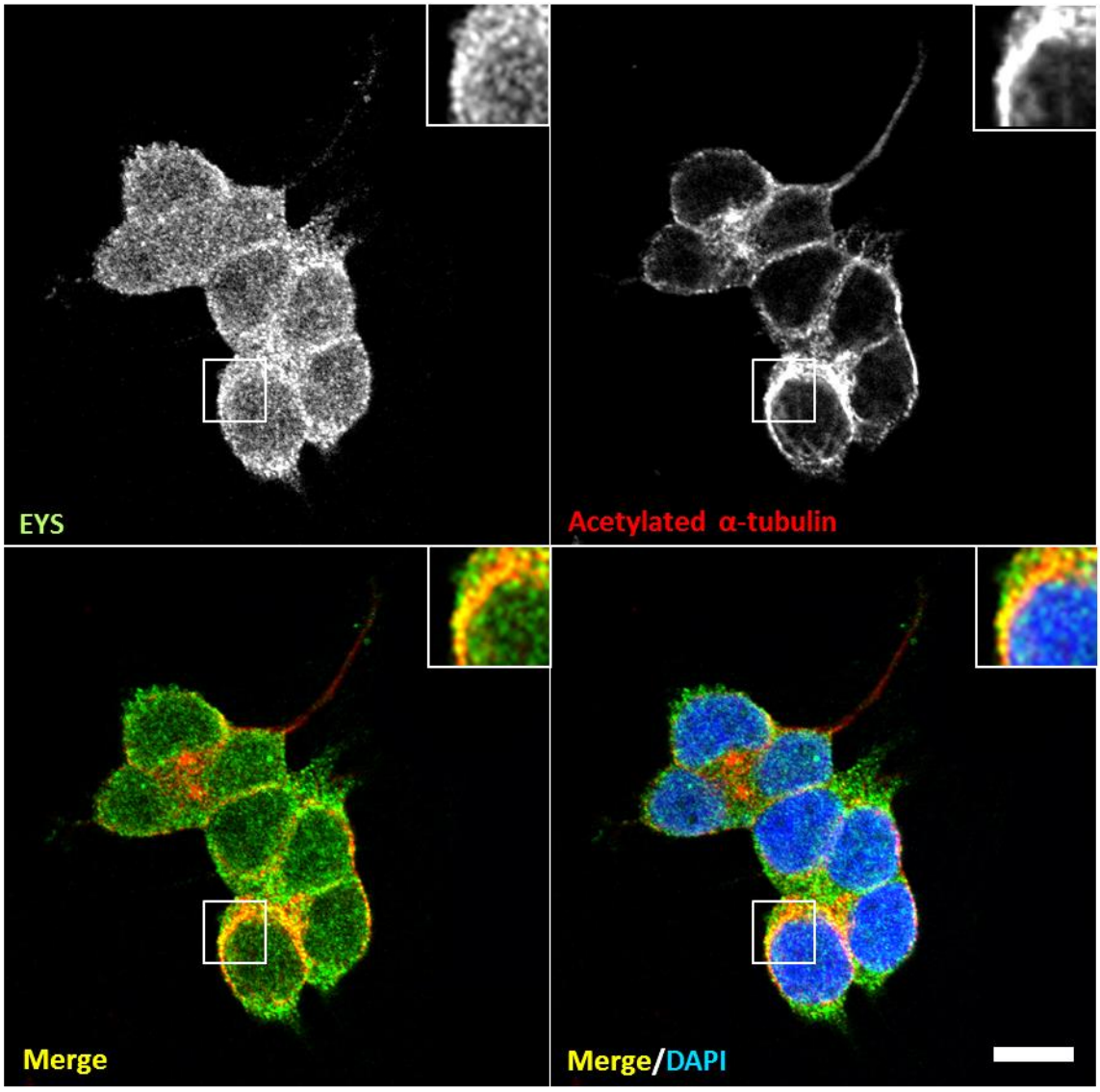

Figure 4.6 Localisation of EYS and acetylated-α-tubulin in a cluster of Y79 cells treated with dibutyryl-cAMP. EYS (green) was detected in the cell cytoplasm whereas microtubules (red) were seen throughout the cytoplasm and one long membrane protrusion is visible, which most likely corresponds to the primary cilium. The zoomed inserts represent the areas demarcated by the white squares in the images. Immunolabelling was performed with anti-EYS1 rabbit and anti-acetylated-α-tubulin mouse antibodies. Secondary antibodies were Alexa Fluor 488 conjugated goat anti-rabbit and Cyanine 3 conjugated goat anti-mouse. Nuclei were stained with DAPI (blue). Scale bar: 10 μm.

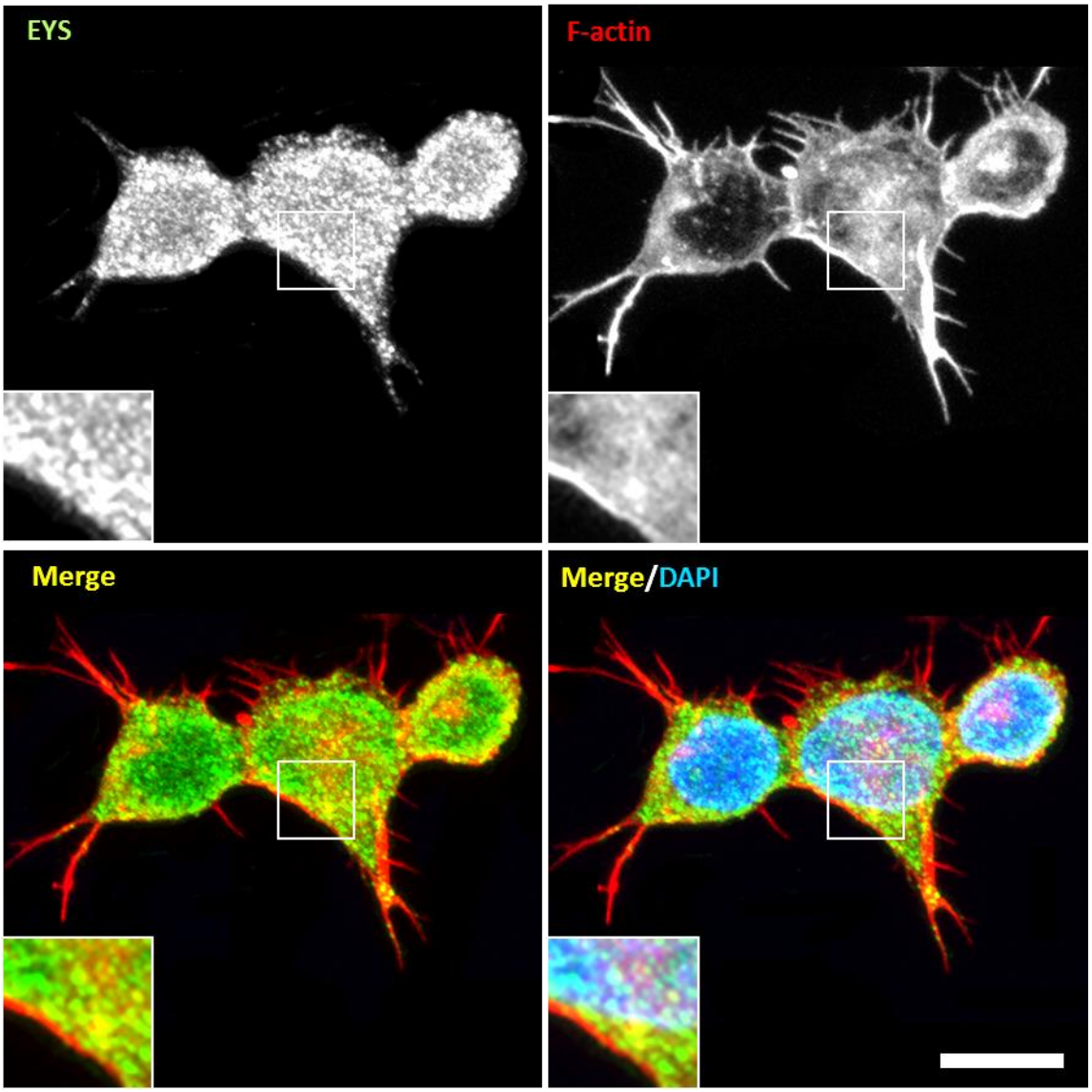

Figure 4.7 Localisation of EYS and F-actin in a cluster of Y79 cells treated with dibutyryl-cAMP. F-actin (red) was concentrated under the cell membrane and present in the membrane protrusions whereas EYS was mostly concentrated in the main cell body, in the areas that most likely represent the cytoplasm; very little signal is present in the protrusions and the two proteins seem to have distinctly separate localisation patterns. The zoomed inserts represent the areas demarcated by the white squares in the images. The cells were immunolabelled with anti-EYS1 rabbit antibody and stained with AlexaFluor 594-conjugated phalloidin dye. A secondary antibody was Alexa Fluor 488 conjugated goat anti-rabbit. Nuclei were stained with DAPI (blue). Scale bar: 10 μm.

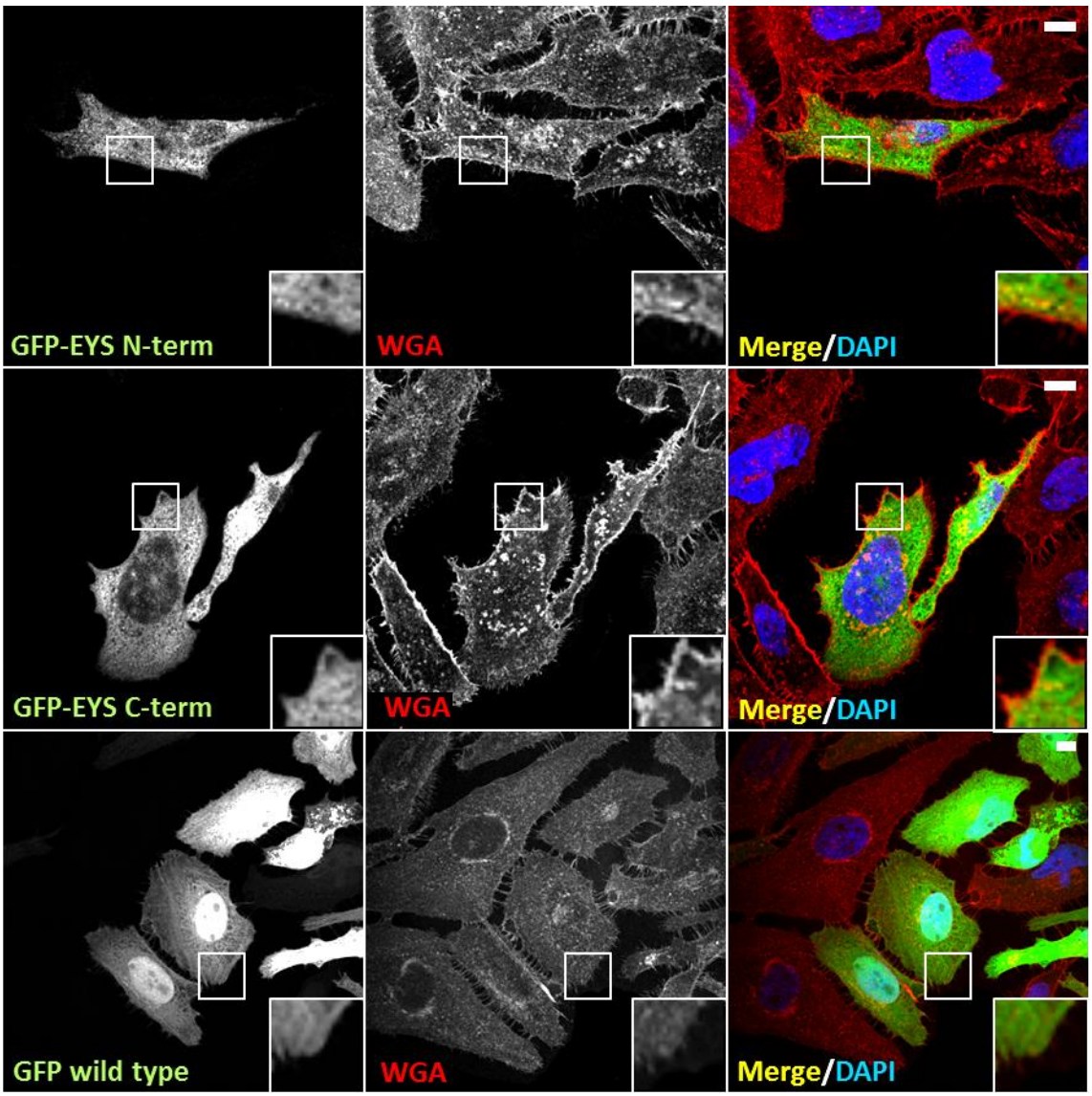

Figure 4.8 Localisation of GFP tagged EYS N-terminal and C-terminal fragments in HeLa cells stained with a membrane marker WGA. EYS N- and C-terminal fragments (green) localise to the cytoplasm and he signal does not overlap with WGA (red). GFP wild type (empty vector) was used as a control. The zoomed inserts represent the areas demarcated by the white squares in the images. Transfected cells were stained with TexasRed conjugated wheat germ agglutinin (WGA) stain. Nuclei were stained with DAPI (blue). Scale bar: 10 μm.

Altogether, the immunofluorescence experiments performed in Y79 and HeLa cell lines demonstrated that EYS could localise to the cytoplasm and possibly to the cell membrane. Variable localisation could be caused by presence of the shorter EYS isoforms 2 and 3; however, anti-EYS1 antibody was demonstrated to only detect EYS isoforms 1 and 4. Therefore, the results obtained in this section can be considered specific for large EYS isoforms 1 and 4.

4.1.2 Characterisation of EYS Isoforms 2 and 3

Since the expression of EYS isoforms 2 and 3 had not previously been addressed experimentally, RT-PCR analysis was performed on a panel of cDNA samples derived from a number of different adult human tissues and cultured cell lines. In the first experiment, full length sequences of EYS isoforms 2 and 3 were sought for in the panel of tissue specific cDNAs and the obtained results are presented in Figure 4.9. The analysis demonstrated that EYS isoforms 2 and 3 are exclusively expressed in the retina and testis and, interestingly, more than one band could be observed in the testis lane for EYS isoform 2, suggesting that there are more EYS variants expressed in this tissue.

When it comes to the cell lines, the analysis demonstrated that EYS isoforms 2 and 3 are expressed in Y79 cells but not in the other tested cell lines, which were SK-N-SH, ARPE-19 and HeLa (Figure 4.10). The lack of expression in SK-N-SH and ARPE-19 cell lines (derived from human neuroblastoma and the RPE respectively) could suggest that the presence of the short EYS variants is restricted to the neural retina.

EYS isoforms 2 and 3 are significantly different in size and domain structure from the other two variants of EYS; therefore, it is not unlikely that EYS isoforms have variable activities in the human body. All of the variants share the same signal peptide which could suggest that they go through similar post-translational processing and localise to the same compartment of the cell.

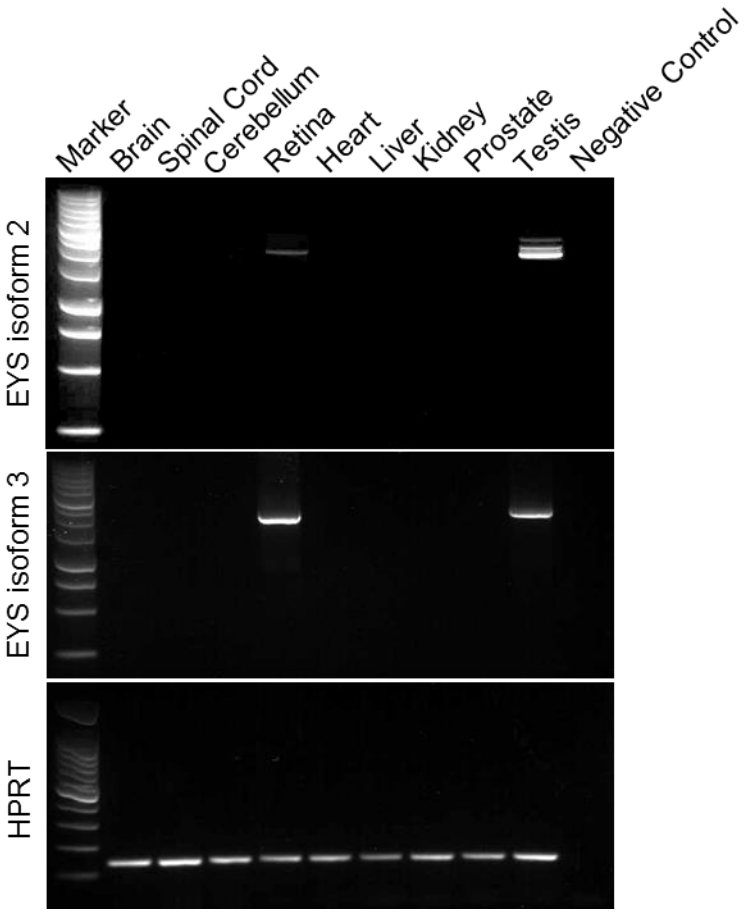

Figure 4.9 RT-PCR analysis of expression of EYS isoforms 2 and 3 in a panel of cDNA sampled derived from human tissues. Primers were designed to cover the entire coding sequence of both isoforms. The predicted sizes of EYS isoform 2 and 3 are 1882 bp and 1796 bp respectively. Positive bands demonstrating presence of the transcripts were observed for both of the isoforms in cDNA derived from the retina and testis. PCR mix without cDNA was used as negative control. A 150 bp fragment of ubiquitously expressed hypoxanthine phosphoribosyltransferase 1 gene (HPRT1) was used as a quality control. Promega 1 kb and 100 bp PCR markers were used to assess sizes of the bands.

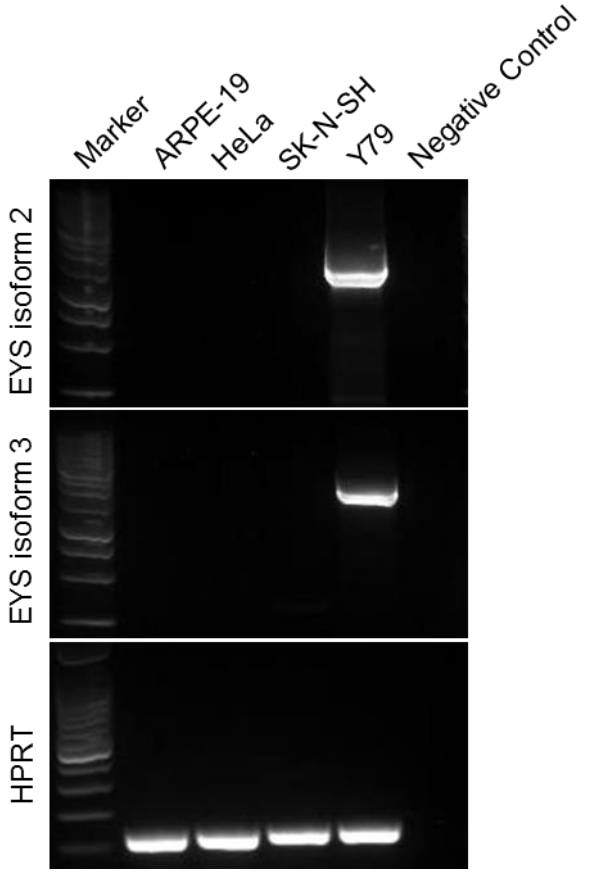

Figure 4.10 RT-PCR analysis of expression of EYS isoforms 2 and 3 in the panel of cDNA derived from four human cell lines. Primers were designed to cover the entire coding sequence of both isoforms. The predicted sizes of EYS isoform 2 and 3 are 1882 bp and 1796 bp respectively. Positive bands demonstrating presence of the transcripts were observed for both isoforms in probes derived from Y79 cells. PCR mix without cDNA was used as negative control. A 150 bp fragment of ubiquitously expressed hypoxanthine phosphoribosyltransferase 1 gene (*HPRT1*) was used as a quality control. Promega 1 kb and 100 bp PCR markers were used to assess sizes of the bands. Cell lines used in the experiment: ARPE-19 – a human retinal pigment epithelial cell line; HeLa – a human epitheloid cervix carcinoma cell line; SK-N-SH – a human neuroblastoma cell line; Y79 – a human retinoblastoma cell line.

In order to look into the subcellular localisation of EYS isoforms 2 and 3, immunocytochemistry experiments were performed. Y79 cells were shown to express all four EYS isoforms endogenously; nonetheless, the available anti-EYS1 antibody was only able to detect EYS isoforms 1 and 4, as described in the previous section. For this reason and in order to ensure that the analysis is specifically focused on EYS isoforms 2 and 3, ectopic expression of GFP tagged constructs was analysed. In the first instance, Y79 cells were investigated as they provide a retina specific environment for the synthesis of EYS proteins. Y79 cells were attached to the glass coverslips and transfected with GFP tagged EYS isoforms 2 and 3; GFP empty vector was used as a control. The results of the experiment are presented in Figure 4.11 and, as it can be observed, GFP tagged EYS isoforms 2 and 3 appear to have an identical expression pattern and localise to the cytoplasm. As expected, the signal from the GFP wild type tag was diffused across the cytoplasm and the nucleus. The subcellular localisation of GFP tagged EYS isoforms 2 and 3 could also overlap with the cell membrane; however, their distribution is similar to the one of GFP wild type which strengthens the hypothesis of the cytoplasmic localisation.

Taking into account the previously mentioned drawbacks to using the Y79 cell line, and that the transfection method for these cells is technically demanding and the efficiency usually low, the GFP tagged constructs were transfected into the HeLa cell line in order to characterise the expression pattern of EYS isoforms with more accuracy. The panel presented in Figure 4.12 shows successfully overexpressed GFP tagged EYS isoforms 2 and 3, and wild type GFP, which was used as a control. The vast majority of the overexpressed EYS isoforms localised to the cytoplasm; however, there was also some signal detected in the cell nuclei. The nuclear localisation was also detected in other experiments; however, it was not a consistently repeated pattern. This would suggest that it can be a result of overexpression or that the localisation of EYS isoforms 2 and 3 is dynamic and modulated by an unknown mechanism. Moreover, there are some stronger green speckles and aggregate-like structures visible for both of the isoforms, which could correspond to transporting vesicles or organelles such as Golgi apparatus; they could also manifest protein degradation.

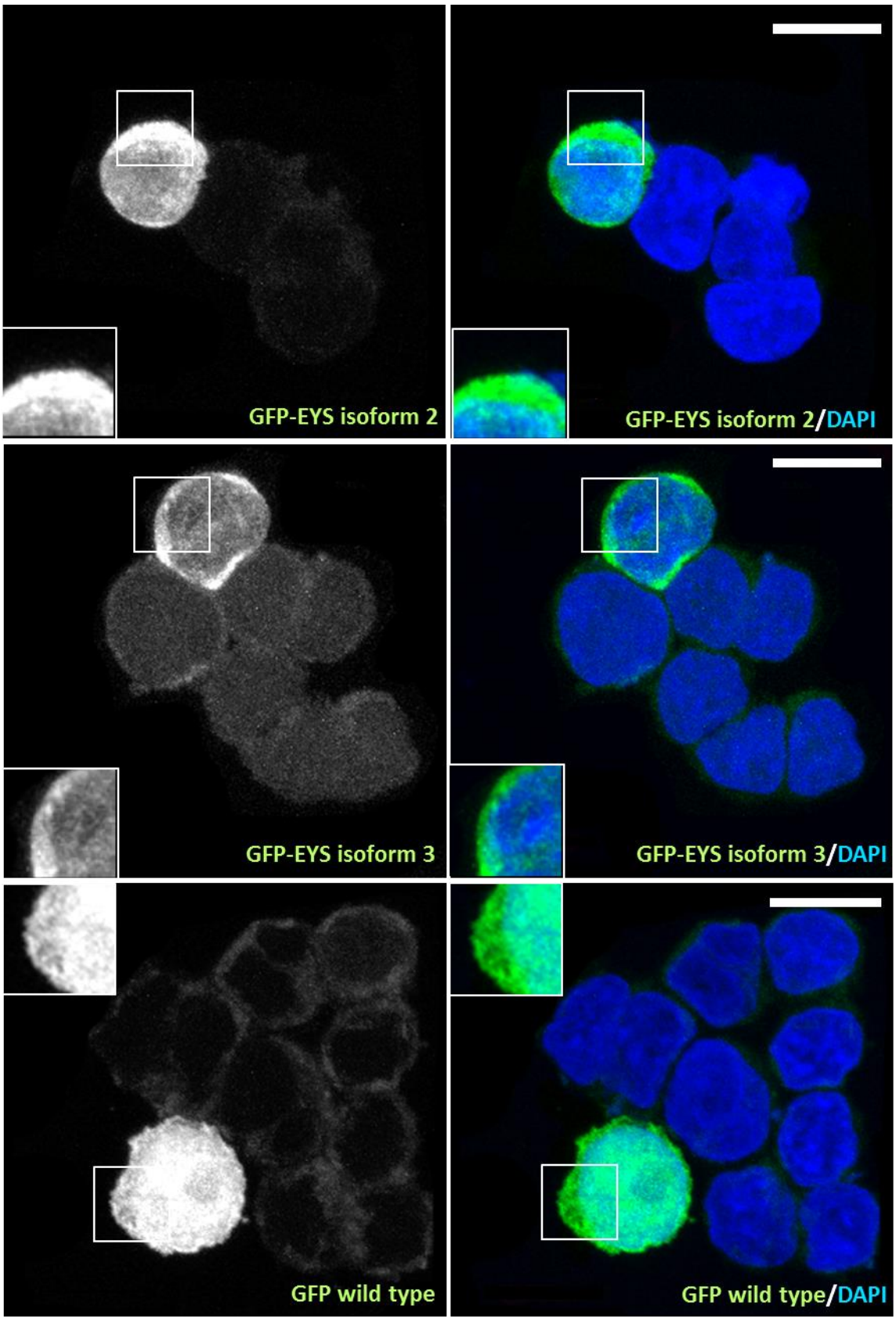

Figure 4.11 Localisation of GFP tagged EYS isoforms 2 and 3 in Y79 cells. Both of the isoforms localised to the cell cytoplasm of transfected Y79 cells. GFP wild type (empty vector) was used as a control of the fluorescent tag. The zoomed inserts represent the areas demarcated by the white squares in the images. Nuclei were stained using DAPI (blue). Scale bar: 10 μm.

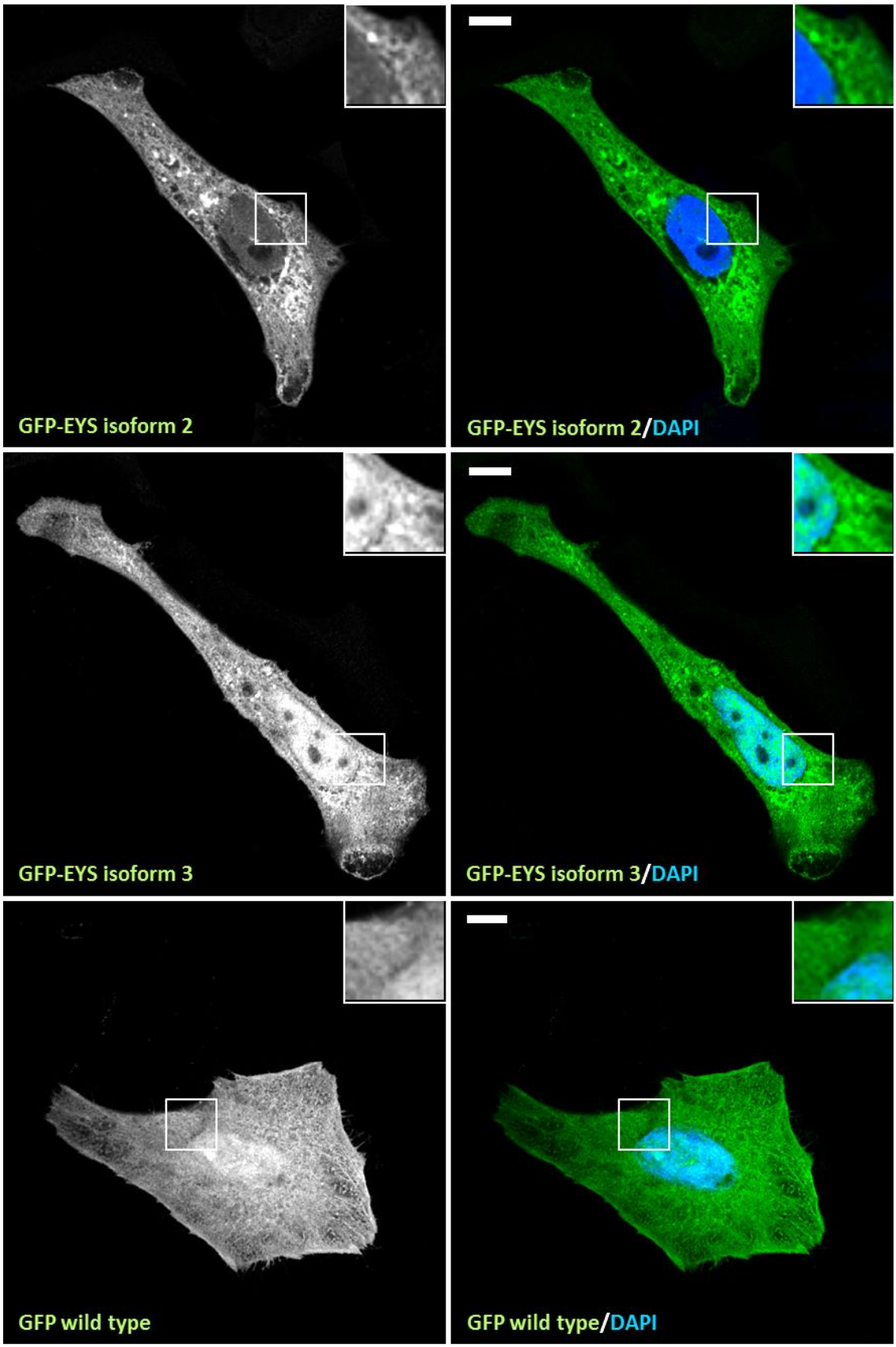

Figure 4.12 Localisation of GFP tagged EYS isoforms 2 and 3 in HeLa cells. EYS isoform 2 localised to the cytoplasm whereas EYS isoform 3 localised to the cytoplasm and the nucleus of transfected HeLa cells. GFP wild type (empty vector) was used as a control of the fluorescent tag. The zoomed inserts represent the areas demarcated by the white squares in the images. Nuclei were stained using DAPI (blue). Scale bar: 10 μm.

To confirm specificity of the experiment, protein extracts were prepared from HeLa cells transfected with GFP tagged EYS isoforms 2 and 3, and the GFP empty vector. Immunoblotting was performed using anti-GFP mouse antibody and as shown in Figure 4.13, protein bands at expected sizes were detected, confirming that tagged EYS isoforms 2 and 3 were successfully overexpressed in HeLa cells.

To delineate the subcellular localisation of EYS isoforms 2 and 3 more accurately, cells transfected with the GFP tagged variants were compared with markers of the particular cellular compartments. In order to highlight the structures present in the cytoplasm, F-actin filaments were stained with fluorophore-conjugated phalloidin and microtubules were immuno-labelled with anti α-tubulin antibody. The cell membrane was stained with a fluorophore-conjugated WGA stain and in order to highlight the Golgi apparatus, immuno-staining with α-giantin antibody was performed.

The panel presented in Figure 4.14 shows the expression pattern of EYS isoform 2 compared with the aforementioned cellular markers. From the staining with phalloidin, it can be concluded that GFP tagged EYS isoform 2 localises to the cytoplasm with the signal being spread up to the cell boundary; no signal was detected in the plasma membrane protrusions.

The cytoplasmic localisation of EYS isoform 2 was re-confirmed by the speckled co-localisation with microtubules, which is indicated by the yellow signal. To check whether EYS isoform 2 resides in the cell membrane, transfected cells were stained with fluorophore-conjugated WGA dye. As it can be seen, EYS isoform 2 does not appear to be present in the cell membrane or the nuclear membrane. To test whether the speckled and aggregate-like signal observed in Figure 4.12 was a result of localisation to the Golgi apparatus, co-labelling with anti-giantin antibody was performed. Co-localisation was not observed, suggesting that the aggregates observed may have been the result of overexpression and/or the protein degradation.

Figure 4.15 presents a panel demonstrating subcellular localisation of EYS isoform 3 compared with the previously described markers. Similarly to EYS isoform 2, EYS isoform 3 localised across the cytoplasm and partially overlapped with actin filaments and microtubules but was not found to reside in the cell membrane, microvilli or the Golgi apparatus. GFP tag expressed on its own is

shown in a panel presented in Figure 4.16 and, as expected, it was found to be diffused across the cytoplasm and the nucleus.

Overall, immunocytochemistry experiments demonstrated that EYS isoforms 2 and 3 localise to the cytoplasm and, occasionally, to the cell nucleus. Neither of the variants was found in the cell membrane, microvilli or the Golgi apparatus.

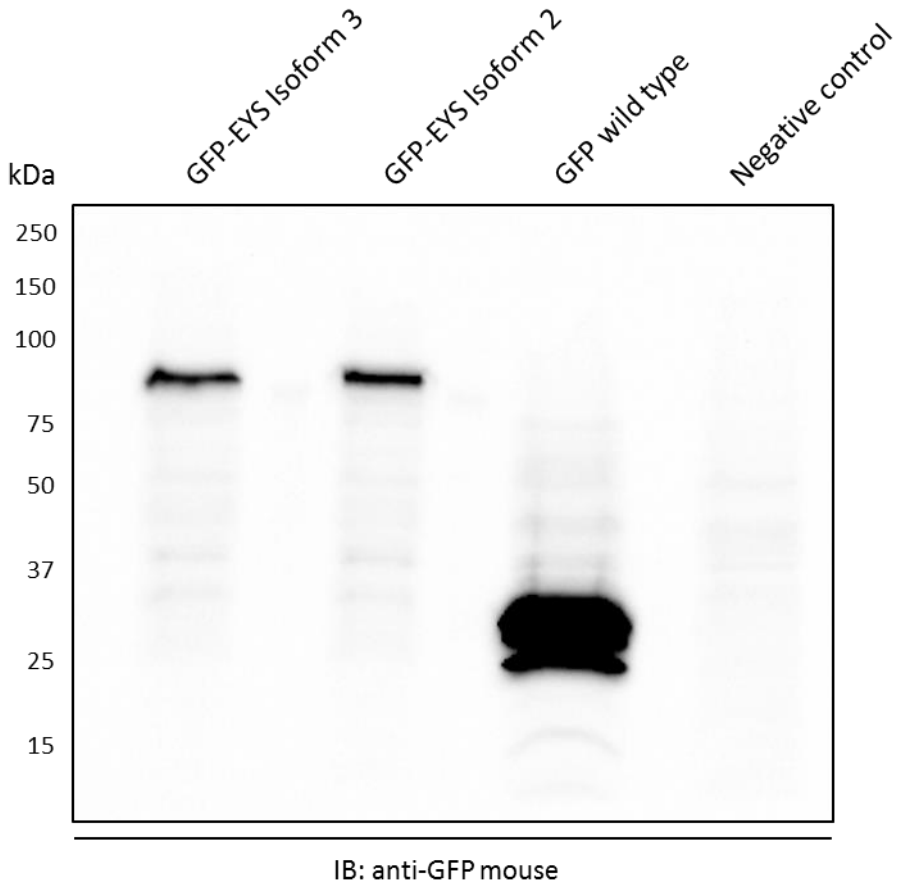

Figure 4.13 Western blot analysis of GFP tagged EYS isoforms 2 and 3. Expected band sizes: GFP-EYS isoform 3 – 94 kDa, GFP-EYS isoform 2 – 97 kDa, GFP wild type – 27 kDa, Protein extract from wild type HeLa cells was used as negative control. Loading was normalised using BCA assay; approximately 30 µg of protein was loaded in each lane. Bio-Rad Precision Plus Protein Standard was used to assess the band size. Anti-GFP mouse primary antibody and HRP conjugated goat anti-mouse secondary antibody were used. IB – immunoblotting.

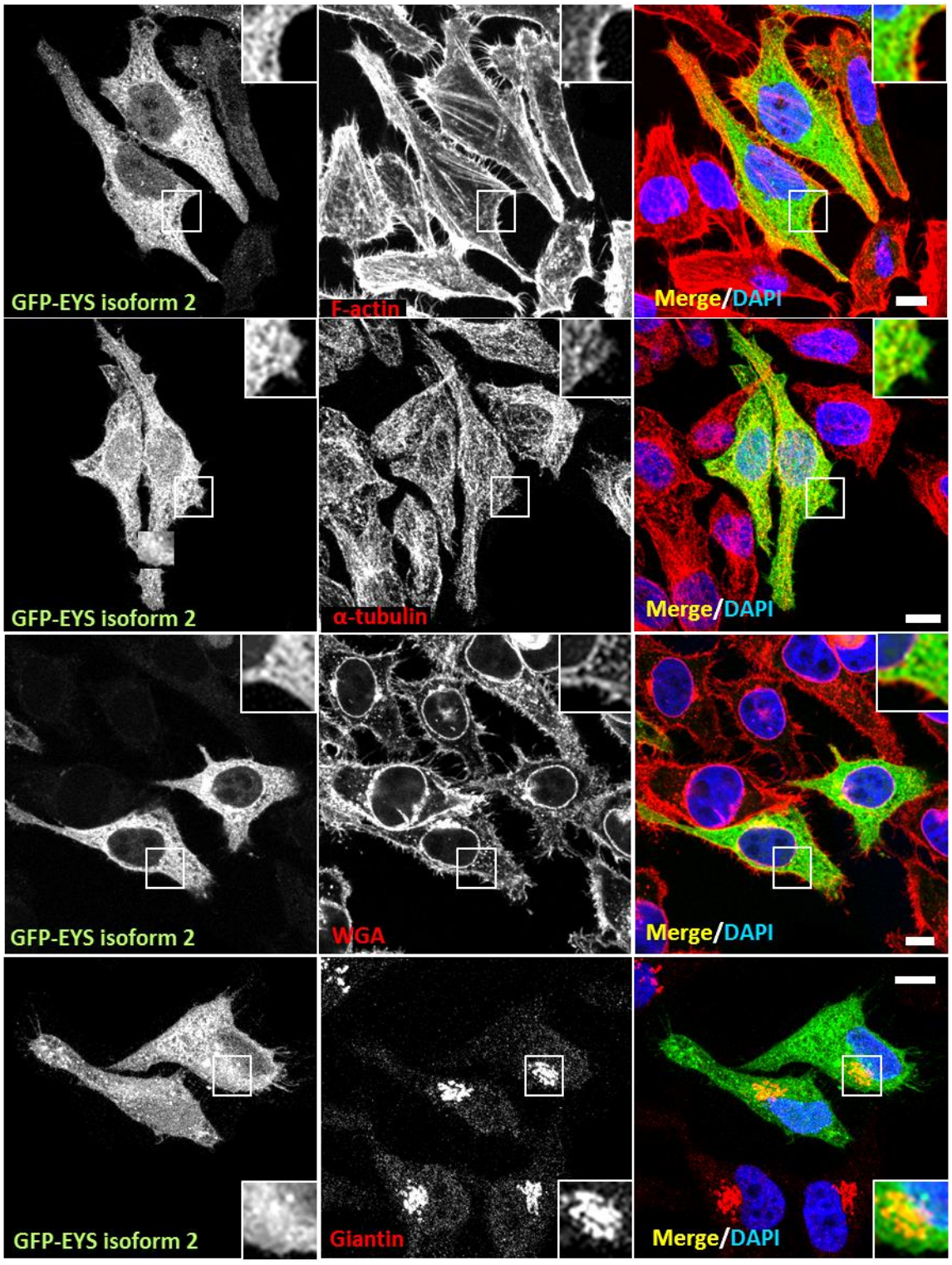

Figure 4.14 Localisation of GFP tagged EYS isoform 2 and a panel of cellular markers in transfected HeLa cells. EYS isoform 2 (green) localised to the cell cytoplasm and occasionally the cell nucleus. The cellular makers (red) were the following organelles: F-actin filaments visualised via staining with AlexaFluor 594-conjugated phalloidin, microtubules stained with anti-α-tubulin mouse antibody, the cell membrane stained with TexasRed conjugated WGA dye and the Golgi apparauts was highlighted by staining with anti-giantin mouse antibody. The zoomed inserts represent the areas demarcated by the white squares in the images. Nuclei were stained with DAPI (blue). Scale bar: 10 μm.

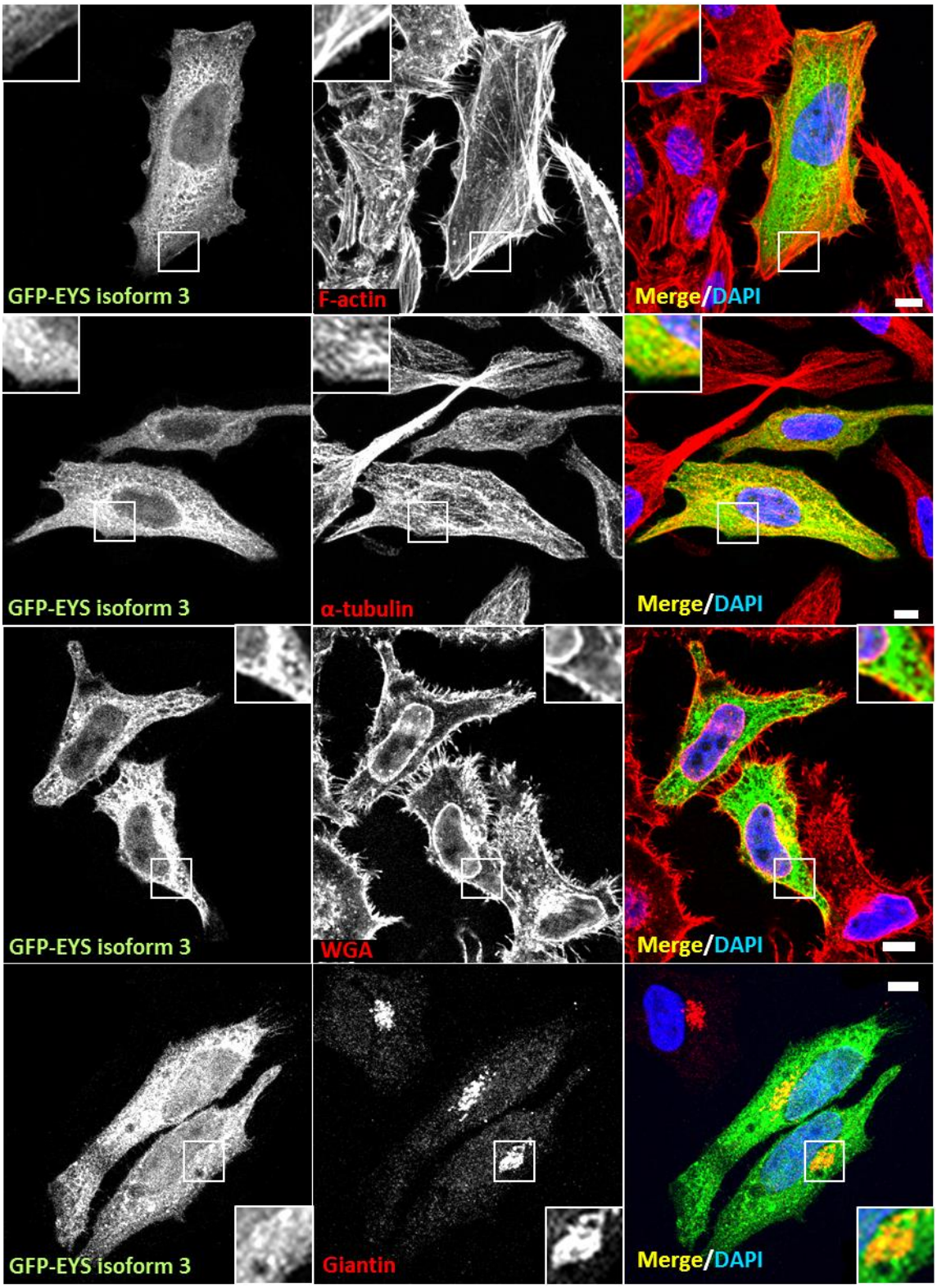

Figure 4.15 Localisation of GFP tagged EYS isoform 3 and a panel of cellular markers in transfected HeLa cells. EYS isoform 3 (green) localised to the cell cytoplasm and occasionally the cell nucleus. The cellular makers (red) were the following organelles: F-actin filaments visualised via staining with AlexaFluor 594-conjugated phalloidin, microtubules stained with anti-α-tubulin mouse antibody, the cell membrane stained with TexasRed conjugated WGA dye and the Golgi apparauts was highlighted by staining with anti-giantin mouse antibody. The zoomed inserts represent the areas demarcated by the white squares in the images. Nuclei were stained with DAPI (blue). Scale bar: 10 μm.

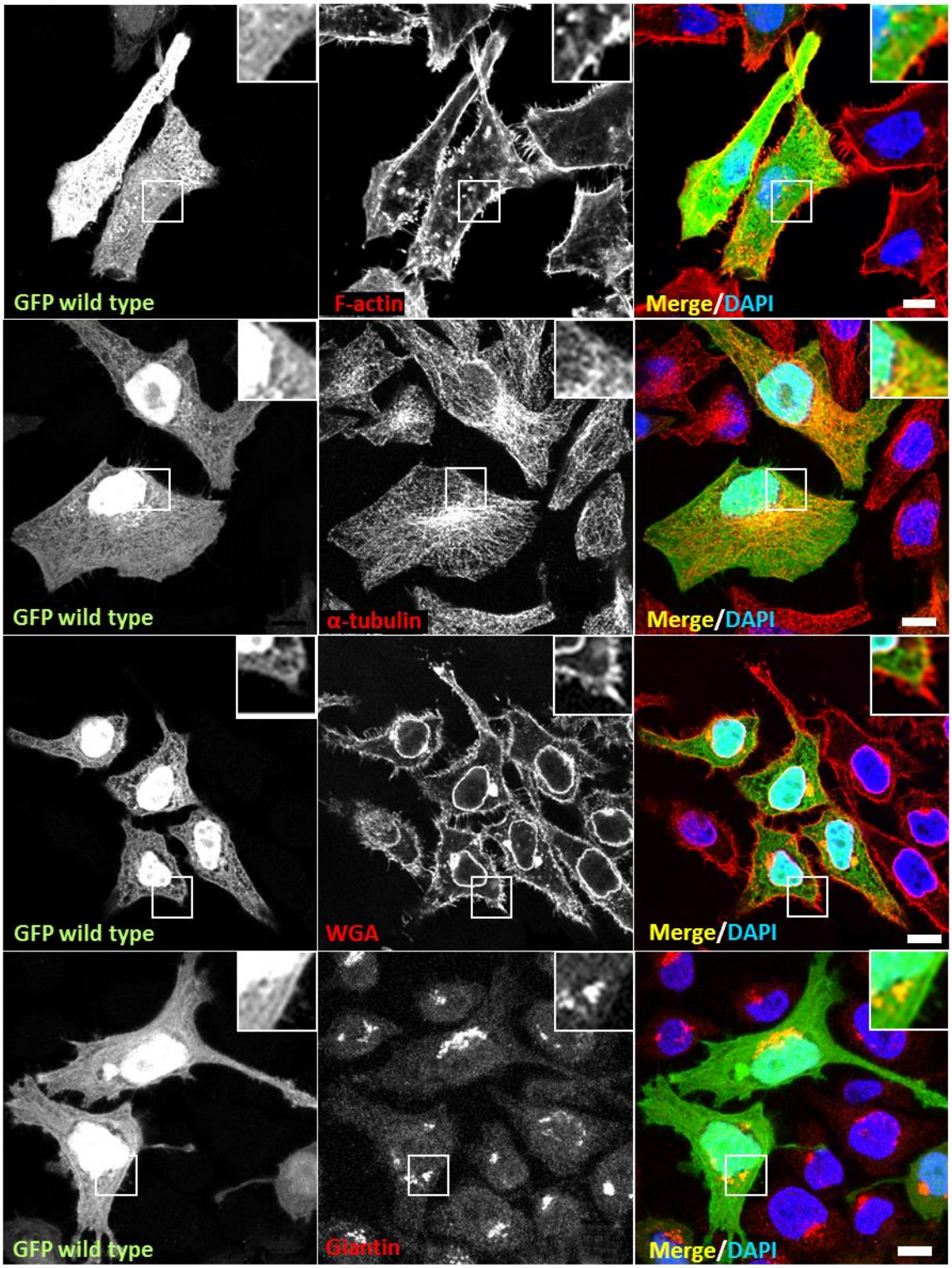

Figure 4.16 Localisation of GFP wild type tag (empty GFP vector) and a panel of cellular markers in transfected HeLa cells. GFP wild type localised to the cell cytoplasm and to the cell nucleus. The cellular makers (red) were the following organelles: F-actin filaments visualised via staining with AlexaFluor 594-conjugated phalloidin, microtubules stained with anti-α-tubulin mouse antibody, the cell membrane stained with TexasRed conjugated WGA dye and the Golgi apparauts was highlighted by staining with anti-giantin mouse antibody. The zoomed inserts represent the areas demarcated by the white squares in the images. Nuclei were stained with DAPI (blue). Scale bar: 10 μm.

4.2 *Ex Vivo* Characterisation of EYS Expression

To investigate the cellular localisation of EYS in a more illustrative model, immunohistochemistry (ICH) experiments were performed. In the first published immunohistochemistry experiment, EYS was reported to localise to the photoreceptor outer segments of the porcine retina (Abd El-Aziz *et al.*, 2008).

In this study, it was aimed to investigate the localisation of EYS more deeply and assess its localisation in the retina derived from an organism more closely related to humans. The best available alternative to human tissue was material explanted from adult crab-eating macaques (*Macaca fascicularis).* To improve credibility of the results, specimens from two different animals were used.

In the first experiment, a single immunostaining was performed to examine the expression pattern of EYS in the monkey retina. Anti-EYS2 antibody was selected as it was raised against an epitope conserved in the genomes of human and crab-eating macaque. As shown in Figure 4.17, EYS was detected in all layers of the retina; however, the strongest signal was detected in the layer corresponding to the connecting cilium and the base of the photoreceptor outer segments. There is also strong signal visible in the lower half of the outer plexiform layer, suggesting that EYS could additionally localise to the synaptic area of photoreceptors or retinal interneurons, and in the ganglion cell layer.

In order to further investigate the potential ciliary localisation of EYS, co-staining with anti-EYS2 and anti-acetylated-α-tubulin antibodies was performed. Acetylated α-tubulin is a component of microtubules and it is commonly used as a marker of the connecting cilium and the ciliary axoneme. Photoreceptor connecting cilium is a structure bridging the inner and outer segments of photoreceptor cells. All proteins residing in the outer segment are synthesised in the inner segment so they must traverse through the connecting cilium to reach their destination. Directly below the connecting cilium, there is the basal body which acts as an organising centre for nucleation of microtubules. The microtubules extend from the basal body to form the axonemal structure that reaches at least half the length of the outer segment (reviewed in Pearring *et al.*, 2013). The micrograph presented in Figure 4.18 suggests that EYS has a similar expression pattern to acetylated α-tubulin, observed as thin whip-like signal extending from the connecting cilium to the photoreceptor outer segment.

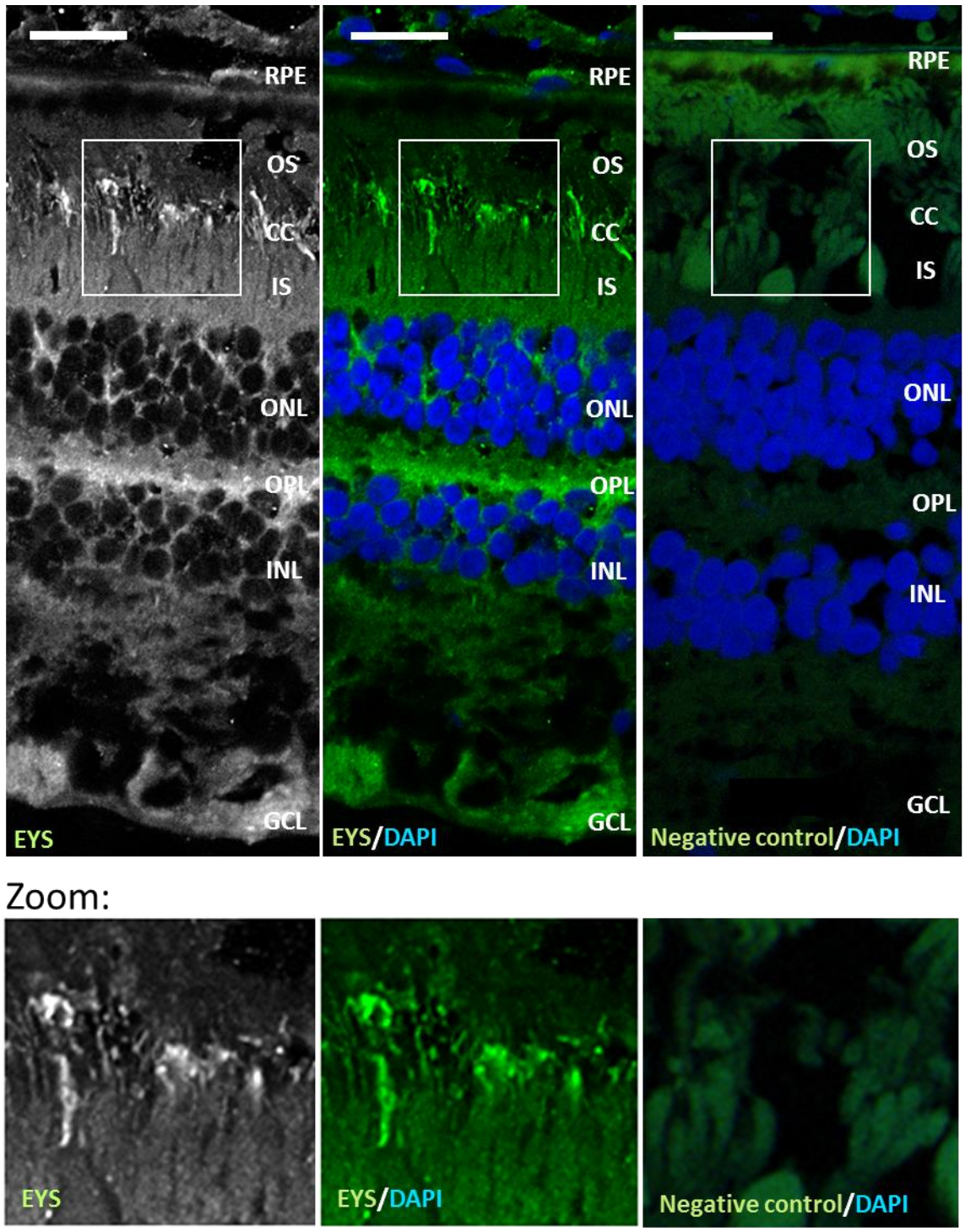

Figure 4.17 Localisation of EYS in the macaque retina. EYS (green) was detected in all layers of the retina; however, significantly stronger signal is visible in the areas corresponding to the connecting cilium and some part of photoreceptor outer segments and outer plexiform layer. The zoomed images (Zoom) are demarcated by the white square in the images. Anti-EYS2 rabbit primary antibody and AlexaFluor488 conjugated goat anti-rabbit secondary antibody were used. DAPI was used to stain cell nuclei (blue). Scale bar: 20 μm. RPE – retinal pigment epithelium, OS – outer segment, CC – connecting cilium, IS – inner segment, OPL – outer plexiform layer, ONL – outer nuclear layer, INL – inner nuclear layer, GCL – ganglion cell layer. Negative control was a specimen labelled with AlexaFluor488 conjugated goat anti-rabbit antibody and DAPI.

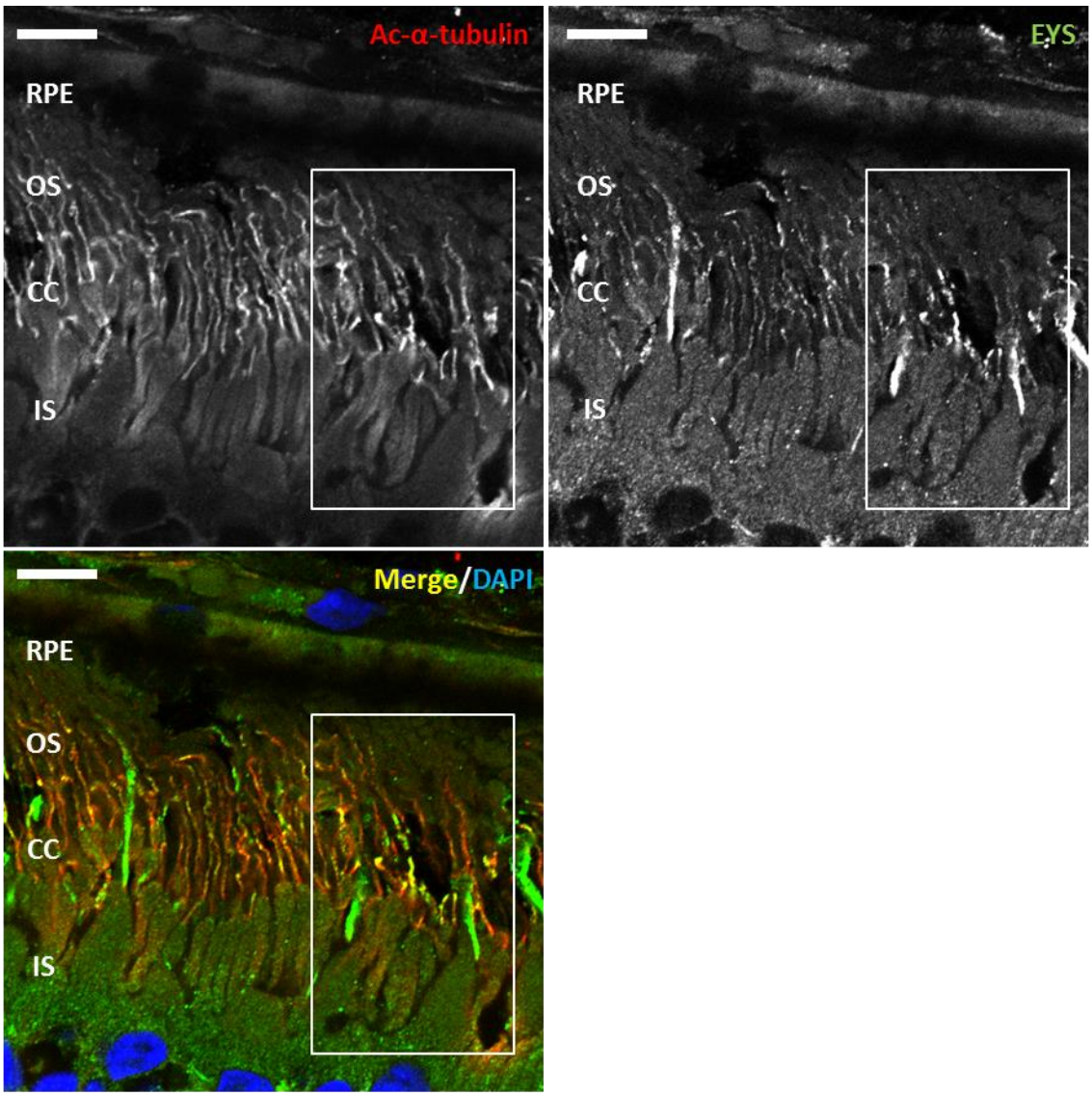

Zoom:

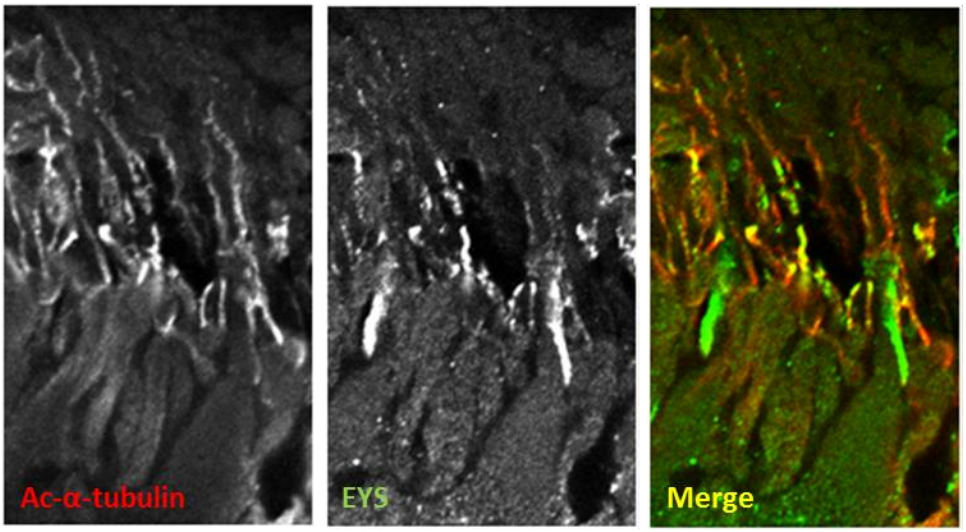

Figure 4.18 Localisation of EYS and acetylated α-tubulin in the macaque. EYS (green) has a similar expression pattern to acetylated α-tubulin (red), observed as thin whip-like signal extending from the connecting cilium to the photoreceptor outer

segment. Acetylated α-tubulin is a structural component and therefore a marker of the photoreceptor ciliary axoneme. Any co-localisation is indicated by yellow/orange signal. The zoomed images (Zoom) are demarcated by the white square in the images. Anti-EYS2 rabbit and anti-acetylated α-tubulin mouse primary antibodies and AlexaFluor488 conjugated goat anti-rabbit and Cyanine 3 conjugated donkey anti-mouse secondary antibodies were used. DAPI was used to stain cell nuclei (blue). Scale bar: 10 μm. RPE – retinal pigment epithelium, OS – outer segment, CC – connecting cilium, IS – inner segment.

This suggests that EYS follows the ciliary axoneme and could be a protein associated with this particular structure.

To ascertain whether EYS localised to the photoreceptor outer segments in the monkey retina, its expression pattern was compared to arrestin that is an outer segment specific protein present in light adapted rod and cone photoreceptors. The micrograph presented in Figure 4.19 shows a co-staining performed with anti-EYS2 (green) and anti-arrestin (red) antibodies. As previously, the EYS signal was detected across the retina with a distinct pattern of thin long fibrils observed in the region of the connecting cilium whereas the staining of arrestin highlighted the layer of the photoreceptor outer segments. The overlap has been observed confirming that EYS localises to the photoreceptor outer segments. Figure 4.20 shows a piece of the same specimen at higher magnification. Here, it can be seen more clearly that the green whip-like signal is present in the region of the connecting cilium and extending above into the outer segment, giving impression that it could overlap with the photoreceptor axoneme.

Since arRP is a condition affecting primarily rods, it was expected that EYS would predominantly localise to this type of photoreceptors. This, however, cannot be determined without performing the analysis utilising rod and cone specific markers.

To confirm whether EYS is present in rods, retinal sections were immuno-labelled with an anti-EYS2 antibody and fluorophore-conjugated WGA stain, specifically binding to rod associated matrix proteins. A micrograph of a stained retina section is presented in Figure 4.21, in which WGA is shown in red and EYS is shown in green. The staining re-confirmed that EYS localises to the region of the connecting cilium and the rod photoreceptor outer segment.

To further examine the co-localisation of EYS and WGA, an image was taken at higher magnification. As shown in Figure 4.22, EYS was detected as thin fibrils

which appear to follow the ciliary axoneme. It also overlapped with the red signal of WGA stain, confirming that EYS is expressed in rods.

To test if EYS is also expressed in cones, co-staining with fluorophore-conjugated PNA, which binds to cone specific matrix proteins, was performed. The result presented in Figure 4.23 demonstrates that EYS is not only associated with rods but it is also present in the cone photoreceptor outer segments. Strikingly, the signal coming from the anti-EYS2 antibody had a very distinct pattern; it is not distributed throughout the outer segments but concentrated on one side of the cell. To verify that observation using a marker that can be immuno-labelled, co-staining of EYS and s-opsin was performed. S-opsin is a protein specifically localising to the s-cone outer segments and in this experiment it was used to highlight that particular structure. The micrograph presented in Figure 4.24 shows an s-cone outer segment highlighted in green and EYS highlighted in red. The expression pattern of EYS is indeed consistent with the previous experiments and it appears as a whip-like structure extending from the connecting cilium into the outer segment.

Immunocytochemistry experiments conducted on monkey retinal sections revealed that EYS could be a ciliary associated protein in both rods and cones. Based on that observation, it can be suggested that EYS may be involved in processes such as maintaining the structure of the ciliary axoneme, intraflagellar transport or signalling pathways. Further research would be required to fully determine the role EYS in photoreceptor cells.

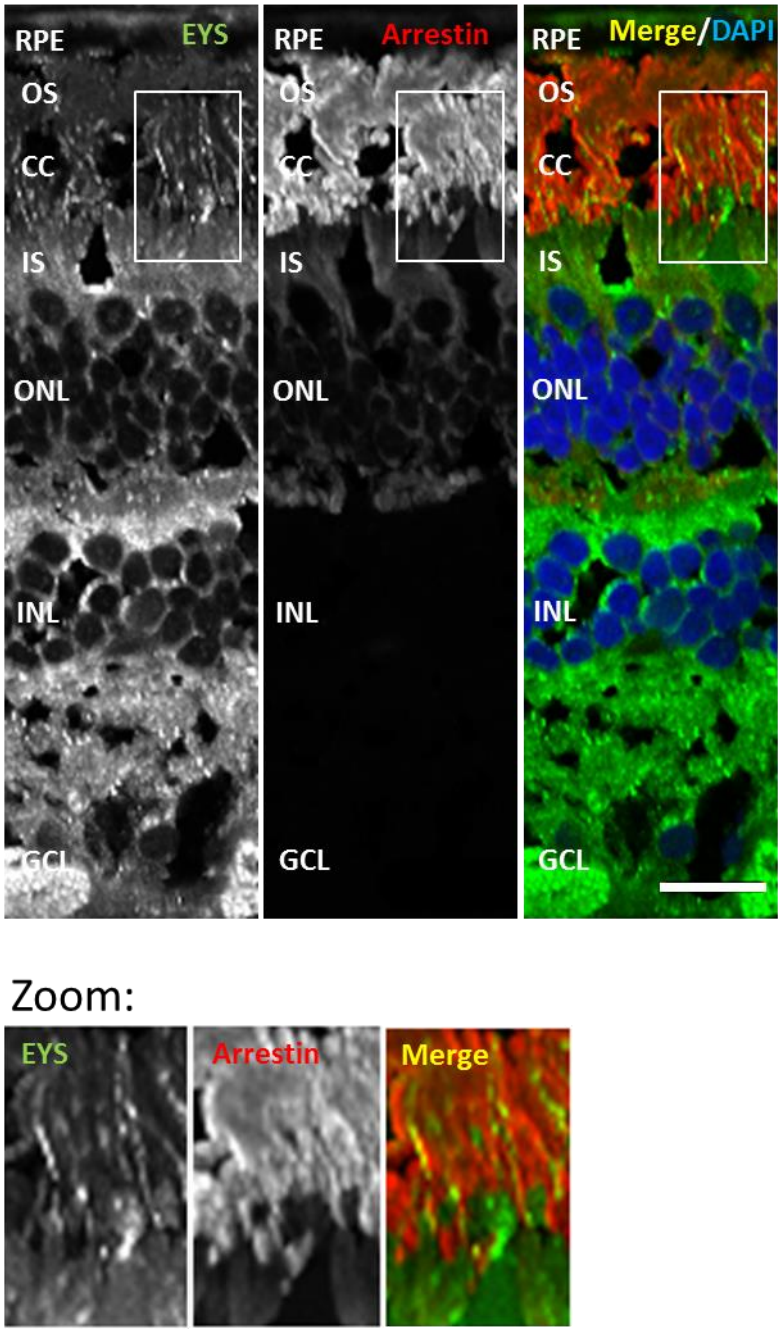

Figure 4.19 Localisation of EYS and arrestin in the macaque retina. The whip-like signal of EYS (green) was detected in the area corresponding to the connecting cilium and outer segments whereas arrestin (red) is specifically localised to the photoreceptor outer segment. The zoomed images (Zoom) are demarcated by the white square in the images. Anti-EYS2 rabbit and anti-arrestin mouse primary antibodies and AlexaFluor488 conjugated goat anti-rabbit and Cyanine 3 conjugated donkey anti-mouse secondary antibodies were used. DAPI was used to stain cell nuclei (blue). Scale bar: 20 µm. RPE – retinal pigment epithelium, OS – outer segment, CC – connecting cilium, IS – inner segment, ONL – outer nuclear layer, INL – inner nuclear layer, GCL – ganglion cell layer.

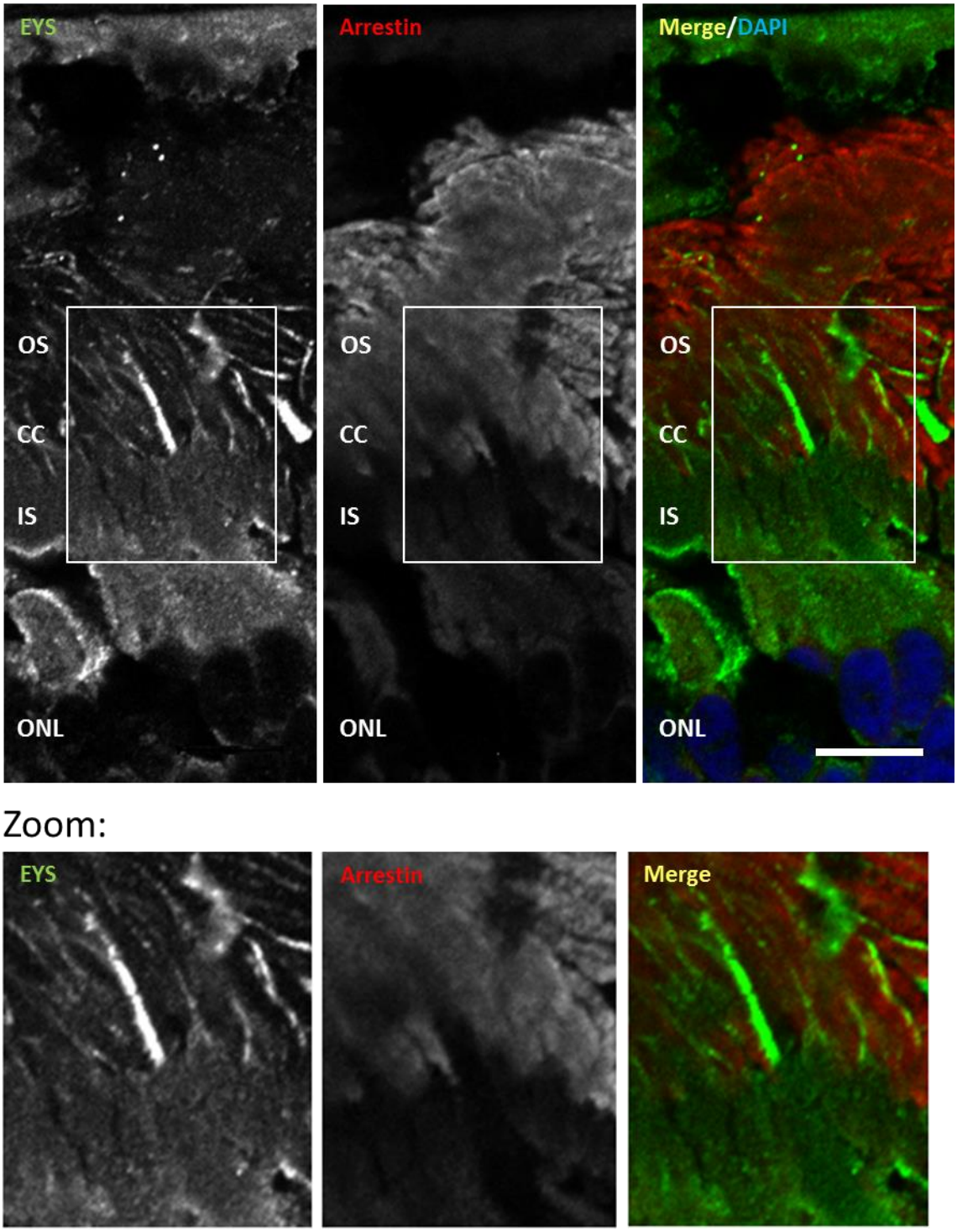

Figure 4.20 Localisation of EYS and arrestin in the macaque retina – a high magnification image. The whip-like signal of EYS (green) was detected in the area corresponding to the connecting cilium and outer segments whereas arrestin (red) is specifically localised to the photoreceptor outer segment. The zoomed images (Zoom) are demarcated by the white square in the images. Anti-EYS2 rabbit and anti-arrestin mouse primary antibodies and AlexaFluor488 conjugated goat anti-rabbit and Cyanine 3 conjugated donkey anti-mouse secondary antibodies were used. DAPI was used to stain cell nuclei (blue). Scale bar: 20 µm. RPE – retinal pigment epithelium, OS – outer segment, CC – connecting cilium, IS – inner segment, ONL – outer nuclear layer.

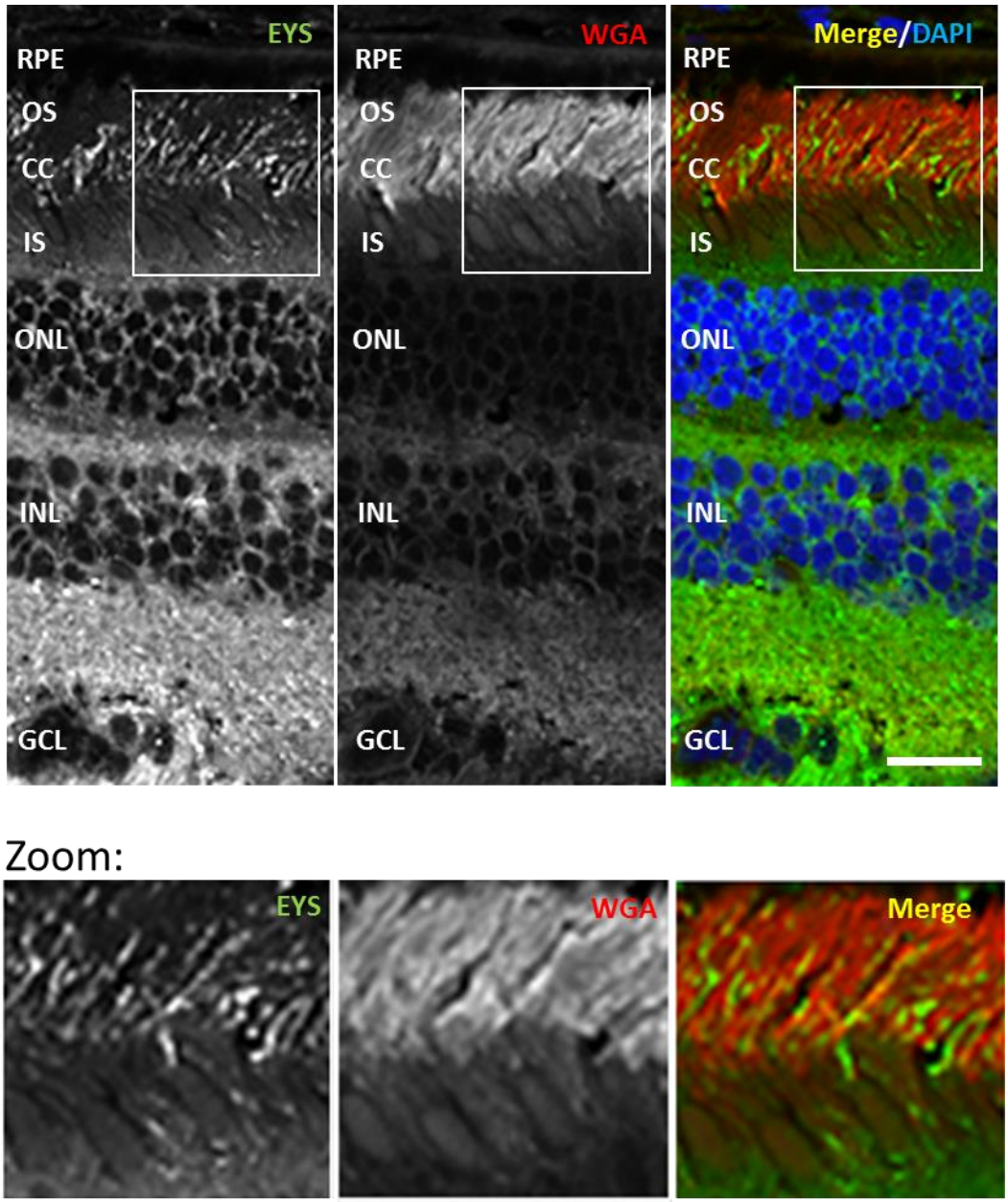

Figure 4.21 Localisation of EYS in the retina stained with the rod specific dye, WGA. EYS (green) was detected in the region of the photoreceptor ciliary axoneme and overlapped with WGA (red). Anti-EYS2 primary antibody (green) and AlexaFluor488 conjugated goat anti-rabbit secondary antibody were used. TexasRed-X-conjugated WGA was used to stain rod associated matrix proteins and DAPI was used to stain cell nuclei (blue). The zoomed images (Zoom) are demarcated by the white square in the images. Scale bar: 20 µm. RPE – retinal pigment epithelium, OS – outer segment, CC – connecting cilium, IS – inner segment, ONL – outer nuclear layer, INL – inner nuclear layer, GCL – ganglion cell layer.

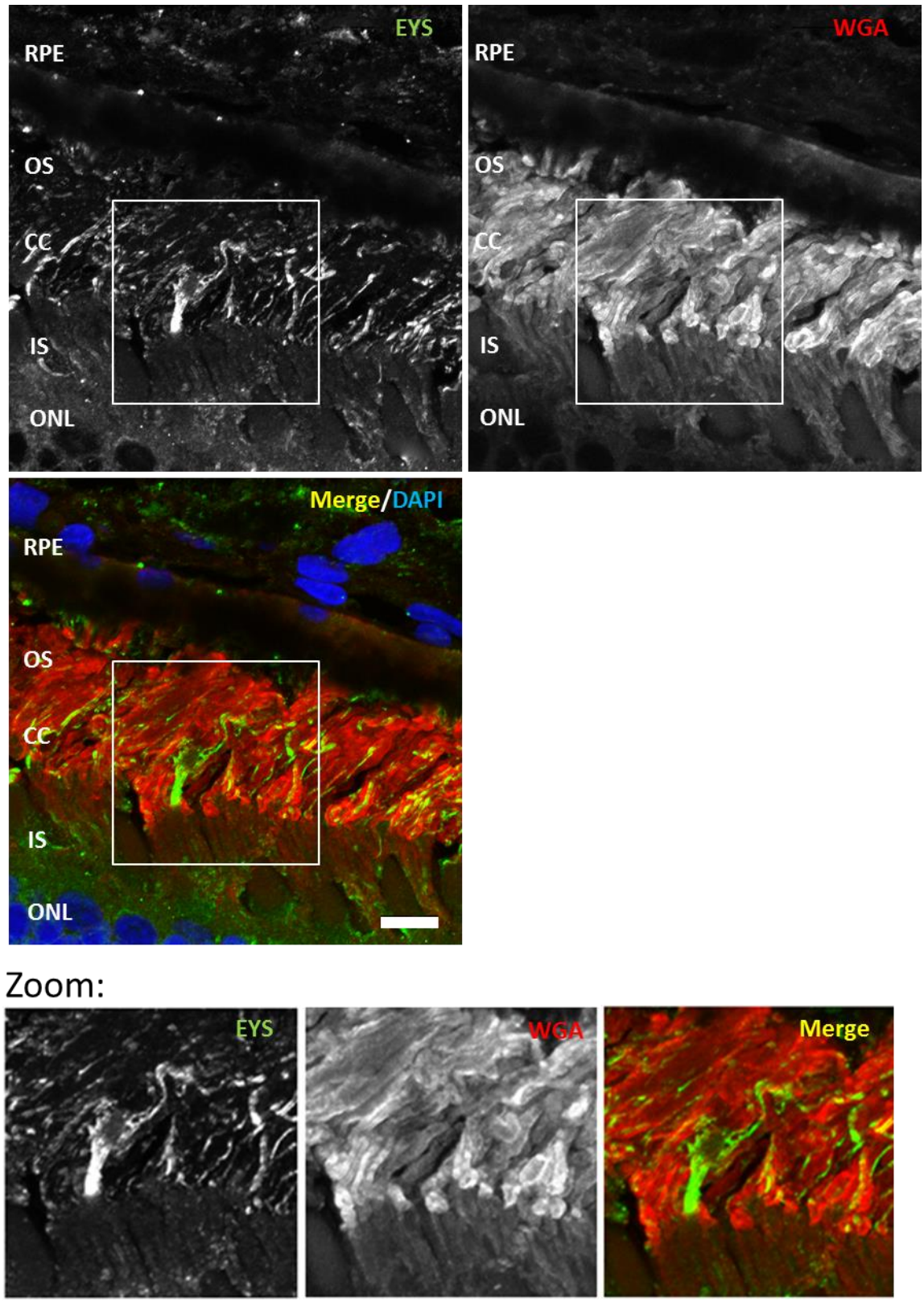

Figure 4.22 Localisation of EYS in the macaque retina stained with the rod specific dye, WGA – a high magnification image. EYS (green) was detected in the region of the photoreceptor ciliary axoneme and overlapped with WGA (red). The zoomed images (Zoom) are demarcated by the white square in the images. Anti-EYS2 primary antibody and AlexaFluor488 conjugated goat anti-rabbit secondary antibody were used. TexasRed-X-conjugated WGA was used to stain rod associated matrix proteins and DAPI was used to stain cell nuclei (blue). Scale bar: 20 µm. RPE – retinal pigment epithelium, OS – outer segment, CC – connecting cilium, IS – inner segment, ONL – outer nuclear layer.

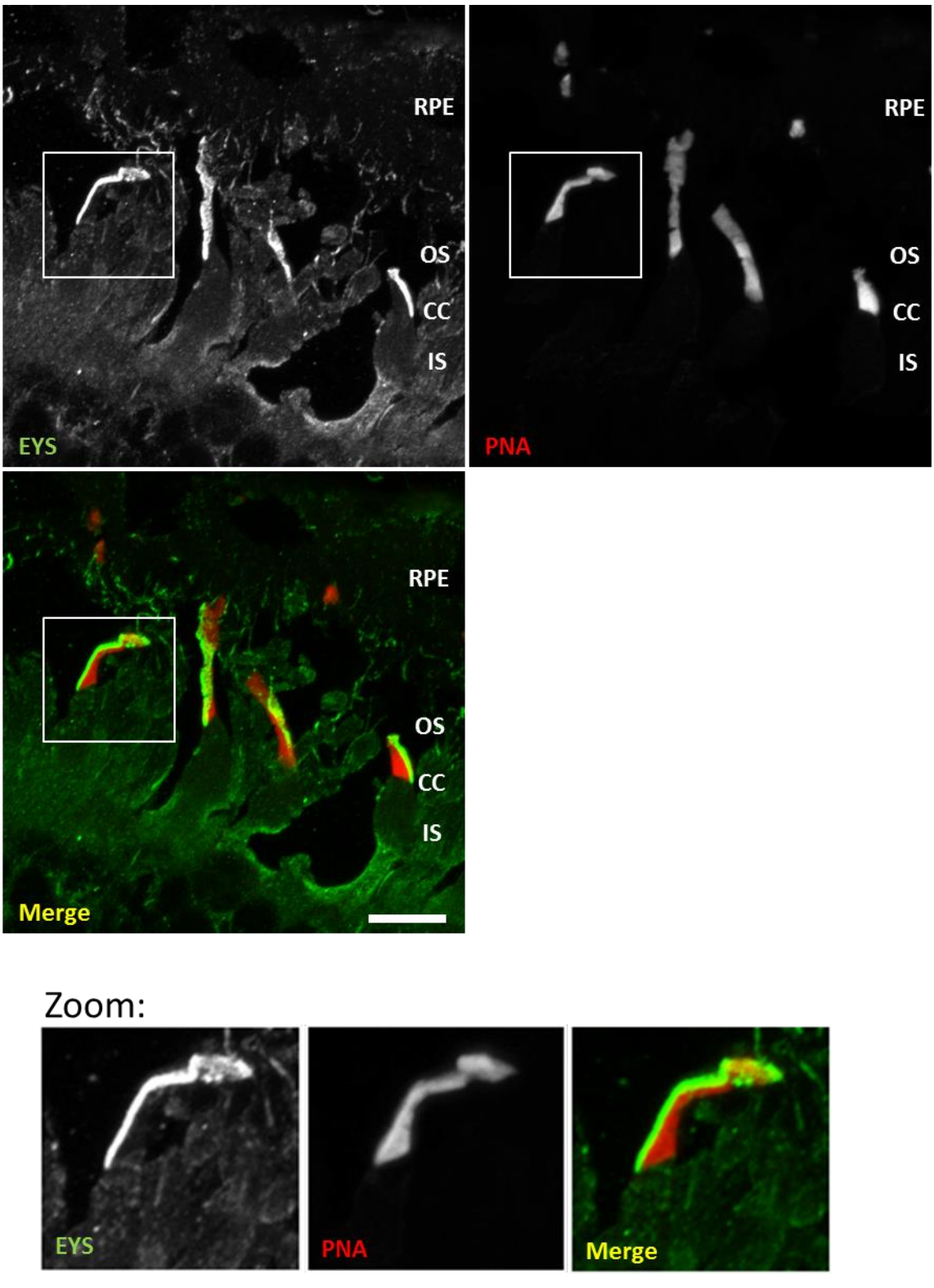

Figure 4.23 Localisation of EYS in the macaque retina stained with a cone specific dye, PNA - a high magnification image . EYS (green) was detected in the region of the photoreceptor ciliary axoneme and it was distinctively concentrated on one side of cone cells, which were highlighted by PNA (red). The zoomed images (Zoom) are demarcated by the white square in the images. Anti-EYS2 primary antibody and AlexaFluor488 conjugated goat anti-rabbit secondary antibody were used. TexasRed-X-conjugated PNA was used to stain cone associated matrix proteins and DAPI was used to stain cell nuclei (blue). Scale bar: 20 µm. RPE – retinal pigment epithelium, OS – outer segment, CC – connecting cilium, IS – inner segment, ONL – outer nuclear layer.

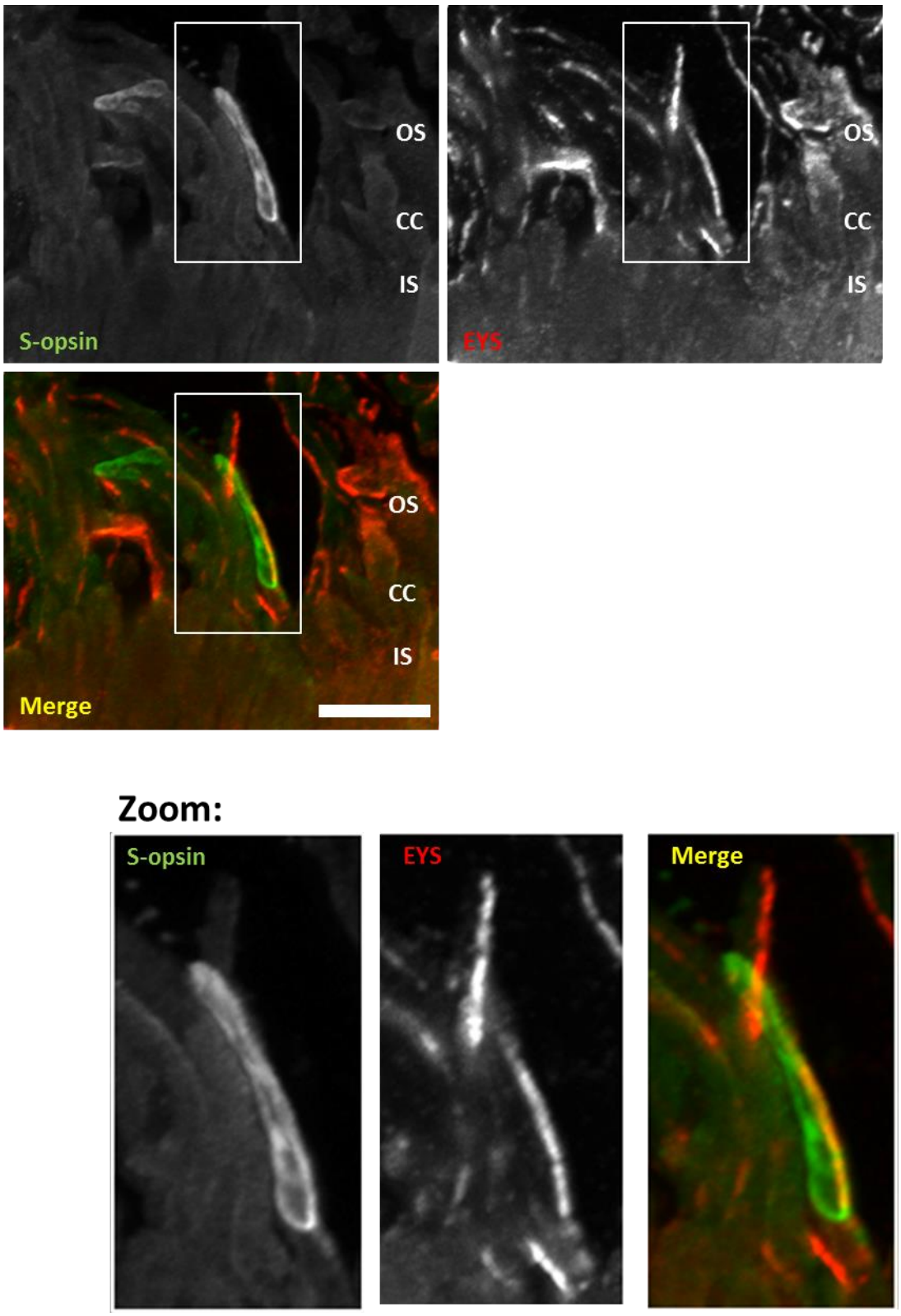

Figure 4.24 Localisation of EYS and S-opsin in the macaque retina. EYS (red) was detected in the region of the photoreceptor ciliary axoneme and the signal was distinctively concentrated on one side of the cone cell and overlapped with the localisation of S-opsin (green), which is a protein specifically localised to the cone outer segments. The zoomed images (Zoom) are demarcated by the white square in the images. Anti-EYS2 and anti-s-opsin primary antibodies and cyanine 3 conjugated donkey anti-goat and AlexaFluor488 conjugated donkey anti-mouse secondary antibodies were used. Scale bar: 10 μm. OS – outer segment, CC – connecting cilium, IS – inner segment.

4.3 Discussion of Chapter 4

The role of EYS protein in the human retina is unquestionably essential for its homeostasis; however, the function it has in the photoreceptor cells is still not fully understood. The experimental work presented in Chapter 4 aimed to expand the fundamental knowledge of EYS and such characterisation was necessary to better understand its significance for human health.

In the first instance, the analysis of online genomic and proteomic databases was performed. In studies published in 2008, EYS was described to be specifically expressed in the retina and *EYS* gene was reported to have either 43 or 44 exons (isoform 1 and 4 respectively). Online databases, however, predicted there can be more than two splicing variants of EYS and surprisingly, the two additional isoforms (isoform 2 and 3) significantly differ in size and domain structure from the canonical protein (Figure 4.1).

Alternative splicing is a dynamically regulated process that contributes to the proteomic diversity and it is especially common for the genes expressed in the nervous system where the synthesis of protein variants determines properties of different types of neurons (reviewed in Li *et al.*, 2007). Therefore, it could be that function and levels of expression of EYS isoforms vary depending on the developmental and/or physiological condition of an organism. In order to supplement previously published expression studies, RT-PCR analysis of short EYS isoforms 2 and 3 was performed. Data obtained demonstrated that full length transcripts of EYS isoforms 2 and 3 are present in the retina and testis, and Y79 cell line. Furthermore, amplification of EYS isoforms 2 from the testicular cDNA resulted in obtaining multiple bands, which could suggest that there are further EYS splicing variants expressed in the testis.

These results are consistent with data published by Collin et al., who aimed to verify expression of EYS isoform 4 in human tissues by amplification of fragments of the gene; such a strategy was most likely undertaken due to the large size of EYS and difficulties with amplification of the full length gene. The group was able to amplify most of the coding exons of EYS isoform 4 in the retina and observed two clearly separated bands in a fragment encompassing exons 41-44, which confirmed the existence of EYS isoform 1. Interestingly, the analysis presented in the paper also included amplification of a fragment spanning exons

9-12, whose sequence is conserved in all EYS isoforms. It resulted in identification of a DNA band in the retina and testis, which implied that EYS isoforms may also be expressed in the testis; however, the presence of this band was not referred to by the authors of the study (Collin *et al.*, 2008).

It should also be mentioned that EYS has been identified by a genome wide association study (GWAS) study as a gene potentially implicated in severe statin induced myopathy, a common side effect of the treatment of hypercholesterolemia (Isackson *et al.*, 2011). The group suggested that there is an EYS isoform specifically expressed in the spinal cord, which comprises of 45 exons and 3196 aa. The published RT-PCR analysis was focused on fragments spanning over exons 27-45 and performed on cDNA samples from the retina, skeletal muscle, brain and spinal cord. The EYS transcripts were suggested to be expressed in all of the tested tissues; however, the longest 45 exon isoform was claimed to be spinal cord specific. The published data is not consistent with the RT-PCR analyses performed by Abd El-Aziz et al. and Collin et al. who reported EYS to be a retina specific gene (Abd El-Aziz *et al.*, 2008; Collin *et al.*, 2008). EYS is a large gene and it may well have multiple isoforms that have variable functions in many tissues of the human body; nevertheless, the spinal cord isoform of EYS has not been annotated in any of the databases and its sequence is not available. Therefore, this isoform has not been included in the study presented herein.

Immunofluorescence experiments were performed in cultured cell lines in order to investigate the subcellular localisation of EYS proteins. In the first instance, localisation of EYS isoforms 1 and 4 was explored. Endogenous patterns of localisation were investigated in Y79 cells, the only cell line known to express EYS proteins. Y79 cells are a suspension cell line, where the cell is mostly made up of a large nucleus with relatively little surrounding cytoplasm. The cells grow in clusters and their organelles are tightly packed around the nucleus, hindering analysis of localisation studies. Cell attachment protocols were successfully optimised and used in the study, although the morphology of Y79 cells does not change much when they are attached to the culture dish. Therefore, cells were treated with dibutyryl-cAMP which encourages differentiation in cells and in the case of Y79s, enhanced the outgrowth of processes and improved visualisation of the cell structures. To better understand the origin of the signal coming from the anti-EYS1 antibody, a selection of markers highlighting different cell structures

were used. The analysis demonstrated that EYS isoform 1 most likely localises to the cytoplasm but could as well reside in the cell membrane. Further research would need to be carried out to fully determine the localisation of EYS in cell lines. One of the directions could be overexpression of full length EYS isoforms 1 and 4 in adherent cell lines, an approach that was attempted in this study and did not yield positive results. This was most likely due to the large size of EYS isoform 1 constructs which were as big as 16 kb and the technology available in the project could not suffice for transfecting with such large plasmids. To have an overview of where EYS domains could localise, N-terminal and C-terminal fragments of EYS were cloned with GFP tag and transfected into HeLa cells. Both of the fragments localised in the cytoplasm and were not present in the cell membrane. This implies that EYS is likely to have cytoplasmic localisation; nonetheless, such hypothesis could only be fully validated by performing research on the full sized protein.

Investigation of subcellular localisation of EYS isoforms 2 and 3 was less demanding. EYS isoforms 2 and 3 are significantly smaller that EYS isoforms 1 and 4 and therefore, it was possible to clone them into tagged vectors and overexpress them in cell lines. Overexpression in the Y79 cell line enabled localisation of the isoforms in the environment that they are naturally synthesised in. Their localisation appeared to be identical to that of EYS isoforms 1 and 4 and the signal was mostly concentrated in the cytoplasm. To better visualise the subcellular localisation of EYS isoforms 2 and 3, they were overexpressed in HeLa cells and compared to a range of markers. These experiments demonstrated that GFP tagged EYS isoforms 2 and 3 localise to the cytoplasm and sporadically to the nucleus; the nuclear localisation was inconsistent between experiments and could imply that EYS isoform 3 has a dynamic localisation and/or function. Another scenario could be that the variable expression pattern is an artefact caused by the protein being overexpressed.

In the previous reports, EYS has been demonstrated to co-localise with rhodopsin in the porcine retina (Abd El-Aziz *et al.*, 2008). Experiments conducted in this project aimed to look into the localisation of EYS more deeply, using retinal tissue sections derived from an animal more closely related to humans. The retinal tissue sections available in this study were explanted from adult crab-eating macaques (*Macaca fascicularis*). In the first instance, single immuno-staining was performed in order to optimise experimental conditions for the anti-EYS2 antibody

and to establish the localisation pattern of EYS in the monkey retina. Signal that was detected highlighted a whip-like structure that appeared in the area corresponding to the connecting cilium and the ciliary axoneme. Signal coming from the anti-EYS2 antibody was also detected in all other layers of the retina; however, it was diffused and significantly weaker, except for the outer plexiform layer and the ganglion cell layer where equally strong signal was detected. It could imply that EYS is expressed in other retinal neurons, which could be investigated in the future.

In order to accurately establish the localisation of EYS in the monkey retina, double immuno-labelling with well characterised cellular markers was performed. Markers used in the study were selected so that it can be assessed whether EYS may be associated with the ciliary axoneme and if it is present in rods, cones or both. The obtained results provided evidence supporting the hypothesis that EYS is likely to be associated with the ciliary axoneme in both rods and cones. This is consistent with the observations made in the porcine retina and re-enforced the previously published hypothesis that EYS resides in the photoreceptor outer segments (Abd El-Aziz *et al.*, 2008).

Altogether, the data presented in this chapter provided additional information regarding EYS genetic structure and localisation in the retina. Expression of EYS isoforms 2 and 3 was for the first time fully characterised by RT-PCR and immunofluorescence studies. Further analysis of EYS isoforms provided evidence implying that EYS is expressed in both rod and cone photoreceptors and it is most likely associated with the ciliary axoneme, where it could be involved in signalling, intraflagellar transport or have a structural role. EYS is an undoubtedly essential component of the human retina and its disruption is associated with arRP; nonetheless, a Japanese patient suffering from a cone-rod dystrophy was reported, carrying a truncating compound heterozygous mutation in *EYS* (Katagiri *et al.*, 2014). This supports the hypothesis that EYS is not only crucial for the functioning of rods but it is also important for the stability of cones. In the future, it would be of paramount importance to conduct similar experiments on human specimens to fully characterise the human orthologue of EYS. Furthermore, the existence of EYS splicing variants should not be underrated and the future research should also focus on their significance in the retina and address their expression and function in the testis.

Another important conclusion can be made regarding the signal peptide of EYS. It has previously been suggested that the N-terminal signal peptide of EYS could direct it to a secretory pathway, making EYS an extracellular protein. Data presented in this chapter imply that EYS is not secreted but resides in the photoreceptor outer segments. Therefore, it could be suggested that the signal peptide is responsible for targeting EYS to the photoreceptor outer segment by, for example, means of vesicular trafficking (reviewed in Pearring *et al.*, 2013).

Overall, a significant amount of data regarding EYS was obtained which not only contributes to better understanding of EYS but also opens new avenues for the design of future research projects.

Chapter 5: Characterisation of the Relationship between EYS and Prominin-1

An intriguing phenomenon in the biology of EYS is its unusual course of evolution, in which the expression of *EYS* was lost in several lineages of mammals, including rodents. EYS, however, has been discovered to be an orthologue of a *Drosophila* protein called spam or spacemaker (Abd El-Aziz *et al.*, 2008; Collin *et al.*, 2008). It has been demonstrated that spam is a secreted extracellular protein, which is a member of network of interactions critical to the formation of the inter-rhabdomeral space (IRS) in the *Drosophila* ommatidium (Husain *et al.*, 2006; Zelhof *et al.*, 2006). Zelhof et al. have also suggested that spam interacts with prominin to counteract the adhesive force of chaoptin during the IRS formation. The group also investigated the relationship of spam and prominin in the *Drosophila* cell line and showed that prominin is required for the localisation of spam to the surface of the cell membrane (Zelhof *et al.*, 2006). Phenotypic analysis of *Drosophila* mutants suggested that the interaction of prominin and spam was required for proper formation of the rhabdomeric photoreceptors, and their human orthologues rescued the mutant phenotype and enabled formation of the IRS when introduced into the *Drosophila* model. This led the authors to suggest that the interaction of spam and prominin may be conserved in humans (Nie *et al.*, 2012). In another study, *Drosophila* spam has been found to be expressed in the mechanoreceptor neurons and it has been shown to protect the neurons from environmental insult by preservation of the cell shape enforced by stiffening of the cell membrane (Cook *et al.*, 2008).

The human orthologue of prominin, Prominin-1, is a pentaspan transmembrane protein that has been shown to be involved in the photoreceptor membranous disk formation, and mutations in *PROM1* gene cause retinal degeneration (see Introduction, section 1.5).

Prominin-1 has been widely studied in vertebrates. It has been shown that in murine photoreceptors it localises to the membrane extensions that give rise to the membrane discs of the outer segments (Maw *et al.*, 2000). It has also been reported that knocking out prominin-1 in mice leads to progressive degeneration of photoreceptors (Zacchigna *et al.*, 2009). In *Xenopus laevis*, prominin-1 has been

demonstrated to be present at the basal disks of rod outer segments and at the outer rims of open disk lamellae of cone outer segments (Han *et al.*, 2012). The known interactome of human Prominin-1 includes Protocadherin-21, a protein involved in the disk membrane morphogenesis, and actin, which is a well-known component of the cytoskeleton (Yang *et al.*, 2008).

In light of the literature data-mining, Prominin-1 is a strong candidate for being an interacting partner of EYS. It is likely that the interaction of the two proteins is conserved in humans and crucial for the proper functioning of human photoreceptors. Prominin-1 was not found to be an interacting partner of EYS in the Y2H screens performed in this study. This, however, does not mean that the interaction does not occur as Prominin-1 is a protein specifically localising to the cell membrane protrusions and, therefore, it is highly likely that it could not have been detected using the GAL4 based Y2H system used in this study.

Since there is strong evidence in support of the interaction taking place in *Drosophila*, the relationship between human orthologues of EYS and Prominin-1 was investigated in this study.

5.1 Immunocytochemistry Studies of EYS and Prominin-1

The first approach to characterise the potential interaction of EYS and Prominin-1 was to analyse their subcellular localisation. To begin with, Y79 cell line was examined as it was known to endogenously express EYS.

To confirm the expression of *PROM1* in Y79 cells, RT-PCR analysis was performed and the result is shown in Figure 5.1. The positive result of the analysis enabled investigation of endogenous expression of Prominin-1 and EYS; however, the first immunofluorescence experiments demonstrated that Prominin-1 is not abundantly expressed in Y79 cells. This may be due to the lack of elaborate membranous structure present in Y79 cells, or due to inefficient binding of the available anti-Prominin-1 antibodies, although, the former scenario should not be the case in light of the immuno-stainings of Y79 cells presented in Chapter 4. Consequently, the endogenous expression of EYS was compared to the ectopic expression of DsRed tagged Prominin-1. Figure 5.2 depicts a cluster of seven Y79 cells, two of which were successfully transfected with DsRed-Prominin-1.

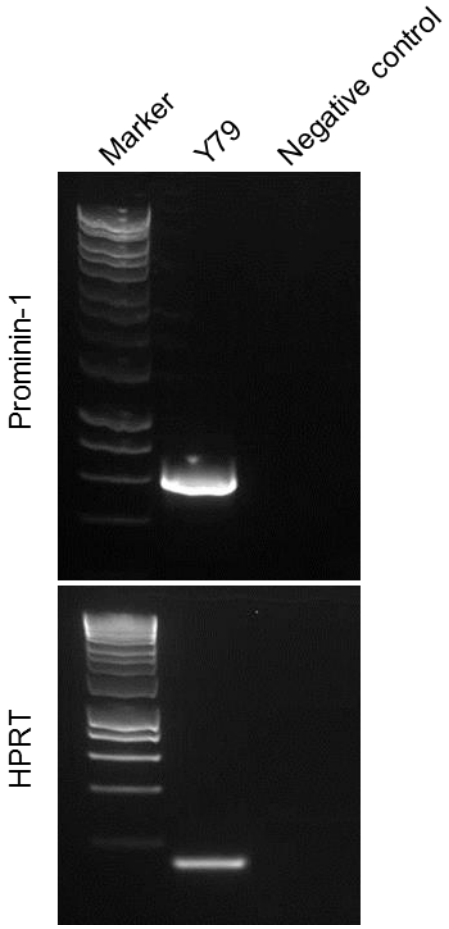

Figure 5.1 RT-PCR analysis of expression of Prominin-1 in cDNA derived from Y79 cells. Primers were designed to cover a fragment of *PROM1* cDNA encompassing exons 20-28 with the expected size of 672 bp. PCR mix without cDNA was used as negative control. A 150 bp fragment of ubiquitously expressed hypoxanthine phosphoribosyltransferase 1 gene (*HPRT1*) was used as a quality control. Bioline Hyperladder I was used to assess sizes of the bands. Y79 – a human retinoblastoma cell line.

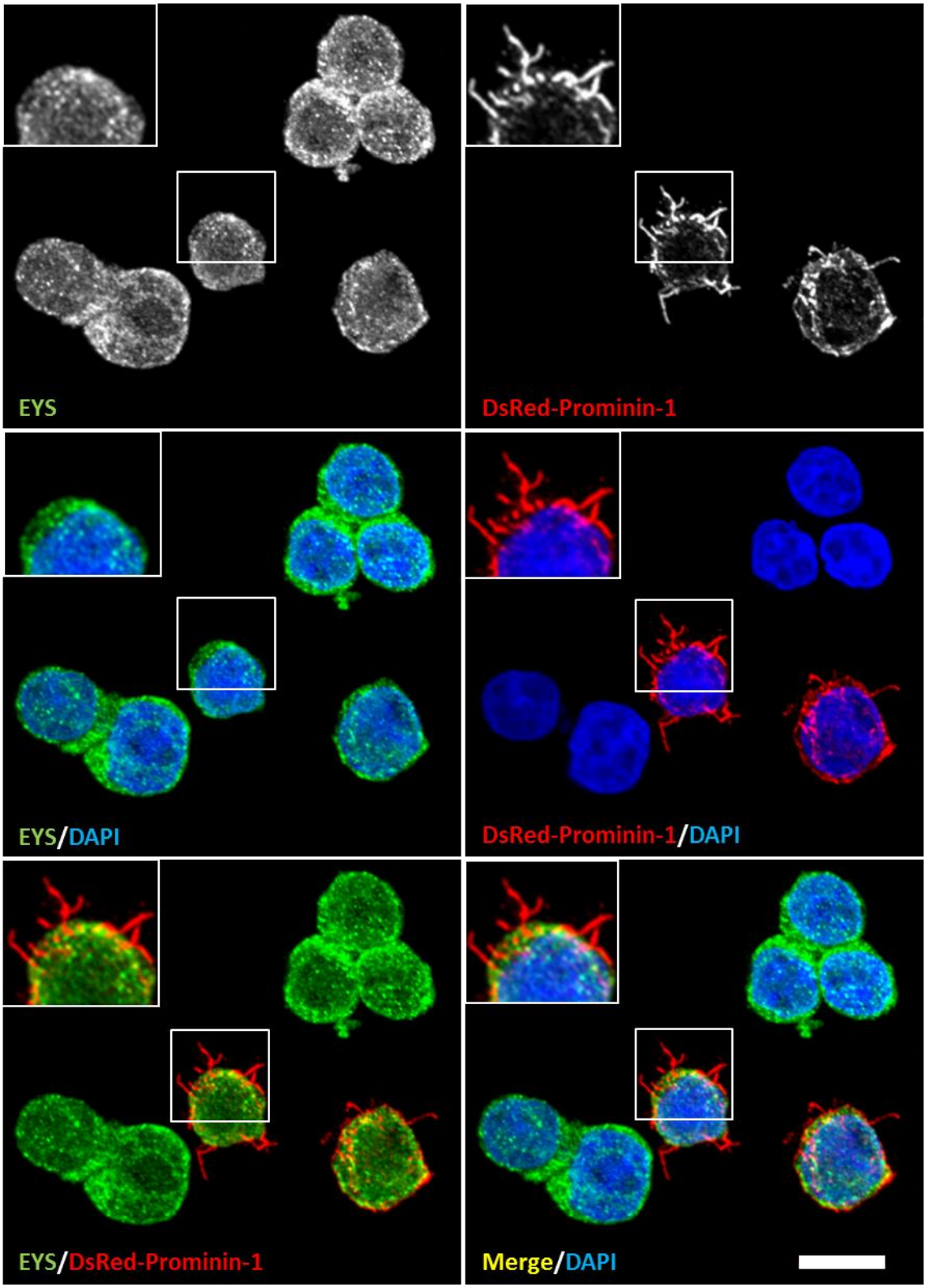

Figure 5.2 Localisation of EYS and DsRed-Prominin-1 in Y79 cells. EYS (green) localised to the cell cytoplasm whereas DS-Red-Prominin-1 localised to the cell membrane microvilli. Co-localisation of the proteins was not been observed. The zoomed inserts represent the area demarcated by the white square in the images. Anti-EYS1 primary and AlexaFluor 488 conjugated goat anti-rabbit secondary antibodies were used. Nuclei were stained with DAPI (blue). Scale bar: 10 μm.

As the micrograph shows, DsRed-Prominin-1 characteristically localised to the cell membrane protrusions whereas EYS was detected as a speckled signal present in the areas that probably correspond to the cytoplasm; it was not detected in the microvilli and co-localisation with Prominin-1 was not observed.

A micrograph of another cell taken at higher magnification is shown in Figure 5.3. The image was taken so that the cell membrane localisation of Prominin-1 is detailed and microvilli of the cell are not well visible here. The micrograph shows that the two examined proteins are unlikely to share the localisation pattern. There is some yellow signal visible in the merged picture that could indicate co-localisation in the area of the cell membrane; however, in such poorly developed cell morphology it could also be random.

The immunocytochemistry experiments presented in Chapter 4 suggested that EYS proteins mainly localise to the cytoplasm and it is known that Prominin-1 has strong preference for the membrane microvilli. One could argue that based on this knowledge it could already be concluded that EYS and Prominin-1 do not co-localise together. However, the experiments performed in the *Drosophila* model demonstrated that spam decorates the surface of the cell membrane only in the presence of prominin, which might participate in recruiting spam to its final destination. A similar phenomenon could be occurring between the human orthologues and the co-expression of Prominin-1 and EYS together could amend the cytoplasmic localisation of EYS proteins.

In order to better understand the subcellular localisation of EYS proteins and Prominin-1, an overexpression approach was undertaken. To begin with, V5 tagged EYS isoform 1 and DsRed tagged Prominin-1 constructs were co-transfected into HeLa cells. It needs to be explained here, that the V5-EYS isoform 1 construct was approximately 16 kb and transfection with such a large plasmid vector, let alone co-transfection with another construct, was extraordinarily challenging. The optimisation of this experiment involved testing several cell lines and numerous commercially available transfection reagents. Most of the tested reagents were liposome based; however, calcium phosphate based methods and electroporation were also attempted with no success.

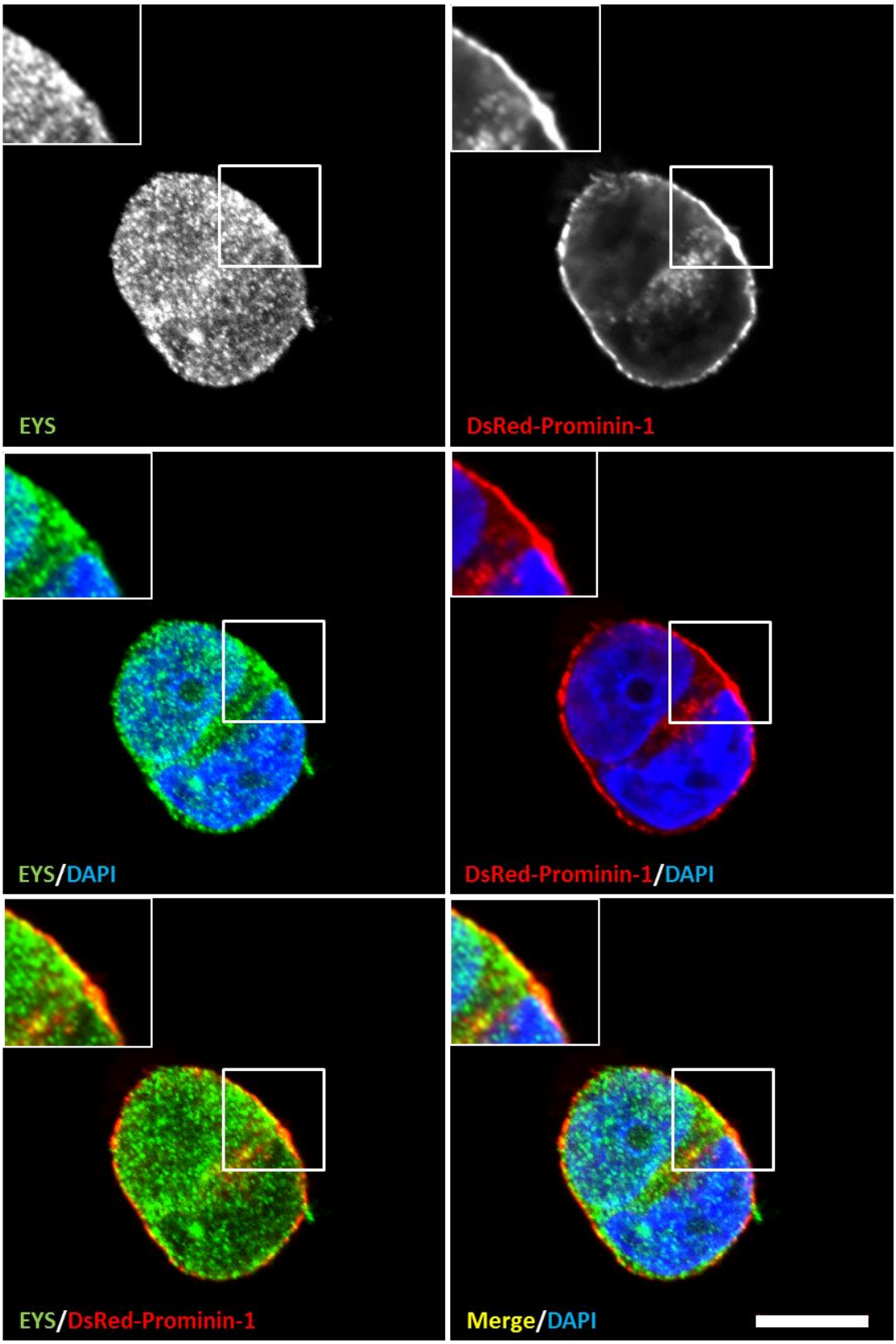

Figure 5.3 Localisation of EYS and DsRed-Prominin-1 in a cluster of two Y79 cells. EYS (green) localised to the cell cytoplasm whereas DS-Red-Prominin-1 I concentrated in the cell membrane. Any co-localisation of the two proteins in indicated by yellow signal. The zoomed inserts represent the area demarcated by the white square in the images. Anti-EYS1 primary and AlexaFluor 488 conjugated goat anti-rabbit secondary antibodies were used. Nuclei were stained with DAPI (blue). Scale bar: 10 μm.

The only reagent which yielded positive results was Effectene (Qiagen, The Netherlands); nevertheless, the efficiency of the co-transfection was very low with only a few positively co-transfected cells observed altogether. From the cell lines tested, HeLa cells were transfected with highest efficiency and, therefore, that particular cell line was used in the experiments. An example of a co-transfected HeLa cell is shown in Figure 5.4. As it can be seen, Prominin-1 localised to the cell membrane and cell membrane protrusions. EYS was not found to localise in the microvilli and the majority of the signal seemed to localise to the cytoplasm; however, there is some yellow signal present that could indicate co-localisation in the cell membrane. More detailed analysis of the co-localisation is difficult as the cells were compromised by the strict conditions of co-transfection which probably had an adverse effect on their structure.

The large size of EYS isoform 1 construct hindered the progress of immunocytochemistry experiments aiming to investigate its relationship with Prominin-1. However, in light of the results described in Chapter 4, it is likely that EYS isoforms 2 and 3 could also interact with Prominin-1. To address this issue, GFP tagged EYS isoforms 2 and 3 were co-transfected with V5-tagged Prominin-1 into HeLa cells. As shown in Figure 5.5 and Figure 5.6, EYS isoforms 2 and 3 share the localisation pattern and both of them localised to the cytoplasm whereas Prominin-1 was specifically detected in the cell membrane, especially in the cell membrane protrusions. There is very little yellow signal visible that could indicate co-localisation, nonetheless, the localisation pattern of EYS isoforms 2 and 3 is undoubtedly distinct from the pattern of Prominin-1.

Figure 5.7 represents a control performed with a GFP empty vector, where it can be observed that GFP on its own has diffused localisation throughout the nucleus and cytoplasm, and is also observed in the microvilli of the cell.

Immunocytochemistry experiments investigating the ectopic expression of EYS proteins and Prominin-1 demonstrated that the proteins of interest do not co-localise in mammalian cell lines. The cytoplasmic localisation of EYS isoforms does not appear to be modulated by the presence of overexpressed Prominin-1. This data show that the phenomenon of prominin recruiting spam to the cell membrane in a *Drosophila* cell line is not observed between the human proteins. The obtained results also imply that the examined proteins do not exist in proximity which means that they are unlikely to physically interact.

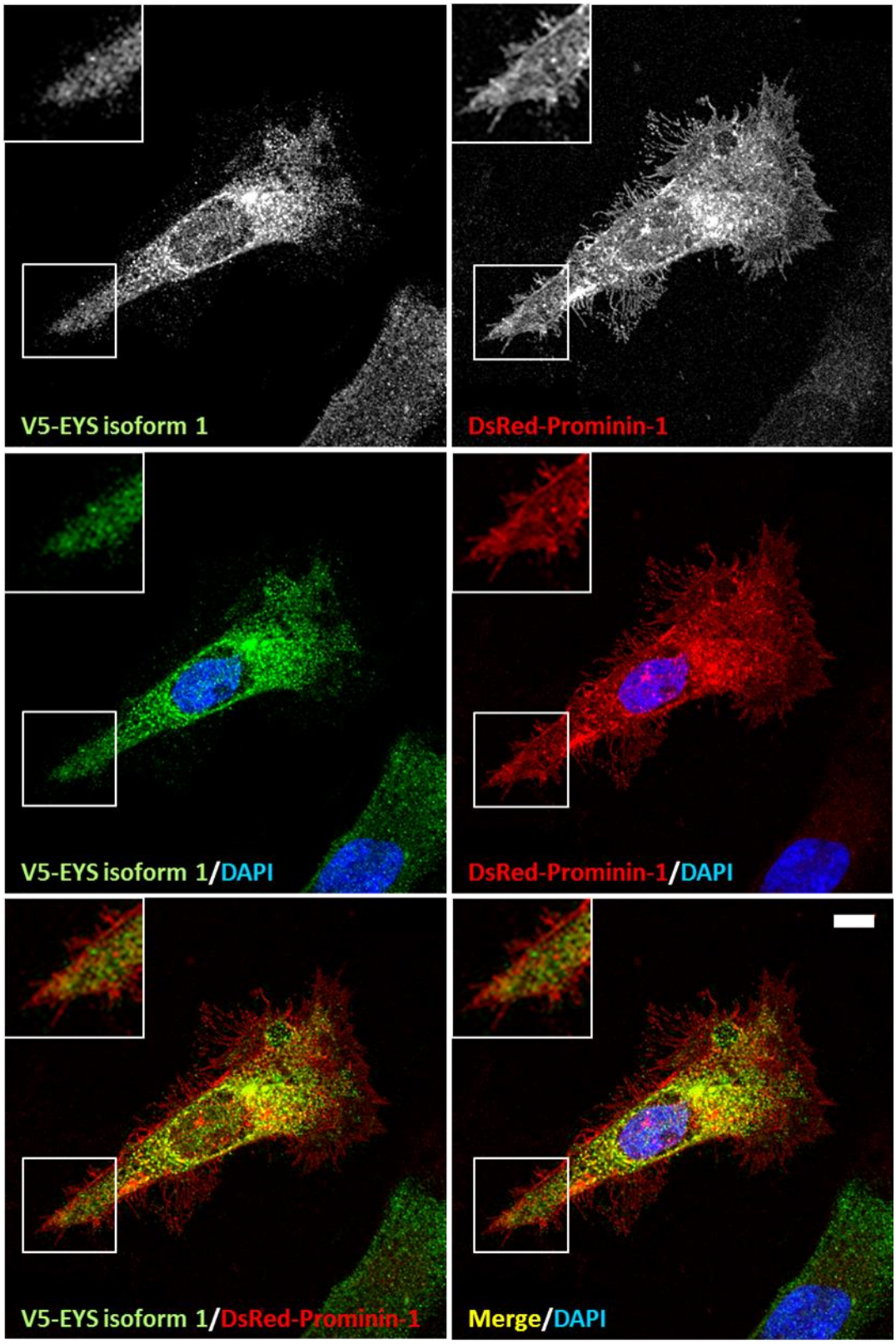

Figure 5.4 Localisation of V5 tagged EYS and DsRed tagged Prominin-1 in HeLa cells. V5-EYS (green) was detected in the cell cytoplasm whereas DsRed-Prominin-1 localised to the cell membrane and cell membrane microvilli. Any potential co-localisation is indicated by the yellow/orange signal. The zoomed inserts represent the area demarcated by the white square in the images. Goat anti-V5 primary and Alexa Fluor 488 conjugated donkey anti-goat secondary antibodies were used. Nuclei were stained with DAPI (blue). Scale bar: 10 μm.

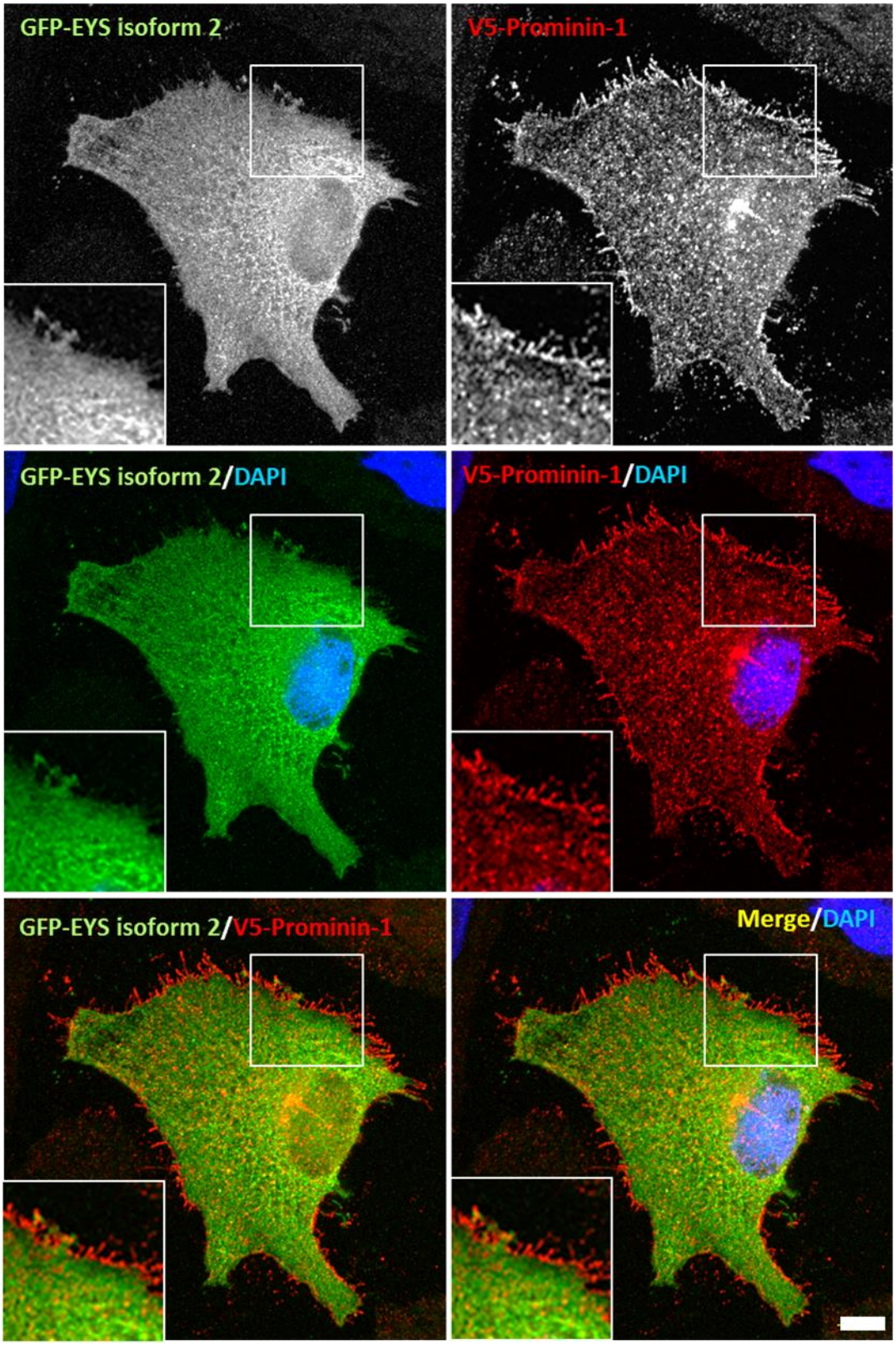

Figure 5.5 Localisation of GFP tagged EYS isoform 2 and V5 tagged Prominin-1 in Hela cells. GFP-EYS isoform 2 localised predominantly to the cell cytoplasm whereas V5-Prominin-1 was concentrated in the cell membrane microvilli. Any potential co-localisation is indicated by the yellow/orange signal. The zoomed inserts represent the area demarcated by the white square in the images. Goat anti-V5 primary and Alexa Fluor 594 conjugated donkey anti-goat secondary antibodies were used. Nuclei were stained with DAPI (blue). Scale bar: 10 µm.

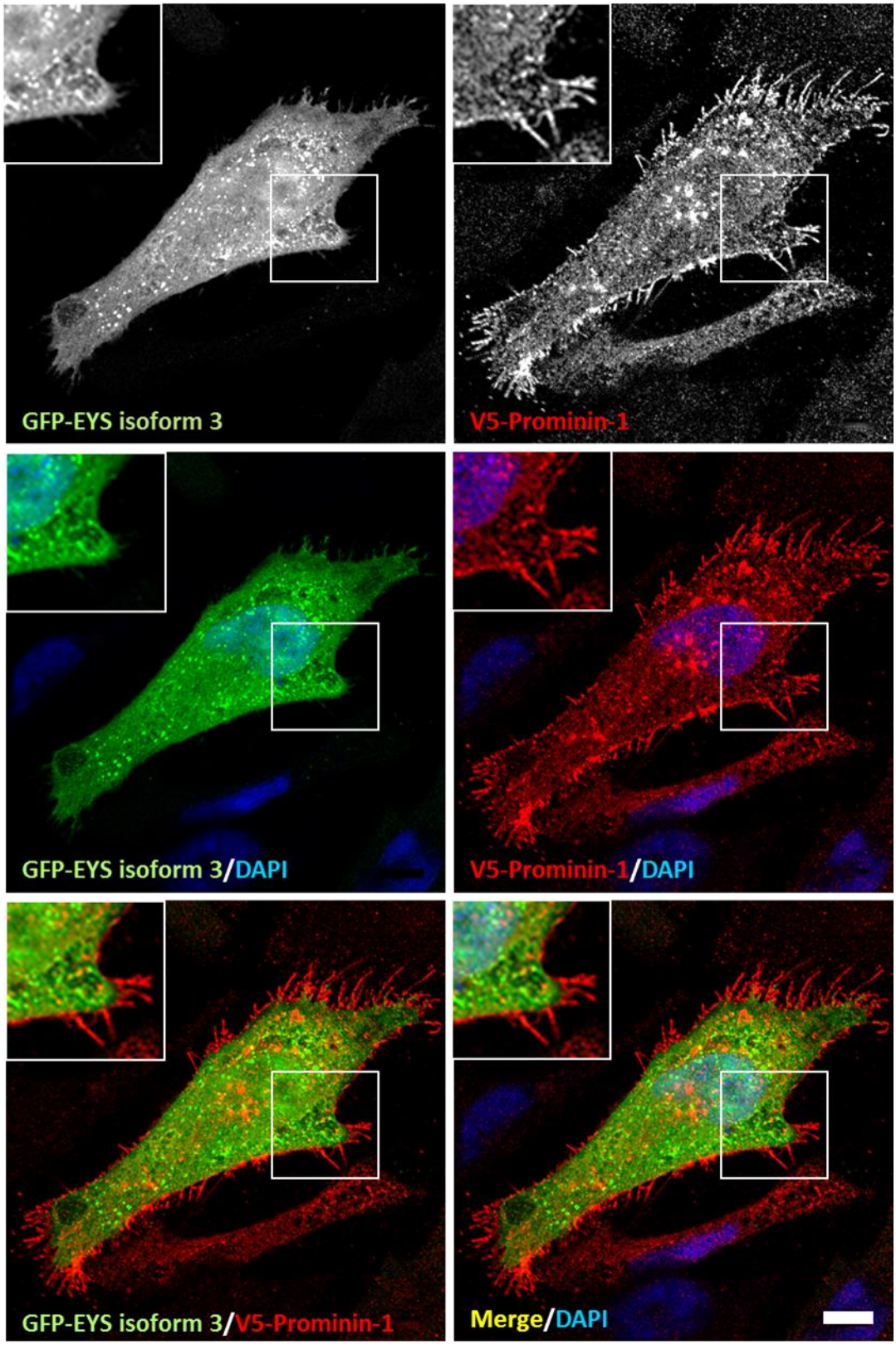

Figure 5.6 Localisation of GFP tagged EYS isoform 3 and V5 tagged Prominin-1 in Hela cells. GFP-EYS isoform 3 localised predominantly to the cell cytoplasm whereas V5-Prominin-1 was concentrated in the cell membrane microvilli. Any potential co-localisation is indicated by the yellow/orange signal. The zoomed inserts represent the area demarcated by the white square in the images. Goat anti-V5 primary and Alexa Fluor 594 conjugated donkey anti-goat secondary antibodies were used. Nuclei were stained with DAPI (blue). Scale bar: 10 μm.

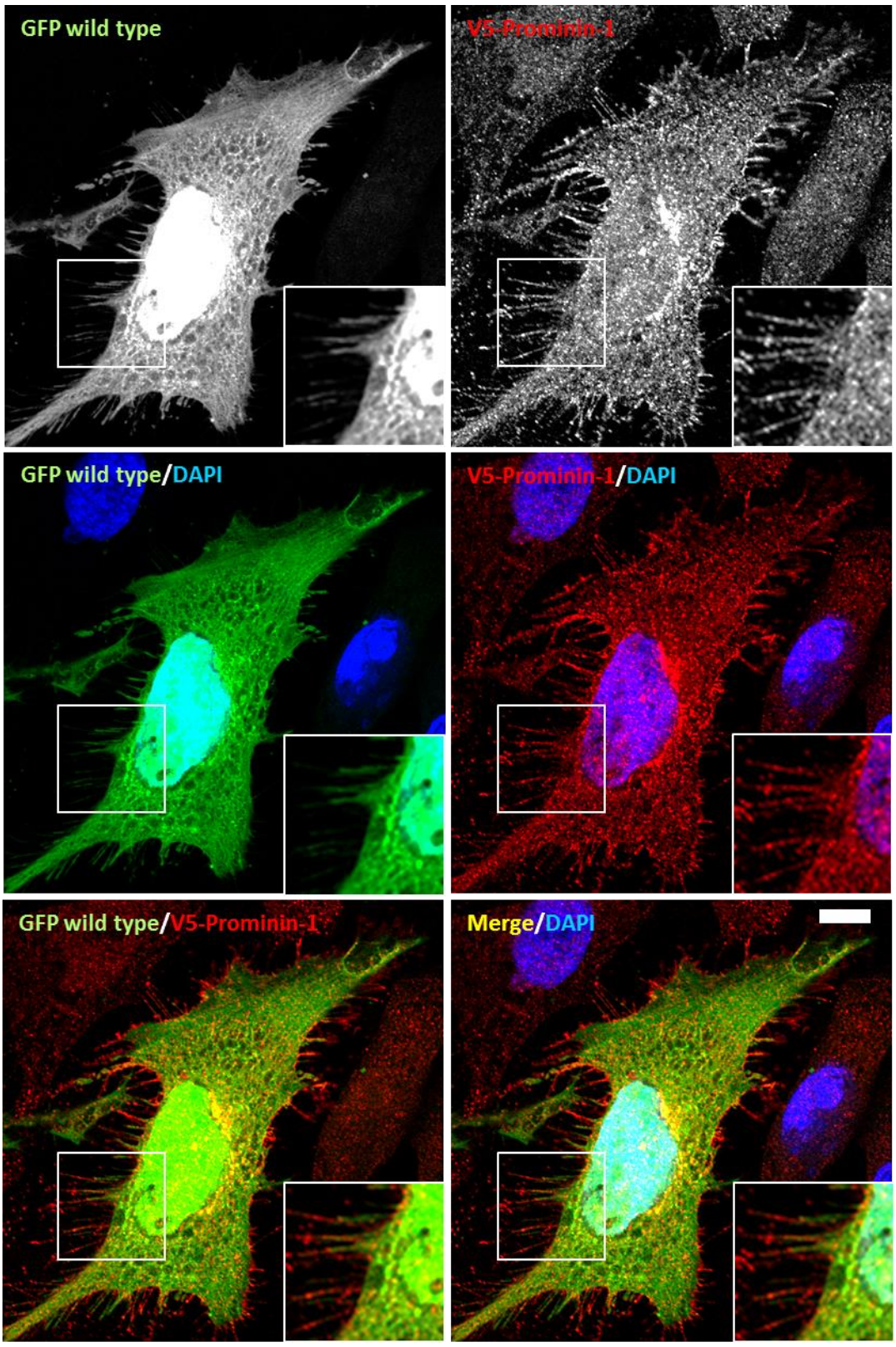

Figure 5.7 Localisation of wild type GFP tag and V5 tagged Prominin-1 in Hela cells. Wild type GFP localised the cell cytoplasm and the nucleus whereas V5-Prominin-1 was concentrated in the cell membrane microvilli. Any potential co-localisation is indicated by the yellow/orange signal. The zoomed inserts represent the area demarcated by the white square in the images. Goat anti-V5 primary and Alexa Fluor 594 conjugated donkey anti-goat secondary antibodies were used. Nuclei were stained with DAPI (blue). Scale bar: 10 μm.

5.2 *Ex Vivo* Analysis of EYS and Prominin-1 Localisation

Data collected from immunocytochemistry experiments demonstrated that human EYS and Prominin-1 do not share the subcellular localisation. In order to have a better understanding of where EYS and Prominin-1 reside in the retina, immunohistochemistry experiments were performed.

The localisation of EYS in the monkey retina was described in Chapter 4 where it was demonstrated that EYS is likely to be a protein associated with the photoreceptor ciliary axoneme. The localisation of Prominin-1 was widely studied and it has been shown that murine prominin-1 localises to the evaginations of the plasma membrane at the base of rod photoreceptor outer segments, where the nascent membranous disks are formed (Maw *et al.*, 2000; Zacchigna *et al.*, 2009). Similar results were obtained when studying the localisation of an orthologue of Prominin-1 in *Xenopus laevis*, where it was found that it localises to the basal disks of rod outer segments and the outer rims of open disk lamellae of cone outer segments (Han *et al.*, 2012).

This data taken together would suggest that EYS and Prominin-1 are not present in the same compartment of the photoreceptor cell; however, such a conclusion would be made based on results coming from different species and could therefore be misleading. To address the co-localisation of EYS and Prominin-1 in a specimen derived from one animal, immunohistochemistry experiments were conducted on retinal tissue sections from adult *Macaca fascicularis*.

Figure 5.8 shows a piece of a retinal section co-labelled with anti-EYS2 and anti-Prominin-1 antibodies. Consistently with observations described in Chapter 4, EYS was detected as a whip-like signal present in the region of the connecting cilium and above, which most likely corresponds to the ciliary axoneme.

The red signal coming from the anti-Prominin-1 antibody appeared to be detected in both types of photoreceptor cells and had a characteristic pattern in each of them. The white arrow indicates a rod cell, in which Prominin-1 was detected as red dots present at the base of the outer segments. This is consistent with the published data demonstrating that prominin localises to the membrane protrusions that are destined to become rod outer segment membranous disks in the mouse retina (Han *et al.*, 2012; Maw *et al.*, 2000).

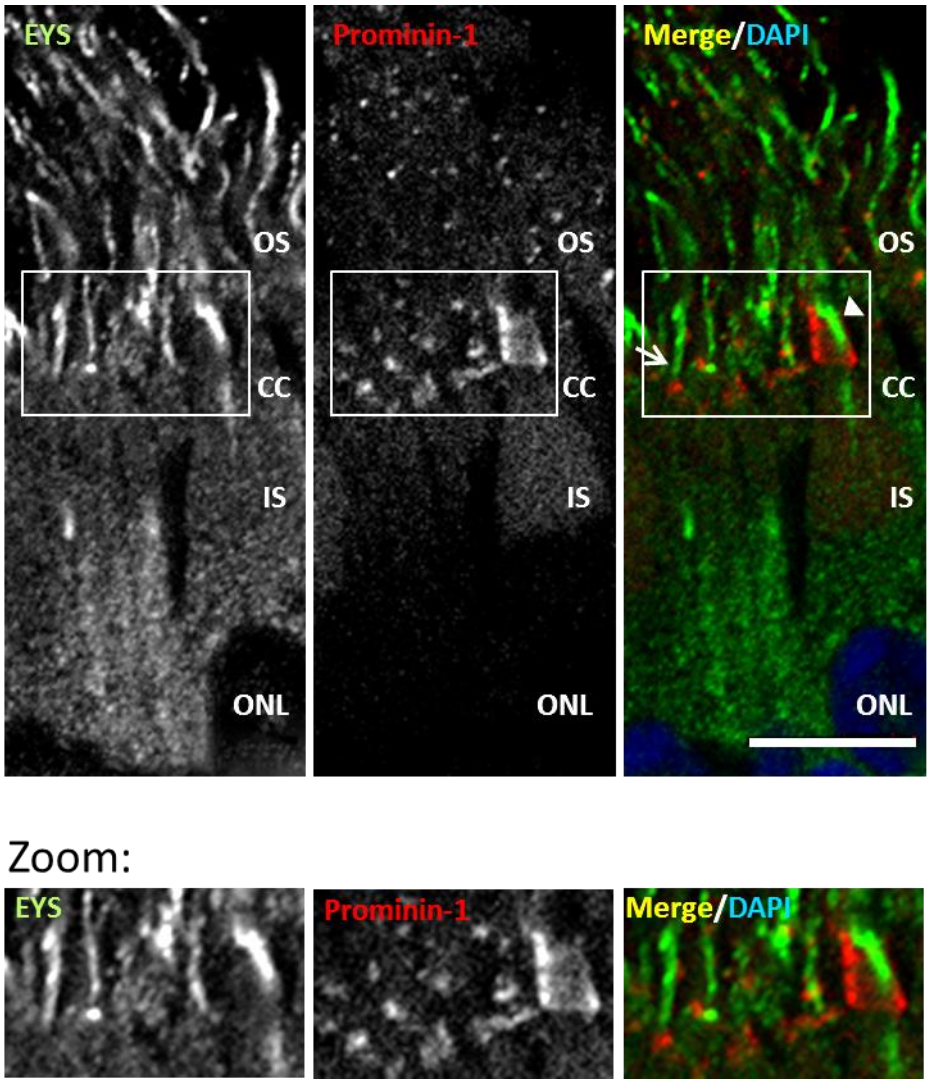

Figure 5.8 Localisation of EYS and Prominin-1 in the macaque retina. The white arrow indicates a rod cell whereas the white arrow head indicates a cone cell. EYS (green) was detected in rods and cones as a whip-like signal in the region of a photoreceptor ciliary axoneme whereas Prominin-1 (red) was detected at the base of the rod outer segments and along the edge of the cone outer segments opposite to the signal of EYS. Co-localisation of the two proteins was not observed. The zoomed images (Zoom) correspond to the areas demarcated by the white square in the images. Anti-EYS2 rabbit and anti-Prominin-1 mouse primary antibodies and AlexaFluor488 conjugated goat anti-rabbit and Cyanine 3 conjugated goat anti-mouse secondary antibodies were used. DAPI was used to stain cell nuclei (blue). Scale bar: 20 µm. OS- outer segment, CC – connecting cilium, IS – inner segment, ONL – outer nuclear layer.

Yellow signal, indicative of co-localisation of the two proteins, was not detected; the red dots identified as Prominin-1 localise clearly just below the green fibril of EYS.

An example of a cone cell illustrating the relationship of EYS and Prominin-1 is indicated by a white arrowhead. As it can be seen, the red signal corresponding to Prominin-1 is concentrated on one side of the indicated cell and such localisation pattern was described by others in a *Xenopus laevis* model; this suggests that the red signal indicates the tips the open disks lamellae (Han *et al.*, 2012). The green signal of EYS is located on the opposite side of the cone outer segment, which is consistent with the observations described in Chapter 4. Such arrangement would suggest that the green signal marks the structure residing opposite to the edges of cone open disks, which could be the ciliary axoneme.

However, the aforementioned localisation pattern was not the only one observed. Figure 5.9 shows two more cone cells photographed at higher magnification. In both of the cells shown, the green fibril of EYS signal is surrounded from both sides by the red signal representing Prominin-1. Such arrangement of the two proteins could be an artefact resulted from sectioning of the retina; the outer segment is conical in shape and Prominin-1 is localised at the tip of the membranous disks whereas EYS is expected to reside in the area of the ciliary axoneme, therefore, cutting of the cell through the tip of the disk could result in a pattern observed in Figure 5.9. Another scenario could be that Prominin-1 localises not only to the cone outer segment but also to the calyceal processes that form a collar around the base of the outer segments of both rod and cone photoreceptors. This hypothesis would need to be verified experimentally, nevertheless, calyceal process have been shown to be present in macaque and human photoreceptor cells, where they house USH1 protein family implicated in Usher syndrome type 1 (USH1)(Sahly *et al.*, 2012). Likewise in rod cells, EYS and Prominin-1 do not seem to share the localisation pattern in cones, which implies they do not exist in proximity in the monkey retina.

Altogether, immunohistochemistry experiments lead to the conclusion that EYS and Prominin-1 do not co-localise in the monkey retina, which suggests that the two proteins do not directly interact.

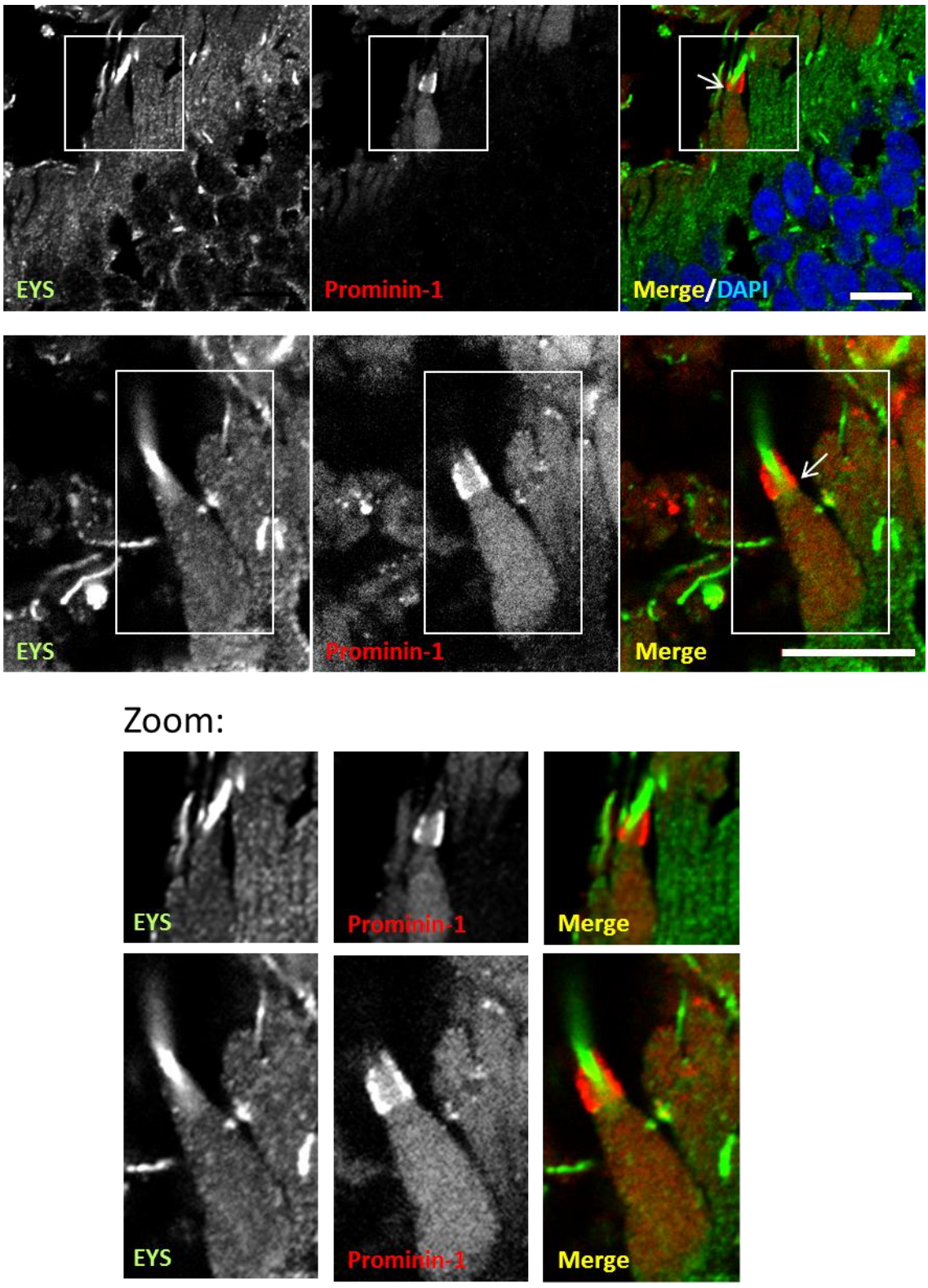

Figure 5.9 Localisation of EYS and Prominin-1 in the macaque retina. The white arrows indicate the analysed cone cells. Prominin-1 (red) was detected along the edges of the cone outer segments whereas EYS (green) was detected in between as a whip-like signal in the region of a photoreceptor ciliary axoneme. The zoomed images (Zoom) correspond to the areas demarcated by the white square in the images. Anti-EYS2 rabbit and anti-Prominin-1 mouse primary antibodies and AlexaFluor488 conjugated goat anti-rabbit and Cyanine 3 conjugated goat anti-mouse secondary antibodies were used. DAPI was used to stain cell nuclei (blue). Scale bar: 20 µm.

5.3 Co-immunoprecipitation of Prominin-1 and EYS Proteins

To fully address the question of whether human orthologues of EYS and Prominin-1 are binding partners, co-immunoprecipitation (Co-IP) assays were performed. Immunofluorescence studies suggested that the two proteins do not co-localise in the tested cell lines and in the monkey retina; however, it could be that the interaction is dynamic and/or takes place only at certain stages of protein trafficking or the retina development.

In the first instance, it was aimed to verify whether Prominin-1 is able to interact with EYS isoforms 1 and 4. As described previously, overexpression of EYS isoform 1 was extremely demanding and therefore, it was not possible to overexpress the two proteins for the purpose of Co-IP assays. To circumvent this issue, Co-IP assay was performed on a protein extract prepared from Y79 cells. For immunoprecipitation of the protein complex, anti-Prominin-1 antibody was used and the presence of EYS was tested by probing the membrane with anti-EYS1 antibody. As shown in Figure 5.10, EYS was detected in the input lane at the expected size of approximately 350 kDa (blot A, red asterisk). Protein bands detected below that size in the same lane might have been a result of protein degradation or non-specific binding of the secondary antibody used. The lanes labelled as 'α-Prom-1' represent the eluted sample from the magnetic beads that had been incubated with anti-Prominin-1 antibody. The lack of a protein band at the size of EYS (~350 kDa) demonstrated the lack of interaction between EYS and Prominin-1. The lanes labelled as '-ve IP' represent a negative control performed by incubation of protein extracts with magnetic beads without a primary antibody. This aimed to test whether protein G attached to the magnetic beads is able to non-specifically bind to the proteins of interest. Blot 'B' represents the same arrangement of samples but it was probed with anti-Prominin-1 antibody. The band marked with a green asterisk in the 'IP α-Prom-1' lane corresponds to the size of Prominin-1 (~100 kDa) and demonstrates that the antibody used in the Co-IP experiments is binding its epitope specifically. It also shows that Prominin-1 was present in the protein extract prepared from Y79 cells. The band, however, is smeared and there is another thin band visible slightly on top of it. This may be due to Prominin-1 being glycosylated, which makes proteins appear as smears

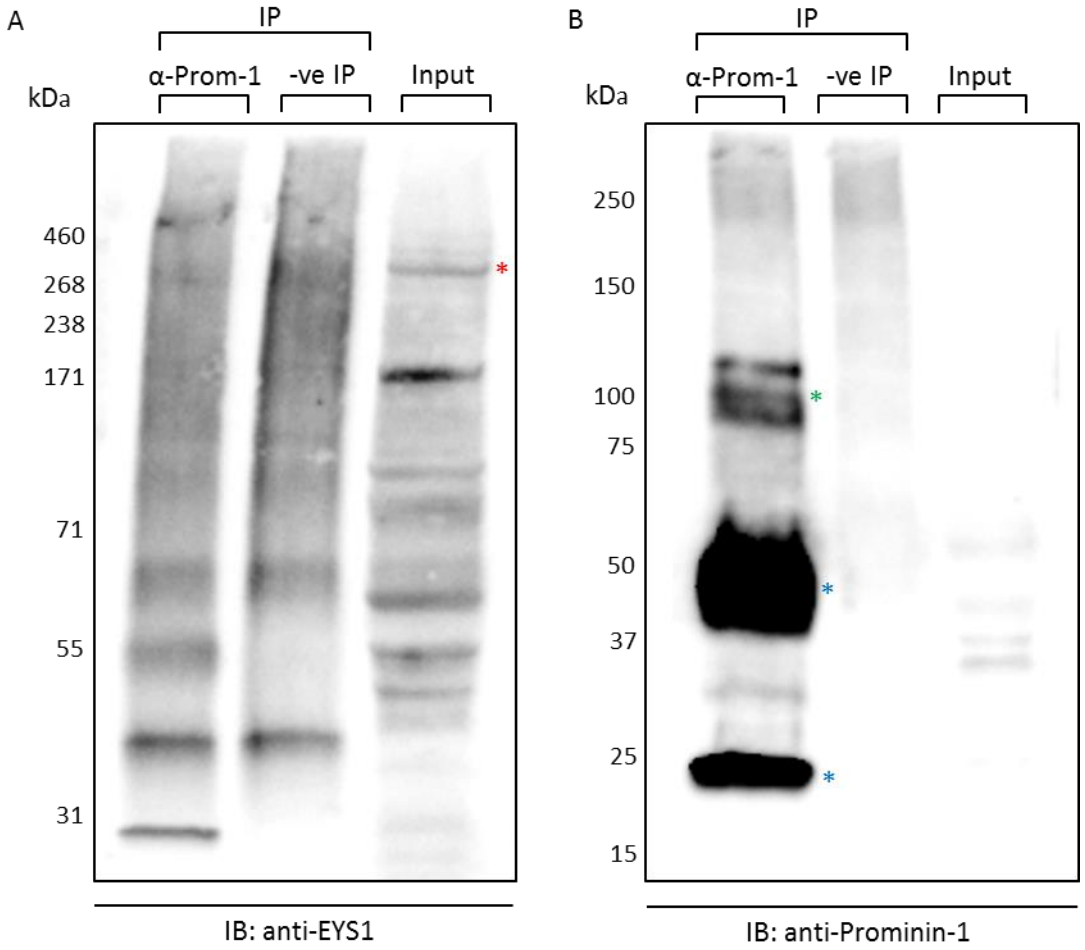

Figure 5.10 Co-immunoprecipitation assay demonstrating lack of interaction between EYS with Prominin-1 in wild type Y79 cells. Blot **'A'** represents membrane probed with anti-EYS1 antibody. The absence of a protein band in the Co-IP lane confirms the lack of interaction. Immunoprecipitation (IP) was performed with mouse anti-Prominin-1 antibody (α-Prom-1). IP performed without an antibody was used as a negative control (-ve IP). Input refers to an extract from wild type Y79 cells and the red asterisk marks the band of EYS isoforms 1 and 4. Blot **'B'** is a control blot probed with anti-Prominin-1 antibody and it demonstrates specificity of the assay; the green asterisk marks the band of Prominin-1 whereas the blue asterisks indicate the antibody heavy and light chains. Loading was normalised using a BCA assay and the samples were resolved by denaturing SDS-PAGE. Secondary antibodies were HRP conjugated goat anti-mouse and goat anti-rabbit antibodies. Expected band sizes: EYS – 350 kDa, Prominin-1 - ~50 kDa. IB – immunoblotting, IP – immunoprecipitation.

rather than sharp bands in immunoblotting; the higher band may correspond to the more heavily glycosylated portion of the protein. Protein bands marked with blue asterisks correspond to the IP antibody heavy chains (~50 kDa) and light chains (~25 kDa). The presence of degraded IP antibody is a result of the elution procedure which is a part of the Co-IP assay protocol. In order to elute samples, magnetic beads are incubated at 70 ˚C in a reducing environment and during that time some of the antibodies bound to the beads may detach. Strikingly, Prominin-1 was not detected in the 'input' lane which was disadvantageous since the 'input' lanes meant to serve as a positive control of the protein size. This suggests that Prominin-1 is not abundantly expressed in Y79 cells but there is enough protein to perform immunoprecipitation assays as it was pulled down by the antibody. Results obtained in Co-IP assays performed on protein extracts from wild type Y79 cells suggest that EYS isoform 1 and 4 do not physically interact with Prominin-1.

The next step was to test whether Prominin-1 is an interacting partner of EYS isoforms 2 and 3. In the case of these two isoforms, advantage was taken of their more convenient size and Co-IP assays were conducted using tagged proteins that were overexpressed in HeLa cells. The experiments were performed using GFP tagged EYS isoforms 2 and 3 and V5 tagged Prominin-1; protein extract from wild type HeLa cells was used as a negative control. Co-IP assays were carried using anti-V5 antibody to pull down protein complexes of overexpressed Prominin-1. Figure 5.11 presents results obtained from Co-IP testing the interaction of EYS isoform 2 and Prominin-1. Blot 'A' represents immunoblotting performed with anti-GFP antibody. The red asterisk in the 'input' lane marks the protein band corresponding to GFP tagged EYS isoform 2; bands of the same size were not detected in the IP lanes and the negative control. Blot 'B' was a control blot containing the same samples but probed using the anti-V5 antibody. The green asterisk marks the band of the pulled down V5-Prominin-1 and blue asterisks correspond to the antibody heavy and light chains. The band corresponding to V5-Prominin-1 detected in the input lane is marked with a purple asterisk. Results of the Co-IP assay implied that V5-Prominin-1 does not physically interact with EYS isoform 2, which is indicated by the lack of a protein band at expected size in the 'α-V5 IP' lane.

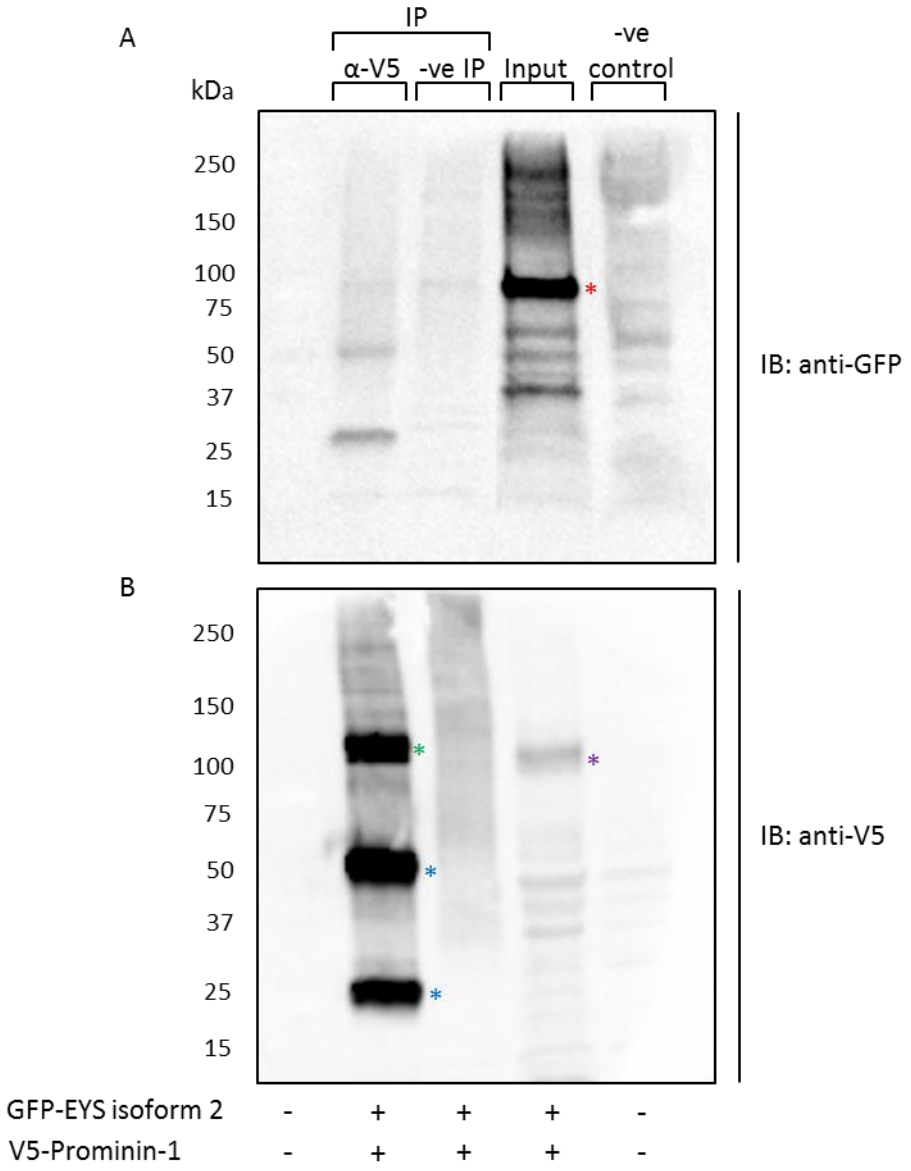

Figure 5.11 Co-immunoprecipitation assay demonstrating lack of interaction between of GFP tagged EYS isoform 2 and V5 tagged Prominin-1 in co-transfected HeLa cells. Blot **'A'** represents the membrane probed with anti-GFP antibody. Immunoprecipitation (IP) was performed with goat anti-V5 antibody. IP performed without an antibody was used as IP negative control (-ve IP). Input refers to an extract from co-transfected HeLa cells whereas the negative control (-ve control) was protein extract from transfected HeLa cells. The red asterisk marks the band of GFP-EYS isoforms 2 in the input lane. The absence of a protein band in the Co-IP lane confirms the lack of interaction. Blot **'B'** is a control blot probed with anti-V5 antibody and it demonstrates specificity of the assay. The green asterisk marks the band of V5-Prominin-1 in the Co-IP lane, the purple asterisks marks the band of v5-Prominin-1 in the input and the blue asterisks indicate the antibody heavy and light chains. Loading was normalised using a BCA assay and the samples were resolved by denaturing SDS-PAGE. Secondary antibodies were HRP conjugated goat anti-mouse and rabbit anti-goat antibodies. The presence of each construct in the loaded sample is denoted by '+' and the absence by '-'. Expected band sizes: GFP-EYS isoform 2 – ~97 kDa, V5-Prominin-1 – ~ 100 kDa. IB – immunoblotting, IP – immunoprecipitation.

Co-IP assay were also performed to test whether EYS isoform 3 is able to interact with Prominin-1. Similarly to EYS isoform 2, HeLa cells were co-transfected with GFP tagged EYS isoform 3 and V5 tagged Prominin-1. Co-IP was performed with anti-V5 antibody and the membranes were probed with anti-GFP and anti-V5 antibodies. As shown in Figure 5.12, interaction between EYS isoform 3 and V5-Prominin was not detected, which can be concluded from the lack of band corresponding to EYS isoform 3 in the IP lane of blot A. The band of EYS isoform 3 is indicated by the red asterisk in the input lane. Blot B was a control blot, where it was shown that anti-V5 antibody binds to V5-Prominin-1; the green asterisk marks the band of V5-Prominin-1, the blue asterisks indicate the antibody heavy and light chains whereas the band of V5-Prominin-1 in the input lane is marked with a violet asterisk.

Altogether, Co-IP assays performed in this study demonstrated that EYS proteins do not complex with Prominin-1, which means that they are unlikely to be interacting partners in humans. However, it could be that the interaction between Prominin-1 and EYS proteins is transient and, therefore, it could not have been detected using the methodology applied in the study.

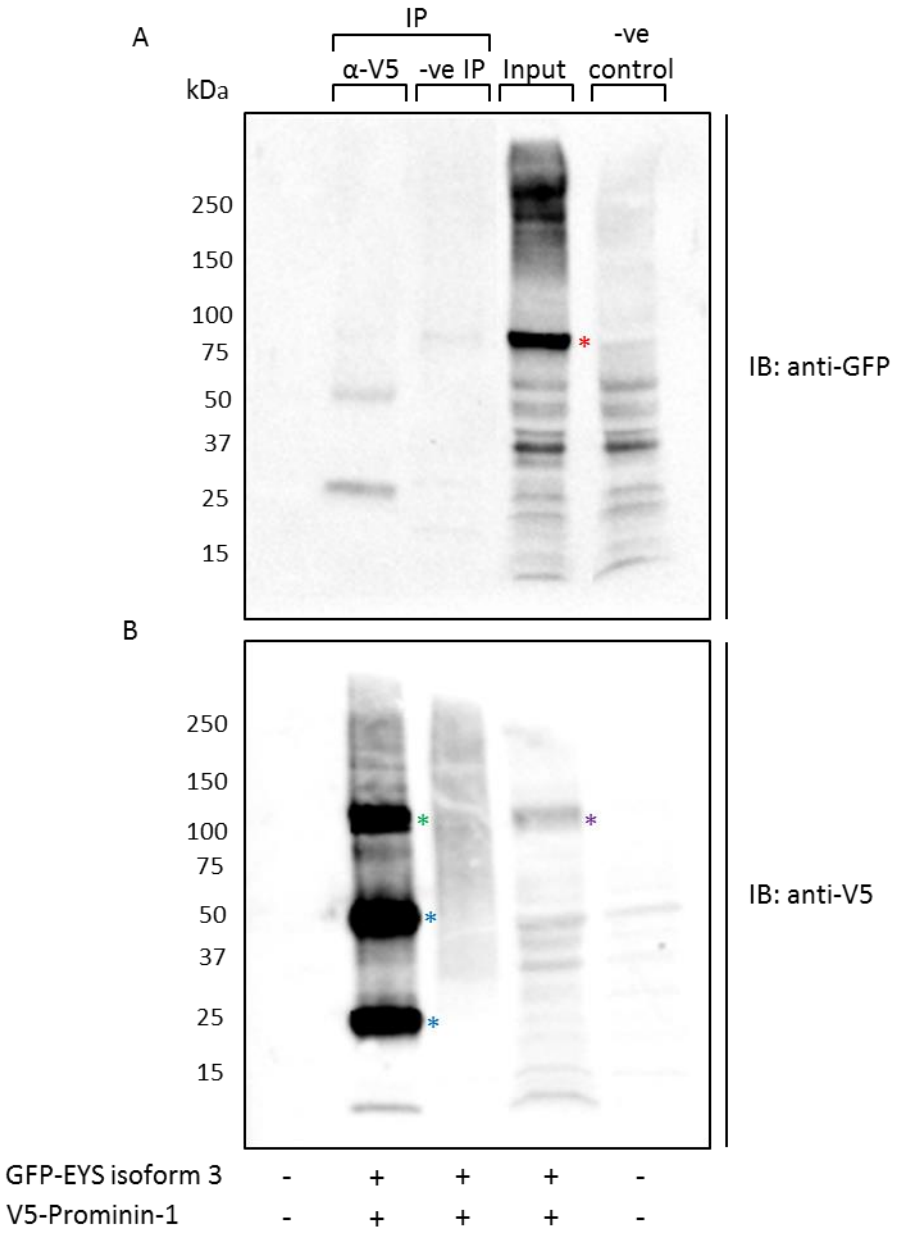

Figure 5.12 Co-immunoprecipitation assay demonstrating lack of interaction between of GFP tagged EYS isoform 3 and V5 tagged Prominin-1 in co-transfected HeLa cells. Blot **'A'** represents the membrane probed with anti-GFP antibody. Immunoprecipitation (IP) was performed with goat anti-V5 antibody. IP performed without an antibody was used as IP negative control (-ve IP). Input refers to an extract from co-transfected HeLa cells whereas the negative control (-ve control) was protein extract from transfected HeLa cells. The red asterisk marks the band of GFP-EYS isoforms 2 in the input lane. The absence of a protein band in the Co-IP lane confirms the lack of interaction. Blot **'B'** is a control blot probed with anti-V5 antibody and it demonstrates specificity of the assay. The green asterisk marks the band of V5-Prominin-1 in the Co-IP lane, the purple asterisks marks the band of v5-Prominin-1 in the input and the blue asterisks indicate the antibody heavy and light chains. Loading was normalised using a BCA assay and the samples were resolved by denaturing SDS-PAGE. Secondary antibodies were HRP conjugated goat anti-mouse and rabbit anti-goat antibodies. The presence of each construct in the loaded sample is denoted by '+' and the absence by '-'. Expected band sizes: GFP-EYS isoform 3 – ~94 kDa, V5-Prominin-1 – ~ 100 kDa. IB – immunoblotting, IP – immunoprecipitation.

5.4 Discussion of Chapter 5

Prominin-1 is a protein implicated in retinal degenerations and it has been suggested that it may be an interacting partner of EYS. The functional link between EYS and Prominin-1 was implied based on extensive research conducted on their *Drosophila* orthologues, spam and prominin. It has been shown that spam is a secreted protein expressed only in the eyes of insects with open rhabdom system, where it interacts with prominin to counteract the adhesive force of chaoptin. This mechanism is a necessary step in the partitioning of the rhabdomeres and creation of the IRS. Moreover, it has been demonstrated that the loss of spam converts the open rhabdom system to the closed system whereas its targeted expression in closed system markedly reorganises the architecture so that it resembles the open system (Husain *et al.*, 2006; Zelhof *et al.*, 2006).

The analysis of *Drosophila* mutant models revealed that presence of human orthologues of spam and prominin is sufficient for the formation of the IRS. Based on this observation, authors of the study suggested that the functional interaction between the two proteins may be conserved in humans and causing retinal degeneration when disrupted (Nie *et al.*, 2012).

Given that the aim of the project was to investigate the interactome of EYS, Prominin-1 was tested as its potential interacting partner. The first approach was to look into the co-localisation of the two proteins in cell lines. EYS proteins and Prominin-1 are endogenously expressed in Y79 cells and therefore, this cell line was looked into in the first instance. The expression of Prominin-1 turned out to be relatively low, to the extent that microvilli, where it normally resides, could not be visualised. To resolve this issue, Y79 cells were transfected with DsRed-Prominin-1 and labelled with anti-EYS1 antibody. The experiment demonstrated that Prominin-1 localises to the cell membrane microvilli present on the surface of Y79 cells whereas EYS does not follow the same pattern of expression; the speckled signal was observed in the regions that could correspond to the cytoplasm and the cell membrane but not cell membrane protrusions. Some yellow signal could be seen at the cytoplasm-cell membrane interface; however, in such modestly developed cell structure, artefacts of immunofluorescence could be mistaken for genuine results.

To better understand the subcellular localisation of the two proteins, an overexpression approach in adherent cells was undertaken. In the first instance, it was attempted to co-transfect HeLa cells with full length EYS isoform 1 and Prominin-1. As it was mentioned previously, transfection with EYS isoform 1 alone is technically challenging and the co-transfection was expected to be even more demanding. Time-consuming and labour intensive optimisation of transfection procedures were conducted, which eventually resulted in obtaining positively co-transfected cells. The efficiency, however, was very low and observations of immuno-localisation of EYS isoform 1 and Prominin-1 could only be made in a few cells. Based on that, it was concluded that EYS isoform 1 and Prominin-1 most likely do not share the same pattern of localisation; however, these observation cannot be considered certain due to the low number of representative cells.

The analysis of co-localisation was also performed for EYS isoforms 2 and 3. The localisation pattern for both of the isoforms was the same, with Prominin-1 residing in the microvilli and EYS fragments being diffused throughout the cytoplasm. No yellow signal was observed at the membrane or at the contact zone of the cell membrane and the cytoplasm, indicating that there is no co-localisation in that subcellular compartment.

The analysis of subcellular co-localisation of proteins is a useful approach to investigate whether the two proteins of interest interact, assuming that the proximity of the two proteins implies interaction. With that borne in mind, it would be reasonable to conclude that Prominin-1 is not an interacting partner of any of the isoforms of EYS. However, the interaction investigated here could be transient and taking place only at some stages of the cell cycle. One certain conclusion that can be made is that none of the EYS isoforms localises to the cell membrane protrusions. It means that the phenomenon of prominin recruiting spam to the surface of the cell membrane of the *Drosophila* cell line does not occur between their human orthologues.

For full verification of the potential co-localisation of EYS and Prominin-1, immunohistochemistry experiments were performed on monkey retinal sections. From experimental work presented in Chapter 4, it was known that EYS may be associated with the ciliary axoneme whereas Prominin-1 was demonstrated to localise to the base of the rod outer segments and outer rims of the cone open disks lamellae in the murine and *Xenopus laevis* models (Han *et al.*, 2012; Maw *et*

al., 2000). In this study, immunohistochemistry experiments were carried out in the adult monkey retinal sections. As expected, EYS was detected in the region corresponding to the ciliary axoneme in rods and cones whereas the signal generated by the anti-Prominin-1 antibody differed between the two types of photoreceptors. In the rod cells, Prominin-1 appeared as speckles localised below the green signal of EYS, which implies that it is localised at the apical region of the rods inner segments. In cones, the red signal was detected either on one side of the cone opposite to the signal of EYS or on both sides of the cell with EYS localising in the middle. In any of the cases, EYS did not appear to co-localise with Prominin-1 which re-enforces the outcomes of the immunocytochemistry experiments. Notably, these results were obtained in the macaque tissue and to fully validate the interaction of EYS and Prominin-1 in humans, it would be necessary to experiment on human retinal specimens, which were not available in this project.

Immunofluorescence experiments indicated that EYS and Prominin-1 do not co-localise together in cell lines and retinal sections. This, however, does not exclude the possibility that the two proteins are capable of binding each other and interact in development or at some stages of trafficking pathways.

To investigate this issue further, Co-IP assays were performed. The interaction between Prominin- 1 and EYS isoforms 1 and 4 was examined in the protein extract prepared from Y79 cells. This strategy was undertaken due to the difficulties with introducing EYS isoform 1 constructs into the cells via transfection. Since both of the proteins of interest are endogenously expressed in Y79 cells, they were considered to be suitable material for conducting Co-IP assays.

The obtained results demonstrated that EYS isoform 1 and 4 do not interact with Prominin-1. Issues were encountered when trying to detect the presence of Prominin-1 in the input control lane containing Y79 lysate, nevertheless, the protein was pulled down by the anti-Prominin-1 antibody attached to the magnetic beads, proving that Prominin-1 was present in the extract. This meant that the expression of Prominin-1 in Y79 cells is not abundant but sufficient for conducting Co-IP assays. Examination of the potential interaction between Prominin-1 and EYS isoforms 2 and 3 was carried out using tagged proteins that were overexpressed in HeLa cells. These experiments demonstrated that neither EYS isoform 2 nor 3 interact with Prominin-1.

Co-IP assay yielded results consistent with the observations made in immunofluorescence experiments and implied that the human orthologues of EYS and Prominin-1 are not interacting partners. An alternative scenario could be that EYS proteins interact with Prominin-1 transiently and such interaction could not have been detected using Co-IP assay that is biased towards stable protein-protein interactions.

Functional interaction between the *Drosophila* orthologues of EYS and Prominin-1 was shown to be essential for the homeostasis of the *Drosophila* photoreceptors. The interaction was suggested to be conserved in humans, making Prominin-1 an interesting candidate for a binding partner of EYS. This was addressed in the study presented herein by performing a range of experiments including immunocytochemistry, immunohistochemistry and co-immunoprecipitation assays. The outcomes of the experiments confirmed that none of the isoforms of EYS co-localise or physically bind Prominin-1. This implies that the two proteins of interest are not strong interacting partners; however, the interaction could still be happening transiently and be a part of a dynamic process taking place during retinal development or protein trafficking. This aspect could be looked into more deeply using advanced methods such as live cell imaging. Furthermore, even if EYS and Prominin-1 do not interact directly, they could still be members of the same multi-protein complex and there could still be a functional link between them. Multi-protein complexes in which EYS and Prominin-1 are potentially involved in could be analysed using mass spectrometry which would reveal proteins that could act as intermediate binding partners of EYS and Prominin-1. Additionally, the problem could be addressed by analysis of animal mutant models checking whether EYS localises properly in *PROM1* mutants and the other way around. This would be a challenging task, mostly because of the absence of EYS in the rodent retina, however, disease modelling using induced pluripotent stem cells could be an alternative.

In spite of the fact the mechanisms taking place in the *Drosophila* model do not seem to be conserved in humans, the research devoted to investigation of EYS and Prominin-1 addressed a very important and previously unexplored area of EYS biology, leading to the exclusion of Prominin-1 from the group of potential binding partners of EYS in humans.

Chapter 6: Mutation Screening of *PROM1* Gene in a Cohort of arRP Patients

Prominin-1 was proposed to be an interacting partner of EYS, the protein of interest in this study. Both Prominin-1 and EYS are vital for the homeostasis of the human retina and mutations in *PROM1* and *EYS* genes lead to retinal degeneration. At the commencement of the project, there had been nearly one hundred disease causing mutations reported in *EYS* and only eight mutations had been reported in *PROM1*. Mutations in *PROM1* have been shown to cause severe retinal degenerations and the phenotype is heterogeneous. The majority of individuals carrying *PROM1* mutations suffer from autosomal recessive RP; however, recessively inherited cone-rod dystrophy and macular degeneration have also been reported. Moreover, one mutation, p.R373C, has been reported to cause autosomal dominant macular degeneration and it has been shown to disrupt morphogenesis of photoreceptor membranous disks in a mouse model (see Introduction, section 1.5).

In the era of next generation sequencing and whole exome sequencing, the number of identified mutations in genes commonly compromised in retinal dystrophies keeps increasing; there are now more than 150 mutations reported in *EYS* and 19 mutations identified in *PROM1* thus far (Appendix A). There is a great discrepancy between the numbers of mutations reported in each of the genes of interest and, therefore, *PROM1* was screened for novel mutations in this study.

6.1 Mutation screening of *PROM1* gene

The panel subjected to screening in this project involved 96 unrelated patients of Caucasian origin, diagnosed with arRP with unidentified causative mutation(s). Sequencing primers were anchored in the intronic sequences to ensure that the splice sites and full exonic sequences are covered. The reference sequence of *PROM1* was derived from Ensembl database; transcript ID ENST00000510224. Analysis of sequence electropherograms revealed seven previously unannotated heterozygous variations present in six unrelated patients (Figure 6.1). Four of the newly identified variants potentially affect the coding

sequence, three of which map to the extracellular domains and one to the transmembrane domain (Figure 6.2). Two of the variations were found in UTR sequences and one at the acceptor splice site. None of the variations was observed in 192 samples of the Human Random Control DNA Panels 1 and 2 (HRC-1 and HRC-2 Caucasian control panels). The obtained results are summarised in Table 6.1.

Substitutions c.181A>G and c.1604A>G alter the amino acid composition of the protein. Potential pathogenicity of substitutions was assessed using software available online (Polyphen-2 and SIFT), although, it needs to be noted that bioinformatics predictions are based on mathematical algorithms and pathogenicity of any mutation needs to be verified by functional experiments. The c.181A>G change is predicted to be non-pathogenic and c.1604A>G is probably damaging according to Polyphen-2, however, both are tolerated according to SIFT, which exemplifies the need for wet-bench experiments to verify potential effects of the mutations.

Deletion c.(620-622)delA causes a frame shift starting at codon 208 and ending at codon 231 where a stop codon is gained after the addition of 22 novel amino acids. A similar effect is caused by the insertion c.(1348-1352)insT which results in a frame shift beginning at codon 452 and gaining a stop codon 12 amino acids further downstream. A premature stop codon can result in the transcript being directed to nonsense mediated decay (NMD), which is an mRNA quality control process preventing production of C-terminally truncated proteins. This could lead to a decrease in the natural expression level of the protein (reviewed in Schweingruber *et al.*, 2013). If the transcript is able to escape NMD, a truncated protein would be synthesised, which could interfere with protein folding and/or affect its function.

Interestingly, the patient carrying the deletion c.(620-622)delA was found to have another mutation in the 5' UTR, c.-307G>A, that could have an impact on the regulation of expression of *PROM1*. It is possible that these mutations have a combined effect on the patient leading to a disease phenotype and form a compound heterozygote; however, it may also be that they reside in the same allele and in this case another variation would have to be identified to explain the recessive inheritance.

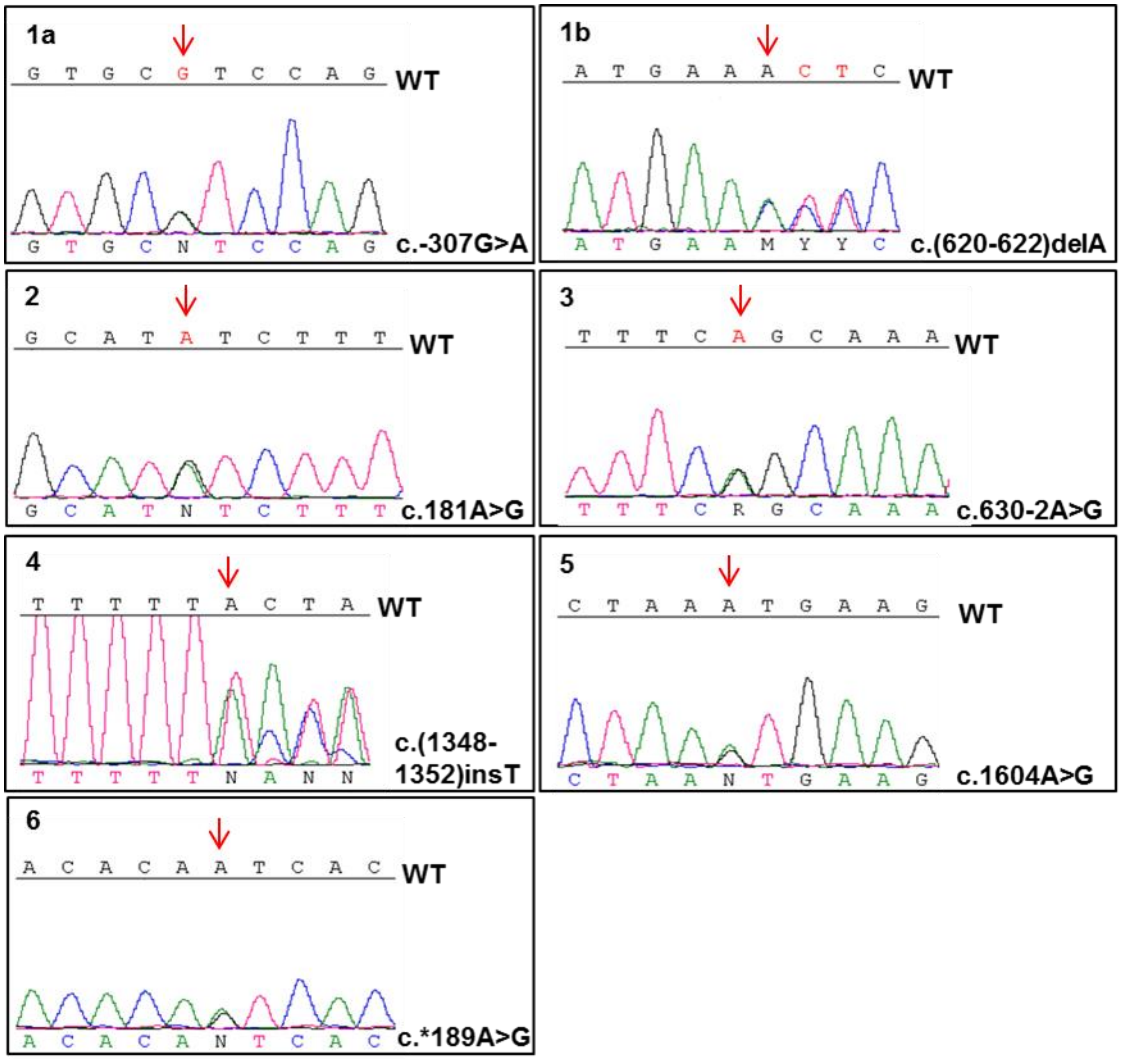

Figure 6.1 Sequence chromatograms showing newly identified variations in *PROM1* in individuals diagnosed with arRP. All of the changes were found in a heterozygous state. Sequence variants were annotated following recommendations of Human Genome Variation Society (HGVS). Red arrows indicate the amended nucleotide or, in case of the insertions and deletion, the first amended nucleotide. WT – 'wild type' refers to a reference sequence derived from Ensembl database.

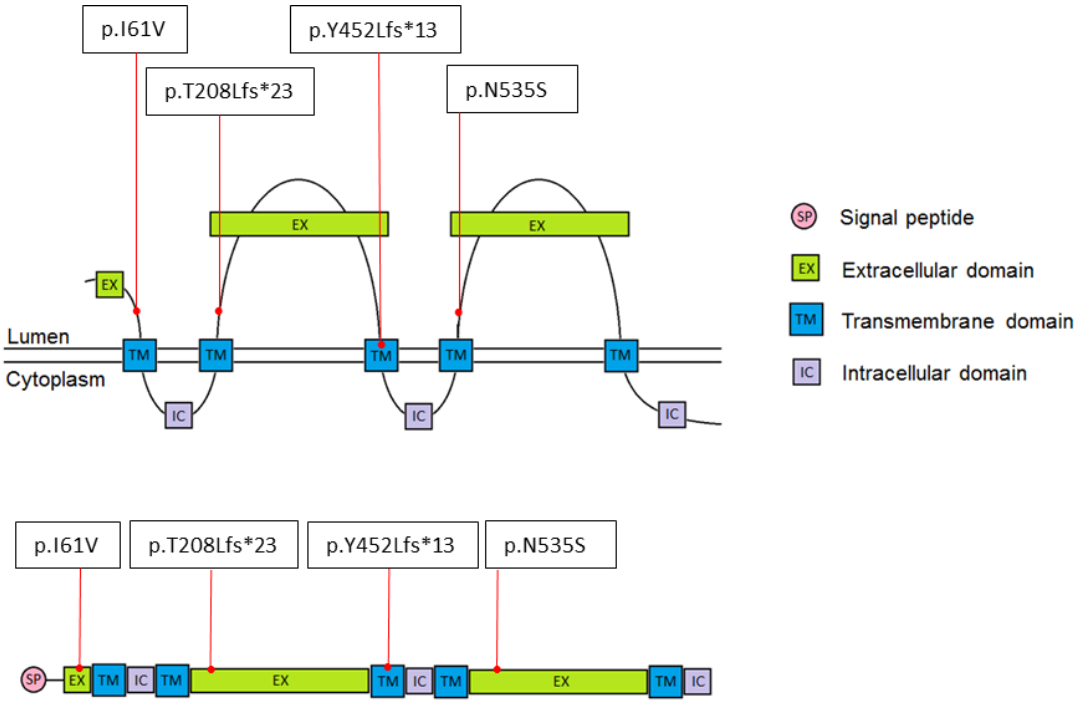

Figure 6.2 Schematic view of Prominin-1 domain structure with the view of distribution of variations identified in the coding sequence of *PROM1*. UTR and splice site variations are not included in this depiction.

Patient number	Position	Nucleotide Change	Amino Acid Change	State	Polyphen2	Sift	Possible effect
1	Exon1 (5'UTR)	c.-307G>A	N/A	hetero-zygous	N/A	N/A	change might have an impact on regulation of gene expression
1	Exon 6	c.(620-622)delA	p.T208Lfs*23	hetero-zygous	N/A	N/A	transcript may undergo NMD or truncated protein may be produced
2	Exon 2	c.181A>G	p.I61V	hetero-zygous	benign	tolerated (0.5)	possible protein function impairment
3	Intron 6-7	c.630-2A>G	N/A	hetero-zygous	N/A	N/A	splice acceptor site may be affected - impaired splicing
4	Exon 13	c.(1348-1352)insT	p.Y452Lfs*13	hetero-zygous	N/A	N/A	transcript may undergo NMD or a truncated protein may be produced - mutation was previously published in homozygous state (Pras et al., 2009)
5	Exon 15	c.1604A>G	p.N535S	hetero-zygous	probably damaging	tolerated (0.47)	possible protein function impairment
6	Exon 28 (3'UTR)	c.*189A>G	N/A	hetero-zygous	N/A	N/A	change might have an impact on regulation of gene expression

Table 6.1 Summary of variations identified in *PROM1* in this study. A cohort of arRP patients was screened for novel mutations resulting in identification of seven novel variants in six unrelated patients. All variants were found in a heterozygous state. Polyphen2 and SIFT software was used to assess pathogenicity of substitutions affecting the coding sequence. NMD refers to nonsense mediated decay of mRNA.

The insertion c.(1348-1352)insT was previously reported in a consanguineous Arab family (Pras *et al.*, 2009). In the published study, three siblings diagnosed with cone-rod dystrophy were found to be homozygous carriers of c.(1348-1352)insT and the parents were unaffected heterozygous carriers (Pras *et al.*, 2009). Variation c.*189A>G was found in the 3' UTR and it could affect regulatory processes of gene expression. The c.630-2A>G substitution found at the splice acceptor site, which could interrupt the normal splicing of the exons, e.g. an exon could be removed or an intron retained, leading to production of a shorter or structurally altered protein.

All of the variations identified in this screen were heterozygous and the panel tested comprised of individuals with recessively inherited retinitis pigmentosa. The mode of inheritance was confirmed in the clinics; however, the DNA samples derived from family members were unavailable to confirm it by direct sequencing. In light of this, it is highly unlikely that the identified mutations are pathogenic; however, the examined individuals may carry other unidentified mutations present in *PROM1*, which could form a compound heterozygote together with the change identified in this study. These could include copy number variations and insertions/deletions of exon(s) and such variations could not have been detected via direct sequencing used in this project. Further research would be required to find a causative genetic variation for the individuals involved in the study.

6.2 Discussion of Chapter 6

Understanding the genetic cause of retinal degenerations is the first step towards understanding the disease and development of potential therapies. One of the genes implicated in retinal dystrophies is *PROM1*, which has been found to be mutated in individuals suffering from arRP, macular degeneration and cone-rod dystrophy. Of note, there could be a functional link between Prominin-1 and EYS proteins, investigation of which was described in Chapter 5.

In this study, a cohort of 96 individuals diagnosed with recessively inherited RP was screened for novel mutations in the *PROM1* gene. The screening resulted in identification of seven previously unidentified changes in six unrelated individuals. Among the identified variations there were five substitutions, one deletion and one insertion. Substitutions identified in the protein coding sequence (c.181A>G and c.1604A>G) were predicted to be most likely tolerated by the bioinformatics software available online. Together with the two other substitutions found in the UTR regions (c.-307G>A and c.*189A>G), these could be rare polymorphisms which can have no effect on the health of the carriers. However, substitutions found in the coding sequence could affect protein folding whereas changes in the UTR regions could have a negative impact on the regulation of gene expression. The substitution affecting a splice acceptor site (c.630-2A>G) may have more serious implications on protein synthesis as it could result in an intron being retained or exon being skipped, which could affect protein folding and function. The identified deletion and insertion (c.(620-622)delA and c.(1348-1352)insT) result in a frameshift leading to introduction of a premature stop codon, which may induce NMD or result in the production of a truncated protein. Notably, the individual carrying deletion c.(620-622)delA was also found to have a change in the 5' UTR, c.-307G>A, and these variants could act together in the disease pathogenesis. More research would be required to verify the effect of the two changes on the biosynthesis of Prominin-1 *in vivo*.

All of the changes identified in the coding sequence of *PROM1* could affect protein folding. This may lead to accumulation of misfolded or unfolded proteins in the endoplasmic reticulum (ER), which in turn could cause a cellular condition known as ER stress resulting in cell death by apoptosis (reviewed in Athanasiou *et al.*, 2013).

Furthermore, all of the variations found in this study are heterozygous and the individuals examined inherited the disease in a recessive manner. Therefore, it cannot be concluded that the identified variations are pathogenic. However, it is likely that the identified changes are loss-of-function mutations and a second allele would have to be mutated to cause the disease; the second undetected genetic variation in *PROM1* would form a compound heterozygote together with the identified change. The second unidentified change could be a copy number variation (CNV), e.g. deletion or insertion of a whole exon, and such a change could not have been identified using direct sequencing method applied in this study. This could be resolved by performing comparative genomic hybridisation (CGH) or employing Next Generation Sequencing (NGS). Once a second variation is found, functional studies of each variation will be required to fully delineate the effect each of them can have on the protein first, and eventually on the homeostasis of photoreceptors. Another possible scenario is that heterozygous mutations in *PROM1* are only pathogenic when inherited together with a variation in another gene, causing a digenic form of RP. The digenic mode of inheritance is not common in photoreceptor degeneration, although there is one report showing that RP can be caused by co-inherited heterozygous mutations in genes encoding Peripherin-2 and Rom-1 (Kajiwara *et al.*, 1994). Extra attention should be drawn to the patient 1 who carries deletion c.(620-622)delA and substitution c.-307G>A in the 5' UTR. The deletion has a truncating effect on the transcript, which undoubtedly affects conformation of the protein or induces NMD. The substitution c.-307G>A could be a non-pathogenic polymorphism but it as well could affect regulatory processes of gene expression. This could be addressed experimentally and if it has an adverse effect on gene expression the two changes could be considered a compound heterozygote, given that it can be shown that they reside in two separate alleles.

Interestingly, *PROM1* is a gene expressed in many tissues including the retina, pancreas, placenta, kidney, liver, lung, brain and heart (Yu *et al.*, 2002); yet, mutations in *PROM1* have only been linked to retinal degeneration and no other obvious pathological signs have been reported. This issue was addressed by Fargeas and colleagues who identified a paralog of *PROM1* gene, *PROM2*. The amino acid identity between Prominin-1 and Prominin-2 has been shown to be less than 30 %; nevertheless, both of the proteins exhibit characteristic structure and strong preference to plasma membrane protrusions. *PROM2*, however, has been

discovered not to be expressed in the eye and this phenomenon was suggested to explain the ocular specific phenotype of *PROM1* mutants; the presence of Prominin-2 could compensate for the absence of Prominin-1 (Fargeas *et al.*, 2003).

Altogether, seven previously unidentified genetic variations were found in the examined cohort of individuals. Since the changes were heterozygous, they cannot be considered as potentially causative of retinal dystrophies. Further research would be required to verify whether the individuals carry more changes in *PROM1* or other parts of their genomes.

Chapter 7: Discussion and Future Perspectives

Retinitis pigmentosa (RP) is a group of retinal degenerative diseases characterised by significant clinical and genetic heterogeneity, with an incidence of approximately 1 in 4000 for a total of more than one million individuals affected worldwide (Hartong *et al.*, 2006). Loss of vision has a devastating effect on quality of life and imposes serious socio-economic burden for patients and their families (Köberlein *et al.*, 2013). Yet, an effective approach to treat photoreceptor degeneration, including RP, has not been developed; the current treatment options are limited to slowing down the progress of the condition. To date, mutations in 84 genes have been identified to be causative of RP by affecting functions such as phototransduction, biosynthesis of proteins or lipid metabolism (RetNet database; https://sph.uth.edu/retnet/home.htm)(Wright *et al.*, 2010). In the era of high-throughput sequencing of individual human genomes, the number of identified disease causing genetic variants is only set to rise. This is invaluable for diagnostic purposes; however, the long term goal towards the development of therapy of blinding diseases can only be achieved via identification of physiological functions of retinopathy associated proteins.

EYS gene was identified at the *RP25* locus on chromosome 6q12, a major locus for autosomal recessive RP. Spanning over 2 Mb, *EYS* is one of the largest genes expressed in the retina (Abd El-Aziz *et al.*, 2008; Collin *et al.*, 2008). Immunofluorescence experiments demonstrated that EYS localises to the photoreceptor outer segments in the porcine retina where it co-localised with rhodopsin (Abd El-Aziz *et al.*, 2008). Interestingly, in the course of mammalian evolution, *EYS* has been lost from several lineages including the armadillo, little brown bat and ruminant lineages. Importantly, *EYS* is not expressed in three rodents: mouse, rat and guinea pig (Abd El-Aziz *et al.*, 2008) commonly used for research purposes in the laboratory. However, it is well conserved in *Drosophila melanogaster* and research conducted in this model revealed that the *Drosophila* orthologue of EYS (eys) is involved in the modelling of the photoreceptor architecture, and that it is a member of a network of interactions necessary for the proper formation of inter-rhabdomeral space (IRS) in the ommatidium. Furthermore, it has been demonstrated that the formation of IRS depends on the

interaction of eys with another well-conserved protein, prominin, and disruption of this interaction causes disorganisation of the rhabdom. It has also been suggested that this interaction may be conserved in humans and be essential for photoreceptor homeostasis (Nie *et al.*, 2012; Zelhof *et al.*, 2006). Studying of eys in the *Drosophila* model also resulted in identification of the role of eys in preservation of the cell shape of the mechanoreceptor neurons by stiffening of the cell membrane (Cook *et al.*, 2008).

Since the discovery of *EYS*, more than 150 mutations have been identified in individuals suffering from autosomal recessive form of RP, making it the major gene implicated in this disease. In spite of the vast knowledge of *EYS* related disease phenotype, the role of EYS protein in the human retina has remained a mystery. The project presented herein aimed to delineate the role of EYS in the human photoreceptors, which is a key point towards undertsanding the mechanisms of RP. Once the role of EYS in pathophysiology of RP is known, it will be possible to investigate whether it can be targeted by gene therapy, drug development or other therapeutical approaches.

7.1 Identification and Characterisation of Interacting Partners of EYS

The approach undertaken to investigate the role of EYS in the retina was to study its interactome. Identification of interacting partners of a protein of interest allows to hypothesise its potential function and opens avenues for further functional research (reviewed in De Las Rivas & Fontanillo, 2010).

The method chosen to identify novel protein-protein interactions (PPIs) in this project was Yeast 2-hybrid (Y2H). Y2H is a genetic screen for the detection of PPIs and the system used in this study was based on the GAL4 transcription activator. Y2H screening was performed using EYS protein bait fragments and a human retinal cDNA library that was previously prepared in the laboratory. Many technical issues had to be dealt with when utilising the system and the difficulties were most likely caused by the large size of EYS and/or its conformation. Extensive screening of the retinal cDNA library resulted in identification of one potential interacting partner, AIPL1. The interaction was detected using an N-terminal fragment of EYS (154-1635 aa) and the prey fragment of AIPL1 mapped to its C-terminal part (281-384 aa). The putative interaction was validated via

immunocytochemistry (ICC) and co-immunoprecipitation (Co-IP) experiments. Validation was performed using the same EYS isoform 1 N-terminal bait fragment (154-1635 aa) and EYS isoforms 2 and 3, which were cloned and characterised at a later stage of the project. EYS isoform 1 (the canonical/full-length protein) could not have been used in the validating experiments due its size, which caused major difficulties with achieving successful overexpression of the tagged protein. Y79 cells, which endogenously express EYS and AIPL1, were not a reliable system for immuno-localisation studies due their poorly developed morphology and they could not have been used as a source of protein for Co-IP due to unavailability of compatible anti-EYS and anti-AIPL1 antibodies; both antibodies available were raised in rabbit. Nonetheless, AIPL1 was demonstrated to co-localise and immunoprecipitate together with EYS isoform 2 and 3 as well as EYS N-terminal bait fragment (bait 3). These results implied that AIPL1 is a novel binding partner of EYS isoforms 2 and 3 and may also be able to interact with EYS isoform 1.

AIPL1 is also implicated in retinal degeneration: mutations in *AIPL1* cause severe early-onset retinal degeneration known as Leber's congenital amaurosis (LCA) (Sohocki *et al.*, 2000). The role of AIPL1 in photoreceptor cells has not been fully understood; however, there is evidence to suggest that it may function as a photoreceptor specific molecular chaperone (Hidalgo-de-Quintana *et al.*, 2008). Furthermore, it has been demonstrated that AIPL1 interacts with and aids in processing of prenylated proteins (Ramamurthy *et al.*, 2003). One such protein is rod cGMP phosphodiesterase (PDE6) which is a critical enzyme in phototransduction; the biosynthesis of a PDE6 heterotetramer requires prenylation of its catalytic subunits and its proper assembly is reliant upon the interaction with AIPL1 (Kolandaivelu *et al.*, 2009). While PDE6 is a protein localising to the photoreceptor outer segment, AIPL1 was demonstrated to reside in the region spanning from the connecting cilium to the synapse (van der Spuy *et al.*, 2002). In this study, it has been shown that EYS is likely to associate to the photoreceptor ciliary axoneme, which makes EYS another example of a protein localising to the photoreceptor outer segment and interacting with AIPL1. Even though EYS is unlikely to be prenylated, it is possible that it is a substrate protein of AIPL1 and requires its chaperoning activity to properly fold and/or localise to its final destination. Interestingly, in the most recent study, AIPL1 has been demonstrated to co-localise at the photoreceptor connecting cilium with EB

proteins, a microtubule binding family of proteins important in the microtubule dynamics, suggesting that the heterocomplex AIPL1-Hsp90 may function at this subcellular compartment (Hidalgo-de-Quintana *et al.*, 2015).

Both EYS and AIPL1 have been shown to be implicated in retinal degenerations and, therefore, it is possible that the two proteins are components of photoreceptor specific pathways that are essential for the homeostasis of the retina, e.g. AIPL1 could assist with the biosynthesis of EYS and the trafficking to the outer segment. The interaction of EYS proteins and AIPL1 has not been investigated by immunohistochemistry and it will be important to carry out such analysis in the future. It would be of best value to perform immunohistochemistry on human specimens which could also be used as a source of protein for Co-IP. These experiments, however, would require obtaining custom made anti-EYS or anti-AIPL1 antibodies raised in an animal other than rabbit; commercially available antibodies have not met the needs of the project due to the questionable specificity.

The identification of AIPL1 as a novel interacting protein partner of EYS did not provide any insights into the specific function that might EYS plays in the photoreceptor outer segments. This triggered the design of further experiments aiming to better characterise EYS, which could help understand what specific role it plays in the retina once it has been fully assembled and trafficked to its final destination.

Another approach to study the interactome of the protein of interest can be investigation of candidate binding partners selected based on the published literature. One such candidate for an interacting partner of EYS was Prominin-1. Prominin-1 is a pentaspan transmembrane protein known to have a strong preference for plasma membrane protrusions and is implicated in retinal degeneration (Maw *et al.*, 2000; Weigmann *et al.*, 1997). Extensive research conducted in a *Drosophila* model suggested that the functional link between the orthologues of EYS and Prominin-1 could be conserved in humans and is vital for the homeostasis of photoreceptor cells (Nie *et al.*, 2012; Zelhof *et al.*, 2006). One of the aims of this study was to verify whether this was the case. The methodology included immunofluorescence used to compare the localisation patterns of the two proteins and Co-IP to verify whether the two proteins associate with each other. ICC and IHC experiments demonstrated that EYS proteins do not co-localise with

Prominin-1 and furthermore, Co-IP assays demonstrated that these two proteins do not complex together.

These results have suggested that the interaction of EYS and Prominin-1 is most likely not conserved in humans; however, it could be that the interaction is transient and/or takes place at certain stages of development. This could be a valid point since the studies of *Drosophila* models revealed that both eys and prominin are expressed at the beginning of rhabdomere formation during the puparium stage of the *Drosophila* development (Zelhof *et al.*, 2006). It is also possible that the functional link between EYS and Prominin-1 exists in fully developed photoreceptors and there are unidentified intermediate interacting partners involved. These aspects remain to be addressed in future research.

As Prominin-1 was considered a potential interacting partner of *EYS* and the number of disease causing mutations is much lower in *PROM1* than in *EYS*, mutation screening of *PROM1* in a panel of arRP patients was carried out. The screening resulted in identification of seven previously unidentified heterozygous changes in six unrelated patients. Since the patients examined were confirmed to inherit the disease in a recessive manner, none of the newly found variations can be considered pathogenic. It could be that the changes are benign or that there are other unidentified variations present in *PROM1* or another gene. In light of this, the genetic background of arRP diagnosed in the panel of patients involved requires further research, preferably by using high throughput methods such as next generation sequencing.

Altogether, identification of novel interacting partners of EYS led to the conclusion that EYS proteins can interact with AIPL1, which may assist with the biosynthesis of EYS in photoreceptor cells. Furthermore, the potential interaction of EYS and Prominin-1 was examined and evidence was provided against the hypothesis that the two proteins interact in adult primates.

Overall, the analysis of EYS interacting partners provided useful insights into its biology; nonetheless, drawing conclusions regarding its possible role in the retina has not been possible and further research would be required to investigate the interactome of EYS more deeply.

7.2 Characterisation of EYS

Elucidating the role of EYS protein in the human retina is vital for understanding mechanisms underlying RP. Experimental efforts to further characterise EYS were necessitated by multiple technical difficulties encountered in Y2H and the resulting low efficiency of the screening. The in-depth analysis of EYS genetic structure as well as subcellular localisation aimed to bring us closer to understanding its function in the retina and ease the design of future studies.

The analysis of genomic online databases followed by RT-PCR analysis resulted in identification of EYS isoforms 2 and 3 which were confirmed to be expressed in the human retina and testis as well as the Y79 cell line. Altogether, there are currently four recognised EYS isoforms: EYS isoform 1 and 4 comprising of 3144 aa and 3165 aa respectively, and two shorter splicing variants, EYS isoforms 2 and 3 made up of 619 aa and 594 aa respectively. The testicular expression of EYS isoforms 2 and 3 is yet to be investigated; however, testes related phenotype has not thus far been reported in males carrying mutations in *EYS*.

The subcellular localisation of EYS isoforms was investigated by performing ICC studies. Overexpressed GFP tagged EYS isoforms 2 and 3 were found to localise mostly to the cytoplasm and occasionally to the cell nucleus. The nuclear expression could be an artefact of transfection and over-expression of the proteins, or it could indicate a potential signalling or transporting type of role for the short EYS isoforms, where they shuttle in between the cytoplasm and nucleus in response to cellular changes. This would be an interesting aspect to address, especially with respect to the interaction with AIPL1, which has previously been shown to modulate the nuclear translocation of NUB1, a protein involved in NEDD8 mediated proteasomal degradation (van der Spuy & Cheetham, 2004). Therefore, it could be that AIPL1 is involved in the translocation of EYS isoforms 2 and 3 between the nucleus and the cytoplasm, as these were shown to associate.

The analysis of EYS isoforms 1 and 4 was challenging due their size and was limited to investigation of endogenous localisation patterns in Y79 cells. This resulted in the conclusion that EYS isoforms 1 and 4 probably localise to the cell cytoplasm and possibly to the cell membrane. The analysis of overexpressed GFP tagged EYS protein fragments suggested their cytoplasmic localisation.

Immunohistochemistry experiments were performed in the *Macaca fascicularis* retinal sections and showed that EYS may be associated with the photoreceptor ciliary axoneme, which is a microtubular structure that plays a role in the structural integrity of photoreceptor outer segments and intraflagellar transport (IFT). It could, therefore, be that EYS plays a role in maintaining the structure of the photoreceptor outer segments by, for example, being a component of the ciliary scaffold. This would be in line with the study published by Cook et al., where it was demonstrated that EYS stiffens the cell membrane of the *Drosophila* cell line (Cook *et al.*, 2008). Another hypothesis can be that EYS is a member of the IFT machinery, which is of central importance for both assembly and maintenance of the cilium. Photoreceptor outer segments do not house the protein synthesis machinery; therefore, the proteins residing in that compartment need to be transported from the inner segment via connecting cilium by means of IFT (Taschner *et al.*, 2012). It could be that EYS is a component of multi-protein motor assemblies, which take part in the very dynamic process of IFT.

The experimental work undertaken to characterise EYS provided further insights into the subcellular localisation of EYS and its genetic structure. This was an important aspect of the project which provided invaluable information on EYS; nonetheless, many questions have remained unanswered. The role of EYS in the human photoreceptors needs to be more deeply investigated to fully understand its importance. More advanced methods such as electron microscopy would have to be employed to research the localisation of EYS in more detail. Furthermore, characterisation and cloning of EYS isoforms 2 and 3 greatly contributed to the analysis of the potential interactions with AIPL1 and Prominin-1; however, the specific role of the short variants of EYS has not yet been addressed. The isoforms of EYS may be multifunctional proteins localising to more than one subcellular compartment. This makes EYS a very challenging protein to investigate and a significant amount of carefully designed research would be required to fully decipher its function in the human body.

7.3 Future Perspectives

The project presented herein involved broad analysis of the biological features of EYS and a few approaches were undertaken: (i) new interacting

partners of EYS were sought for using Y2H, (ii) putative interacting partners identified by Y2H (AIPL1) and by a candidate gene approach (Prominin-1) were characterised by immunofluorescence and Co-IP assays, (iii) subcellular localisation of EYS was better characterised and (iv) mutation screening of *PROM1* in a cohort of arRP patients was conducted. Each stage of the study yielded exciting results and each of them can be elaborated on in the future research projects.

The network of interactions that EYS is involved in has not been fully investigated. Multiple technical issues were encountered which hindered the efficient Y2H screening and in the future, an alternative approach could be undertaken to investigate the interactome of EYS. From the number of available methods, Y2H is one of the most convenient and cost effective methods of high-throughput searching for novel interactions. However, from the project presented herein, it can be concluded that the GAL4 based Y2H is not the most suitable system to study EYS; this is most likely due to its size and/or localisation in yeast cells that prevent the bait-prey complex to travel to the nucleus. As an alternative, a modification of Y2H could be used but this will only be possible if the exact localisation of EYS is known, e.g. membrane split-ubiquitin Y2H (MbY2H) system could be used for the detection of interactions between membrane bound proteins (Brückner *et al.*, 2009). An alternative approach could be to employ affinity purification in tandem with mass spectrometry (AP-MS). The advantage of the method is that it allows identification of PPIs under native conditions, i.e. using mammalian cells, the multicomponent complexes are pulled down allowing investigation of the network of interaction more comprehensively by mass spectrometry (Ngounou Wetie *et al.*, 2014). The method, however, requires transfection and expression of the tagged protein of interest in the cell line. This imposes serious limitations since transfection with tagged EYS isoform 1 was challenging using standard laboratory protocols. Transfection using commercially available reagents as well as electroporation did not bring satisfactory results; however, the solution could be to work on tagged EYS protein fragments. Alternatively, it could be attempted to find a method of efficient introduction of such large plasmids into the cell lines of interest, for example, by employing viral vectors that are capable of carrying large DNA constructs (Waehler *et al.*, 2007). The bottleneck in this approach can be the transfection of viral constructs carrying a gene of interest into the packaging cell line, which could be hindered by the size

of *EYS*. This issue could be addressed by using the recently developed dual AVV vectors which are capable of efficient transduction of large genes in smaller fragments that are then reconstituted into full sized genes (Trapani *et al.*, 2014). Construction of viral vectors for EYS would not only contribute to the AP-MS approach but would also enable more detailed characterisation of the localisation pattern of overexpressed EYS isoform 1 and could be a starting point for working on gene therapy approach to treat arRP.

Furthermore, since AP-MS makes it possible to look into to the protein complexes, it could also be used to verify whether EYS complexes with Prominin-1. This would address part of the question of whether there is a functional link between the two proteins; whether the two associate in development remains to be investigated once a suitable and viable option for an animal model becomes available for investigating endogenous expression of EYS.

Prominin-1 has been considered as a potential interacting partner of EYS based on previously published literature and there is rationale for some other proteins to be potential interacting partners of EYS. In this study, co-localisation of EYS and acetylated α-tubulin has been shown. This interaction could be examined using immunohistochemistry to see if they also co-localise in human tissue and Co-IP to verify whether the two proteins physically bind. Furthermore, EYS was shown to co-localise with RP1 in the monkey retina (unpublished data from our laboratory) and the same experimental approach could be used to test this interaction. Interestingly, mutations in *RP1* have been shown to cause RP and the protein it encodes is specifically biosynthesised in the retina where it is a part of the ciliary axoneme (Liu *et al.*, 2002; Pierce *et al.*, 1999). It has also been shown that RP1 is a microtubule-associated protein that may be essential for the correct stacking of outer segment discs (Liu *et al.*, 2003; Liu *et al.*, 2004a). Co-localisation of EYS and RP1 could suggest that EYS, similarly to RP1, plays a role in structural organisation of the outer segment and proper stacking of membranous disks; Co-IP assays could be performed to verify whether the two proteins physically bind. This would enhance the hypothesis that EYS is a ciliary axoneme associated protein and it may have a structural function.

One of the achievements of the project is the cloning and characterisation of EYS isoforms 2 and 3. They have been demonstrated to localise to the cytoplasm and, therefore, they could be used as baits in the GAL4 based Y2H system with

more success. Performing the Y2H screening using EYS isoforms 2 and 3 could be a major step in investigation of their role in the human retina and potentially other tissues such as testis. Looking into their interacting partners would provide insights into their potential function and the same interacting partners could be tested for EYS isoform 1 and 4. The technical issues encountered in this project could be avoided as EYS isoforms 2 and 3 constitute merely ~20 % of the longest isoform and their size should not affect the performance of Y2H. Furthermore, antibodies could be raised against EYS isoform 2 and 3 and they could be used for immunohistochemistry studies, which would provide information on their localisation *in vivo*.

Moreover, the Y2H data obtained in this project have been validated using ICC and Co-IP. Further validation could be undertaken using ICH performed on human specimens. This would be the most illustrative model; however, the co-localisation of EYS and AIPL1 could not be assessed unless new antibodies against any of the two proteins are available. It would also be interesting to examine whether any of the published disease causing mutations in either EYS or AIPL1 impair the interaction between the two proteins.

The subcellular localisation of EYS was investigated in the monkey retina and it appeared that EYS may be a ciliary axoneme associated protein. Further analysis would be necessary to validate whether this localisation is the same in the human retina, most preferably using electron microscopy.

Studying EYS proteins is challenging mostly due to the size of EYS isoform 1. The second feature of EYS that adds difficulty is its absence in rodents, which excludes the most common animal models, i.e. mouse and rat, from the *in vivo* research of EYS. Instead, larger animals such as rabbits or dogs would have to be used to study EYS *in vivo*, which makes the research of EYS more challenging experimentally and ethically. Future perspectives for addressing these issues have arisen from the stem cell research, especially the development of the patient derived induced pluripotent stem cells (iPSC). Patient derived iPSC cells can be used for a variety of applications ranging from elucidating the mechanisms of disease causing mutations to drug screening and testing of gene therapy (reviewed in Jayakody *et al.*, 2015; Yvon *et al.*, 2015). Modelling of retinal degeneration has been successfully demonstrated using tissue material derived from RP patients with distinct mutations in *RP1*, *RP9*, *PRPH2* and *RHO* genes. The obtained rod

photoreceptors were used for characterisation of the course of degeneration and for drug testing (Jin *et al.*, 2011). A similar approach could be undertaken to study EYS and to begin with, its localisation could be looked into in wild type and mutated models. Stem cell based models are a promising tool for studying proteins like EYS and in that respect, the absence of EYS in mouse models of retinal diseases can be turned into an advantage. Rodent models of retinal degeneration could serve as null environment for stem cell based approaches, e.g. patient derived iPSCs could be differentiated into photoreceptors precursors and transplanted into mouse models; the comparison of photoreceptors derived from RP patients with the healthy controls would provide insights into the mechanisms underlying *EYS* specific arRP. Furthermore, the patient derived iPSCs could be subjected to CRISPR-based genome editing to correct the disease causing mutation and the obtained photoreceptor precursors could be transplanted into murine models to examine whether they can develop into properly functioning photoreceptors; such an approach could be turned into a therapeutic strategy for RP (reviewed in Tucker *et al.*, 2014). Testing human derived stem cells in murine models has been successfully conducted, making the suggested approach feasible (Lamba *et al.*, 2009).

More opportunities for further research come from the mutation screening performed in the project. This could be elaborated on further and the patients' DNA samples should preferentially be submitted for the whole exome sequencing, enabling identification of the underlying cause of arRP. The effect of mutations on the homeostasis of the photoreceptor cells could subsequently be addressed experimentally.

The research project presented herein aimed to elucidate the role of EYS in the human retina by identification and characterisation of its interacting partners. Indeed, it has brought us closer to understanding its function and determining why mutations in *EYS* cause arRP. Moreover, the results of the project have opened new avenues for long term and exciting future research opportunities. Since mutations in *EYS* are the major cause of arRP, it will be of paramount importance to undertake the challenge of researching EYS further in order for the individuals suffering from arRP and their families to receive benefit from the biomedical research.

Chapter 8: Appendices

Appendix A. Mutations Identified in *PROM1* to Date

Mutations in *PROM1* have been shown to be causative of retinal degeneration. The causative variants reported to date are summarised in Table 8.1.

	Nucleotide change	Amino acid change	Inherit-ance	Disease	Reference
1	c.1841delG	p.G614Efs*13	R	Retinal degeneration and polydactyly	(Maw *et al.*, 2000)
2	c.1726C>T	p.Q576*	R	arRP accompanied by macular degeneration	(Zhang *et al.*, 2007)
3	c.1117C>T	p.R373C	D	Autosomal dominant macular degeneration	(Yang *et al.*, 2008)
4	c.1349insT	p.Y452fs*13	R	Cone rod dystrophy	(Pras *et al.*, 2009)
5	c.869delG	p.S290Ifs*2	R	arRP	(Permanyer *et al.*, 2010)
6	c.1142–1G>A	N/A	R	Cone rod dystrophy	(Littink *et al.*, 2010)
7	c.1557C>A	pY519*	R	arRP	(Song *et al.*, 2011)
8	c.1532C>A	p.T520K	R	arRP	(Gonzalez-del Pozo *et al.*, 2011)
9	c.442A>T	p.K148*	R	arRP	(Jinda *et al.*, 2014)
10	c.642T>A c.1209_1229	p.Y214* pQ403_S410delinsH	R, comp. het	arRP	(Eisenberger *et al.*, 2013)
11	c.2011A>T c.510-1G>A	p.K671* p.?	R, comp. het	Simplex RP	(Wang *et al.*, 2014)
12	c.730C>T c.1354_1355insT	p.R244* p.Y452fs*	R, comp. het	Simplex RP	(Wang *et al.*, 2014)
13	c.139delC c.1238T>A	p.H47Ifs*12 p.V413D	R, comp. het	arRP	(Xu *et al.*, 2014)

14	c.1157T>A	p.L386*	?	Cone rod dystrophy	(Glöckle *et al.*, 2014)
15	c.1530>CG	p.Y510*	R	arRP	(Abu-Safieh *et al.*, 2013)
16	c.1984-1G>T	N/A	R	arRP	(de Castro-Miró *et al.*, 2014)
17	c.2373+5G>T	N/A	R	arRP	(Chen *et al.*, 2013)
18	c.1355_1356insT c.622delA	p.Y453Lfs p.T208Lfs	R, comp. het)	arRP	(Zhao *et al.*, 2015)
19	c.1983+1G>T c.730c>7	p.R228*	R, comp. het)	cone rod dystrophy	(Zhang *et al.*, 2014)

Table 8.1 Summary of mutations reported in *PROM1* to date. Variants were annotated in accordance with recommendations of Human Genome Variation Society (HGVS). R - recessive inheritance, D – dominant inheritance, R comp. het. – recessive inheritance, compound heterozygote, ? – inheritance unspecified.

Appendix B. Oligonucleotides for Sequencing EYS cDNA

In this study, the cloning of genes of interest was performed on several different occasions and each time inserts were sequenced to check the integrity of the sequence and to verify the reading frame. Primers used for sequencing of EYS, PROM1 and AIPL1 are summarised in Table 8.2, Table 8.3 and Table 8.4 respectively.

Primer	Sequence (5' ->3')
Forward 1	ATGACTGACAAATCAATCGTCA
Reverse 1	CCCAAAAACCAGCAATCTCTG
Forward 2	GACAGTGAAACAGCAGTTCTG
Reverse 2	CACATTCACAAATGAAAC
Forward 3	GTGAGTTTTCATTAGTACCATGTCA
Forward 4	TTCTTTCTGGCTGCAAACTG
Forward 5	CAAGTGTGTCCCAGGATTTA
Reverse 5	CTTCCCAATCAGATAGGCAC
Forward 6	TATGTCTGTGCCCACCCCTT
Forward 7	TGTGAAATAAATCTAGATGA
Forward 7A	GGATCTGTGTTGATGGGC
Reverse 7	GATATTCATTAATAAGTTCTGTGC
Forward 8	ATCACCATGTCTACATGGTG
Forward 8a	TTCTTTGTGGTGATGAAATA
Forward 9	CAGCAAAACACAGTCTTCTT
Forward 10	ATATCTAAACAGGTAACCAT
Forward 11	CATTGTCCCTTCACAAACTA
Reverse 11	ATGCAACATTGGTGGTGAC
Forward 12	CTTCAGAATGGTCCAAATGG
Forward 12a	CTTACTTTGTCTTCACTGGAA
Forward 13	CATGTACTCGGAAAACCCCT
Reverse 13	GTGGCATACATCCTGCTGGC
Forward 14	GGAACATAACAGAACTGTTA
Forward 15	GCCACGTCCCTTGGTGTGCT
Forward 16	AGGAGCGAGCCCCTCAATCT
Forward 16a	CTGCATTTCATTACCTCATG
Forward 17	CTGCATTTCATTACCTCATG
Forward 18	CCATGGCAATAGAAAATGAA
Forward 19	GCTCAAAATGAAGAAAATGA
Forward 20	ACTATCATTCTAGAAACTCT
Forward 21	TTCTTACAGTTGCCTGTGTA

Table 8.2 Summary of primers used for sequencing *EYS* cDNA.

Primer	Sequence (5'->3')
Forward 1	ATGGCCCTCGTACTCGGC
Reverse 1	GCAGGCAATTCATAATTCCAA
Reverse 2	CATAATCAATTTTGGATTCATAT
Forward 2	TGGAGAAATGCACCAGCGACAG
Forward 3	ATCAAATATATATTGGCCCAG
Forward 4	ATCCATCAAGTGAAACCTGC
Forward 5	CTTGAATTCCATTGGTTCAG
Forward 6	ATGCCACCCCGACCACCCG
Forward 7	GCATACTGGAAGCATAAG
Forward 8	ACAGGGAATGGATTGTTGGAG
Forward 9	CTGTGTAGCTACATTATCGAC

Table 8.3 Primers used for sequencing *PROM1* cDNA.

Primer	Sequence (5' ->3')
Forward 1	ATGGATGCCGCTCTGCTCCTGAACG
Reverse 1	GGAGCTCGCCCGTGCCCCCGTGC
Forward 2	GAGTGGCACGTGCACACGTGC
Reverse 2	GTAATCACTCGGGGCATCAACCTGC
Forward 3	GCTGAAGAAGGAGGAGTACTATG
Forward 4	GCCACCCGCACAGTCATCCACAGAG

Table 8.4 Primers used for sequencing *AIPL1* cDNA.

Appendix C. Oligonucleotides for Gateway Cloning

For gateway cloning of proteins of interest, primers containing *attB* sequences had be designed. The *att* flanked PCR products were cloned into pDONR/Zeo entry vectors then, into destination vectors of interest. The primer designed for cloning using Gateway system are summarised in Table 8.5, Table 8.6 and Table 8.7.

Primer	Sequence (5' ->3')
AIPL1-attB1-F - Forward	GGGGACAAGTTTGTACAAAAAAGCAGGCTTC ATGGATGCCGCTCTGCTCCTGAACG
AIPL1-attB2-R - Reverse, with stop codon	GGGGACCACTTTGTACAAGAAAGCTGGGTG TCAGTGCTGCAGCGAGTGCCCTG
AIPL1-attB2-R - Reverse, without stop codon	GGGGACCACTTTGTACAAGAAAGCTGGGTG GTGCTGCAGCGAGTGCCCTG

Table 8.5 Gateway compatible primers for cloning of *AIPL1* into the pDONR/Zeo entry vector. Att sequences are highlighted in green and stop codon is in red.

Primer	Sequence (5'->3')
PROM1-attb1-F - Forward	GGGGACAAGTTTGTACAAAAAAGCAGGCTTC ATGGCCCTCGTACTCGGCTCCCTG
PROM1-attb2-R - Reverse, with stop codon	GGGGACCACTTTGTACAAGAAAGCTGGGTG TCAATGTTGTGATGGGCTTGTC
PROM1-attb2-R - Reverse, without stop codon	GGGGACCACTTTGTACAAGAAAGCTGGGTG ATGTTGTGATGGGCTTGTC

Table 8.6 Gateway compatible primers for cloning of *PROM1* into the pDONR/Zeo entry vector. Att sequences are highlighted in green and stop codon is in red.

Primer	Sequence (5' ->3')
NUB1-attB1-F - Forward	GGGGACAAGTTTGTACAAAAAAGCAGGCTTC ATGGCACAAAAGAAATATCTTCAAG
NUB1-attB2-R - Reverse, with stop codon	GGGGACCACTTTGTACAAGAAAGCTGGGTGTTA GTTTTTCTTTGTTGCTGACTTC
NUB1-attB2-R - Reverse, without stop codon	GGGGACCACTTTGTACAAGAAAGCTGGGTG GTTTTTCTTTGTTGCTGACTTC

Table 8.7 Gateway compatible primers for cloning of *NUB1* into the pDONR/Zeo entry vector. *Att* sequences are highlighted in green and stop codon is in red.

Appendix D. Oligonucleotides for Cloning EYS isoforms 2 and 3

In the study, GFP and 3XFLAG tagged EYS isoforms 2 and 3, and EYS N-terminal (1-1635 aa) fragment were used. Primers used for cloning each of the proteins into the pEGFP-C3 vector are summarised in Table 8.8 whereas Table 8.9 shows primers used for cloning into the p3XFLAG-Myc-CMV vector.

Primer	Restriction site	Sequence (5'->3')
EYS isoform 2 Forward	XhoI	CCCTCGAGATGACTGACAAATCAATCGTC
EYS isoform 2 Reverse	KpnI	GGGGTACCTATTCTTACGATAAATCCCACC
EYS isoform 3 Forward	XhoI	CCCTCGAGATGACTGACAAATCAATCGTC
EYS isoform 3 Reverse	KpnI	GGGGTACCAATGATACATAAATACCTGGG
EYS N-terminal (1-1635 aa) Forward	XhoI	CCCTCGAGATGACTGACAAATCAATCGTC
EYS N-terminal (1-1635 aa) Reverse	KpnI	GGGGTACCACTCTTTTTAGAAGGAAATAAAG

Table 8.8 Summary of primers used for cloning of EYS isoforms 2 and 3 and N-terminal (1-1635 aa) fragment into pEGFP-C3 vector.

Primer	Restriction site	Sequence (5'->3')
EYS isoform 2 Forward	EcoRI	GGAATTCAATGACTGACAAATCAATCGTC
EYS isoform 2 Reverse	KpnI	GGGGTACCTATTCTTACGATAAATCCCACC
EYS isoform 3 Forward	EcoRI	GGAATTCAATGACTGACAAATCAATCGTC
EYS isoform 3 Reverse	KpnI	GGGGTACCAATGATACATAAATACCTGGG
EYS N-terminal (1-1635 aa) Forward	BglIII	CAGATCTGATGACTGACAAATCAATCGTC
EYS N-terminal (1-1635 aa) Reverse	KpnI	GGGGTACCACTCTTTTTAGAAGGAAATAAAG

Table 8.9 Summary of primers used for cloning of EYS isoforms 2 and 3 and N-terminal (1-1635 aa) fragment into p3XFLAG-Myc-CMV vector.

Appendix E. Oligonucleotides Used for RT-PCR Analysis

RT-PCR analysis was performed to examine the expression levels of *EYS* isoforms 2 and 3 in a panel of human tissue derived cDNA samples as well as cell lines. It was also used to check the expression of *PROM1* gene in Y79 cells by amplification of its fragment. Expression of *HPRT* gene was used as a quality control of cDNA samples. The primer pairs are summaries in Table 8.10.

Primer	Sequence (5'->3')
EYS isoform 2 Forward	CCCGAAAATGACTGACAAATC
EYS isoform 2 Reverse	GCCACTAAATCAAACTTATATTC
EYS isoform 3 Forward	CCCGAAAATGACTGACAAATC
EYS isoform 3 Reverse	CTGCTCAAATGATACATAAATACC
PROM1 Forward	ACAGGGAATGGATTGTTGGAG
PROM1 Reverse	GTTCATTCTTAAAGCACTACCCAGA
HPRT Froward	GGGACATAAAAGTAATTGGTG
HPRT Reverse	GCGACCTTGACCATCTTTGG

Table 8.10 Primer pairs used in the RT-PCR analysis throughout the study.

Appendix F. Oligonucleotides Specific for Vectors

Vector specific primers were used to verify the integrity of cloned inserts or, in case of pGADT7-Rec vector, to identify the insert Table 8.11. In case of pBD-GAL4-DEST vector, primers anchored in the insert were used to verify the frame and the integrity of cloned insert; hence they are not listed here.

Vector	Primer	Sequence (5'->3')
pDONR/Zeo	M13 Forward	GTAAACGACGGCCAG
	M13 Reverse	CAGGAAACAGCTATGAC
pGADT7-Rec	MATCHMAKER 5' AD LD-Insert Screening Amplimer	CTATTCGATGATGAAGATACCCCACCAAACCC
	MATCHMAKER 3' AD LD-Insert Screening Amplimer	GTGAACTTGCGGGGTTTTTCAGTATCTACGATT
	T7 Sequencing Primer	TAATACGACTCACTATAGGGC
	3' AD Sequencing Primer	AGATGGTGCACGATGCACAG
pAD-GAL4-DEST	pAD-GAL4-DEST Reverse	AAACCACTGTCACCTGGTTGG
	pAD-GAL4-DEST Forward	GTGCACGATGCACAGTTGAAGT

Table 8.11 Summary of vector specific primers used in the study.

Appendix G. Sequences of Preys Identified in Y2H Screen 4

From all of the screens performed in the study, only Y2H screen 4 resulted in identification of preys carrying fragments of gene coding sequences. The outputs of sequencing are summarised in Table 8.12.

Colony number	Identified protein	Sequence
1	Homo sapiens nuclear factor I/A (NFIA)	CAMGAAAGGTWSWCTTCKATACAKACTSACTATCMSSGCRAGYK CCRCCATGGAGTACCCATACGACGTACCAGATTACGCTCATATGG CCATGGAGGCCAGTGAATTCCACCCAAGCAGTGGTATCAACGCAG AGTGGCCATTATGGCCGGGGGGAGCAGCCAAGGCAAGGTGCAC AACCCATTCCTTCCCACCCCAATGTTGCCACCGCCACCGCCACCAC CGATGGCCAGGCCTGTGCCTCTGCCGGTGCCAGACACAAAGCCTC CAACCACGTCAACAGAAGGAGGTGCAGCCTCCCCCACGTCACCAA CCTACTCGACACCCAGCACCTCCCCCGCAAACCGATTCGTCAGTGT TGGACCACGGGATCCAAGCTTTGTAAATATCCCTCAACAGACACA GTCCTGGTACCTGGGATAAAAGTTGCAGCGTCCCACCATCCACCA GACAAACCACCTGACCCCTTCTCAACTCTGTAACATGGACGCAACC TCAACCCAGCGCAGTTACAACTTCACTATCAGCGGAAGGGGAGAA AAACCGATTCAAATCAACTTGTACATGGAAACAGCAAGCATTATG GTCAAACAGCAAGGCCATAACCTTTTGGGATTTTTTTTTTTTTAAA AWAYTTTAGGRACKGTKGWAWTTTCTCAWAKGGKGCTGRAAAK GGTTGGSCTTTGWAACATTTGAAGTGTTTCCAKGGWAGCGTGAG MATWAGGTRACGTGGCTAGCGRAGRACWACCCTTGCTCACTGA YTTCCTGTTGWAACACACTTTTCYTTACGRAGCCTGGCTGTTTCAM AGTATTTTCATGAATTTTACCCACACAGGTGTGATCCTCCTTTGAG CATTGAGGAGGCACATGCARAACTAAATCTTTTGTAGTAGCTGAR ATCTGCAAWATATAACGGGACAGTCAAAGGCAATGTTTTTTCTGT AAMAWATTGAAAAAAAAAAATGCAGTTAWATCCTTTTTTATTTG TCATTAAGTTTGTTTTGGTCAGCAGTCAGCAGTTAAGTWATATAA AMATGGACCCGCAAGAMAATGAAATCCACTCAMATGGCARAAC CATTCGAAAATGCAAACTACTACTACTAACGCTCAGTCTTTAAAGT TGAATGCTGCMACTTAAMATA
2	Homo sapiens small EDRK-rich factor 2 (SERF2)	AAATAAAAGGAGWCTTTATACGACTCACTATAGGGCGAGCGCCG CCATGGAGTACCCATACGACGTACCAGATTACGCTCATATGGCCA TGGAGGCCAGTGAATTCCACCCAAGCAGTGGTATCAACGCAGAG TGGCCATTATGGCCGGGGAAGGAGGAACCCAAGTGGCTTTGTGG CTTCGTGTCCAACCCTCATGCCCTTCGCCTGTGTGCCTGGAGCCAG TCCCACCACGCTCGCGTTTCCTCCTGTAGTGCTCACAGGTCCCAGC ACCGATGGCATTCCCTTTGCCCTGAGTCTGCAGCGGGTCCCTTTTG TGCTTCCTTCCCCTCAGGTAGCCTCTCTCCCCCTGGGCCACTCCCG GGGGTGAGGGGGTTACCCCTTCCCAGTGTTTTTTATTCCTGTGGG GCTCACCCCAAAGTATTAAAAGTAGCTTTGTAATACAAAAAAAAA AAAAAAAAAAAAAAAAAAAMMYYYYSSSCCCKCCCSSKCYYWWRR GWGGGGGKWWYMWWWSSGRWWYWCWWMRKYYYMRRYYY MMAAWWAAWYCMAAAWMMMRSAAAMMCCCCSYKTTYWM MCA

4	Homo sapiens eukaryotic translation initiation factor 3, subunit L (EIF3L)	AAAGSAAGGRGWCTTTAATACGACTCACTATAGGGCGAGCGCCR CCATGGAGTACCCATACGACGTACCAGATTACGCTCATATGGCCA TGGAGGCCAGTGAATTCCACCCAAGCAGTGGTATCAACGCAGAG TGGCCATTATGGCCGGTGAGCAGATGCATGCGCTGCTGGCCATTG CCCTCACGATGTACCCCATGCGTATCGATGAGAGCATTCACCTCCA GCTGCGGGAGAAATATGGGGACAAGATGTTGCGCATGCAGAAAG GTGACCCACAAGTCTATGAAGAACTTTTCAGTTACTCCTGCCCCAA GTTCCTGTCGCCTGTAGTGCCCAACTATGATAATGTGCACCCCAAC TACCACAAAGAGCCCTTCCTGCAGCAGCTGAAGGTGTTTTCTGAT GAAGTACAGCAGCAGGCCCAGCTTTCAACCATCCGCAGCTTCCTG AAGCTCTACACCACCATGCCTGTGGCCAAGCTGGCTGGCTTCCTG GACCTCACAGAGCAGGAGTTCCGGATCCAGCTTCTTGTCTTCAAA CACAAGATGAAGAACCTCGTGTGGACCAGCGGTATCTCAGCCCTG GATGGTGAATTTCAGTCAGCCTCAGAGGTTGACTTCTACATTGAT AAGGACATGATCCACATCGCGGACACCAAGGTCGCCAGGCGTTAT GGGGATTTCTTCATCCGTCAGATCCACAAATTTGAGGAGCTTAATC GAACCCTGAAGAAGATGGGACAGAGACCTTGATGATATTCACAC ACATTCAGGAACCTGTTTTGATGTATTATAGGCAGGAAGTGTTTTT GCTACCGTGAAACCTTTACCTAGATCAGCCATCAGCCTGTCAACTC AGTTAACAAGTTAACGACCGAAGTGTTTCAAGTGGATCTCAGTAA GGATCTTGGAGCCTACTMACAAACAAARAAAAGAGACYTGTKCG GCGCTGGCTTTAAGGKGGCMTCGATCGGATCATCGAGYCARCTG CTAATGATCGTAAATWCGAAACGTSAGTTCAC
5	Homo sapiens eukaryotic translation initiation factor 3, subunit L (EIF3L)	GSGTAAAAGAGWCTTTATACGACTCACTATAGGGCGAGCGCCRC CATGGAGTACCCATACGACGTACCAGATTACGCTCATATGGCCAT GGAGGCCAGTGAATTCCACCCAAGCAGTGGTATCAACGCAGAGT GGCCATTATGGCCGGTGAGCAGATGCATGCGCTGCTGGCCATTGC CCTCACGATGTACCCCATGCGTATCGATGAGAGCATTCACCTCCA GCTGCGGGAGAAATATGGGGACAAGATGTTGCGCATGCAGAAAG GTGACCCACAAGTCTATGAAGAACTTTTCAGTTACTCCTGCCCCAA GTTCCTGTCGCCTGTAGTGCCCAACTATGATAATGTGCACCCCAAC TACCACAAAGAGCCCTTCCTGCAGCAGCTGAAGGTGTTTTCTGAT GAAGTACAGCAGCAGGCCCAGCTTTCAACCATCCGCAGCTTCCTG AAGCTCTACACCACCATGCCTGTGGCCAAGCTGGCTGGCTTCCTG GACCTCACAGAGCAGGAGTTCCGGATCCAGCTTCTTGTCTTCAAA CACAAGATGAAGAACCTCGTGTGGACCAGCGGTATCTCAGCCCTG GATGGTGAATTTCAGTCAGCCTCAGAGGTTGACTTCTACATTGAT AAGGACATGATCCACATCGCGGACACCAAGGTCGCCAGGCGTTAT GGGGATTTCTTCATCCGTCAGATCCACAAATTTGAGGAGCTTAATC GAACCCTGAAGAAGATGGGACAGAGACCTTGATGATATTCACAC ACATTCAGGAACCTGTTTTGATGTATTATAGGCAGGAAGTGTTTTT GCTACCGTGAAACCTTTACCTAGATCAGCCATCAGCCTGTCAACTC AGTTAACAAGTTAAGGACCGAAGTGTTTCAAGTGGATCTCAGTAA AGGATCTTTGGAGCCTACAAACAAAAAGAAAAACYKKGKCGGSGC TGGCTTWRAGRGGGKTGGCWYCGATWCGGGATYCCTCYCGRRYT CRRAGYTGCAAAWGAATCSKAAAATCCGGAATCGCCCSCKTCTAT TTTWTYYC

9	Homo sapiens nuclear factor I/A (NFIA)	AMAMAAGTWRWCTTCTGATACAKACTSACTATCMSSAGCRAGYK CACGCCATGGAGTACCCATACGACGTACCAGATTACGCTCATATG GCCATGGAGGCCAGTGAATTCCACCCAAGCAGTGGTATCAACGCA RAGTGGCCATTATGGCCGGGGGGAGCAGCCAAGGCAAGGTGCA CAACCCATTCCTTCCCACCCCAATGTTGCCACCGCCACCGCCACCA CCGATGGCCAGGCCTGTGCCTCTGCCGGTGCCAGACACAAAGCCT CCAACCACGTCAACAGAAGGAGGTGCAGCCTCCCCCACGTCACCA ACCTACTCGACACCCAGCACCTCCCCCGCAAACCGATTCGTCAGTG TTGGACCACGGGATCCAAGCTTTGTAAATATCCCTCAACAGACAC AGTCCTGGTACCTGGGATAAAAGTTGCAGCGTCCCACCATCCACC AGACAAACCACCTGACCCCTTCTCAACTCTGTAACATGGACGCAAC CTCAACCCAGCGCAGTTACAACTTCACTATCAGCGGAAGGGGAGA AAAACCGATTCAAATCAACTTGTACATGGAAACAGCAAGCATTAT GGTCAAACAGCAAAGGCCATAACCTTTTGGGATTTTTTTTTTTTWA AAATAYTTWAGGRACKGTKGWAWTTYCYCATAKGGKGCKGRAAA KGGTKGGSCTTKGWAACATTTGAAGKGTTYCCAKGGTASCGKGAG CATWAGGTRACGTGGCTAGCGRAGAACWACCCTKGCTCACKGAC TYCYKGTTGTAACACACTTTCCTTACGGAGCCTGGCTGTTTCACAG TATTTCATGAATTTACCCACACAGGTGTGATCCTCCTTGAGCATTG AGGAGGCACATGAGAACTAAATCTTTTGTAGTAGCTGAGATCTGC AATATAWAACGGGACAGTCAAAGGGCAATGTTTTTTTCTGTAAM ATATTGAAAAARAAAAATGCAGTAWATCCTTTTTTATTGTTCCATT AGTTTGTTGGTCAGCAGTCAGCAGTAGTAWAWAACATGGCCCCG CAGACATGATCCACTCMATGCTGACATCGAAATGGCACTACTACT MTACGTTCAGTTTCSCACAAGCCTTGGAAGTGCTGCACTTACAT
11	Homo sapiens aryl hydrocarbon receptor interacting protein-like 1 (AIPL1)	CCATAAAGGAGWCTTTATACGACTCACTATAGGGCGAGCGCCRC CATGGAGTACCCATACGACGTACCAGATTACGCTCATATGGCCAT GGAGGCCAGTGAATTCCACCCAAGCAGTGGTATCAACGCAGAGT GGCCATTATGGCCGGGAGGCCAAGGCGGACCTCCAGAAAGTGCT GGAGCTGGAGCCGTCCATGCAGAAGGCGGTGCGCAGGGAGCTG AGGCTGCTGGAGAACCGCATGGCGGARAAGCAGGAGGAGGAGC GGCTGCGCTGCCGGAACATGCTGAGCCAGGGTGCCACGCAGCCT CCCGCAGAGCCACCCACAGAGCCACCCGCACAGTCATCCACAGAG CCACCTGCAGAGCCACCCACAGCACCATCTGCAGAGCTGTCCGCA GGGCCCCCTGCAGAGCCAGCCACAGAGCCACCCCCGTCCCCAGG GCACTCGCTGCAGCACTGAGCCCCCTGAGGCCCACAGCCACCCAG GCAGGGAGCAAGTGGCCTGGTCACTTCTGGTTCGATTGACCAGG ATCGTGGTGTCACTTTTTAAAATTTAAAATTAATTTTTGAAATCAA AGTCAGACACACCCATGGTAAAAAAAAAAAAAAAAAAAAAAAA AAMWSKKYYSSGSSSYYYSGSCYTYKRRRGGGTGGSWMYRRWYM SGGRYYCCYYSRMSCYRGRYSKGMAAAWRAYYKWAAAWYKSGRA AAACCAMMATTTTKTTMYMAAAAG

12	Homo sapiens nuclear factor I/A (NFIA)	TYSRKTRTWSTWCTYKATACAKACYSAMTATCMSSGCWAAGYKM YRSCATGGAGTACCCATACGACGTACCAGATTACGCTCATATGGCC MYGGAGGCCAGTGAATTCCACCCAAGCAGTGGTATCAACGCAGA GTGGCCATTATGGCCGGGGGGAGCAGCCAAGGCAAGGTGCACA ACCCATTCCTTCCCACCCCAATGTTGCCACCGCCACCGCCACCACC GATGGCCAGGCCTGTGCCTCTGCCGGTGCCAGACACAAAGCCTCC AACCACGTCAACAGAAGGAGGTGCARCCYCCCCCMMSKYMMCC AACCTACTCGACACCCAGCACCTCCCCCGCAAACCGATTCGTCAGT GTTGGACCACGGGATCCAAGCTTTGTAAATATCCCTCAACAGACA CAGTCCTGGTACCTGGGAWAAAAGTTGCAGCGTCCCACCATCCA CCAGACAAACCACCTGACCCCTTCTCAACTCTGTAACATGGACGCA ACCTCAACCCAGCGCAGTTACAACTTCACTATCAGCGGAAGGGGA RAAAAACCGATTCAAATCAACTTGTACATGGAAACAGCAAGCATT ATGGTCAAACAGCAAGGGCCATAACCCTTTGGGATTTTTTTTTTTT TTTTAAAAATACTTAGGGAMCKGKTTGTAAATTTTCTCATATGGTG CTGGAAAATGGKTTGGGGCCTTTGTAMMATTTGGAAGTGTTTCC ATGGTAGCGTGAGCATTAAGTGARCGTGCCTAGCGGGAGGACTA CCCTTGCTCACTGACTTCCTGTTGTACACACTTTCTACGAGACCTG GCTGTTCACAGTATTCATGATTTACCCMCAAGGKTGAATCCTCCTG ACATTGAGAGCACATGGAAACTTAGTCTTTGATAGCTGGAATTCG CATATASCGGACGTCAAGGCCAGTTTCGWACATGAG
15	Palmitoyl-protein thioesterase 2 (PPT2)	TAAGAAAGAGWCTTTATACGACTCACTATAGGGCGAGCGCCGCC ATGGAGTACCCATACGACGTACCAGATTACGCTCATATGGCCATG GAGGCCAGTGAATTCCACCCAAGCAGTGGTATCAACGCAGAGTG GCCATTATGGCCGGGCACAGGCACACCAAAGCCTGACATCTGCTT TCCAAGGCCACCACTTGGTCTCTGGACCGAGGAGTTCCTGGGGAC CCCTGAATATATCCTCAGGAGAGCCAAGGTTCAATGCAGGTCTCA TAAAGGGTACGGTTGGAGTGCCAGGCTGTGTGGGARATACCGGC CATTGGACACCTCACTATGACCCCCCGGGCCAATAGAGTCTTCAA CCCAAAAGAATCCCGCAGATAAACCTTCAAGGTGGTCGAAGGGG CGTGGAAGCATGGAAGAGAGACACAAGGAGAGACAAAGTGAGT TACTGCTGGGATCCTGGACCTCCTCCCCACAGGGTGAACCCTTCA GCTCAGGAGTCACAGAGAGGGCTCTGGAATAAGGTGGGACAGT GGCTAGAAGGGGAAGTAATCCCAGGGGGCTCACCAGTTGCTCCT CCATCTCCAGGAMGGTCTCATTTGCATCATAGAAACCAAAGAAGC TACAAAGAGATTGGGGGGGARGTTATCAGAAGAGCTGGAGAAA ATCTGGCCGGGCGCAGTGGCACACGCCTGTAATTGCAGCACTTTG GGAGGCCAAGGAGGGCAAATCACCTGAGCCAGAGTTCAAGACCA GCCTGACCAAAATGGTGAACCCCATCTCTACTAAAATACAAAATTA GCTGGGCATGGTGGCAGATGCCTGCAGCCCAGCTACCCAGAGCT GAAGCAGATATTACTTGACCAGAGGGKKGGAAGTTGCATTGAGT CGAGATCGCACCACTGCACTCAGCTGGTGACGAGCGGACYCATCT CAAAGAAGAAGGAKAGCAASAACAMATAAAAACCTGTSGCCSCT CSCCTTTAARGGKGCATCGATCCGGATCMTCGAGCCTCGACTGCA GAKATCTGCATCGAACGACGTYAATGTACGG

16	Homo sapiens fibulin 1 (FBLN1)	AATAYAGAGWCTTTATACGACTCACTATAGGGCGAGCGCCGCCA TGGAGTACCCATACGACGTACCAGATTACGCTCATATGGCCATGG AGGCCAGTGAATTCCACCCAAGCAGTGGTATCAACGCAGAGTGG CCATTATGGCCGGGGGAAGGTGAGCCCCCACAGTGGGGTGGTGG CCCTCACCAAGCCTGTCCCCGAGCCCAGGGACTTGCTCCTGACCG TCAAGATGGATCTCTCTCGCCACGGCACCGTCAGCTCCTTTGTGGC CAAGCTTTTCATCTTTGTGTCTGCAGAGCTCTGAGCACTCGCTTCG CGTCGCGGGGTCTCCCTCCTGTTGCTTTCCTAACCCTGCCCTCCGG GGCGTTAATAAAGTCTTAGCAAGCGTCCCACACAGCGAAAAAAAA AAAAAAAAAAAAAAAAAAMYKKYSSSSCSSKYYSSSYYYYKRRRGG GGGGSWWYMRWWSSGRRWWCYYYSRRKYYMRRYYKSMAAW WRAWYSRAAAWWYSWRAAAAMCCSCSGGTSYMMMAAA
19	Homo sapiens small EDRK-rich factor 2 (SERF2)	AAGAAAGAGWCTTTATACGACTCACTATAGGGCGAGCGCCGCCA TGGAGTACCCATACGACGTACCAGATTACGCTCATATGGCCATGG AGGCCAGTGAATTCCACCCAAGCAGTGGTATCAACGCAGAGTGG CCATTATGGCCGGGGAAGGAGGAACCCAAGTGGCTTTGTGGCTT CGTGTCCAACCCTCATGCCCTTCGCCTGTGTGCCTGGAGCCAGTCC CACCACGCTCGCGTTTCCTCCTGTAGTGCTCACAGGTCCCAGCACC GATGGCATTCCCTTTGCCCTGAGTCTGCAGCGGGTCCCTTTTGTGC TTCCTTCCCCTCAGGTAGCCTCTCTCCCCCTGGGCCACTCCCGGGG GTGAGGGGGTTACCCCTTCCCAGTGTTTTTTATTCCTGTGGGGCTC ACCCCAAAGTATTAAAAGTAGCTTTGTAATACAAAAAAAAAAAAA AAAAAAAAAAAAAAMYYKYYSSSSCCKCCYSSKYYYYWRRRWGGG GGKWWMMWWYSSGRWWCCYYWMRKKYYRRMYYKMSAWWR RAWYYWAAWMMSSWRAACAMCCCSSGGTTTTYMMCAAA
22	Homo sapiens eukaryotic translation initiation factor 3	TSARAAGAGWCTTTATACGACTSACTATAGGGCGAGCGCCRCCTG GAGTACCCATACGACGTACCAGATTACGCTCATATGGCCATGGAG GCCAGTGAATTCCACCCAAGCAGTGGTATCAACGCAGAGTGGCCA TTATGGCCGGTGAGCAGATGCATGCGCTGCTGGCCATTGCCCTCA CGATGTACCCCATGCGTATCGATGARAGCATTCACCTCCAGCTGC GGGAGAAATATGGGGACAAGATGTTGCGCATGCAGAAAGGTGA CCCACAAGTCTATGAAGAAMTTTTCAGTTACTCCTGCCCCAAGTTC CTGTCGCCTGTAGTGCCCAACTATGATAATGTGCACCCCAACTACC ACAAAGAGCCCTTCCTGCAGCAGCTGAAGGTGTTTTCTGATGAAG TACAGCAGCAGGCCCAGCTTTCAACCATCCGCAGCTTCCTGAAGC TCTACACCACCATGCCTGTGGCCAAGCTGGCTGGCTTCCTGGACCT CACAGAGCAGGAGTTCCGGATCCAGCTTCTTGTCTTCAAACACAA GATGAAGAACCTCGTGTGGACCAGCGGTATCTCAGCCCTGGATG GKGAATTTCAGTCAGCCYCAGARGGTTGACTTCTACATTGATAAG ACATGATCCACATCGCGGACACCAAGGTCGCCAGGCGTWTTKGG GGRAWTTCTTCATCCGTCARATCCACAAATTTGGAGGGAGCTTAA TCGAAACCCTGAAGAAGATGGACAGAGACCCTTGATGATATTCAC ACACATTCAGAACTGGTTTTGATGTATATAGGCAGAAGKGKTTTTT TGCYTACCGKGAACCTTACCTARATCAGCCATCAGCTGTCAACTCA GTACAGTATGACCGAGTGTTCAGTGAATCTCAGTAAGGATCTTGA GCCTAAAAAAAAAARAAAAAACTGCGCACTCGCYCTAAGGTGGG CTGTACGAATCACTGGTCGACGYAGAKATCTGGATCAGACACGCT ATATTAAWGGRAG

24	Homo sapiens ubiquitin A-52 residue ribosomal protein fusion product 1 (UBA52)	TCSGCAAGTGSWCTTTATACKACTCACTATAGGGCGAGCGCCRCC ATGGAGTACCCATACGACGTACCAGATTACGCTCATATGGCCATG GAGGCCAGTGAATTCCACCCAAGCAGTGGTATCAACGCARAGTG GCCATTATGGCCGGGAGGTGGCATTATTGAGCCTTCTCTCCGCCA GCTTGCCCARAAATACAACTGCGACAAGATGATCTGCCGCAAGTG CTATGCTCGCCTTCACCCTCGTGCTGTCAACTGCCGCAAGAAGAA GTGTGGTCACACCAACAACCTGCGTCCCAAGAAGAAGGTCAAATA AGGTTGTTCTTTCCTTGAAGGGCAGCCTCCTGCCCAGGCCCCGTG GCCCTGGAGCCTCAATAAAGTGTCCCTTTCATTGACTGGAAAAAA AAAAAAAAAAAAAAAAAAAAAAAYKKKSSSSSSSSKYYSSSYYYWWR RRGGGGGGSWMWMMWWSSGRWMYCYMYSMKYYKMRSKYKS MAWWKRAWYSWAAAWYKSWRAAAMCCSSSGGKKKTTTYMAA AA
26	Homo sapiens cytochrome c oxidase subunit VIIc (COX7C), nuclear gene encoding mitochondrial protein	TAAGAAGAGWCTTTATACGACTCACTATAGGGCGAGCGCCGCCA TGGAGTACCCATACGACGTACCAGATTACGCTCATATGGCCATGG AGGCCAGTGAATTCCACCCAAGCAGTGGTATCAACGCARAGTGG CCATTATGGCCGGGGAAGGTCGTGAAAAAAAAGGTCTTGGTGAG GTGCCGCCATTTCATCTGTCCTCATTCTCTGCGCCTTTCGCARAGCT TCCAGCAGCGGTATGTTGGGCCAGAGCATCCGGAGGTTCACAAC CTCTGTGGTCCGTAGGAGCCACTATGAGGAGGGCCCTGGGAAGA ATTTACCATTTTCAGTGGAAAACAAGTGGTCGTTACTAGCTAAGAT GTGTTTGTACTTTGGATCTGCATTTGCTACACCCTTCCTTGTAGTAA GACACCAACTGCTTAAAACATAAGGATGTTTCAGTTCCTCCATTTA ACAGATATGAAGAGCATTTTAAGAGGTGCAGCCTCTGGAAGTGG ATCAAACTAGAACTCATATGCCATACTAGATATGTTCGTCAATAAA CTTATGACGTGAAAAAAAAAAAAAAAAAAAAAAAAAAAAAAAA AARRRAAAAAAAAAAAAAAAAAAAAMYYYYTTYSSSSSSKKKKKKK YYYWARRRWGGGGGYWMWWAWMSGGRWYCCCYYSRSYYSRR YKYKRAAAAAAMYYMAAYAYWMSRAAAMCGGKTTTTTWWWYA CAAA

Table 8.12 Summary of coding sequences identified in Y2H screen 4. The sequencing outputs include the whole sequence identified using the pGADT7-Rec vector specific primers.

Appendix H. Summary of Preys Carrying Non-coding Sequences

The preys carrying non-coding sequences identified in Y2H screening are summarised in Table 8.13.

Y2H screen 4, bait 3	
Colony number	**Prey identified**
3	Homo sapiens cDNA FLJ46255 fis,
6	Homo sapiens solute carrier organic anion transporter family, member 5A1 (SLCO5A1)
7	Homo sapiens ADP-ribosylation factor 1 (ARF1), transcript variant 2
8	Homo sapiens ADP-ribosylation factor 1 (ARF1), transcript variant 2
10	Homo sapiens spleen focus forming virus (SFFV) proviral integration oncogene spi1 (SPI1), transcript variant 1
13	unidentified sequence
14	Homo sapiens carboxylesterase 2 (CES2), transcript variant 1
17	Homo sapiens kinesin family member 1A (KIF1A), transcript variant 2
18	unidentified sequence
20	unidentified sequence - prey fragment smaller than 200 bp
21	Homo sapiens ADP-ribosylation factor 1
23	unidentified sequence - prey fragment smaller than 200 bp
25	unidentified sequence
27	unidentified sequence
28	unidentified sequence
Y2H screen 5, bait 6	
Colony number	**Prey identified**
1	Homo sapiens heterogeneous nuclear ribonucleoprotein A0 (HNRNPA0)
2	Homo sapiens mitofusin 2 (MFN2), nuclear gene encoding mitochondrial protein
3	Homo sapiens latent transforming growth factor beta binding protein 2 (LTBP2)
Y2H screen 6, bait 8	
Colony number	**Prey identified**
1	Homo sapiens MSTP112 (MST112)
2	Homo sapiens spleen focus forming virus (SFFV) proviral integration oncogene spi1 (SPI1)
3	Homo sapiens solute carrier family 38, member 3 (SLC38A3)
4	Homo sapiens chromosome 19 clone CTB-189B5,
5	unidentified sequence
6	Homo sapiens mRNA; cDNA DKFZp434J194 (from clone DKFZp434J194).
7	Homo sapiens macrophage erythroblast attacher (MAEA), transcript variant 1
8	Homo sapiens neurobeachin (NBEA), transcript variant 1

9	Homo sapiens kinesin family member 1A (KIF1A), transcript variant 2
Y2H screen 7, bait 7	
Colony number	**Prey identified**
1	Homo sapiens MAU2 chromatid cohesion factor homolog (C. elegans) (MAU2)

Table 8.13 Summary of preys carrying intronic sequences identified in Y2H.

Appendix I. Characterisation of Anti-EYS1 and Anti-EYS3 Antibodies

Anti-EYS1 rabbit antibody was a custom made antibody acquired by Bhattacharya laboratory. It was raised against an epitope that was common for all four EYS isoforms. As it was described in the chapter devoted to characterisation of EYS, the antibody is capable of detecting EYS isoforms 1 and 4 in the extracts from Y79 cells. To test if it as well able to detect EYS isoforms 2 and 3, immunoblotting was performed on protein extracts containing overexpressed 3XFLAG constructs. As a positive control, 3XFLAG-VAX2 was used whereas the negative control was extract from untransfected HeLa cells. As shown in Figure 8.1, anti-EYS1 antibody was unable to detect EYS isoforms 2 and 3. The bands detected by anti-EYS1 antibody have the same pattern in all of the lanes and they were most likely non-specifically detected by either primary or secondary antibodies.

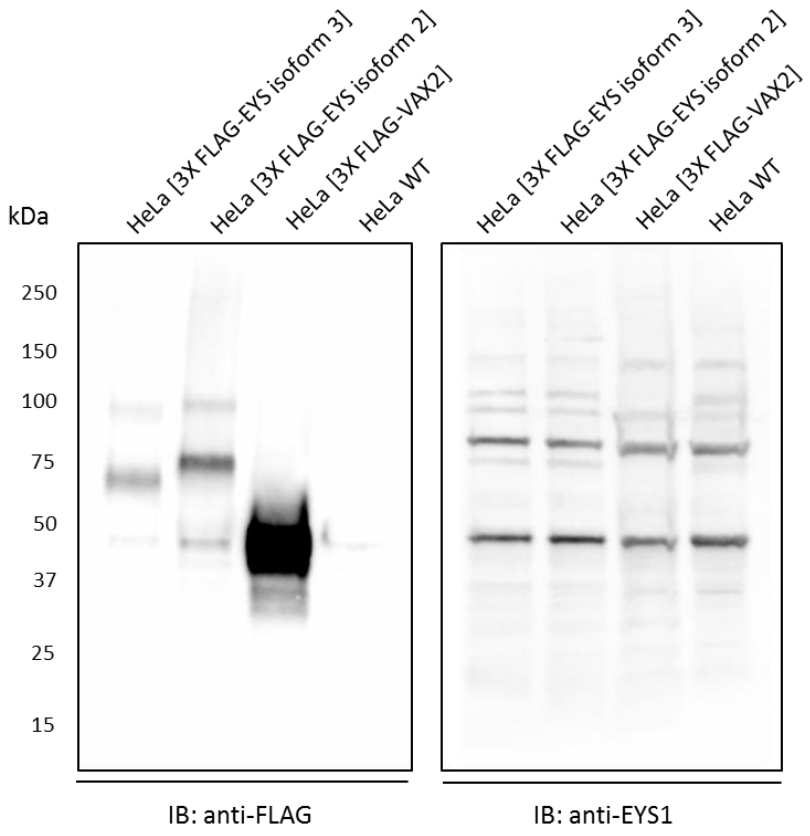

Figure 8.1 Immunoblotting testing whether anti-EYS1 antibody can detect EYS isoforms 2 and 3. The blot on the left was probed with anti-FLAG mouse antibody whereas the blot on the right was probed with anti-EYS1 rabbit antibody. Secondary antibodies used were HRP conjugated anti-mouse and anti-rabbit antibodies. Precision Plus Protein standard was used to assess the band size. BCA assay was used to normalise loading. Expected protein sizes: 3xFLAG-EYS isoform 2 – ~72 kDa, 3xFLAG-EYS isoform 3 – ~69 kDa, 3XFLAG-VAX2 - ~ 40 kDa.

The same type of analysis was performed for anti-EYS3 polyclonal goat antibody which was purchased from SantaCruz, USA. The result is presented in Figure 8.2 and it can be concluded that this antibody is unable to detected EYS isoforms 2 and 3 either.

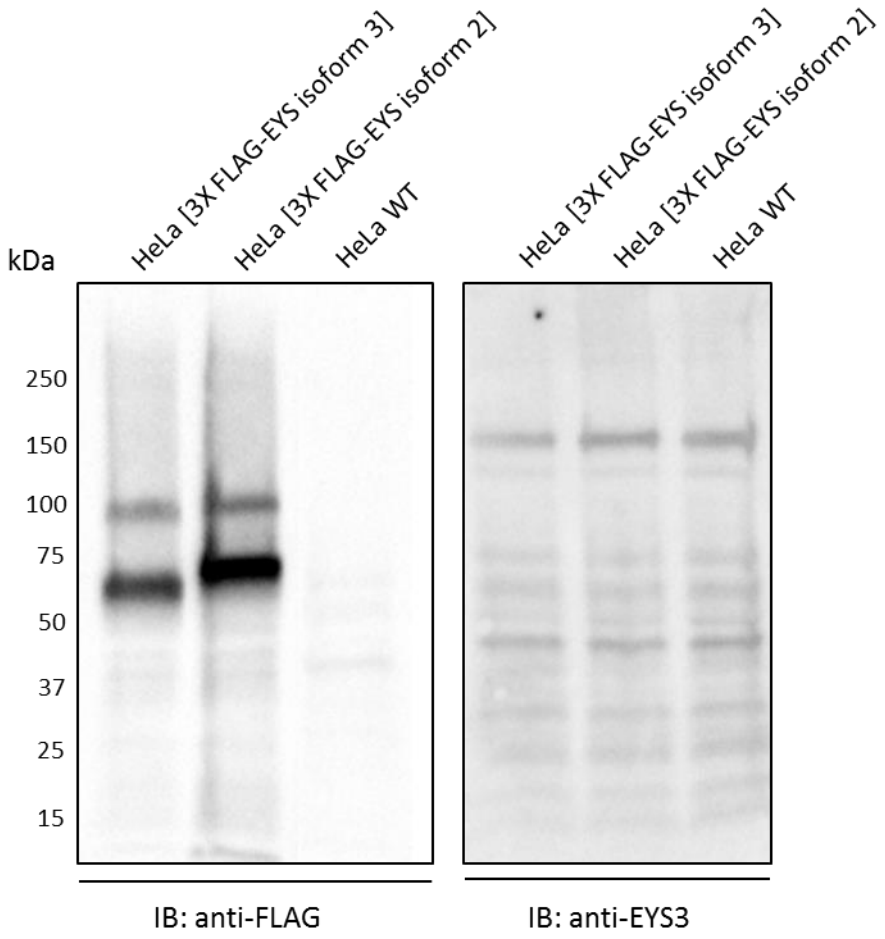

Figure 8.2 Immunoblotting testing whether anti-EYS3 antibody can detect EYS isoforms 2 and 3. The blot on the left was probed with anti-FLAG mouse antibody whereas the blot on the right was probed with anti-EYS3 goat antibody. Secondary antibodies used were HRP conjugated anti-mouse and anti-goat antibodies. Precision Plus Protein standard was used to assess the band size. BCA assay was used to normalise loading. Expected protein sizes: 3xFLAG-EYS isoform 2 – ~72 kDa, 3xFLAG-EYS isoform 3. IB – immunoblotting.

Bibliography

Abd El-Aziz, M. M., Barragan, I., O'Driscoll, C. A., Goodstadt, L., Prigmore, E., Borrego, S., Mena, M., Pieras, J. I., El-Ashry, M. F., Safieh, L. A., Shah, A., Cheetham, M. E., Carter, N. P., Chakarova, C., Ponting, C. P., Bhattacharya, S. S. & Antinolo, G. (2008). EYS, encoding an ortholog of Drosophila spacemaker, is mutated in autosomal recessive retinitis pigmentosa. *Nat Genet* 40, 1285-1287.

Abd El-Aziz, M. M., El-Ashry, M. F., Chan, W. M., Chong, K. L., Barragan, I., Antiñolo, G., Pang, C. P. & Bhattacharya, S. S. (2007). A novel genetic study of Chinese families with autosomal recessive retinitis pigmentosa. *Ann Hum Genet* 71, 281-294.

Abd El-Aziz, M. M., O'Driscoll, C. A., Kaye, R. S., Barragan, I., El-Ashry, M. F., Borrego, S., Antiñolo, G., Pang, C. P., Webster, A. R. & Bhattacharya, S. S. (2010). Identification of novel mutations in the ortholog of Drosophila eyes shut gene (EYS) causing autosomal recessive retinitis pigmentosa. *Invest Ophthalmol Vis Sci* 51, 4266-4272.

Abu-Safieh, L., Alrashed, M., Anazi, S., Alkuraya, H., Khan, A. O., Al-Owain, M., Al-Zahrani, J., Al-Abdi, L., Hashem, M., Al-Tarimi, S., Sebai, M. A., Shamia, A., Ray-Zack, M. D., Nassan, M., Al-Hassnan, Z. N., Rahbeeni, Z., Waheeb, S., Alkharashi, A., Abboud, E., Al-Hazzaa, S. A. & Alkuraya, F. S. (2013). Autozygome-guided exome sequencing in retinal dystrophy patients reveals pathogenetic mutations and novel candidate disease genes. *Genome Res* 23, 236-247.

Adzhubei, I. A., Schmidt, S., Peshkin, L., Ramensky, V. E., Gerasimova, A., Bork, P., Kondrashov, A. S. & Sunyaev, S. R. (2010). A method and server for predicting damaging missense mutations. *Nat Methods* 7, 248-249.

Akey, D. T., Zhu, X., Dyer, M., Li, A., Sorensen, A., Blackshaw, S., Fukuda-Kamitani, T., Daiger, S. P., Craft, C. M., Kamitani, T. & Sohocki, M. M. (2002). The inherited blindness associated protein AIPL1 interacts with the cell cycle regulator protein NUB1. *Hum Mol Genet* 11, 2723-2733.

Arai, Y., Maeda, A., Hirami, Y., Ishigami, C., Kosugi, S., Mandai, M., Kurimoto, Y. & Takahashi, M. (2015). Retinitis Pigmentosa with EYS Mutations Is the Most

Prevalent Inherited Retinal Dystrophy in Japanese Populations. *J Ophthalmol* 2015, 819760.

Athanasiou, D., Aguilà, M., Bevilacqua, D., Novoselov, S. S., Parfitt, D. A. & Cheetham, M. E. (2013). The cell stress machinery and retinal degeneration. *FEBS Letters* 587, 2008-2017.

Audo, I., Sahel, J. A., Mohand-Saïd, S., Lancelot, M. E., Antonio, A., Moskova-Doumanova, V., Nandrot, E. F., Doumanov, J., Barragan, I., Antinolo, G., Bhattacharya, S. S. & Zeitz, C. (2010). EYS is a major gene for rod-cone dystrophies in France. *Hum Mutat* 31, E1406-1435.

Bandah-Rozenfeld, D., Littink, K. W., Ben-Yosef, T., Strom, T. M., Chowers, I., Collin, R. W., den Hollander, A. I., van den Born, L. I., Zonneveld, M. N., Merin, S., Banin, E., Cremers, F. P. & Sharon, D. (2010). Novel null mutations in the EYS gene are a frequent cause of autosomal recessive retinitis pigmentosa in the Israeli population. In *Invest Ophthalmol Vis Sci* 51, pp. 4387-4394. United States.

Barragan, I., Borrego, S., Pieras, J. I., Gonzalez-del Pozo, M., Santoyo, J., Ayuso, C., Baiget, M., Millan, J. M., Mena, M., Abd El-Aziz, M. M., Audo, I., Zeitz, C., Littink, K. W., Dopazo, J., Bhattacharya, S. S. & Antinolo, G. (2010). Mutation spectrum of EYS in Spanish patients with autosomal recessive retinitis pigmentosa. *Hum Mutat* 31, E1772-1800.

Bett, J. S., Kanuga, N., Richet, E., Schmidtke, G., Groettrup, M., Cheetham, M. E. & van der Spuy, J. (2012). The inherited blindness protein AIPL1 regulates the ubiquitin-like FAT10 pathway. *PLoS One* 7, e30866.

Bonilha, V. L., Rayborn, M. E., Bell, B. A., Marino, M. J., Pauer, G. J., Beight, C. D., Chiang, J., Traboulsi, E. I., Hollyfield, J. G. & Hagstrom, S. A. (2015). Histopathological comparison of eyes from patients with autosomal recessive retinitis pigmentosa caused by novel EYS mutations. *Graefes Arch Clin Exp Ophthalmol* 253, 295-305.

Brückner, A., Polge, C., Lentze, N., Auerbach, D. & Schlattner, U. (2009). Yeast two-hybrid, a powerful tool for systems biology. *Int J Mol Sci* 10, 2763-2788.

Burns, M. E. & Pugh, E. N., Jr. (2010). Lessons from photoreceptors: turning off g-protein signaling in living cells. In *Physiology (Bethesda)* 25, pp. 72-84. United States.

Caufield, J. H., Sakhawalkar, N. & Uetz, P. (2012). A comparison and optimization of yeast two-hybrid systems. *Methods* 58, 317-324.

Chen, X., Zhao, K., Sheng, X., Li, Y., Gao, X., Zhang, X., Kang, X., Pan, X., Liu, Y., Jiang, C., Shi, H., Rong, W., Chen, L. J., Lai, T. Y., Wang, X., Yuan, S., Liu, Q., Vollrath, D., Pang, C. P. & Zhao, C. (2013). Targeted sequencing of 179 genes associated with hereditary retinal dystrophies and 10 candidate genes identifies novel and known mutations in patients with various retinal diseases. *Invest Ophthalmol Vis Sci* 54, 2186-2197.

Chizzolini, M., Galan, A., Milan, E., Sebastiani, A., Costagliola, C. & Parmeggiani, F. (2011). Good epidemiologic practice in retinitis pigmentosa: from phenotyping to biobanking. *Curr Genomics* 12, 260-266.

Collin, R. W., Littink, K. W., Klevering, B. J., van den Born, L. I., Koenekoop, R. K., Zonneveld, M. N., Blokland, E. A., Strom, T. M., Hoyng, C. B., den Hollander, A. I. & Cremers, F. P. (2008). Identification of a 2 Mb human ortholog of Drosophila eyes shut/spacemaker that is mutated in patients with retinitis pigmentosa. In *Am J Hum Genet* 83, pp. 594-603. United States.

Cook, B., Hardy, R. W., McConnaughey, W. B. & Zuker, C. S. (2008). Preserving cell shape under environmental stress. *Nature* 452, 361-364.

de Castro, E., Sigrist, C. J., Gattiker, A., Bulliard, V., Langendijk-Genevaux, P. S., Gasteiger, E., Bairoch, A. & Hulo, N. (2006). ScanProsite: detection of PROSITE signature matches and ProRule-associated functional and structural residues in proteins. *Nucleic Acids Res* 34, W362-365.

de Castro-Miró, M., Pomares, E., Lorés-Motta, L., Tonda, R., Dopazo, J., Marfany, G. & Gonzàlez-Duarte, R. (2014). Combined genetic and high-throughput strategies for molecular diagnosis of inherited retinal dystrophies. *PLoS One* 9, e88410.

De Las Rivas, J. & Fontanillo, C. (2010). Protein–Protein Interactions Essentials: Key Concepts to Building and Analyzing Interactome Networks. *PLoS Comput Biol* 6, e1000807.

Duke-Elder, S. S. (1958). The Eye in Evolution. United Kingdom: St. Louis, The C.V. Mosby Company, Henry Kimpton Publishers.

Eisenberger, T., Neuhaus, C., Khan, A. O., Decker, C., Preising, M. N., Friedburg, C., Bieg, A., Gliem, M., Charbel Issa, P., Holz, F. G., Baig, S. M., Hellenbroich, Y., Galvez, A., Platzer, K., Wollnik, B., Laddach, N., Ghaffari, S. R., Rafati, M.,

Botzenhart, E., Tinschert, S., Börger, D., Bohring, A., Schreml, J., Körtge-Jung, S., Schell-Apacik, C., Bakur, K., Al-Aama, J. Y., Neuhann, T., Herkenrath, P., Nürnberg, G., Nürnberg, P., Davis, J. S., Gal, A., Bergmann, C., Lorenz, B. & Bolz, H. J. (2013). Increasing the yield in targeted next-generation sequencing by implicating CNV analysis, non-coding exons and the overall variant load: the example of retinal dystrophies. *PLoS One* 8, e78496.

Fargeas, C. A., Florek, M., Huttner, W. B. & Corbeil, D. (2003). Characterization of prominin-2, a new member of the prominin family of pentaspan membrane glycoproteins. In *J Biol Chem* 278, pp. 8586-8596. United States.

Fargeas, C. A., Huttner, W. B. & Corbeil, D. (2007). Nomenclature of prominin-1 (CD133) splice variants - an update. In *Tissue Antigens*, pp. 602-606. Denmark.

Fields, S. & Song, O. K. (1989). A NOVEL GENETIC SYSTEM TO DETECT PROTEIN PROTEIN INTERACTIONS. *Nature* 340, 245-246.

Forsythe, E. & Beales, P. L. (2013). Bardet-Biedl syndrome. *Eur J Hum Genet* 21, 8-13.

Glöckle, N., Kohl, S., Mohr, J., Scheurenbrand, T., Sprecher, A., Weisschuh, N., Bernd, A., Rudolph, G., Schubach, M., Poloschek, C., Zrenner, E., Biskup, S., Berger, W., Wissinger, B. & Neidhardt, J. (2014). Panel-based next generation sequencing as a reliable and efficient technique to detect mutations in unselected patients with retinal dystrophies. *Eur J Hum Genet* 22, 99-104.

Gonzalez-del Pozo, M., Borrego, S., Barragan, I., Pieras, J. I., Santoyo, J., Matamala, N., Naranjo, B., Dopazo, J. & Antinolo, G. (2011). Mutation screening of multiple genes in Spanish patients with autosomal recessive retinitis pigmentosa by targeted resequencing. In *PLoS One*, p. e27894. United States.

Hamel, C. (2006). Retinitis pigmentosa. *Orphanet J Rare Dis* 1, 40.

Han, Z., Anderson, D. W. & Papermaster, D. S. (2012). Prominin-1 Localizes to the Open Rims of Outer Segment Lamellae in Xenopus laevis Rod and Cone Photoreceptors. *Investigative Ophthalmology & Visual Science* 53, 361-373.

Hartong, D. T., Berson, E. L. & Dryja, T. P. (2006). Retinitis pigmentosa. *Lancet* 368, 1795-1809.

Hidalgo-de-Quintana, J., Evans, R. J., Cheetham, M. E. & van der Spuy, J. (2008). The Leber Congenital Amaurosis Protein AIPL1 Functions as Part of a

Chaperone Heterocomplex. *Investigative ophthalmology & visual science* 49, 2878-2887.

Hidalgo-de-Quintana, J., Schwarz, N., Meschede, I. P., Stern-Schneider, G., Powner, M. B., Morrison, E. E., Futter, C. E., Wolfrum, U., Cheetham, M. E. & van der Spuy, J. (2015). The Leber congenital amaurosis protein AIPL1 and EB proteins co-localize at the photoreceptor cilium. *PLoS One* 10, e0121440.

Hosono, K., Ishigami, C., Takahashi, M., Park, D. H., Hirami, Y., Nakanishi, H., Ueno, S., Yokoi, T., Hikoya, A., Fujita, T., Zhao, Y., Nishina, S., Shin, J. P., Kim, I. T., Yamamoto, S., Azuma, N., Terasaki, H., Sato, M., Kondo, M., Minoshima, S. & Hotta, Y. (2012). Two novel mutations in the EYS gene are possible major causes of autosomal recessive retinitis pigmentosa in the Japanese population. *PLoS One* 7, e31036.

Husain, N., Pellikka, M., Hong, H., Klimentova, T., Choe, K.-M., Clandinin, T. R. & Tepass, U. (2006). The Agrin/Perlecan-Related Protein Eyes Shut Is Essential for Epithelial Lumen Formation in the Drosophila Retina. *Developmental Cell* 11, 483-493.

Isackson, P. J., Ochs-Balcom, H. M., Ma, C., Harley, J. B., Peltier, W., Tarnopolsky, M., Sripathi, N., Wortmann, R. L., Simmons, Z., Wilson, J. D., Smith, S. A., Barboi, A., Fine, E., Baer, A., Baker, S., Kaufman, K., Cobb, B., Kilpatrick, J. R. & Vladutiu, G. D. (2011). Association of common variants in the human eyes shut ortholog (EYS) with statin-induced myopathy: evidence for additional functions of EYS. *Muscle Nerve* 44, 531-538.

Ivanov, A. S., Zgoda, V. G. & Archakov, A. I. (2011). [Protein interactomics technologies]. *Bioorg Khim* 37, 8-21.

Iwanami, M., Oshikawa, M., Nishida, T., Nakadomari, S. & Kato, S. (2012). High prevalence of mutations in the EYS gene in Japanese patients with autosomal recessive retinitis pigmentosa. In *Invest Ophthalmol Vis Sci* 53, pp. 1033-1040. United States.

Jaszai, J., Fargeas, C. A., Florek, M., Huttner, W. B. & Corbeil, D. (2007). Focus on molecules: prominin-1 (CD133). In *Exp Eye Res* 85, pp. 585-586. England.

Jaszai, J., Fargeas, C. A., Graupner, S., Tanaka, E. M., Brand, M., Huttner, W. B. & Corbeil, D. (2011). Distinct and conserved prominin-1/CD133-positive retinal cell populations identified across species. *PLoS One* 6, e17590.

Jayakody, S. A., Gonzalez-Cordero, A., Ali, R. R. & Pearson, R. A. (2015). Cellular strategies for retinal repair by photoreceptor replacement. *Progress in Retinal and Eye Research* 46, 31-66.

Jin, Z.-B., Okamoto, S., Osakada, F., Homma, K., Assawachananont, J., Hirami, Y., Iwata, T. & Takahashi, M. (2011). Modeling Retinal Degeneration Using Patient-Specific Induced Pluripotent Stem Cells. *PLoS ONE* 6, e17084.

Jinda, W., Taylor, T. D., Suzuki, Y., Thongnoppakhun, W., Limwongse, C., Lertrit, P., Suriyaphol, P., Trinavarat, A. & Atchaneeyasakul, L. O. (2014). Whole exome sequencing in Thai patients with retinitis pigmentosa reveals novel mutations in six genes. *Invest Ophthalmol Vis Sci* 55, 2259-2268.

Kajiwara, K., Berson, E. L. & Dryja, T. P. (1994). Digenic retinitis pigmentosa due to mutations at the unlinked peripherin/RDS and ROM1 loci. *Science* 264, 1604-1608.

Kamitani, T., Kito, K., Fukuda-Kamitani, T. & Yeh, E. T. (2001). Targeting of NEDD8 and its conjugates for proteasomal degradation by NUB1. *J Biol Chem* 276, 46655-46660.

Kandel, E. R., Schwartz, J. H. & Jessell, T. M. (1991). Principles of Neural Science, Third Edition. Center for Neurobiology and Behavior, College of Physicians and Surgeons of Columbia University and The Howard Hughes Medical Institute: Appleton & Lange.

Karman, S. B., Diah, S. Z. & Gebeshuber, I. C. (2012). Bio-inspired polarized skylight-based navigation sensors: a review. *Sensors (Basel)* 12, 14232-14261.

Katagiri, S., Akahori, M., Hayashi, T., Yoshitake, K., Gekka, T., Ikeo, K., Tsuneoka, H. & Iwata, T. (2014). Autosomal recessive cone–rod dystrophy associated with compound heterozygous mutations in the EYS gene. *Documenta Ophthalmologica* 128, 211-217.

Kaufman, P. L. & Alm, A. (2003). Adler's Physiology of the Eye. Third Edition. USA: Mosby.

Keegan, L., Gill, G. & Ptashne, M. (1986). Separation of DNA binding from the transcription-activating function of a eukaryotic regulatory protein. *Science* 231, 699-704.

Kito, K., Yeh, E. T. & Kamitani, T. (2001). NUB1, a NEDD8-interacting protein, is induced by interferon and down-regulates the NEDD8 expression. *J Biol Chem* 276, 20603-20609.

Kolandaivelu, S., Huang, J., Hurley, J. B. & Ramamurthy, V. (2009). AIPL1, a protein associated with childhood blindness, interacts with alpha-subunit of rod phosphodiesterase (PDE6) and is essential for its proper assembly. *J Biol Chem* 284, 30853-30861.

Kolb, H., Fernandez, E. & Nelson, R. (1995). Webvision: The Organization of the Retina and Visual System University of Utah, Health Sciences Center: Internet, Public Domain.

Kyritsis, A., Tsokos, M. & Chader, G. (1984). Attachment culture of human retinoblastoma cells: Long-term culture conditions and effects of dibutyryl cyclic AMP. *Experimental Eye Research* 38, 411-421.

Köberlein, J., Beifus, K., Schaffert, C. & Finger, R. P. (2013). The economic burden of visual impairment and blindness: a systematic review. *BMJ Open* 3, e003471.

Lamba, D. A., Gust, J. & Reh, T. A. (2009). Transplantation of human embryonic stem cell-derived photoreceptors restores some visual function in Crx-deficient mice. *Cell Stem Cell* 4, 73-79.

Li, Q., Lee, J.-A. & Black, D. L. (2007). Neuronal regulation of alternative pre-mRNA splicing. *Nat Rev Neurosci* 8, 819-831.

Littink, K. W., Koenekoop, R. K., van den Born, L. I., Collin, R. W., Moruz, L., Veltman, J. A., Roosing, S., Zonneveld, M. N., Omar, A., Darvish, M., Lopez, I., Kroes, H. Y., van Genderen, M. M., Hoyng, C. B., Rohrschneider, K., van Schooneveld, M. J., Cremers, F. P. & den Hollander, A. I. (2010). Homozygosity mapping in patients with cone-rod dystrophy: novel mutations and clinical characterizations. In *Invest Ophthalmol Vis Sci*, pp. 5943-5951. United States.

Liu, Q., Lyubarsky, A., Skalet, J. H., Pugh, E. N. & Pierce, E. A. (2003). RP1 is required for the correct stacking of outer segment discs. *Invest Ophthalmol Vis Sci* 44, 4171-4183.

Liu, Q., Zhou, J., Daiger, S. P., Farber, D. B., Heckenlively, J. R., Smith, J. E., Sullivan, L. S., Zuo, J., Milam, A. H. & Pierce, E. A. (2002). Identification and subcellular localization of the RP1 protein in human and mouse photoreceptors. *Invest Ophthalmol Vis Sci* 43, 22-32.

Liu, Q., Zuo, J. & Pierce, E. A. (2004a). The retinitis pigmentosa 1 protein is a photoreceptor microtubule-associated protein. *J Neurosci* 24, 6427-6436.

Liu, X., Bulgakov, O. V., Wen, X. H., Woodruff, M. L., Pawlyk, B., Yang, J., Fain, G. L., Sandberg, M. A., Makino, C. L. & Li, T. (2004b). AIPL1, the protein that is defective in Leber congenital amaurosis, is essential for the biosynthesis of retinal rod cGMP phosphodiesterase. *Proc Natl Acad Sci U S A* 101, 13903-13908.

Majumder, A., Gopalakrishna, K. N., Cheguru, P., Gakhar, L. & Artemyev, N. O. (2013). Interaction of aryl hydrocarbon receptor-interacting protein-like 1 with the farnesyl moiety. *J Biol Chem* 288, 21320-21328.

Maw, M. A., Corbeil, D., Koch, J., Hellwig, A., Wilson-Wheeler, J. C., Bridges, R. J., Kumaramanickavel, G., John, S., Nancarrow, D., Röper, K., Weigmann, A., Huttner, W. B. & Denton, M. J. (2000). A frameshift mutation in prominin (mouse)-like 1 causes human retinal degeneration. *Human Molecular Genetics* 9, 27-34.

Millán, J. M., Aller, E., Jaijo, T., Blanco-Kelly, F., Gimenez-Pardo, A. & Ayuso, C. (2011). An update on the genetics of usher syndrome. *J Ophthalmol* 2011, 417217.

Miraglia, S., Godfrey, W., Yin, A. H., Atkins, K., Warnke, R., Holden, J. T., Bray, R. A., Waller, E. K. & Buck, D. W. (1997). A novel five-transmembrane hematopoietic stem cell antigen: isolation, characterization, and molecular cloning. *Blood* 90, 5013-5021.

Mishra, M. & Knust, E. (2013). Analysis of the Drosophila compound eye with light and electron microscopy. *Methods Mol Biol* 935, 161-182.

Moses, K. (2006). Evolutionary biology: fly eyes get the whole picture. In *Nature* 443, pp. 638-639. England.

Nathans, J. (1999). The evolution and physiology of human color vision: insights from molecular genetic studies of visual pigments. In *Neuron*, pp. 299-312. United States.

Ng, P. C. & Henikoff, S. (2002). Accounting for human polymorphisms predicted to affect protein function. *Genome Res* 12, 436-446.

Ngounou Wetie, A. G., Sokolowska, I., Woods, A. G., Roy, U., Deinhardt, K. & Darie, C. C. (2014). Protein-protein interactions: switch from classical methods to proteomics and bioinformatics-based approaches. *Cell Mol Life Sci* 71, 205-228.

Nie, J., Mahato, S., Mustill, W., Tipping, C., Bhattacharya, S. S. & Zelhof, A. C. (2012). Cross species analysis of Prominin reveals a conserved cellular role in invertebrate and vertebrate photoreceptor cells. *Dev Biol* 371, 312-320.

Pearring, J. N., Salinas, R. Y., Baker, S. A. & Arshavsky, V. Y. (2013). Protein sorting, targeting and trafficking in photoreceptor cells. *Prog Retin Eye Res* 36, 24-51.

Permanyer, J., Navarro, R., Friedman, J., Pomares, E., Castro-Navarro, J., Marfany, G., Swaroop, A. & Gonzalez-Duarte, R. (2010). Autosomal recessive retinitis pigmentosa with early macular affectation caused by premature truncation in PROM1. In *Invest Ophthalmol Vis Sci* 51, pp. 2656-2663. United States.

Pierce, E. A., Quinn, T., Meehan, T., McGee, T. L., Berson, E. L. & Dryja, T. P. (1999). Mutations in a gene encoding a new oxygen-regulated photoreceptor protein cause dominant retinitis pigmentosa. *Nat Genet* 22, 248-254.

Pras, E., Abu, A., Rotenstreich, Y., Avni, I., Reish, O., Morad, Y. & Reznik-Wolf, H. (2009). Cone-rod dystrophy and a frameshift mutation in the PROM1 gene. In *Mol Vis* 15, pp. 1709-1716. United States.

Ramamurthy, V., Roberts, M., van den Akker, F., Niemi, G., Reh, T. A. & Hurley, J. B. (2003). AIPL1, a protein implicated in Leber's congenital amaurosis, interacts with and aids in processing of farnesylated proteins. *Proceedings of the National Academy of Sciences* 100, 12630-12635.

Remington, L. A. (2005). *Clinical Anatomy of the Visual System*. USA: Elsevier.

Ridge, K. D., Abdulaev, N. G., Sousa, M. & Palczewski, K. (2003). Phototransduction: crystal clear. In *Trends Biochem Sci* 28, pp. 479-487. England.

Roper, K., Corbeil, D. & Huttner, W. B. (2000). Retention of prominin in microvilli reveals distinct cholesterol-based lipid micro-domains in the apical plasma membrane. *Nat Cell Biol* 2, 582-592.

Ross, C. A. & Akimov, S. S. (2014). Human-induced pluripotent stem cells: potential for neurodegenerative diseases. *Hum Mol Genet* 23, R17-26.

Sahly, I., Dufour, E., Schietroma, C., Michel, V., Bahloul, A., Perfettini, I., Pepermans, E., Estivalet, A., Carette, D., Aghaie, A., Ebermann, I., Lelli, A., Iribarne, M., Hardelin, J.-P., Weil, D., Sahel, J.-A., El-Amraoui, A. & Petit, C. (2012). Localization of Usher 1 proteins to the photoreceptor calyceal processes, which are absent from mice. *The Journal of Cell Biology* 199, 381-399.

Scheufler, C., Brinker, A., Bourenkov, G., Pegoraro, S., Moroder, L., Bartunik, H., Hartl, F. U. & Moarefi, I. (2000). Structure of TPR Domain–Peptide Complexes: Critical Elements in the Assembly of the Hsp70–Hsp90 Multichaperone Machine. *Cell* 101, 199-210.

Schweingruber, C., Rufener, S. C., Zünd, D., Yamashita, A. & Mühlemann, O. (2013). Nonsense-mediated mRNA decay - mechanisms of substrate mRNA recognition and degradation in mammalian cells. *Biochim Biophys Acta* 1829, 612-623.

Shichida, Y. & Matsuyama, T. (2009). Evolution of opsins and phototransduction. *Philosophical Transactions of the Royal Society of London B: Biological Sciences* 364, 2881-2895.

Smith, P. K., Krohn, R. I., Hermanson, G. T., Mallia, A. K., Gartner, F. H., Provenzano, M. D., Fujimoto, E. K., Goeke, N. M., Olson, B. J. & Klenk, D. C. (1985). Measurement of protein using bicinchoninic acid. *Analytical Biochemistry* 150, 76-85.

Sohocki, M. M., Bowne, S. J., Sullivan, L. S., Blackshaw, S., Cepko, C. L., Payne, A. M., Bhattacharya, S. S., Khaliq, S., Qasim Mehdi, S., Birch, D. G., Harrison, W. R., Elder, F. F., Heckenlively, J. R. & Daiger, S. P. (2000). Mutations in a new photoreceptor-pineal gene on 17p cause Leber congenital amaurosis. *Nat Genet* 24, 79-83.

Song, J., Smaoui, N., Ayyagari, R., Stiles, D., Benhamed, S., MacDonald, I. M., Daiger, S. P., Tumminia, S. J., Hejtmancik, F. & Wang, X. (2011). High-throughput retina-array for screening 93 genes involved in inherited retinal dystrophy. In *Invest Ophthalmol Vis Sci* 52, pp. 9053-9060. United States.

Sun, X., Pawlyk, B., Xu, X., Liu, X., Bulgakov, O. V., Adamian, M., Sandberg, M. A., Khani, S. C., Tan, M. H., Smith, A. J., Ali, R. R. & Li, T. (2010). Gene therapy with a promoter targeting both rods and cones rescues retinal degeneration caused by AIPL1 mutations. *Gene Ther* 17, 117-131.

Tan, M. H., Smith, A. J., Pawlyk, B., Xu, X., Liu, X., Bainbridge, J. B., Basche, M., McIntosh, J., Tran, H. V., Nathwani, A., Li, T. & Ali, R. R. (2009). Gene therapy for retinitis pigmentosa and Leber congenital amaurosis caused by defects in AIPL1: effective rescue of mouse models of partial and complete Aipl1 deficiency using AAV2/2 and AAV2/8 vectors. *Hum Mol Genet* 18, 2099-2114.

Taschner, M., Bhogaraju, S. & Lorentzen, E. (2012). Architecture and function of IFT complex proteins in ciliogenesis. *Differentiation* 83, S12-22.

Trapani, I., Colella, P., Sommella, A., Iodice, C., Cesi, G., de Simone, S., Marrocco, E., Rossi, S., Giunti, M., Palfi, A., Farrar, G. J., Polishchuk, R. & Auricchio, A. (2014). Effective delivery of large genes to the retina by dual AAV vectors. *EMBO Mol Med* 6, 194-211.

Tucker, B. A., Mullins, R. F. & Stone, E. M. (2014). Stem cells for investigation and treatment of inherited retinal disease. *Hum Mol Genet* 23, R9-R16.

van der Spuy, J. (2006). Focus on molecules: the aryl hydrocarbon receptor interacting protein-like 1 (AIPL1). *Exp Eye Res* 83, 1307-1308.

van der Spuy, J., Chapple, J. P., Clark, B. J., Luthert, P. J., Sethi, C. S. & Cheetham, M. E. (2002). The Leber congenital amaurosis gene product AIPL1 is localized exclusively in rod photoreceptors of the adult human retina. *Hum Mol Genet* 11, 823-831.

van der Spuy, J. & Cheetham, M. E. (2004). The Leber congenital amaurosis protein AIPL1 modulates the nuclear translocation of NUB1 and suppresses inclusion formation by NUB1 fragments. *J Biol Chem* 279, 48038-48047.

van der Spuy, J., Kim, J. H., Yu, Y. S., Szel, A., Luthert, P. J., Clark, B. J. & Cheetham, M. E. (2003). The expression of the Leber congenital amaurosis protein AIPL1 coincides with rod and cone photoreceptor development. *Invest Ophthalmol Vis Sci* 44, 5396-5403.

Waehler, R., Russell, S. J. & Curiel, D. T. (2007). Engineering targeted viral vectors for gene therapy. *Nat Rev Genet* 8, 573-587.

Wang, F., Wang, H., Tuan, H.-F., Nguyen, D. H., Sun, V., Keser, V., Bowne, S. J., Sullivan, L. S., Luo, H., Zhao, L., Wang, X., Zaneveld, J. E., Salvo, J. S., Siddiqui, S., Mao, L., Wheaton, D. K., Birch, D. G., Branham, K. E., Heckenlively, J. R., Wen, C., Flagg, K., Ferreyra, H., Pei, J., Khan, A., Ren, H., Wang, K., Lopez, I., Qamar, R., Zenteno, J. C., Ayala-Ramirez, R., Beatriz Buentello, V., Fu, Q., Simpson, D. A., Li, Y., Sui, R., Silvestri, G., Daiger, S. P., Koenekoop, R. K., Zhang, K. & Chen, R. (2014). Next generation sequencing-based molecular diagnosis of retinitis pigmentosa: identification of a novel genotype-phenotype correlation and clinical refinements. *Human genetics* 133, 331-345.

Weigmann, A., Corbeil, D., Hellwig, A. & Huttner, W. B. (1997). Prominin, a novel microvilli-specific polytopic membrane protein of the apical surface of epithelial cells, is targeted to plasmalemmal protrusions of non-epithelial cells. *Proc Natl Acad Sci U S A* 94, 12425-12430.

Wright, A. F., Chakarova, C. F., Abd El-Aziz, M. M. & Bhattacharya, S. S. (2010). Photoreceptor degeneration: genetic and mechanistic dissection of a complex trait. *Nat Rev Genet* 11, 273-284.

Xu, Y., Guan, L., Shen, T., Zhang, J., Xiao, X., Jiang, H., Li, S., Yang, J., Jia, X., Yin, Y., Guo, X., Wang, J. & Zhang, Q. (2014). Mutations of 60 known causative genes in 157 families with retinitis pigmentosa based on exome sequencing. *Hum Genet* 133, 1255-1271.

Yang, Z., Chen, Y., Lillo, C., Chien, J., Yu, Z., Michaelides, M., Klein, M., Howes, K. A., Li, Y., Kaminoh, Y., Chen, H., Zhao, C., Al-Sheikh, Y. T., Karan, G., Corbeil, D., Escher, P., Kamaya, S., Li, C., Johnson, S., Frederick, J. M., Zhao, Y., Wang, C., Cameron, D. J., Huttner, W. B., Schorderet, D. F., Munier, F. L., Moore, A. T., Birch, D. G., Baehr, W., Hunt, D. M., Williams, D. S. & Zhang, K. (2008). Mutant prominin 1 found in patients with macular degeneration disrupts photoreceptor disk morphogenesis in mice. *J Clin Invest* 118, 2908-2916.

Yau, K. W. & Hardie, R. C. (2009). Phototransduction motifs and variations. In *Cell* 139, pp. 246-264. United States.

Yu, Y., Flint, A., Dvorin, E. L. & Bischoff, J. (2002). AC133-2, a novel isoform of human AC133 stem cell antigen. *J Biol Chem* 277, 20711-20716.

Yvon, C., Ramsden, C. M., Lane, A., Powner, M. B., da Cruz, L., Coffey, P. J. & Carr, A.-J. F. (2015). Using Stem Cells to Model Diseases of the Outer Retina. *Computational and Structural Biotechnology Journal* 13, 382-389.

Zacchigna, S., Oh, H., Wilsch-Brauninger, M., Missol-Kolka, E., Jaszai, J., Jansen, S., Tanimoto, N., Tonagel, F., Seeliger, M., Huttner, W. B., Corbeil, D., Dewerchin, M., Vinckier, S., Moons, L. & Carmeliet, P. (2009). Loss of the cholesterol-binding protein prominin-1/CD133 causes disk dysmorphogenesis and photoreceptor degeneration. In *J Neurosci* 29, pp. 2297-2308. United States.

Zelhof, A. C., Hardy, R. W., Becker, A. & Zuker, C. S. (2006). Transforming the architecture of compound eyes. In *Nature*, pp. 696-699. England.

Zhang, F. L. & Casey, P. J. (1996). Protein prenylation: molecular mechanisms and functional consequences. *Annu Rev Biochem* 65, 241-269.

Zhang, Q., Zulfiqar, F., Xiao, X., Riazuddin, S. A., Ahmad, Z., Caruso, R., MacDonald, I., Sieving, P., Riazuddin, S. & Hejtmancik, J. F. (2007). Severe retinitis pigmentosa mapped to 4p15 and associated with a novel mutation in the PROM1 gene. *Hum Genet* 122, 293-299.

Zhang, X., Ge, X., Shi, W., Huang, P., Min, Q., Li, M., Yu, X., Wu, Y., Zhao, G., Tong, Y., Jin, Z. B., Qu, J. & Gu, F. (2014). Molecular diagnosis of putative Stargardt disease by capture next generation sequencing. *PLoS One* 9, e95528.

Zhao, L., Wang, F., Wang, H., Li, Y., Alexander, S., Wang, K., Willoughby, C., Zaneveld, J., Jiang, L., Soens, Z., Earle, P., Simpson, D., Silvestri, G. & Chen, R. (2015). Next-generation sequencing-based molecular diagnosis of 82 retinitis pigmentosa probands from Northern Ireland. *Human Genetics* 134, 217-230.